Molecular activation mechanism of RNA polymerase II degradation factor Def1

Kotryna Temcinaite

University College London

and

The Francis Crick Institute

PhD Supervisor: Dr Jesper Svejstrup

A thesis submitted for the degree of

Doctor of Philosophy

University College London

September 2016

Declaration

I Kotryna Temcinaite confirm that the work presented in this thesis is my own. Where information has been derived from other sources, I confirm that this has been indicated in the thesis.

Abstract

Transcribing RNA polymerase II (RNAPII) is prone to stalling and arrest due to its inability to efficiently bypass DNA lesions. RNAPII stalled at a DNA lesion triggers the transcription-coupled nucleotide excision repair (TC-NER) pathway to immediately repair the lesion and allow transcription to progress. However, if the TC-NER pathway fails, the so-called 'last resort pathway' is activated. The last resort pathway leads to the removal of stalled RNAPII from DNA, clearing the way for other repair factors. Ubiquitin signalling plays a crucial role in this pathway.

The last resort pathway is comprised of several ubiquitin-dependent steps. Rpb1, the largest subunit of RNAPII, undergoes two sequential ubiquitylation events: first, mono-ubiquitylation is carried out by ubiquitin ligase Rsp5, and then poly-ubiquitylation by the Elongin-Cullin complex. These steps enable the ubiquitin-dependent chaperone Cdc48, together with its adaptor proteins Ubx4 and Ubx5, to disassemble RNAPII from chromatin, and present it to the proteasome. Importantly, for the second ubiquitylation step to occur, RNAPII degradation factor Def1 undergoes ubiquitin- and proteasome-dependent activation, which allows it to bind RNAPII and recruit the Elongin-Cullin complex.

This thesis focuses on the molecular detail of Def1 activation in response to DNA damage in *Saccharomyces cerevisiae,* utilising a number of *in vivo* and *in vitro* techniques. It suggests that Cdc48, together with a specific adaptor protein, is required for the Def1 activation process. These observations add important new information about the last resort pathway and raise intriguing questions about the interplay between these two Cdc48-dependent steps in the pathway.

Acknowledgement

First and foremost, I would like to thank my PhD supervisor Jesper Svejstrup for the opportunity to work in his lab on an exciting and challenging project, and for his guidance and advice over the four years.

I would also like to thank all the members of the Svejstrup lab for creating a friendly and stimulating work environment, for good scientific discussions, and for support. I would especially like to thank Michelle Harreman for being a teacher, a collaborator, and a friend; and Hannah Williams for all the help and support over the course of my PhD. I would also like to acknowledge my thesis committee – Simon Boulton and John Diffley – not only for useful discussions regarding my project, but also for invaluable advice outside of research.

Last but not least, I would like to thank (already a Dr) Ross Coron as well as my family and friends for their endless and unconditional support, encouragement, and understanding.

Table of Contents

Table of figures

List of tables

Abbreviations

4-NQO	4-Nitroquinoline 1-oxide
5-FOA	5-Fluoroorotic Acid
AAA	ATPases Associated with diverse cellular Activities
ADP	Adenosine diphosphate
AMC	7-amino-4-methylcoumarin
APC	Anaphase-promoting complex
ARS	ATP regeneration system
ATP	Adenosine triphosphate
AZ	Antizyme
BSA	Bovine serum albumin
CHX	Cycloheximide
Ci	Cubitus interruptus
CP	Core particle
CPD	Cyclobutane pyrimidine dimer
CRL	Cullin-RING ligases
CS	Cockayne syndrome
CSB	Cockayne syndrome B protein
CTD	C-terminal domain
CUE	Coupling of ubiquitin to ER degradation domain
CV	Column volume
DNA	Deoxyribonucleic acid
DTT	Dithiothreitol
DUB	De-ubiquitylating enzyme
EDTA	Ethylenediaminetetraacetic acid
EM	Electron microscopy
ER	Endoplasmic reticulum
ERAD	ER-associated protein degradation
FPR	Phenylalanine-proline-arginine motif
GAL	Galactose
GGR	Global genome repair
GLU	Glucose

GRR	Glycine Rich Repeat motif
GST	Glutathione-S-Transferase
GYF	Glycine-tyrosine-phenylalanine domain
HbYX	Hydrophobic-tyrosine-X motif
HECT	Homologous to the E6AP carboxyl terminus
HF	His-Flag tag
HTM	His-Tev-Myc tag
IAA	Indole-3-acetic acid
IBR	In-between-RING domain
IP	Immunoprecipitation
IPT	Immunoglobulin-like fold, Plexins, Transcription factors domain
IPTG	Isopropyl *β*-D-1-thiogalactopyranoside
JAMM	JAB1/MPN/Mov34 metalloenzyme motif proteases
KoAc	Potassium Acetate
LN	Liquid nitrogen
MBP	Maltose binding protein
mRNA	Messenger RNA
MTH	Myc-TEV-His tag
NAT	Nourseothricin-sulfate
NEB	New England Biolabs
NEM	N-ethylmaleimide
NER	Nucleotide excision repair
NTS	Non-transcribed strand
ODC	Ornithine decarboxylase
OLE	Oleic acid
Otu	Ovarian tumour proteases
PBS	Phosphate buffered saline
PCNA	Proliferating cell nuclear antigen
PCR	Polymerase chain reaction
PDD	Processing determinant domain
PI	Protease Inhibitor mix
Pi	Inorganic phosphate group
Poly-Q	Poly-glutamine repeats
PP1	Protein serine/threonine phosphatase 1

pr-Def1	Processed-Def1 protein
PTM	Post-translational modification
PUB	PNGase/UBA or UBX domain
PUL	PLAA, Ufd3, and Lub1 domain
RBR	RING-in-between-RING
RING	Really Interesting New Gene domain
RNA	Ribonucleic acid
RNAPII	RNA polymerase II
RP	Regulatory particle
rRNA	Ribosomal RNA
RT	Room temperature
SDS	Sodium dodecyl sulphate
SOCS	Suppressor of cytokine signaling protein family
SUMO	Small ubiquitin-like modifier
TC-NER	Transcription coupled nucleotide excision repair
TE	Tris-EDTA buffer
TM	Transmembrane domain
tRNA	Transfer RNA
TS	Transcribed strand
ts	Temperature sensitive strain
UBD	Ubiquitin Binding domain
Ub	Ubiquitin
UBA	Ubiquitin-associated domain
UBX	Ubiquitin regulatory X domain
UEV	Ubiquitin E2 variant domain
UIM	Ubiquitin-interacting motif
Usp	Ubiquitin-specific proteases
UV	Ultra-violet
VBM	VCP binding motif
VIM	VCP interacting motif
VCP	Valosin-containing protein, now called p97
WT	Wild-type (W303-1A *S. cerevisiae* strain)
XP	Xeroderma pigmentosum
Znf	Zinc finger domain

1 Introduction

Due to the fact that Def1 is a yeast protein, and the pathway it is involved in is best described in *Saccharomyces cerevisiae*, the introduction mostly focuses on the yeast system, however, relevant mammalian homologues are mentioned throughout.

1.1 The ubiquitin system

1.1.1 Ubiquitin

Ubiquitin is a small 8.5 kDa protein, which can be covalently attached via an iso-peptide bond to lysine residues on other cellular proteins, and acts as a post-translational modification (PTM). It is highly conserved in eukaryotes (Figure 1.1 A), but not present in prokaryotic organisms. Ubiquitin was first described as a signal for selective protein degradation (Ciechanover et al. 1980; Wilkinson et al. 1980) and later discovered to be involved in many other cellular processes by altering protein-protein interactions or governing their subcellular localisation and activity (reviewed in (Finley et al. 2012)).

Unlike most other PTMs, ubiquitin is special in its ability to form chains. Ubiquitin itself contains 7 lysine residues (Figure 1.1 B) that can act as a receptor for further ubiquitylation events. In addition, the N-terminus is also susceptible to conjugation of further ubiquitin molecules. This configurations allows complex ubiquitin chain formation, including mixed linkages and branched chains (Peng et al. 2003; H. T. Kim et al. 2007). Linkage formation is regulated and different linkage chains are thought to perform different signalling functions inside the cell.

Further adding complexity to the ubiquitin signalling system, are the discoveries of ubiquitin modifications. Ubiquitin has been found to be both phosphorylated and actetylated under physiological conditions. Acetylation of ubiquitin was demonstrated to inhibit poly-ubiquitin chain formation (Ohtake et al. 2015). The first reported ubiquitin phosphorylation site was Ser57 (Peng et al. 2003), followed by further additions to the list from other studies (Swatek & Komander 2016). Several proteomics screens have also identified ubiquitin to be modified with a small

ubiquitin-like modifier (SUMO) (Galisson et al. 2011; Lamoliatte et al. 2013; Hendriks et al. 2014).

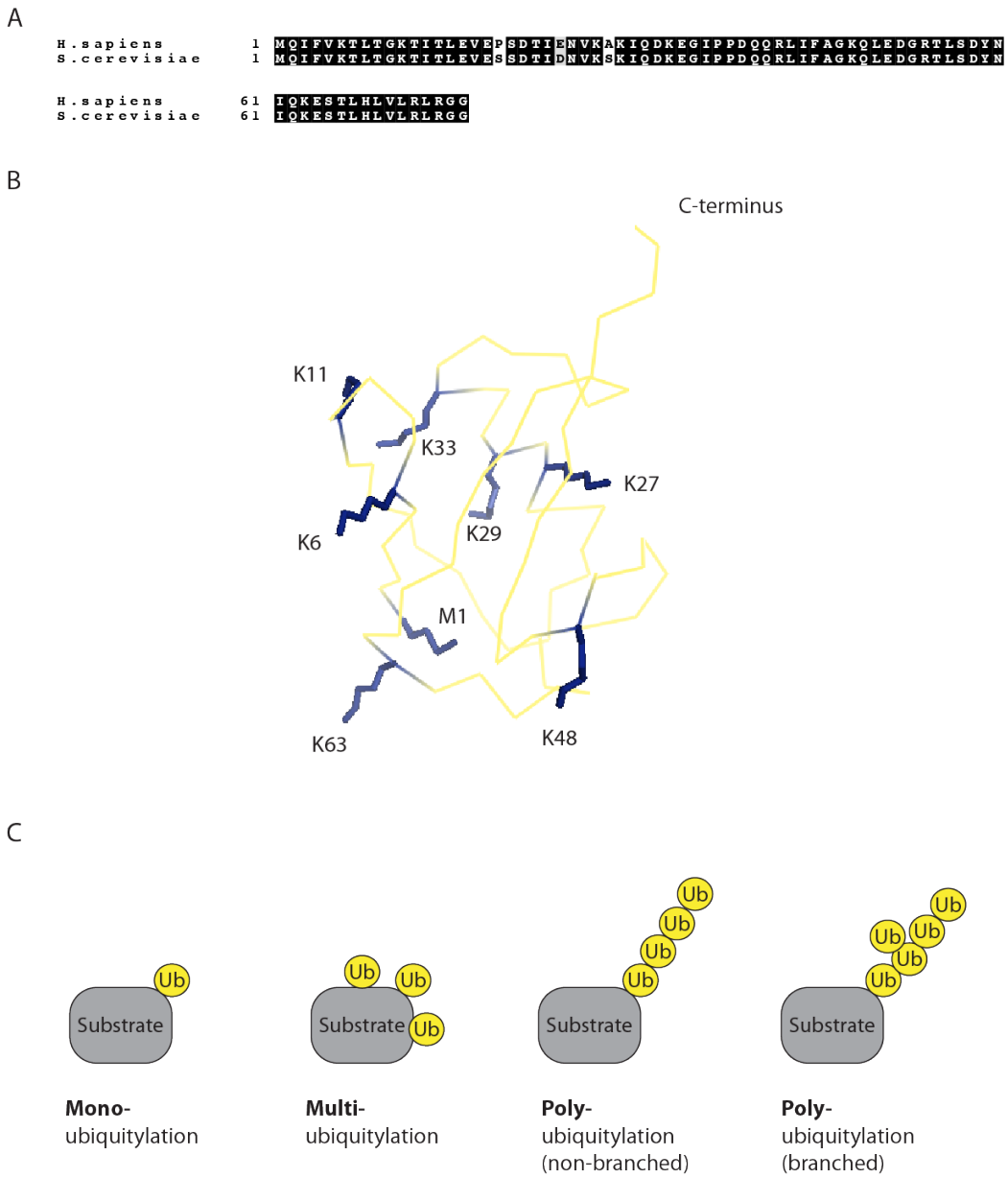

Figure 1.1. Ubiquitin structure.
A – sequence alignment of human (top) and yeast (bottom) ubiquitin. ***B*** – Ubiquitin structure (pdb 1UBQ (Vijay-Kumar et al. 1987)), with residues, involved in ubiquitin chain formation highlighted in blue. *C* – Different modes of ubiquitylation.

A vast number of diverse ubiquitin signals can be generated – a substrate can be mono-ubiquitylated, multi-ubiquitylated, or poly-ubiquitylated (Figure 1.1 C). Taking into account that ubiquitin can be linked in chains by 8 different types of linkages, lysine residues in each ubiquitin can be additionally modified with either acetyl

groups or SUMO, and there are 11 potential phosphorylation sites present on each ubiquitin molecule, the variety of ubiquitin signals is further expanded. This allows for very dynamic and intricate signalling inside the cell, which remains poorly understood.

1.1.2 Ubiquitylation cascade

In order for ubiquitin to become covalently attached to a target protein, a cascade of reactions carried out by three different enzymes is required. The reaction starts with the activation of ubiquitin. This is the only step in the ubiquitylation process requiring ATP. It is performed by a ubiquitin-activating (E1) enzyme. *Saccharomyces cerevisiae* has only one ubiquitin-activating enzyme, Uba1 (Finley et al. 2012). The use of an ATP molecule allows the formation of a high-energy thoiester bond between the catalytic cysteine of Uba1 and ubiquitin (Figure 1.2 A). Next, ubiquitin is transferred to a catalytic cysteine of a ubiquitin-conjugating enzyme E2 (Olsen & Lima 2013). The final step in the cascade is performed by the E3 ubiquitin ligases that directly or indirectly transfer ubiquitin onto the substrate (Figure 1.2 B).

While there is only one E1 enzyme in yeast, the number of recognised E2s and E3s is rapidly increasing, with over 10 E2s and over 60 E3s identified, adding to the complexity of the ubiquitin system (Finley et al. 2012). One E2 enzyme is capable of interacting with several E3s, and each E3 enzyme has more than one substrate, thus significantly expanding the ubiquitylation network. In humans, the complexity of ubiquitin system is expanded by larger numbers of enzymes involved in ubiquitylation – there are eight E1 enzymes reported (Schulman & Harper 2009), over 40 E2s (Valimberti et al. 2015), and the estimate of over 600 E3s (Berndsen & Wolberger 2014).

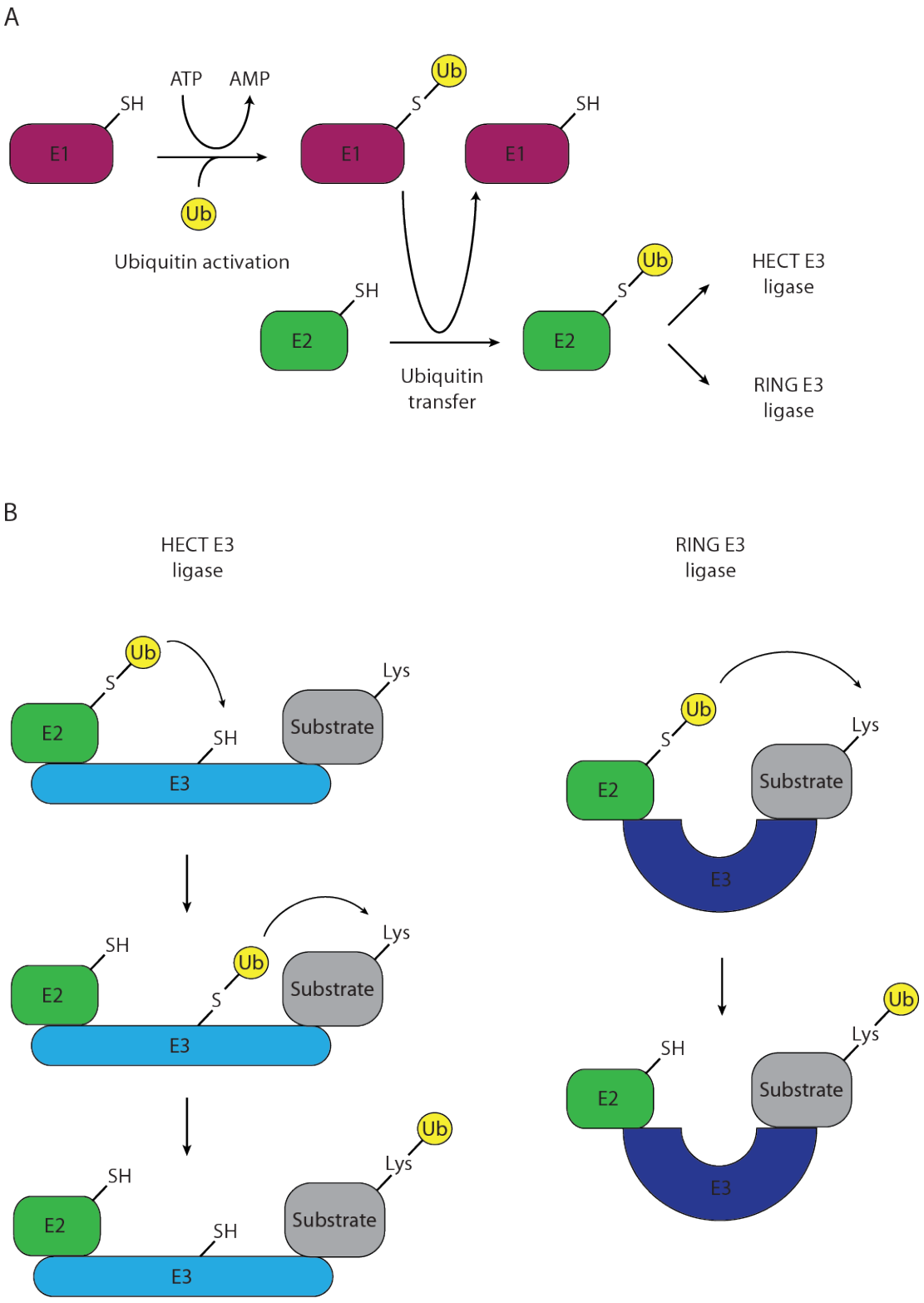

Figure 1.2. The ubiquitylation cascade.
A – Ubiquitin is conjugated to an E1 ubiquitin activating enzyme in an ATP-dependent manner. Then the ubiquitin is transferred to an E2 ubiquitin conjugating enzyme further working with either HECT or RING family E3 ubiquitin ligases. ***B*** – Schematics

highlighting the differences between HECT and RING E3 ubiquitin ligases. HECT E3 ligases catalyse a two-step reaction, first conjugating ubiquitin to their catalytic cysteine residue and then transferring it to the substrate, while RING E3 ligases catalyse a direct transfer of ubiquitin from E2 to the substrate.

The E1 enzyme has only one function in the ubiquitylation cascade – ubiquitin activation. In contrast, E2s have been shown to play a more complicated role in the system. Not only have E2 enzymes been demonstrated to be involved in the determination of the ubiquitin chain topology (Eddins et al. 2006; Suryadinata et al. 2013), they also might be implicated in determining substrate specificity for E3 enzymes (Bernier-Villamor et al. 2002; Somesh et al. 2007), allowing additional flexibility in substrate recognition.

The E3 enzymes can be split into two families according to their structure and mode of action – RING domain and HECT domain-containing E3s (Figure 1.2 B). HECT domain E3s first accept ubiquitin from an E2 enzyme onto their active site cysteine and then catalyse a transfer of the ubiquitin onto a substrate. This type of mechanism is achieved by the coordination between the N-lobe responsible for binding the E2 and the catalytic C-lobe of the HECT domain connected by a flexible linker (L. Huang et al. 1999; Verdecia et al. 2003). The best-described example of a HECT E3 ligase in *S. cerevisiae* is Rsp5, which is involved in many cellular processes (Huibregtse et al. 1995; Kaliszewski & Zoładek 2008) and will be revisited in subsequent chapters due to its role in the 'last resort' pathway for RNA polymerase II (RNAPII) ubiquitylation and degradation (1.4.3).

Rsp5 belongs to the Nedd4 (neural cell-expressed developmentally downregulated) ubiquitin ligase family, and is the only E3 ligase in yeast from this family of ubiquitin ligases, which are involved in various cellular processes (Kaliszewski & Zoładek 2008). All E3 ligases in this family share a similar structure: they are composed of the catalytic HECT domain, several WW domains, and the C2 domain. The Rsp5 C2 domain mediates the interaction with phosphorylated phosphatidylinositols, and is important for the localisation of Rsp5 at endosomal membranes for the regulation of membrane protein trafficking (Dunn et al. 2004). Rsp5 also has been reported to harbour two nuclear localisation signals (NLS) and one nuclear export signal (NES),

enabling it to shuttle between the nucleus and the cytoplasm (Cholbinski et al. 2011).

Apart from its role in membrane protein trafficking and the 'last resort' pathway (1.4.3), Rsp5 together with E2 Ubc4 has also been implicated in the regulation of mRNA nuclear export factor Hpr1 (Gwizdek et al. 2005). It has also been implicated in both tRNA and rRNA processing and transport (Domanska & Kaminska 2015). Moreover, genetic studies have suggested that Rsp5 works upstream of anaphase-promoting complex (APC) in the same pathway for mitotic chromatin assembly, although the exact role of Rsp5 in this process remains unresolved (Arnason et al. 2005).

The three Rsp5 WW domains play a role in substrate recognition. They are thought to recognise PXY, PPXY or LPXY motif, but not all Rsp5 substrates identified in a protein microarray screen contain such motifs (Gupta et al. 2007). The substrates without the canonical WW recognition motif are hypothesised to bind Rsp5 via other domains or require adaptor proteins for recognition (Kaliszewski & Zoładek 2008). An example of such Rsp5 adaptor protein is Bsd2, a protein required for the ubiquitylation of a vacuolar carboxypeptidase, Cps1, while both Bsd2 and Tre1 adaptors are required for the Rsp5-dependent ubiquitylation of the manganese transporter, Smf1 (Sullivan et al. 2007). The presence of adaptor proteins expands the repertoire of Rps5 substrates. However, the largest subunit of RNAPII, Rpb1, in the last resort pathway is directly recognised by the Rsp5 WW domains (Beaudenon et al. 1999).

In contrast to the HECT family ligases, that essentially catalyse two reactions during the ubiquitin transfer, the RING family ligases do not themselves have an active site as such, but instead catalyse a direct attack of the substrate lysine on the E2~Ub bond. The RING domain is responsible for binding to the E2 and stimulating the ubiquitin transfer to the substrate (Lorick et al. 1999). The catalysis of the reaction is achieved both through the altered conformation of the E2 upon binding an E3 RING ubiquitin ligase (Ozkan et al. 2005) and correct catalytic orientation (Duda et al. 2008; Plechanovová et al. 2012).

The largest sub-set of RING E3 ligases is known as Cullin RING ligases (CRLs). These multisubunit ligases are composed of the scaffold protein – cullin, a RING-box protein, carrying a domain similar to the RING domain from single-subunit E3 ligases, and an adaptor protein, which is responsible for substrate binding (Feldman et al. 1997; Skowyra et al. 1997). A CRL important for this thesis is the Elongin-Cullin complex, involved in the last resort pathway (1.4.3). It is formed by Cul3 binding to the Rbx1/Hrt1 (the RING domain protein) via the C-terminus, while the N-terminus of Cul3 binds to Elc1. Elc1 is a SKP1-like adaptor protein, which heterodimerises with the substrate receptor Ela1.

In addition to the Cul3 complex with the Ela1, Elc1, and Rbx1 proteins, involved in the last resort pathway, Cul3 has also been reported to assemble in a complex with Elc1, the SOCS (suppressor of cytokine signalling) box adaptor protein Rad7, and the RING-finger protein Rad16 (Gillette et al. 2006). This complex is responsible for the ubiquitylation of Rad4, a global genome repair (GGR) factor. Rad4 together with Rad23 was shown to recognise DNA lesions that locally destabilize the Watson-Crick double helix, such as cyclobutane pyrimidine dimers (CPDs) (J.-H. Min & Pavletich 2007). Interestingly, Rad4 became ubiquitylated by the Cul3/Elc1/Rad7/Rad16 complex and degraded in response to UV irradiation, which is thought to be the alternative, Rad23-independent, pathway for nucleotide excision repair (NER), requiring *de novo* protein synthesis (Gillette et al. 2006). However, the regulation of the two alternative NER pathways and the role the CRL plays in this process remains unresolved.

Both types of E3 enzymes (HECT and RING) are able to form ubiquitin chains on substrates. Ubiquitin chains on substrates are formed by sequential addition of ubiquitin moieties on top of one another. The processivity of CRLs is ensured by the electrostatically driven interaction between E2 and cullin, allowing the E2 to be quickly reloaded several times, while still interacting with the same substrate (Kleiger et al. 2009). The HECT ligases require ubiquitin re-loading to build a ubiquitin chain and due to steric hindrance, ubiquitin-loaded E2 cannot access the ubiquitin-binding site on the C-lobe before the E3 transfers its ubiquitin on the substrate (Maspero et al. 2013). Moreover, it is also possible for several distinct E2/E3 complexes to be involved in poly-ubiquitylation of a single substrate

(Rodrigo-Brenni & Morgan 2007; Parker & Ulrich 2009; Harreman et al. 2009). This is again of particular relevance for the last resort pathway, where sequential action by Rsp5 and the Elongin-Cullin complex is required for RNAPII poly-ubiquitylation (1.4.3.1, 1.4.3.2).

Interestingly, priming of CRLs has also been described in the mammalian system. ARIH1, an E3 ligase belonging to the Ariadne subfamily of RING-in-between-RING (RBR) ligases was shown to physically associate with CLRs and catalyse the first ubiquitylation step in the reaction (Scott et al. 2016). RBR family ligases have three main domains: two RING domains interspaced by cysteine-rich zinc finger domain, also called an in-between RING (IBR) domain. The RBR family ligases function like HECT E3 ligases – they bind E2s via one RING domain, and transfer ubiquitin to the catalytic cysteine on the second RING domain (D. M. Wenzel et al. 2011). This family of E3 ligases is not present in yeast. ARIH1 was shown to specifically bind neddylated CUL1, CUL2, CUL3, and CUL4A complexes, which subsequently leads to the stimulation of ARIH1 ligase activity (Kelsall et al. 2013). RBX1 protein in complex with a cullin is not only required to achieve this activation, but also actively guides ARIH1 to mono-ubiquitylate the CRL substrate (Scott et al. 2016). Such priming of CRLs allows a faster poly-ubiquitylation of the substrate and also adds a Nedd8-specific regulation step (Scott et al. 2016). There is a clear parallel between this system and Rsp5 priming Elongin-Cullin complex in the last resort pathway (1.4.3.1, 1.4.3.2).

1.1.3 De-ubiquitylating enzymes

Ubiquitylation is a reversible modification – de-ubiquitylating enzymes (DUBs) are able to trim and remove ubiquitin chains from substrates by hydrolysing the isopeptide bond. So far around 20 DUBs have been identified in yeast (Finley 2009), and over a 100 DUBs in humans (Hutchins et al. 2013). In yeast, based on their structure and sequence, all DUBs are divided into four families: the Usp (ubiquitin-specific proteases) family, the Otu (ovarian tumour proteases) family, and the JAMM (JAB1/MPN/Mov34 metalloenzyme motif proteases) and Uch (ubiquitin C-terminal hydrolases) families (Finley et al. 2012). DUBs have a broad range of

substrates (Schaefer & Morgan 2011) and no single DUB is essential for survival in yeast. Nevertheless, individual DUBs typically show clear selectivity for specific ubiquitin linkages (Mevissen et al. 2013; Yu Ye et al. 2012).

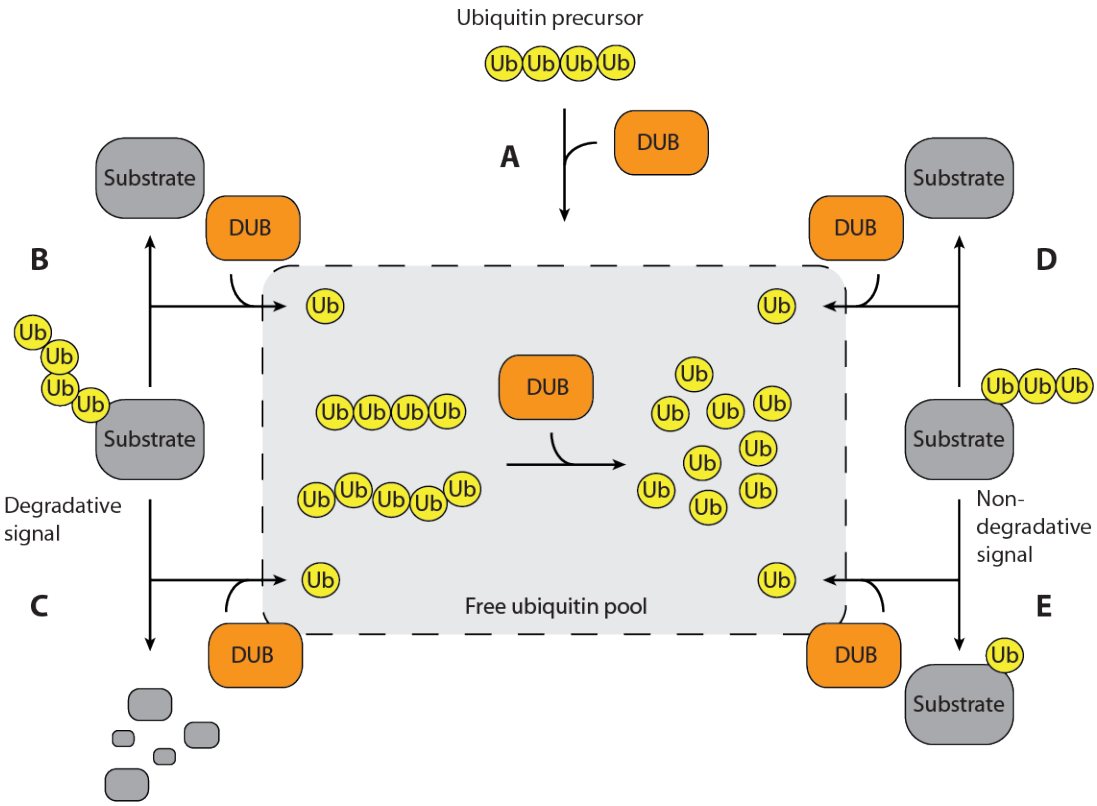

Figure 1.3. Cellular roles of DUBs.
A – generating mono-ubiquitin from linear ubiquitin precursor; B – rescuing substrates from degradation by removing the degradative signal; C – recycling ubiquitin when a ubiquitylated substrate is degraded; D – removing non-degradative signal from the substrate; E – modifying the ubiquitin signal and changing the substrate function/activity.

DUBs play several major roles in the cell (Figure 1.3). Three out of four ubiquitin-encoding genes in yeast code for a linear ubiquitin fusion and DUBs are required to generate free ubiquitin from these precursors. Secondly, by removing ubiquitin chains from modified proteins, DUBs can reverse their fate, e.g. rescue protein from degradation. DUBs also play an important role in ubiquitin homeostasis by recycling ubiquitin from proteins destined for degradation, and finally, they are able to edit ubiquitin chains by trimming, potentially allowing the exchange of one ubiquitin signal for another.

Interestingly, a recent study of a mammalian proteasome-associated DUB USP14 (Ubp6 in yeast) has demonstrated that USP14 has a preference for multi-ubiquitylated substrates over substrates carrying a single poly-ubiquitin chain, suggesting that the proteasome in the presence of USP14 is able to differentiate between a substrate carrying a single-poly-ubiquitin chain and a multi-ubiquitylated substrate (B.-H. Lee et al. 2016). USP14 was able to remove multiple ubiquitin chains *en bloc* from a model substrate, an 88-residue amino-terminal element of cyclin B1, until a single ubiquitin chain was left, and the prevalence of the last ubiquitin chain was suggested to be due to the distance between the ubiquitin chain and the place of attachment between the substrate and USP14 (B.-H. Lee et al. 2016).

Functions of DUBs are regulated in several different ways. Both phosphorylation and ubiquitin-like modifications can alter DUB activity (Reiley et al. 2005; Solé et al. 2011; Todi et al. 2009). The other major mode of DUB regulation is via its binding partners and allosteric regulation, i.e. Ubp3 becomes activated upon association with Bre5 (M. Cohen et al. 2003) and Ubp2 was found to associate with the E3 Rsp5, antagonising its Lys-63 chain formation (Kee et al. 2006; Kee et al. 2005). This association has relevance for the last resort pathway (1.4.3) as the Rsp5 ubiquitin ligase is responsible for the first ubiquitylation step in the pathway (Harreman et al. 2009). Moreover, Ubp3 also plays an important role in the last resort pathway, rescuing the RNAPII complexes targeted for degradation via its de-ubiquitylation activity (Kvint et al. 2008).

1.1.4 Ubiquitin binding domains

Each ubiquitin signal inside the cell has to be recognised correctly and a vast number of different ubiquitin chain topologies provides a challenge, since all of them might be signalling a different protein fate. The ubiquitin signal can be recognised by ubiquitin binding domains (UBDs), which are small and capable of forming autonomous folding units (Hofmann 2009), or short peptide sequences capable of interacting with ubiquitin (Fradet-Turcotte et al. 2013).

The common feature shared between all UBDs is their non-covalent association with the ubiquitin signal. The binding affinities are usually low, with dissociation constants typically in the hundreds of micromolar range (Hurley et al. 2006; Hicke et al. 2005) (Table 1-1). The ubiquitin surface recognised by UBDs typically comprises a hydrophobic patch including the highly-conserved Ile-44 residue on ubiquitin (Figure 1.4 A), while a UBD usually contributes an α-helix to the interaction (Hofmann 2009). However, other binding surfaces are also important and the subtle differences between the family members leads to different binding affinities and specificities (Raasi et al. 2005). Obviously, a UBD is in itself unlikely to ensure specificity in the interaction between a UBD containing protein and its ubiquitylated partner. Specificity is thus additionally ensured by coordinating the interaction between ubiquitin and UBD with other interaction surfaces in the proteins in question (Parker et al. 2007): the ubiquitin-UBD interaction often merely enhances the association between proteins that already have other interaction motifs or domains.

Table 1-1. Ubiquitin binding affinities of some ubiquitin binding domains.
Adapted from (Hicke et al. 2005)

Ubiquitin-binding domain	Domain size (amino acids)	Ubiquitin binding affinity (K_d)
CUE	42-43	2-160 μM (mono-ubiquitin)
UBA	45-55	10–500 μM (mono-ubiquitin) 0.03–9 μM (poly-ubiquitin)
UEV	~145	100–500 μM (monoubiquitin)
UIM	~20	100–400 μM (mono- or poly-ubiquitin)

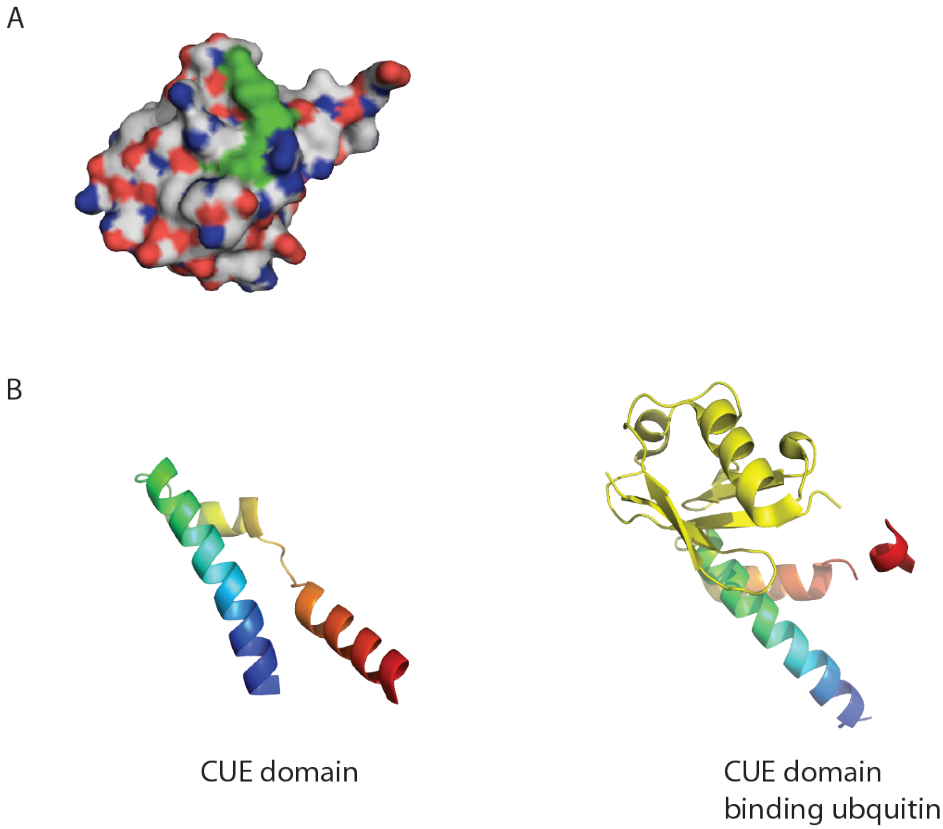

Figure 1.4. Ubiquitin and ubiquitin-interacting domains.
A – The structure of ubiquitin (pdb 1UBQ (Vijay-Kumar et al. 1987)) with the hydrophobic patch Leu8-Ile44-Val70 highlighted in green on a surface representation. Acidic areas are shown in red and basic in blue. ***B*** – (left) The CUE domain of yeast Vps9 protein (pdb 1MN3 (Prag et al. 2003)), (right) the CUE domain of yeast Vps9 protein interacting with ubiquitin (pdb 1P3Q (Prag et al. 2003)).

UBDs are also sometimes able to differentiate between ubiquitin linkages in a poly-ubiquitin chain. Although the most straightforward way for differentiation between the linkages would be a specific recognition of the surface that is only accessible in one specific type of ubiquitin-ubiquitin linkage, there are actually no documented examples of such strategy at the time of writing. However, concomitant binding of two K48-linked ubiquitin molecules by a single UBD has been reported. For example, the second ubiquitin-associated (UBA) domain in the DNA damage response factor, Rad23, preferentially binds to K48 chains by sandwiching its UBA domain between the two K48-linked ubiquitin molecules (Varadan et al. 2005). Another binding strategy is the cooperation between several UBDs in the same protein. This leads to the increased avidity for ubiquitin and can also contribute to the chain specificity expressed via the linker length between the UBDs (Sims & R.

E. Cohen 2009). Overall, different ubiquitin chains have their thermodynamically preferred states, which are stabilised by the association with a specific interacting UBD (Husnjak & Dikic 2012).

UBDs play various roles inside the cell. They can act to prevent poly-ubiquitylation of a substrate (Herrador et al. 2013), guide the ubiquitin conjugation reaction by orienting the incoming ubiquitin molecules (Shih et al. 2003), and even promote ubiquitylation without the involvement of an E3 ubiquitin ligase (Hoeller et al. 2007), apart from their general function in ubiquitin recognition. Unsurprisingly, as a part of the ubiquitin signalling system, UBDs are involved in a very broad spectrum of cell signalling (Hofmann 2009; Acconcia et al. 2009).

A UBD important for this thesis is the CUE (*C*oupling of *U*biquitin to *E*R degradation) domain (Figure 1.4 B), since it is found at the N-terminus of the Def1 protein (1.4.3.6). The CUE domain was first described in the Vps9 protein, involved in protein trafficking (Donaldson et al. 2003; Shih et al. 2003). The structure of a CUE domain with ubiquitin revealed that the CUE domain binds the conserved hydrophobic Leu8-Ile44-Val70 patch on ubiquitin (Kang et al. 2003). It has been implicated in binding both mono-ubiquitin and poly-ubiquitin chains (Shih et al. 2003; Bagola et al. 2013), and was shown to be required to promote mono-ubiquitylation of Vps9 by the Rsp5 ubiquitin ligase (Shih et al. 2003). Moreover, the CUE domain from Vps9 was shown to be able to dimerise and bind a single ubiquitin moiety, thus increasing the binding affinity (Prag et al. 2003). Intriguingly, the CUE domain on Def1 may not actually bind ubiquitin, but instead a ubiquitin-homology domain in the Ela1 protein, thus bringing the Ela1-Elc1-Cul3 ubiquitin ligase to a stalled RNAPII (Wilson, Harreman, Taschner, et al. 2013). This process is described in detail in (1.4.3).

1.1.5 The ubiquitin signal

Ubiquitin signalling is involved in many cellular processes, such as endocytosis, regulation of gene transcription, intracellular cell signalling, DNA damage repair, and protein degradation. For example, ubiquitylation of histones represents one of

the major modifications on chromatin and ubiquitylation of histone H2A is associated with condensed chromatin (Mimnaugh et al. 1997; Levinger & Varshavsky 1982). On the other hand, mono-ubiquitylation of histone H2B has also been implicated in the regulation of transcription by RNA polymerase II (RNAPII), having a stimulatory effect (Pavri et al. 2006). Histone ubiquitylation also guides other post-translational modifications, such as methylation and acetylation (Yi Zhang 2003), illustrating its importance.

Different ubiquitin chain linkages have been linked to different processes in the cell. K6- and K33-linked ubiquitin chains were found to be up-regulated in response to DNA damage (Elia et al. 2015). K6 chains have also been implicated in mitochondrial homeostasis (Durcan et al. 2014), while, besides K48, K11 and linear ubiquitin chains have been observed to play a role in proteasomal degradation, especially related to cell-cycle control (Grice et al. 2015; M. Min et al. 2015). K27 chains might be involved in the DNA-damage response (Gatti et al. 2015) and K33 chains have been implicated in many cellular processes, with a recent report suggesting an involvement in post-Golgi membrane protein trafficking (Yuan et al. 2014). It is clear that there are tendencies for some ubiquitin chains to be associated with certain cellular processes, although there are no strict divisions.

From the canonical ubiquitin chains (K48 and K63), traditionally K63 chains are associated with non-proteolytic functions. K63 chains have been implicated in the inflammatory response and regulation of endosomal sorting pathways. However, the most relevant function of K63 chains to this thesis is that in DNA damage repair.

The best-described involvement of K63 chains in DNA damage repair is the ubiquitylation of proliferating cell nuclear antigen (PCNA). PCNA forms a ‘sliding-clamp’, which replicative polymerases attach to during replication, thus enhancing their processivity. Upon encountering a DNA lesion that the processive replicative polymerase cannot cope with, the replication fork stalls at the site of the lesion and PCNA becomes ubiquitylated. The first step in the ubiquitylation cascade is mono-ubiquitylation on PCNA Lys-164, carried out by E3 ligase Rad18 together with the E2 Rad6 (Hoege et al. 2002). This step may be followed by the expansion of the mono-ubiquitylation to a K63-linked poly-ubiquitin chain by the E3 ligase Rad5,

together with Ubc13-Mms2 E2 complex, which signals for error-free damage avoidance using sister-strand recombination (H Zhang & C. W. Lawrence 2005).

K48 chains are the most common type of ubiquitin chains, and have been shown to target proteins to the proteasome for degradation. It has been suggested that at least a tetra-ubiquitin chain is required for efficient substrate targeting to the proteasome (Thrower et al. 2000). Further studies started to re-define this notion, demonstrating that two di-ubiquitin chains can lead to efficient degradation as well (Lu et al. 2015). The structure and function of the proteasome is discussed in detail in the next sub-chapter (1.2).

Overall, ubiquitin is involved at some level in most, if not all, cellular processes and the signalling system is highly complex due to the number of different chain linkages and modifications of ubiquitin itself, all recognised and acted on by different effectors. The field of ubiquitin signalling has significantly expanded over the recent years revealing this complexity, but it many cases more studies are needed to completely elucidate the exact role ubiquitin plays.

1.2 The proteasome

1.2.1 Structure of the proteasome

The 26S proteasome is formed of 33 subunits, all together corresponding to a 2.5 MDa complex (Finley et al. 2012). It is highly evolutionarily conserved and found in all eukaryotes. The 26S proteasome is made of two sub-particles – the 19S regulatory subcomplex and the 20S catalytic core particle (Figure 1.5). The 19S regulatory particle is responsible for substrate recognition, while the 20S particle harbours the active sites for protein degradation. The 20S core particle (CP) is capped by the 19S regulatory particle (RP) either at one or both ends (Peters et al. 1993), and this association requires ATP (Smith et al. 2005). Both CP and RP structures are discussed in more detail below.

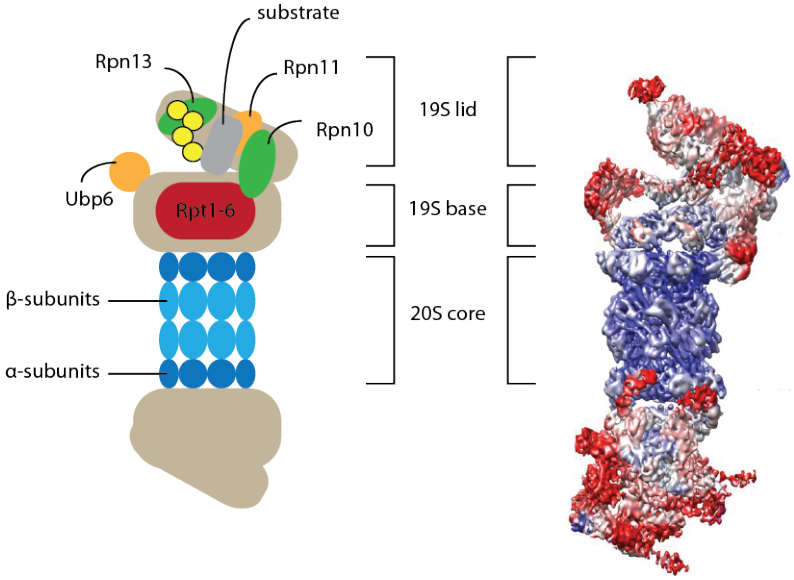

Figure 1.5. Structure of the 26S proteasome.
(left) A schematic representation of the 26S proteasome. ATPase subunits Rpt1-6 are represented in red, DUBs associated with the proteasome – Ubp6 and Rpn11 – orange, ubiquitin-interacting subunits Rpn13 and Rpn10 – green, β- subunits – light blue, α-subunits – dark blue, substrate – grey, ubiquitin – yellow. (right) The cryo-EM structure of the yeast 26S proteasome (pdb 4B4T (Beck et al. 2012)). The structure is coloured according to resolution from blue (6.5 Å) to red (8.5 Å).

1.2.1.1 The core particle (CP)

The CP is formed of four concentric rings (2 α rings and 2 β rings) and shows a two-fold symmetry, with each ring being a heteroheptamer. The active sites are physically sequestered from the surroundings and found inside the barrel. Only three β subunits are catalytically active, β1, β2, and β5, each of them carrying a different active site - trypsin-like, caspase-like, and chymotrypsin-like, respectively (Heinemeyer et al. 1997). This allows a rather non-specific degradation of a wide range of substrates.

The four rings altogether form a catalytic chamber and two antechambers on each side. The antechambers formed by α and β rings have been shown to provide the environment required to maintain the substrate in the unfolded state (Sharon et al. 2006; Ruschak et al. 2010). The centre of the α ring is also known as the gate and regulates the passage of substrates, only allowing completely unfolded proteins to pass (T. Wenzel & Baumeister 1995), since the pore is occupied by the N-termini

from the α subunits (Groll et al. 2000). The α subunits also provide a binding interface for the RP to dock onto (Smith et al. 2007).

Overall, the CP provides high concentration of active sites with low specificity (i.e. general proteolytic activity) within a closed space (Finley 2009) – ideal conditions to degrade any unfolded protein, but no way of selecting its targets. This selective role is performed by the regulatory particle, comprised of the lid and the base protein assemblies (Glickman et al. 1998). The RP is also responsible for de-ubiquitylation (for ubiquitin recycling) and unfolding of the substrates before they enter the 20S particle for degradation (Glickman et al. 1998; Navon & Goldberg 2001).

1.2.1.2 The regulatory particle (RP)

The regulatory particle is formed of two sub-complexes – the base and the lid (Figure 1.5). The base is made of Rpt1-6 subunits (forming a hexamer with ATPase activity), and Rpn1, Rpn2, Rpn10, and Rpn13 subunits, with the latter two acting as substrate receptors. Although it was initially thought that the base subunits made contact with the CP, while the lid was covering the central pore, Rpn2, Rpn10, and Rpn13 were later shown to be located away from the CP and to not make any physical contacts with it (Sakata et al. 2012).

All Rpt proteins forming the Rpt ring of the base particle are members of the ATPases associated with diverse cellular activities (AAA) family. They use ATP to generate mechanical force to unfold the protein substrate and translocate it through the channel. This mechanism of action was inferred from studies of a bacterial ATP-dependent protease, ClpXP (Aubin-Tam et al. 2011), and structural rearrangements of the Rpt ring observed during substrate degradation (Matyskiela et al. 2013). The Rpt ring is directly coupled to the 20S core particle by insertion of C-terminal hydrophobic-tyrosine-X (HbYX) motifs, present in three out of six Rpt proteins (Rpt2, 3, and 5) into specific pockets of α subunits of the CP (Smith et al. 2007; Tian & Matouschek 2006), allowing synergistic action.

The base also has three substrate receptors – Rpn1, Rpn10, and Rpn13. Rpn10 has been shown to bind ubiquitin chains (Elsasser et al. 2004), while Rpn1 acts as a receptor for ubiquitin-like (UBL) domains (Elsasser et al. 2002), and Rpn13 can bind both ubiquitin and UBLs (Husnjak et al. 2008; Schreiner et al. 2008). Rad23, Dsk2, and Ddi1 have both UBL and ubiquitin-associated (UBA) domains and have been described as shuttle factors delivering ubiquitylated proteins to the proteasome (Elsasser et al. 2002; Rosenzweig et al. 2012), due to their ability to simultaneously bind ubiquitylated proteins and interact with the proteasome.

The lid particle is composed of Rpn3, Rpn5, Rpn6, Rpn7, Rpn8, Rpn9, Rpn11, Rpn12, and Sem1 proteins. It is positioned laterally to the base and forms many contacts with the base subunits (Lander et al. 2012; Lasker et al. 2012). A cryo-electron microscopy (EM) structure of the yeast 26S proteasome revealed that Rpn8/Rpn11 heterodimer connects with the base and the 20S CP at the periphery and Rpn3, Rpn5, Rpn6, Rpn7, Rpn9, and Rpn12 form a horseshoe-like structure, positioning Rpn11 directly above the AAA-ATPase N-ring for de-ubiquitylation of the substrates immediately before unfolding (Beck et al. 2012).

The main function of the lid is de-ubiquitylation of incoming proteins and it is performed by the Rpn11 subunit. Rpn11 is a zinc-metalloprotease capable of cleaving off ubiquitin chains at the base, removing the chain entirely (Verma et al. 2002). Another deubiquitylase associated with the proteasome is Ubp6. However, it is not a stoichiometric component of the proteasome (Hanna et al. 2007) and only becomes associated with the proteasome via the Rpt1 subunit when its catalytic site is occupied by ubiquitin (Aufderheide et al. 2015; Bashore et al. 2015). Unlike Rpn11, Ubp6 trims ubiquitin chains starting from the outermost ubiquitin in the chain (Guterman & Glickman 2004).

1.2.1.3 Structural dynamics of protein degradation

Recent EM studies have captured the 26S proteasome in several different conformational states: s1, s2, and s3 (Unverdorben et al. 2014), revealing the dynamics of proteasome action. S1 is the predominant state in the absence of

substrate under ATP hydrolysis conditions (Beck et al. 2012; Lander et al. 2012; Lasker et al. 2012) and represents the ground state of the proteasome. The s3 state is observed in the presence of the substrate or the slowly-hydrolysable ATP analogue, ATPγS (Sledz et al. 2013; Matyskiela et al. 2013). The s2 state represents an intermediate state between s1 and s3, potentially corresponding to the proteasome engaged with the substrate, but not yet committed for degradation (Finley et al. 2016). Taken together, these structural states may reflect the changes in the proteasome during the substrate degradation cycle.

1.2.1.4 Proteasome activators

Even though the canonical 26S proteasome is formed by the 20S and 19S subunits, other proteins can replace the regulatory 19S particle on top of the 20S cylinder. Generally, these factors are referred to as proteasome activators (Finley et al. 2012). Approximately 20% of the proteasomes in yeast are hybrid RP–CP–Blm10 particles (Schmidt et al. 2005). Blm10 opens the CP gate by binding to the CP and inserting its C-terminal HbYX motif in the α5/α6 pocket, but this type of opening is considerably smaller compared to the 19S RP, however, could provide access for an unfolded protein (Sadre-Bazzaz et al. 2010). Blm10 was shown to promote degradation of the transcription factor, Sfp1, required for the expression of ribosomal protein genes (Lopez et al. 2011), and also takes part in assembly of the CP (Fehlker et al. 2003) and its nuclear import (Weberruss et al. 2013).

Cdc48, a ubiquitin-dependent segregase, which is discussed in detail in subsequent sections (1.3), is hypothesised to be able to act as an activator of the CP due to its homohexameric structure and C-terminal HbYX motifs (Finley et al. 2016). An association between Cdc48 and the 20S proteasome has been determined in archaea (Barthelme & Sauer 2012; Barthelme et al. 2014); however, whether Cdc48 carries all the same functions in eukaryotes remains to be elucidated. Recently, a functional association between the human homologue of Cdc48 (called p97), and the 20S proteasome was suggested based on the analysis of the D592N and D592H mutations in human p97, found in amyotrophic lateral sclerosis (ALS): these disease-related mutations appear to be in the elements

required for association between the 20S proteasome and Cdc48 in archaea (Barthelme et al. 2015).

1.2.2 Proteasomal function and its regulation

1.2.2.1 Degradation signals

One of the main functions of the proteasome is in quality-control protein degradation. For quality-control purposes, degron signals governed by protein folding and assembly play an important role – they allow ubiquitin ligase recognition and targeting for degradation via ubiquitylation. For example, nuclear quality control ligase San1 recognises misfolded proteins directly through exposed hydrophobic motifs (Fredrickson et al. 2011; Rosenbaum et al. 2011), and ubiquitylates them, targeting for proteasomal degradation.

Another type of degron recognised by ubiquitin ligase is the N-end rule degron, recognised by the N-end rule ubiquitin ligase Ubr1. It is determined by the N-terminal amino acid residue of the substrate protein (Bachmair et al. 1986; Bartel et al. 1990; Choi et al. 2010). Usually, the destabilising N-terminal residues are not present on newly synthesised proteins, but appear as a result of the action of proteases (Varshavsky 2011). However, recently, the group of substrates recognised by the Ubr1 ubiquitin ligase has been expanded significantly with the observation that Ubr1 is capable of recognising un-acetylated N-terminal methionine if it is followed by a hydrophobic residue (H.-K. Kim et al. 2014). These results suggest that N-end rule degron might be a more general degradation pathway then previously thought, since the majority of cellular proteins have an N-terminal methionine residue. The N-end degrons are recognised by specific ubiquitin ligases that poly-ubiquitylate these proteins, targeting them for proteasomal degradation.

1.2.2.2 Structural requirements for protein degradation

It is clear that substrate recognition is mostly carried out by the ubiquitin ligases, marking substrates with the ubiquitin signal, directing them to the proteasome.

However, there are some additional requirements in order for the proteasome to successfully degrade the substrate (Figure 1.6). Generally, the proteasomal degron has been described as bi-partite – requiring both the proteasome targeting signal (typically ubiquitin), and a disordered region in the substrate (with no strict sequence requirements), where the proteasome can initiate (Prakash et al. 2004; Takeuchi et al. 2007). After initiation, unfolding and degradation of the substrate happens processively and bi-directionally from the initiation site (C. Lee et al. 2001; Piwko & Jentsch 2006).

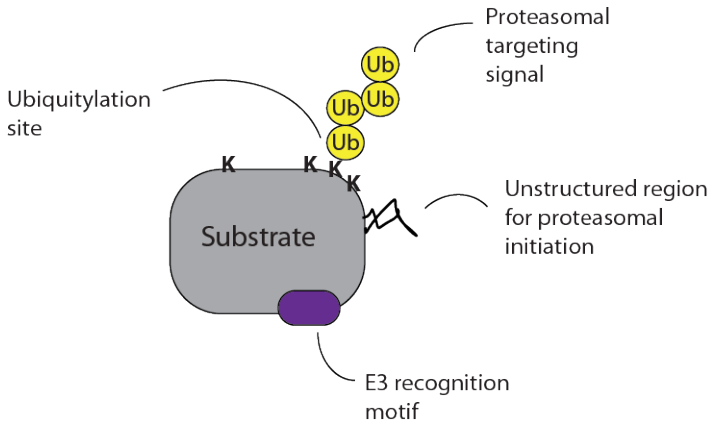

Figure 1.6. General requirements for proteasomal degradation.
The tripartite degradation signal (Guharoy et al. 2016) consists of an E3 ubiquitin ligase recognition motif, proteasomal targeting signal (usually K48 ubiquitin chains), and an unstructured region within the protein in proximity to the targeting signal, where the proteasome can initiate.

The length requirement for a disordered sequence to act as an initiation signal has been estimated to be around 30 amino acids and it also needs to be separated in space from the proteasome-targeting signal (Inobe et al. 2011). When an unstructured region is not naturally present in the protein, in some cases ubiquitylation can induce the formation of such a region on the substrate (Hagai & Levy 2010). It has also been demonstrated that the ubiquitin tag and the unstructured initiation sequence can act in *trans*, with the component carrying the unstructured region being the one degraded (Prakash et al. 2008). The proteasome degradation signal has been recently proposed to be tripartite, thus simultaneously ensuring the diversity and specificity of substrates. The tri-partite signal is composed of a peptide motif required for the substrate recognition by E3 ligase, a

secondary site with ubiquitylatable lysines, and finally a structurally disordered initiation site for the proteasome (Guharoy et al. 2016) (Figure 1.6).

Nevertheless, there are examples of proteins degraded by the proteasome in a ubiquitin-independent manner. In such cases, a ubiquitin signal is replaced by a different factor that can target the substrate to the proteasome. The best-described example of ubiquitin-independent proteasomal degradation is ornithine decarboxylase (ODC) (Y. Murakami et al. 1992). Here, another protein, antizyme (AZ), is required to direct it for degradation. AZ interacts with ODC and acts to target it to the proteasome while also inducing a conformation change in ODC, exposing its C-terminal degradation signal (M Zhang et al. 2003). AZ alone is not recognised by the proteasome, but AZ-ODC complex has the same binding site on the proteasome as ubiquitylated proteins (M Zhang et al. 2003).

As discussed above, canonical protein degradation by the proteasome requires the substrate to be targeted to the proteasome, usually by a poly-ubiquitin signal, which is recognised by ubiquitin receptors, typically on the regulatory particle, and an unstructured region where the proteasome can initiate. Ubiquitin is removed and recycled prior to substrate degradation, and ATP is needed for the translocation-coupled unfolding of the protein so that it can pass through the gate into the proteasome degradation chamber.

1.2.2.3 Regulation of proteasomal degradation

Although a lot of protein degradation control happens at the level of targeting only the correct substrates to the proteasome, the function of the proteasome can also be controlled globally. A conserved ubiquitin ligase Hul5 was found to be associated with the proteasome under proteasome-stress conditions and be able to both ubiquitylate proteasome substrates to aid their degradation (Crosas et al. 2006) and modify the proteasome itself, altering its activity (Besche et al. 2014; Jacobson et al. 2014).

Another layer of proteasome activity regulation in yeast comes through enhanced levels of transcription. A negative feedback loop exists involving the Rpn4 protein, which acts a constitutive substrate for the proteasome and also regulates transcription of all proteasomal subunits (Xie & Varshavsky 2001). When the proteasome is unable to degrade Rpn4 efficiently, its elevated levels thus promote increased synthesis of new proteasome subunits.

1.2.3 Partial proteasomal processing

Apart from its main function in complete degradation of the substrate, the proteasome also plays an exciting role in the regulation of protein activity. Such regulation is achieved via partial proteasomal processing, where a substrate is not completely degraded and where the released protein fragment has a different activity from the full-length protein. This type of regulation has been described for only a handful of proteins. Mammalian transcription factor NF-κB subunits p50 and p52 come from precursors p105 and p100, respectively (Fan & Maniatis 1991; Palombella et al. 1994; Heusch et al. 1999). Yeast transcription factors Spt23 and Mga2 (distantly related to NF-κB) also undergo activation by partial proteasomal processing (Hoppe et al. 2000). The same is true for an unrelated transcription factor Cubitus interruptus (Ci) in *Drosophila melanogaster* (Aza-Blanc et al. 1997; C. H. Chen et al. 1999; Tian et al. 2005) and its vertebrate homologues Gli2 and Gli3 (B. Wang et al. 2000; Pan & B. Wang 2007; Pan et al. 2006), the yeast RNA polymerase II (RNAPII) degradation factor, Def1 (Wilson, Harreman, Taschner, et al. 2013), and another yeast transcription factor, Sp1 (Su et al. 1999) (Figure 1.7 A).

For the processing of p105 that leads to the formation of NF-κB subunit p50, the N-terminal Rel homology domain (RHD), required for dimerization and transcription factor activity, and the following glycine-rich region (GRR) are important (Orian et al. 1999; Moorthy et al. 2006). The proteasome degrades the C-terminal portion of the protein, which normally acts as an inhibitor by binding the N-terminal nuclear localisation signal and preventing the protein from being imported into the nucleus, while the N-terminus is protected from proteasomal degradation by the GRR (Lin & S. Ghosh 1996). The generation of NF-κB subunit p52 is thought to follow a similar mechanism (Heusch et al. 1999). Ubiquitylation is also required for these

processing reactions, with mono-ubiquitylation being sufficient as a signal (Kravtsova-Ivantsiv et al. 2009). Interestingly, the p105 protein expressed in yeast also becomes processed (Palombella et al. 1994; Kravtsova-Ivantsiv et al. 2009), arguing for a conserved mechanism for partial proteasomal processing, and suggesting that all the key signals for the processing reaction are, at least in this case, likely to be present in protein sequence and structure.

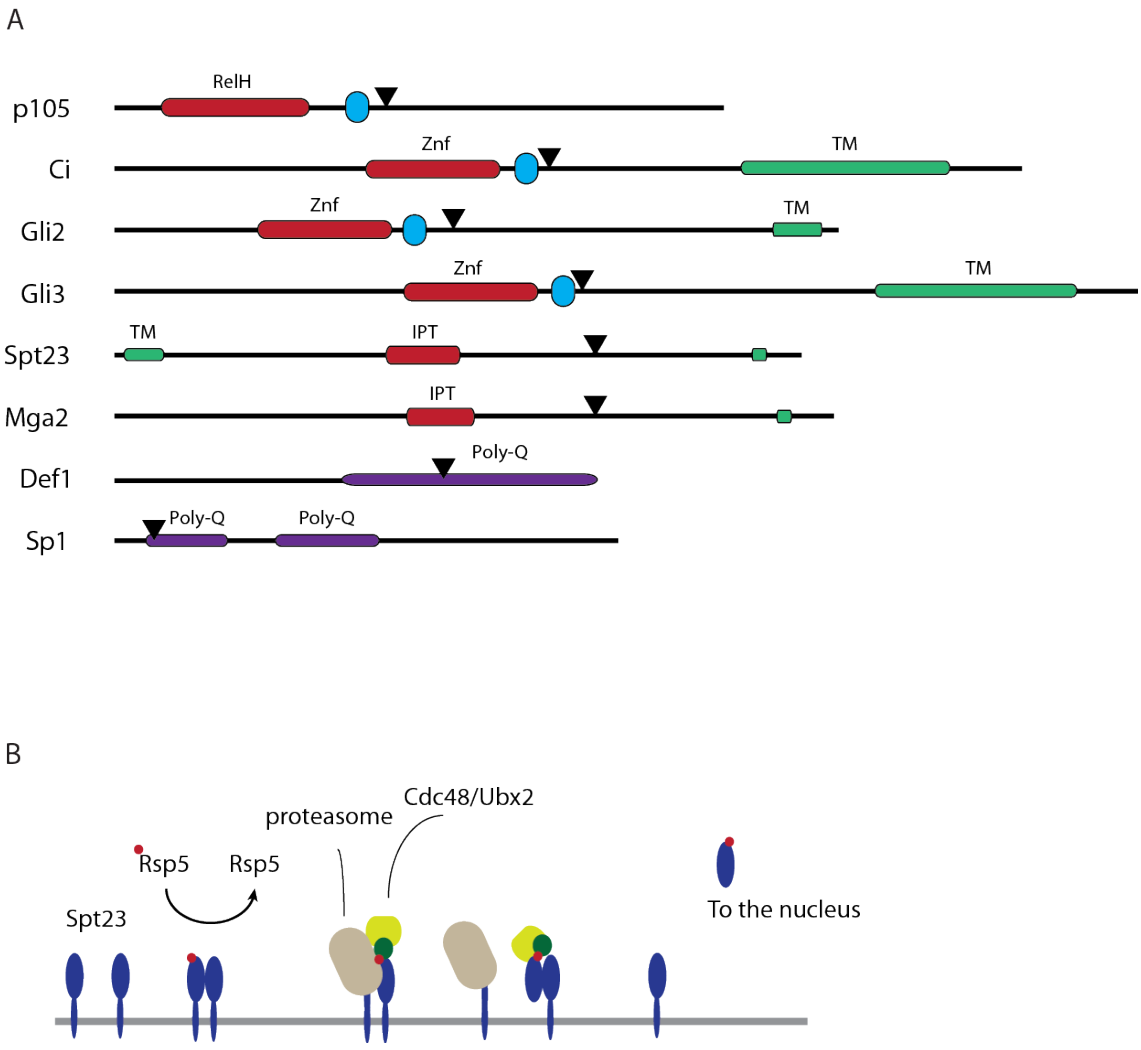

Figure 1.7. Partial proteasomal processing.
A – Examples of proteins susceptible to partial proteasomal processing, with the highlighted structural elements important for the reaction. Triangle marks the processing site, although it might be dynamic. Red – tightly folded domain or dimerization domain: Rel homology domain in p105, Zn finger domain in Ci, Gli2, and Gli3, IPT domain in Spt23 and Mga2; blue – glycine rich region (GRR) or low complexity region; green – transmembrane domains; purple – glutamine-rich regions. ***B*** – A schematic representation of Spt23 partial proteasomal processing. Spt23 – blue, ubiquitin – red, the proteasome – beige, Cdc48-Ufd1-Npl4 complex light green, Ubx2 –

dark green. Mono-ubiquitylation of Spt23 by Rsp5 is followed by partial proteasomal processing, potentially stimulated by Cdc48. After the cleavage step is complete Cdc48 with its cofactors play a role in dissolution of a reaction intermediate where the processed form of Spt23 is still associated with membrane-bound full-length form.

Ci, as well as the Gli2 and Gli3 proteins, are part of hedgehog (Hh) signalling pathway (B. Wang et al. 2000). In the presence of Hh signalling, Ci is in a full-length, activated state, however if the signal is absent, the C-terminal transactivation domain is degraded by the proteasome, leaving the N-terminus of the protein, which acts as a transcriptional repressor (Aza-Blanc et al. 1997). The processing determinant domain (PDD) enriched in asparagine, serine, and glutamine residues, and the strongly folded Zn finger domains, are both required for processing (Tian et al. 2005). Gli3 is processed in a similar way to Ci, while Gli2 is processed to a much smaller extent (Pan & B. Wang 2007). In the same manner as Ci, PDD is required for the processing of Gli3 (Pan & B. Wang 2007); however, a ubiquitylation site in proximity to the PDD is also required, with the position of the ubiquitylation site playing a critical role in processing (Schrader et al. 2011).

Mechanistic studies of the proteasome showed that it can initiate degradation on a circular substrate and that at least two polypeptide chains can fit through the channel (C. Lee et al. 2002; C.-W. Liu et al. 2003). The current model for partial proteasomal processing, based on limited biochemical data, suggests a two-step mechanism – proteasome cleavage initiated at an internal site and bi-directional degradation up to a stop site (Piwko & Jentsch 2006). The model is based on the observation that partial proteasomal processing requires an unstructured region of 20-30 amino acids in proximity to a tightly-folded domain (Tian et al. 2005; Piwko & Jentsch 2006). Additionally, a glycine-rich region in NF-κB was demonstrated to play an important role in halting the degradation and facilitating the release of processed product (Orian et al. 1999). As an exception to the rule, Sp1 seems to be lacking a clear stop-signal (Figure 1.7 A), but its glutamine-rich regions may act to reduce proteasome processivity (Kraut et al. 2012).

Two models can explain the requirement for low complexity sequence, such as the glycine-rich region in NF-κB. One possibility is that low complexity regions can slip out of the proteasome pore due to the lack of interactions with the pore loops in the

proteasome, facilitating release; while another model proposes that low complexity sequences poorly transduce the pulling force generated by the proteasome to the substrate and thus are 'slippery' (Nassif et al. 2014). The analysis of the effect that glycine-alanine repeats have on proteasomal processing suggested that these repeats make the coupling between nucleotide hydrolysis and the work performed on the substrate less efficient (Hoyt et al. 2006). Further examination of degradation processivity on a model substrate revealed that a low-complexity sequence is also more likely to prevent the proteasome from unfolding an adjacent domain, rather than facilitating a faster release (Kraut et al. 2012).

Interestingly, *in vitro* studies demonstrated that two strongly-folded domains can protect each other from degradation by the proteasome without directly interacting with each other, simply by competing for proteasome's unfolding activity (Kraut & Matouschek 2011). This model has been suggested to be applicable to Spt23 processing, since Spt23 lacks an obvious 'slippery' low complexity sequence that might facilitate release from the proteasome (Nassif et al. 2014). However, it has also been suggested that the IPT dimerisation domain plays a role as a stop signal in Spt23 (Rape et al. 2001), and that the 'slippery sequence' is not required for partial proteasomal processing in yeast due to a lower processivity of yeast proteasomes (Kraut et al. 2012).

Another interesting mechanistic observation is that for partial proteasomal processing, mono-ubiquitylation of a substrate is enough to target it to the proteasome (Rape et al. 2001; Kravtsova-Ivantsiv et al. 2009), while degradation usually requires poly-ubiquitin chains. This raises an interesting question of whether there are distinct binding sites on the proteasome for mono- and poly-ubiquitylated substrates and if additional factors play a role in partial proteasomal processing by recognising the mono-ubiquitin signal and delivering the substrate to the proteasome.

In the case of Spt23 processing, other factors, apart from the proteasome, have been implicated in the reaction (Figure 1.7 B). Spt23 is an ER-membrane-bound transcription factor, involved in the regulation of the OLE (oleic acid) pathway in yeast, which controls membrane fluidity (S Zhang et al. 1999; Hoppe et al. 2000).

The activation of Spt23 (synthesised as a precursor, p150) was found to be proteasome-dependent and require ubiquitylation by Rsp5 ubiquitin ligase, resulting in the release of an N-terminal 90 kDa fragment (p90), that can travel to the nucleus to perform its function as a transcription factor (Hoppe et al. 2000; Shcherbik et al. 2004). Subsequently, mutations in *NPL4*, *UFD1*, and *CDC48* were shown to perturb the processing of Spt23 (Hitchcock et al. 2001). Indeed, the role of Cdc48 was proposed to be the dissolution of the Spt23 processing intermediate, where a processed form of one of the proteins in a dimer is still associated with a full-length p150 partner (Rape et al. 2001). These results were followed by the discovery that the UBX domain protein, Ubx2, which acts as an adaptor for Cdc48 and is found associated with the ER membrane, is required for targeting of Cdc48 to Spt23 (Kolawa et al. 2013). It has also been proposed that Cdc48 is not only required for the resolution of the processing intermediate, but also for the stimulation of the processing by the proteasome (Kolawa et al. 2013). Overall, these results demonstrate that the proteasome does not act alone in the partial proteasomal processing of Spt23 – it requires Cdc48 with its accessory factors, such as Npl4, Ufd1, and Ubx2. However, whether Cdc48 is required for the actual processing step or only for the dissolution of p90/p150 dimer, remains elusive.

The discovery that the RNAPII degradation factor Def1 becomes processed by the proteasome started to draw a more general mechanism of protein activation by the proteasome in yeast. It is also worth noting, that unlike other examples of proteins undergoing partial proteasomal processing, Def1 is not a transcription factor. In the manner similar to Spt23, Def1 first has to be ubiquitylated by Rsp5 ubiquitin ligase, and requires a functional proteasome for its processing (Wilson, Harreman, Taschner, et al. 2013). However, unlike Spt23, Def1 is not tethered to a membrane, and the proteasomal processing generates an active form, processed-Def1 (pr-Def1), which lacks a C-terminal nuclear export signal, and thus allows the active form to accumulate in the nucleus, where it can perform its function in the last resort pathway (Wilson, Harreman, Taschner, et al. 2013) (discussed in detail in (1.4.3)). However, whether any additional factors are required for Def1 processing and the location of the processing reaction (nucleus or cytoplasm) remains unclear. It is also not completely understood what is the signal for partial proteasomal processing of Def1.

In summary, partial proteasomal processing seems to require signals that are similar to those involved in proteasomal degradation. First, the proteins have to be targeted to the proteasome and a region where the proteasome can initiate should be present as well. However, an additional feature able to stop the proteasome and release the processed product is essential. A strongly folded domain, or an interaction with a partner protein, seem to be able to fulfil this role. However, there are differences between partial proteasomal processing in yeast and higher eukaryotes – the examples of partial proteasomal processing in yeast lack a low complexity, 'slippery' sequence in proximity to a tightly folded domain. Nevertheless, the discovery of more proteins undergoing partial proteasomal processing both in yeast and mammalian systems could change this view.

1.3 The ubiquitin-dependent segregase, Cdc48

1.3.1 Function of Cdc48

Cdc48 was first discovered in a genetic screen in yeast, as mutations in the *CDC48* gene caused cell cycle arrest (Moir et al. 1982). It is a highly conserved, homohexameric protein. The mammalian homologue of Cdc48 is the p97 protein, named after its molecular weight. Cdc48 belongs to the AAA ATPase family, and is involved in many diverse cellular functions. The human p97 has also been implicated in many diseases, such as cancer, Paget's disease of bone, and several neurodegenerative disorders (Watts et al. 2004; Yamamoto et al. 2004; Barthelme et al. 2015). The findings discussed below come from investigations into both yeast Cdc48 and mammalian p97 due to the fact that they share 65% sequence identity (Pye et al. 2006); not surprisingly, the data so far suggest a very similar mode of action.

Cdc48 is an abundant cellular protein, mostly found in the cytosol, but it has also been reported to associate with endoplasmic reticulum (ER) and Golgi membranes (Acharya et al. 1995; Latterich et al. 1995). A sub-fraction of the protein is also found in the nucleus (Madeo et al. 1998). Cdc48 undergoes many different post-translational modifications in the cell. They have been suggested to regulate the

ATPase activity, adaptor binding, and cellular localisation (Ewens et al. 2010). Cdc48 has been reported to become phosphorylated on serine and threonine residues in response to different signals (Madeo et al. 1998; Livingstone et al. 2005). Mass spectrometry experiments revealed that Cdc48 can also be acetylated (Mori-Konya et al. 2009). Additionally, in mammals, p97 has been reported to be methylated, which results in the inhibition of the ATPase activity (Kernstock et al. 2012; Cloutier et al. 2013). SUMO and ubiquitin modifications have also been detected; however, their effect on Cdc48 remains unclear (Peng et al. 2003; Wohlschlegel et al. 2004).

The best studied functions of Cdc48 include membrane fusion (Latterich et al. 1995) and ER-associated protein degradation (ERAD) (Rabinovich et al. 2002; Jarosch et al. 2002; Braun et al. 2002). As discussed earlier, Cdc48 is also involved in the partial proteasomal processing of the yeast transcription factor Spt23 (1.2.3) (Rape et al. 2001). All Cdc48 functions seem to be linked to ubiquitin signalling. Cdc48 has been demonstrated to bind ubiquitin (Meyer 2002) to extract proteins from protein complexes, binding partners, and from chromatin (Rape et al. 2001; Verma et al. 2011; Maric et al. 2014), hence the functional term ‘segregase’ is often used to describe it. The segregation of proteins is achieved by translating ATP hydrolysis into mechanical force, resulting in conformational change and rotation in Cdc48 (Rouiller et al. 2002).

However, segregation is not the only function of Cdc48. It has also been reported to regulate the extent of ubiquitylation of bound substrates. Such regulation is achieved via the interaction with a set of ubiquitin-editing co-factors, such as the ubiquitin chain extender E4 enzyme Ufd2, a ubiquitin-binding factor Ufd3, and Otu1 deubiquitylase (Richly et al. 2005; Rumpf & Jentsch 2006). Being involved in the extension of ubiquitin chains, prevention of further ubiquitylation, and de-ubiquitylation of bound substrates, Cdc48 has been proposed to act as a ‘gearbox’, controlling the fate of its substrates, by going ‘forward’ with further ubiquitylation, ‘neutral’ with prevention of further ubiquitylation, and ‘reverse’ with de-ubiquitylation activities (Jentsch & Rumpf 2007).

Support for the 'molecular gearbox' model comes from the dual role Cdc48 plays in the Spt23 pathway. Together with Ufd1–Npl4 and Ubx2 it is required for freeing the active p90 form of Spt23 from the p150 precursor (1.2.3). However, in a separate investigation Cdc48 was also shown to function with Ufd2 and Rad23 in the degradation of p90 (Richly et al. 2005). Ufd2 plays an important role in this case by extending the ubiquitin chain of the substrate and handing the substrate directly to the proteasome shuttle co-factor Rad23 (Koegl et al. 1999; I. Kim et al. 2004). In this case, the role of Cdc48 in editing the ubiquitin chain completely changes the fate of the substrate. However, it is not clear what leads to these different outcomes upon the substrate interaction with Cdc48.

1.3.2 Structure of Cdc48

Cdc48 has two ATPase domains – D1 and D2, connected by a short linker, and an N-terminal domain, often referred to as the N-domain (Figure 1.8). The structure of Cdc48 and its correlation with the nucleotide binding states has not been investigated in detail, and most results in this field come from studies of mammalian p97. However, due to the high sequence identity, the mechanisms of action of the two proteins are expected to be similar.

The D1 and D2 domains are formed by six protomers coming together in a barrel-like structure. ATP binding to the D1 domain promotes hexamerisation (Baek et al. 2013). Conformational changes in the protomers can result in open and closed conformations of the D1 and D2 domains (Pye et al. 2006). D1 and D2 rings are arranged in a head-to-tail manner, with the D1 ring being more stable than the D2. Hence, it has been suggested that it is the D2 ring undergoing major structural changes during the ATPase cycle (Q. Wang et al. 2003). However, further studies have suggested an interprotomer motion-transmission model stating that the nucleotide-dependent motion is transmitted between the two ATPase domains of one protomer with the help of a neighbouring protomer and finally results in the changes in the N-terminal domain (G. Li et al. 2012; C. Huang et al. 2012).

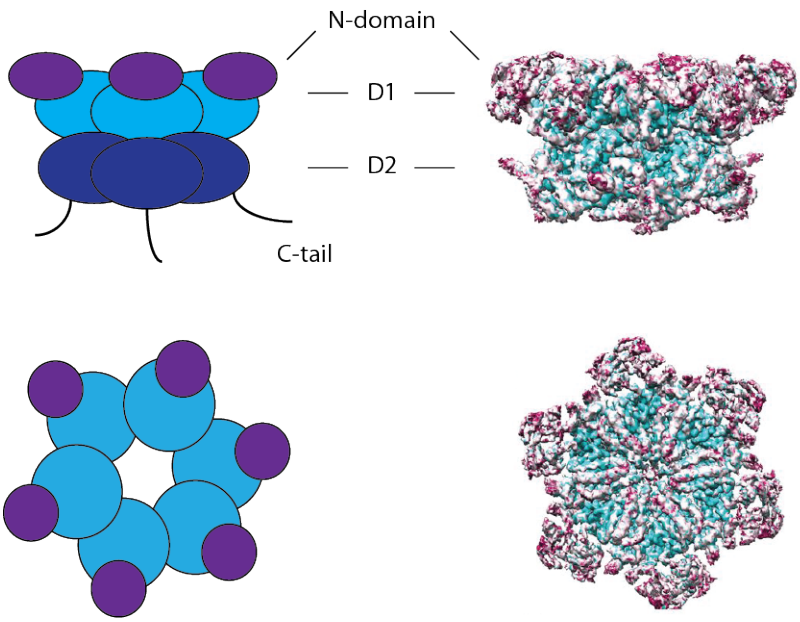

Figure 1.8. The structure of Cdc48/p97.
(left) schematic representation of the structure, side view – top, top view – bottom. D1 ring – light blue, D2 ring – dark blue, N-domain – purple. (right) Cryo-EM structure of human p97 (pdb 5FTK (Banerjee et al. 2016)), the structure is coloured according to the resolution from cyan (2 Å) to magenta (6 Å).

The D2 ring is thought to be the domain responsible for the major ATPase activity, since the mutations in D2 significantly inhibit the ATPase activity, but the equivalent mutations in D1 have a lesser effect in *in vitro* assays (Song et al. 2003). However, a separate study suggested that both D1 and D2 participate in ATP hydrolysis and that the ATP hydrolysis cycles are alternating between the two domains (Yihong Ye et al. 2003). It is worth noting that different assays and protein mutants were used in the conflicting studies. The discrepancy remains unresolved. Nevertheless, cryo-EM studies of p97 suggest negative cooperativity between the ATPase rings, such that ATP hydrolysis can happen in only one ring at a time (Beuron et al. 2006). Interestingly, a positive cooperativity between ATPase domains has been suggested for Cdc48 in biochemical assays (Fröhlich et al. 1995) as well as a p97 homolog of *Caenorhabditis elegans* (Nishikori et al. 2011). Despite the unresolved issue over the major ATPase activity contributor, it is clear that for the function *in vivo*, the ATPase activity of both D1 and D2 domains is needed (Esaki & Ogura 2010).

The question of whether during substrate unfolding by Cdc48, substrates thread through the Cdc48 pore also remains unsolved. Substrate threading through the middle pore has been suggested to be an unlikely scenario, as the D2 ring is wider, but the D1 ring is relatively narrow with histidine residues constricting the pore (DeLaBarre et al. 2006). Both ATPase domains go through motion upon the ATPase cycle and structurally locking them has detrimental effects for the cell (DeLaBarre & Brunger 2005; Esaki & Ogura 2010). However, the D2 domain is thought to generate the driving force in substrate unfolding, since the D2 mutants defective in ATP binding or hydrolysis seem to be able to bind the substrates, but are defective in their release (Pye et al. 2006; DeLaBarre & Brunger 2005). On the other hand, the association between the 20S proteasome and Cdc48 in archaea (Barthelme & Sauer 2012; Barthelme et al. 2014) points to the possibility that Cdc48 is able to thread a peptide through the central pore. Molecular dynamics simulations of this process suggest that less work is required for the translocation of substrate from the D1 towards the D2 compartment than in the opposite direction (Tonddast-Navaei & Stan 2013), in agreement with the assembly architecture of the archaeal 20S-Cdc48 proteasome (Barthelme et al. 2014).

The insights into the structural requirements for proteasomal degradation support the hypothesis that complete unfolding of a substrate by Cdc48 is unnecessary, since an unstructured region of around 30 amino acids is sufficient as an initiation site for proteasomal degradation (Tian et al. 2005; Piwko & Jentsch 2006; Verhoef et al. 2009). It has been demonstrated that the addition of an unstructured region can convert a substrate from requiring Cdc48 for degradation, to being degraded in a Cdc48-independent manner (Beskow et al. 2009).

The N-domain residing at the periphery of D1 is the least conserved part of Cdc48 (Q. Wang et al. 2004). It was demonstrated to bind ubiquitylated substrates in *in vitro* studies; however, this binding is dependent on the nucleotide state and is not observed in the presence of ADP (Rape et al. 2001; Dai & C. C. Li 2001). The N-domain is also responsible for the interaction with adaptor proteins (discussed in detail in the next section (1.3.3)), such as Ubx1 (also known as Shp1 in yeast, or p47 in mammals) and Ufd1-Npl4 (Meyer 2002). Additionally, the N-terminal domain was suggested to have a putative motif recognising SUMO (Hannich et al. 2005).

However, it is not known whether the N-domain is able to bind both co-factors and ubiquitylated proteins simultaneously. Cryo-EM studies also showed that the N-domain is not necessary for hexamerisation or ATP-hydrolsis, but it is responsive to the ATPase cycles, being flexible in different nucleotide states apart from the ATP hydrolysis step (Rouiller et al. 2002).

The C-terminal tail of Cdc48 is highly disordered and has not been visualised by EM or crystallography (Q. Wang et al. 2004). It is also highly flexible and susceptible to trypsin digestion (Q. Wang et al. 2003). The C-terminus of Cdc48 carries a phosphorylation site, regulating the nuclear import of the protein. Phosphorylation leads to a structural change and the exposure of a nuclear import signal (Madeo et al. 1998). The C-terminal tail may also modulate the ATPase activity via protein-protein interactions or further post-translational modifications (Baek et al. 2013).

1.3.3 Cdc48 co-factors

It is widely believed that the Cdc48 co-factors (also known as adaptors) specifically target Cdc48 to various pathways and substrates. Most co-factors interact with Cdc48 via one or more of the several defined motifs. The N-domain binding domains are the UBX (ubiquitin regulatory X) domain, UBX-like domain, SHP box (also known as Binding Site 1), VCP binding motif (VBM), and VCP interacting motif (VIM), while the C-tail binding domains are the PUB (PNGase/UBA or UBX) and PUL (PLAA, Ufd3, and Lub1) domains (Stolz et al. 2011). PUB, VIM and VBM domains are only present in higher eukaryotes (Yeung et al. 2008). Some of the co-factors have overlapping binding sites on Cdc48, creating exclusive and hierarchical interactions.

1.3.3.1 The UBX domain proteins

The UBX domain is an 80-residue domain forming a hydrophobic interaction with Cdc48 and is a close structural homologue to ubiquitin (Buchberger et al. 2001; Dreveny et al. 2004) (Figure 1.9 A). However, UBX domains have a conserved

arginine residue and a conserved phenylalanine-proline-arginine (FPR) sequence, which is specific to the UBX domains and is not found in ubiquitin or other ubiquitin-like proteins (Buchberger et al. 2001). Cdc48 binds UBX domains stronger than ubiquitin itself. Structural studies of p97 in complex with p47 (human homologue of yeast Ubx1 protein) revealed that the FPR motif is important for the p47-p97 interaction and that the UBX domain in p47 interacts with the N-domain of p97, binding at the interface of two subdomains (Dreveny et al. 2004).

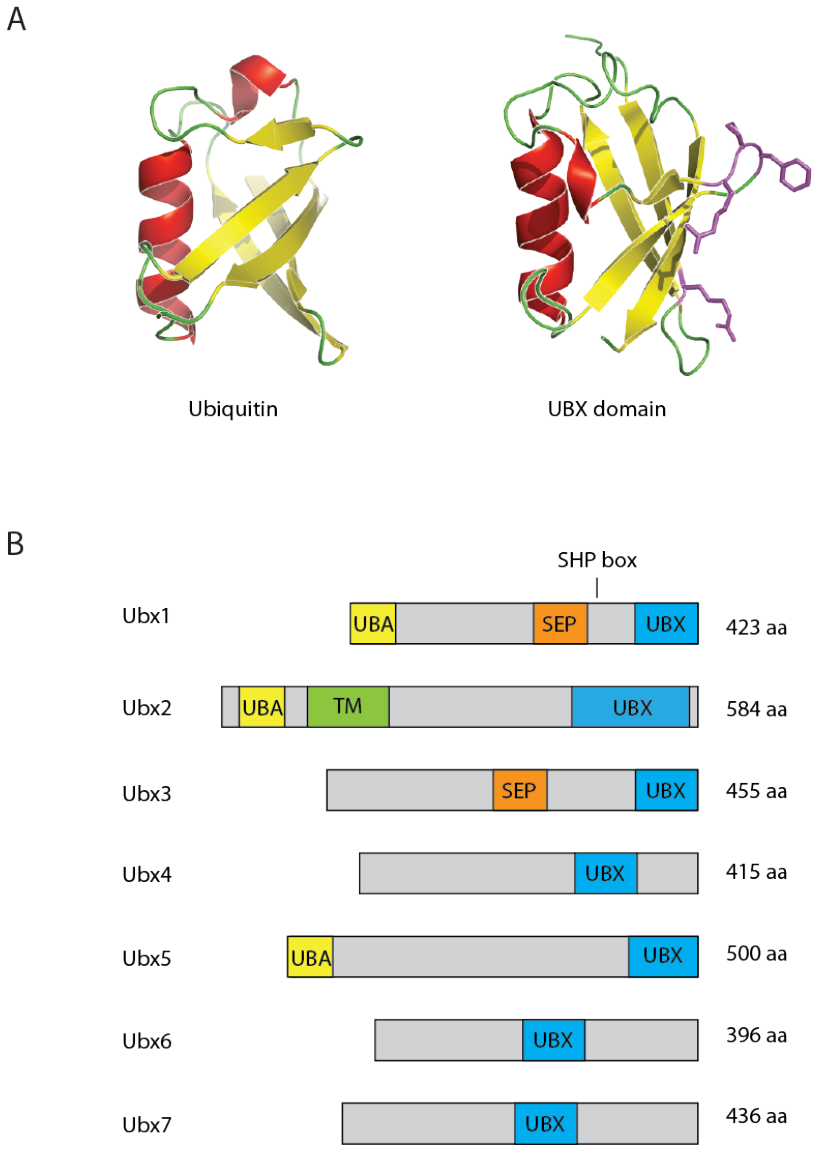

Figure 1.9. The UBX domain.
A – the comparison between ubiquitin structure (left) and the UBX domain from human FAF1 protein (pdb 3QX1), with the unique R…FPR feature highlighted in magenta. ***B*** – All UBX containing proteins in *S. cerevisiae.* All of them carry a UBX domain (blue), some also have a ubiquitin-binding UBA domain (yellow), transmembrane domain

(green) and SEP domain (orange). In addition, Ubx1 also carries an additional Cdc48-interacting motif – SHP box.

In *S. cerevisiae,* there are seven proteins containing a UBX domain – Ubx1 (Shp1) and Ubx2 to Ubx7 (Figure 1.9 B). Some of these also contain ubiquitin-binding UBA domains in addition to the UBX domain, aiding their function as substrate-recruiting co-factors (Schuberth et al. 2004). Apart from the UBX and UBA domains, Ubx1 also carries an additional Cdc48 binding domain – a SHP box (Sato & Hampton 2006). As has been demonstrated with mammalian proteins, the SHP box is always found upstream of the UBX domain and binds p97 in the area overlapping with UBX binding (Isaacson et al. 2007). This observation suggests that Ubx1 can have several different Cdc48 binding modes.

1.3.3.2 Substrate recruiting and substrate modifying co-factors

Functionally, Cdc48 co-factors can be subdivided into two groups – substrate recruiting and substrate modifying co-factors. Substrate recruiting co-factors usually have both substrate- and Cdc48-interacting domains. Ubx1, Ubx2, and Ubx5 proteins are able to carry out this function due to their N-terminal UBA and C-terminal UBX domains (Schuberth et al. 2004). Indeed, as mentioned earlier (1.2.3), Ubx2 was implicated in targeting Cdc48 to process Spt23 (Kolawa et al. 2013), and, as will be discussed later (1.4.3.4), Ubx5 plays a role in the removal of RNAPII arrested at a DNA lesion (Verma et al. 2011). However, unlike Ubx1, Ubx5 and Ubx2 are considered to be co-adaptors, being compatible with Cdc48 interacting with the Ufd1-Npl4 heterodimer (Schuberth & Buchberger 2008) and indeed only being able to stably associate with Cdc48 in the presence of Udf1-Npl4, as demonstrated with the mammalian counterpart proteins (Hänzelmann et al. 2011).

The major substrate-recruiting Cdc48 co-factors exhibit mutually exclusive binding – Cdc48 cannot bind Ubx1 and Ufd1-Npl4 simultaneously (Meyer et al. 2000). This might suggest different cellular functions or molecular activities for the respective complexes. Npl4 associates with Cdc48 via a UBX-like ubiquitin fold domain (Bruderer et al. 2004), while Ufd1 carries a SHP box. Only one Ufd1-Npl4 heterodimer associates with a p97 hexamer, binding two adjacent protomers (Pye et al. 2007), while different stoichiometries were reported for Ubx1 binding – either

6 or 3 Ubx1 molecules were reported to associate with one Cdc48 hexamer (Kondo et al. 1997; Beuron et al. 2006; Rouiller et al. 2000), most likely due to experimental differences.

The second functional group of Cdc48 co-factors is substrate-processing co-factors, comprised of very diverse members. A well-characterised example is the Ufd2 E4 ubiquitin chain elongator. It has been shown to associate with the C-tail of Cdc48 and elongate the ubiquitin chain of substrates recruited to Cdc48 by the Ufd1-Npl4 complex (Koegl et al. 1999). Additionally, Ufd2 is able to associate with Rad23 and Dsk2 (proteasome shuttle factors) and aid the transfer of substrates from Cdc48 to the proteasome (Richly et al. 2005). Ufd2 also shares its binding site on Cdc48 with Ufd3 protein, which is thought to regulate Ufd2 activity by blocking its association with Cdc48 (Rumpf & Jentsch 2006). Interestingly, the homologues of Ufd2 from higher eukaryotes interact with the N-domain of p97 via a VBM motif instead, showing a divergent evolutionary pathway (Boeddrich et al. 2006; Morreale et al. 2009).

Another example of substrate processing adaptor is a deubiquitylase, Otu1. Otu1 interacts with Cdc48 via a UBX-like domain and cleaves K48 ubiquitin chains (Rumpf & Jentsch 2006). Otu1 has been shown to be able to associate with Cdc48 at the same time as Ufd3, the inhibitor of Ufd2 ubiquitin chain extension activity (Rumpf & Jentsch 2006). This switch in co-factors completely changes the outcome of substrates interacting with Cdc48. Interestingly, there also seems to be a functional bias in co-factor association with Cdc48, where substrate-recruiting co-factors are more likely to interact with the N-terminus of the protein, and substrate-processing co-factors bind Cdc48 at the C-terminus (Madsen et al. 2009), directing different substrates to different fates.

How the co-factors affect Cdc48 ATPase activity has not been studied extensively. Co-factors binding the N-domain are more likely to have an effect on the ATPase activity, since motions in the N-domain were observed during the ATPase cycle (Rouiller et al. 2002). Indeed, binding of p47 to the N-domain has been shown to result in the decrease in the ring diameter of p97 (Kondo et al. 1997) and decrease its ATPase activity (Meyer et al. 1998). Later studies suggested that p47 is able to

both increase and decrease the ATPase activity of p97, depending on the concentration and, presumably, binding stoichiometry (Xiaoyi Zhang et al. 2015). An interesting possibility would be that p47/Ubx1 binding via UBX domain and SHP box leads to different functional outcomes.

1.4 The interface between transcription and DNA damage

1.4.1 Transcription

Transcription is a fundamental cellular process, allowing information to flow from DNA via RNA to proteins. Transcription is also a highly regulated process, catalysed by DNA-dependent RNA polymerase complexes. In eukaryotes, there are three RNA polymerases: RNA polymerase I is responsible for ribosomal RNA (rRNA) production, RNA polymerase II (RNAPII) is responsible for messenger RNA (mRNA) production, while RNA polymerase III produces transfer RNAs (tRNAs). RNAPII is responsible for the bulk transcription in the cell and it will be discussed in more detail.

RNAPII is a 550 kDA complex formed of 12 subunits, Rpb1 to Rpb12. Many structural and biochemical studies helped to define both the structure and mechanism of RNAPII. X-ray crystallography structures were obtained of both the enzyme alone (Cramer et al. 2001; Bushnell & Kornberg 2003; Armache et al. 2003) and the transcription complex (Gnatt et al. 2001), as well the more recent cryo-EM studies revealed the structure of transcription pre-initiation complex (K. Murakami et al. 2013), all giving mechanistic insight into transcription. Generally, RNAPII is subdivided into four mobile elements - Core, Clamp, Shelf, and Jaw Lobe. The Core is comprised of Rpb3, 10, 11, 12 and the active centre formed by regions of Rpb1 and Rpb2 (Gnatt et al. 2001). A cleft, which is formed by all four elements, directs the incoming DNA into the buried active site (Figure 1.10) and is operated by the Clamp to form open and closed conformations (Gnatt et al. 2001). The DNA duplex is unwound upstream of the active site and the non-transcribed strand (NTS) is found on the outside of the complex (Gnatt et al. 2001). DNA-RNA hybrid formed during transcription is melted by a loop termed Lid, acting as a wedge and directing RNA strand towards a separate exit channel, while Rudder

prevents the association between DNA and RNA strands by forming an interaction with the DNA strand (see Figure 1.10) (Gnatt et al. 2001).

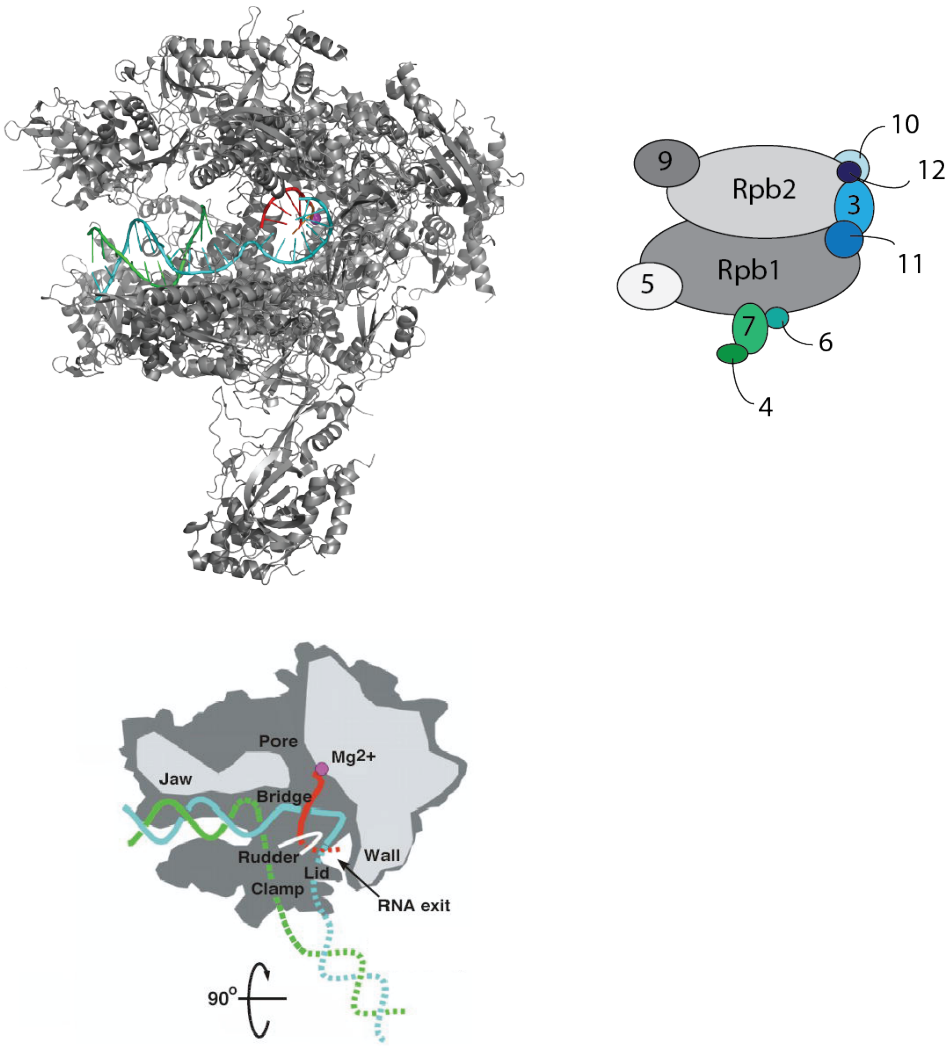

Figure 1.10. The structure of RNAPII complex.
Top left – the structure of the RNAPII elongation complex (pdb 4A3F (Cheung & Cramer 2011)): RNAPII complex is grey, TS – cyan, NTS – green, RNA – red, catalytic Mg ion – magenta. Top right – schematic representation of RNAPII subunits, the Rpb8 subunit is not visible, since it is behind the complex. Bottom – schematic representation of mRNA synthesis highlighting the structural elements. Colouring the same as top. Adapted from (Hahn 2004).

A ratchet mechanism has been proposed for the movement of the polymerase – RNAPII is thought to fluctuate between the pre- and post-translocated states, until a nucleotide comes in, binds in the active site and locks it in the post-translocated state (Bar-Nahum et al. 2005). Then the forward movement is generated by a conformational change in the flexible Bridge helix, which can bend and straighten

to push the polymerase. In this way, the incoming nucleotide and the flexible Bridge element above the active site act as two ratchet devices promoting forward transcription (Bar-Nahum et al. 2005). An important consequence of this model is that RNAPII can not only move forwards, but also backtrack.

The transcription process can be subdivided into three stages – initiation, elongation, and termination. The initiation stage is the most regulated one in the process, since a plethora of activators and repressors play a role in transcription initiation, while RNAPII termination is coupled to the processing of newly synthesised pre-mRNA (Richard & Manley 2009; X. Liu et al. 2013). However, for the purpose of this thesis, transcription elongation and transcription stalling are discussed in greater detail.

1.4.1.1 Transcription elongation and pausing

During transcription elongation the polymerase is thought to move by diffusion (Brownian motion) between a pre-translocation state, where a nucleotide has been added to the mRNA chain, a post-translocation state, in which the polymerase has shifted forward by a single nucleotide, and a backtracked state, when the polymerase has moved one or several nucleotides backwards extruding the newly synthesised RNA chain from the active site (X. Liu et al. 2013) (Figure 1.11). This mechanism requires and allows quality control and removal of incorrectly inserted nucleotides, and involves great processivity. RNA polymerase is able to cover large genes – the human dystrophin gene is 2.3 Mbp long and has to be transcribed in one go (Tennyson et al. 1995). In contrast to DNA polymerases making long DNA-DNA hybrids, the DNA-RNA hybrid is only 8-9 nucleotides long, meaning that if RNAPII elongation complex dissociates, the RNA product is lost. However, even though RNAPII does not let go of the DNA strand during transcription, it is not a continuous process and the polymerase is prone to stalling and pausing.

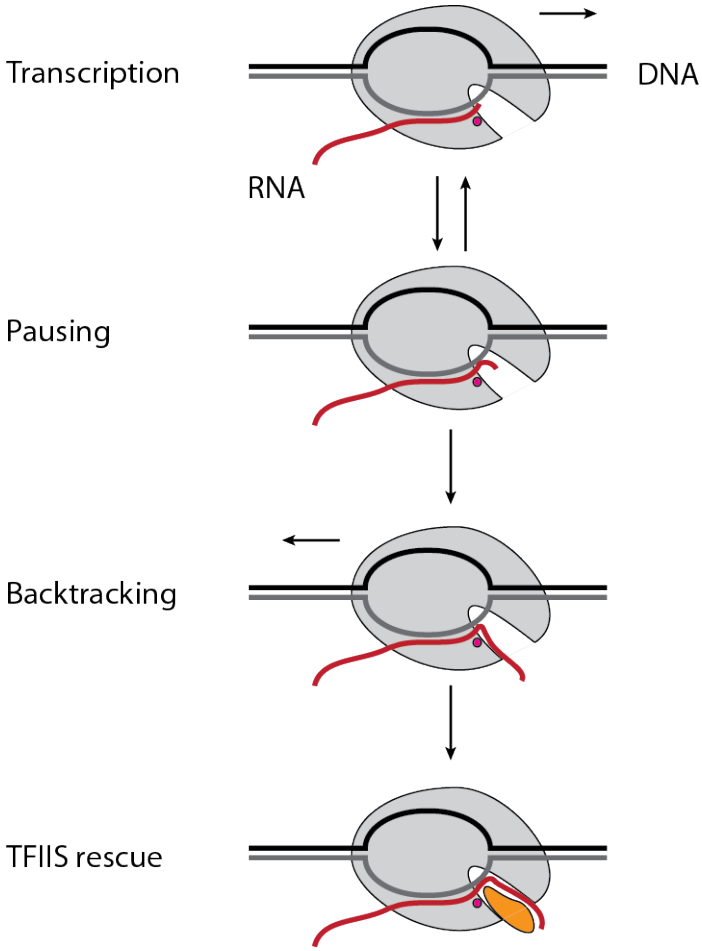

Figure 1.11. RNAPII backtracking.
A schematic representation of RNAPII backtracking. RNA – red, TS – dark grey, NTS – black, RNAPII complex – light grey, TFIIS – orange, catalytic Mg ion – magenta. When the polymerase backtracks, the newly synthesised RNA strand is displaced from the active site and expelled from the complex. TFIIS stimulates the cleavage of displaced RNA and helps to re-align it in the active site for further addition of nucleotides.

Stalling and pausing of the polymerase has been observed both by early footprinting experiments and more recent single molecule studies (Krummel & Chamberlin 1992; Chubb et al. 2006; Galburt et al. 2007; Larson et al. 2012). Certain DNA regions might be harder to transcribe than others, contributing to the pausing of the polymerase – it has been suggested that weak RNA-DNA hybrid formation directly leads to backtracking (Nudler et al. 1997). Sequences rich in guanine and able to form G4 DNA have also been shown to interfere with transcription *in vitro* if present on the non-transcribed strand (Tornaletti et al. 2008). Moreover, a plethora of other factors and circumstance, including topological constraints, nucleosomes, and DNA damage have been reported to cause RNAPII

stalling or arrest (García-Rubio & Aguilera 2012). The effect of RNA polymerase pausing in bacteria can sometimes be overcome by strong promoters, which result in more molecules travelling on the gene (Epshtein & Nudler 2003). The same is true for eukaryotes with two different processes contributing to this effect – de-chromatisation of the template (Bintu et al. 2011) and trailing polymerases being able to help by pushing a paused, leading polymerase complex (Saeki & Svejstrup 2009).

Experiments monitoring transcription at nucleotide resolution in *S. cerevisiae* revealed that pausing is common *in vivo* and implicated nucleosomes in the process (Churchman & Weissman 2011). Interestingly, transcription rates reported *in vivo* and *in vitro* on a naked DNA template do not differ significantly (Singh & Padgett 2009; Izban & Luse 1992a), even though *in vitro* nucleosomes significantly inhibit transcription and promote backtracking (Orphanides et al. 1998; Kireeva et al. 2005). Generally, RNAPII is though to first pause if the forward movement is blocked, then backtrack by extruding 8 nucleotides of newly synthesised RNA from the active site to a conserved backtrack site and become arrested in this position due to the trapping of the active site trigger loop (Cheung & Cramer 2011). As mentioned earlier, a backtracked RNAPII can be rescued by the action of TFIIS (Figure 1.11).

Some single molecule studies suggested that transcription (not RNAPII) pausing observed in experiments are likely to be generated by the polymerase backtracking on the template (Galburt et al. 2007; Depken et al. 2009). An alternative view also exists proposing that pausing might be caused by many different mechanisms, including regulatory pausing (J. Zhou et al. 2013). In bacteria, a certain type of sequence-specific pauses that are not backtracked have been identified and termed non-ubiquitous pausing (Neuman et al. 2003; Herbert et al. 2006). Even if pausing does not involve backtracking, upon a prolonged pause the polymerase may become persistently arrested (Gu & Reines 1995).

Different elongation factors play important roles in promoting transcription elongation. The best know transcription factor for its ability to rescue a backtracked RNAPII is transcription elongation factor TFIIS. TFIIS can promote read-through of

DNA roadblocks formed by DNA-interacting proteins, as well as difficult to transcribe sequences (Reines & Mote 1993). TFIIS works by stimulating the RNAPII-mediated cleavage of nascent RNA, when RNAPII is backtracked so that it has lost contact with the 3' hydroxyl end of the transcript. (Izban & Luse 1992b). Transcript cleavage, by the RNAPII active site, generates a new 3' hydroxyl end for the active site to continue forward translocation (Figure 1.11). This stimulatory activity of TFIIS has been demonstrated to be essential for transcription and cell viability (Sigurdsson et al. 2010). However, TFIIS is unable to facilitate transcription over bulky lesions, such as cyclobutane pyrimidine dimers (CPDs) *in vitro* (Donahue et al. 1994; Selby et al. 1997). These constitute strong blocks to transcript elongation (Brueckner et al. 2007).

It is worth noting, that elongation factors are not the only factors ensuring efficient transcription. Histone chaperones, chromatin remodelling factors, and histone modifying enzymes are required to reconfigure the chromatin during transcription and restore its original state after the RNAPII complex has travelled through (Selth et al. 2010). This is usually achieved either by temporary displacement or modification of nucleosomes (Kristjuhan & Svejstrup 2004). A SWI-SNF remodeler, RSC, can stimulate RNAPII transcription over mono-nucleosomes *in vitro* (Carey et al. 2006). A histone chaperone FACT (*fa*cilitates *c*hromatin *t*ranscription) has also been implicated in transcription elongation most likely by destabilising the nucleosome structure and allowing the RNAPII complex passage (Orphanides et al. 1998; Belotserkovskaya et al. 2003).

1.4.1.2 Regulation of RNA polymerase II

An important domain in the regulation of RNAPII is the C-terminal tail of Rpb1, which is composed of 26 Tyr-Ser-Pro-Thr-Ser-Pro-Ser sequence repeats in yeast (P. Liu et al. 2010). Although it is not required for the catalytic activity of polymerase, deletion or significant truncation of the C-terminal domain (CTD) leads to cell death (West & Corden 1995). Remarkably, all residues in the CTD hepta-peptide repeat can be modified during transcription – tyrosine, the serines, and threonine undergo phosphorylation, while the prolines are susceptible to switches

between the *cis* and *trans* isomers. Specific CTD modifications are linked to specific stages in transcription: phosphorylation of Ser5 is enriched at the promoter, while Ser2 phosphorylation is associated with transcription elongation and termination, and they dynamically change with the progression of RNAPII through the gene (Mayer et al. 2010). The CTD functions as a binding platform for different RNAPII co-factors with the different phosphorylation states determining their binding (Komarnitsky et al. 2000). Additionally, bivalent marks on adjacent repeats can also be recognised by certain factors (A. Ghosh et al. 2011), directing them to the transcribing RNAPII at very precise moments in the cycle. Binding of these co-factors enables and regulates co-transcriptional processes such as transcript capping, splicing, transcript cleavage and polyA addition, and transcriptional termination (Mischo & Proudfoot 2013).

Ubiquitin also plays an important role in transcription regulation. Many transcription factors undergo poly-ubiquitylation and degradation, ensuring a short-duration transcription signal (Salghetti et al. 2000). Other transcription factors need to undergo mono-ubiquitylation to become active *in situ* (Salghetti et al. 2001) or, as discussed earlier (1.2.3), initiate a longer activation process, e.g. partial processing by the proteasome (Hoppe et al. 2000). Additionally, ubiquitylation of Rpb1 and Rpb2 subunits by the ubiquitin ligase Asr1 was reported to result in expulsion of Rpb4 and 7 subunits, thus modulating the RNAPII subunit composition and inactivating the polymerase (Daulny et al. 2008). Efficient transcription also relies on ubiquitylation of chromatin. Mono-ubiquitylation of histone H2B was observed to de-compact chromatin (Fierz et al. 2011) and recruit other chromatin re-modelling factors (Sun & Allis 2002).

1.4.1.3 Transcription in the presence of DNA damage

The immediate effect that DNA damage has on transcription is steric hindrance, interfering with reading the DNA strand. RNA polymerases form a very strong complex on DNA and cannot spontaneously dissociate from the template (Dalal et al. 2006). Such stability is necessary for efficient and processive gene transcription;

however, it also means that transcribing RNAPII can become blocked by DNA lesions, with potentially detrimental consequences (Svejstrup 2007).

It has been demonstrated that UV irradiation of cells is followed by a global transcription shutdown (Mayne & Lehmann 1982). The global transcriptional repression is thought to be mediated at least partly via phosphorylation of free RNAPII molecules on the CTD, preventing transcription initiation (Rockx et al. 2000; Heine et al. 2008). However, in response to UV, a subset of genes becomes up-regulated, such as genes involved in the nucleotide excision repair (NER) pathway (Al-Moghrabi et al. 2003), required to deal with DNA damage.

RNAPII is able to bypass small DNA lesions in the transcribed strand (TS) and most lesions in the non-transcribed strand (NTS). RNA polymerases were shown to able to transcribe over abasic sites (W. Zhou & Doetsch 1993; W. Zhou et al. 1995). Oxidative lesions, such as 8-oxoguanine, thymine glycol, and 5-hydroxyuracil can stall RNAPII, but this effect can be overcome with the help of general transcription factors (Charlet-Berguerand et al. 2006). However, bulky lesions, such as UV induced cyclobutane pyrimidine dimers (CPDs) and 6-4 photoproducts cause RNAPII arrest (Donahue et al. 1994), most likely due to steric hindrance. The same effect on the polymerase was observed with single-strand breaks (Kathe et al. 2004) and inter-strand crosslinks (Jung & Lippard 2006; Damsma et al. 2007), illustrating that the polymerase stalls as it is unable to bypass bulky lesions and breaks.

Structural studies of RNAPII in the context of DNA damage has revealed that in the case of CPDs, the lesion enters the active site of RNAPII, which leads to misincorporation of uridine in the mRNA, which in turn blocks translocation (Brueckner et al. 2007). However, a more recent study has observed some translesion transcription activity *in vitro*, which happens at a very slow rate, but nevertheless might be able to contribute to UV resistance *in vivo* (Walmacq et al. 2012).

It has been observed that certain lesions are repaired much faster if they are found on the transcribed strand by the TC-NER pathway (discussed in the next section

(1.4.2)) and proposed that RNAPII is able to act as a damage sensor. An interesting question is how stalled RNAPII signals the damage and initiates the TC-NER pathway. The evidence that RNAPII itself does not change conformation upon encountering CPDs (Brueckner et al. 2007) argues against an allosteric model for the initiation of TC-NER. If there is no change in RNAPII structure, a polymerase stalled at a DNA lesion may not be distinguishable from a polymerase stalled due to the depletion of ribonucleotides (Somesh et al. 2005), or polymerase collisions (Hobson et al. 2012). Interestingly, it has been demonstrated in mammalian cells that blockage of transcription (without DNA damage) is capable of activating the DNA damage response by p53 phosphorylation (Derheimer et al. 2007). In general, it seems reasonable to presume that modification of RNAPII, or other factors associating with it, label the polymerase as being stalled at DNA damage.

RNAPII permanently stalled at a lesion will have detrimental effects to the cell – due to its size it might block the access to the DNA repair factors and also form a roadblock to any other processes happening on DNA. It has been demonstrated in an *in vitro* system that RNAPII is capable of shielding a CPD lesion from recognition by photolyase (Donahue et al. 1994). In cells there are two pathways preventing the destructive consequences of RNAPII stuck at a DNA lesion – transcription-coupled nucleotide excision repair (TC-NER), and the last resort pathway for the removal of RNAPII and proteasomal degradation of its largest subunit, Rpb1; both are discussed below.

1.4.2 Transcription-coupled nucleotide excision repair (TC-NER)

The nucleotide excision repair pathway is responsible for the removal of various lesions from DNA by excision, as the name suggests. There are two main branches of the pathway – a global genome repair (GGR), which will eventually deal with most bulky lesions across the genome, and transcription-coupled nucleotide excision repair (TC-NER), a fast pathway which is specifically responsible for the removal of DNA lesions in the transcribed strand of active genes. It is widely thought that RNAPII acts as a sensor for the damage and initiates TC-NER.

The preferential repair of transcribed genes has been observed in both yeast and higher eukaryotes (Terleth et al. 1989; Bohr 1985) and the difference between repair rates in the transcribed strand (TS) repair and the non-transcribed strand (NTS) of the same gene ruled out the possibility of open chromatin structure contributing to better accessibility of lesions (Sweder & Hanawalt 1992). Experiments with temperature-sensitive RNAPII mutants in yeast revealed the requirement for active transcription in the TC-NER pathway (Leadon & D. A. Lawrence 1992; Sweder & Hanawalt 1992). The model for TC-NER suggests that RNAPII stalled at a lesion initiates the pathway and that it has to be moved to allow access for the repair factors (Lainé & Egly 2006).

TC-NER in yeast is generally dependent on Rad26 (Cockayne syndrome protein B in mammals). Rad26 is a DNA-dependent helicase, containing a SNF2-like DNA helicase/translocase domain, but DNA unwinding activity for Rad26 has not been observed (Guzder et al. 1996). A role for pushing stalled RNAPII away from the DNA lesion and creating access to repair factors was proposed. The *E. coli* homologue of Rad26, Mfd, is directly involved in moving RNA polymerase either by translocation or by causing it to be released from DNA (Park et al. 2002). Rad26 might be able to perform a similar function in yeast, and CSB in humans.

The role of Rad26 in TC-NER is somewhat complicated. An involvement of Rad26 in transcription elongation has been observed *in vivo,* suggesting that Rad26 might also play a role as a general elongation factor (S. K. Lee et al. 2001). Later, Rad26 was suggested to be associated with elongating RNAPII indirectly, due to the fact that it is recruited to coding sequences in a RNAPII-dependent manner (Malik et al. 2010). Rad26 was also hypothesised to play a role as a histone chaperone (Malik & Bhaumik 2012; Malik et al. 2012), and observed to modulate transcription over DNA lesions (S.-K. Lee et al. 2002; Yu et al. 2003). Interestingly, upon overexpression of Rad26, faster DNA damage repair rates were observed on both TS and NTS (Bucheli & Sweder 2004), and Rad26 was observed to have a role in DNA damage repair in repressed genes (S. Li et al. 2007). However, it is possible that these effects are still mediated via RNAPII, due to pervasive antisense transcription (Xu et al. 2009).

Upon induction of DNA damage in yeast, Rad26 has been reported to become phosphorylated on serine 27, by a DNA damage checkpoint kinase, Mec1, (Taschner et al. 2010), resulting in enhanced activity of the TC-NER pathway. It might be mediated via the elevated activity of the Rad26 ATPase, since Ser27 is found in the auto-inhibitory leucine latch motif (S. Li 2015), which might be released upon modification. However, the phosphorylation of Ser27 was not observed to significantly influence the ATPase activity *in vitro* (Taschner et al. 2010).

In human cells, CSB has been shown to recruit nucleotide excision repair factors and TFIIH to a stalled RNAPII (Fousteri et al. 2006). Rad26 may also play a role in recruitment of TFIIH to stalled RNAPII, since it is not required for TC-NER close to transcription initiation sites, where TFIIH is presumably still associated with RNAPII after transcriptional initiation (Tijsterman et al. 1997). An alternative model for the Rad26's role in the TC-NER could be the displacement of TC-NER repressors from the RNAPII complex, either directly or indirectly (S. Li 2015). Even though different hypotheses exist, it is still not entirely clear how Rad26 or CSB mediate the TC-NER pathway.

The *Δrad26* strain, however, retains some TC-NER activity (Verhage et al. 1996), and an alternative, RNAPII subunit Rpb9-dependent pathway has been suggested, with Rpb4 playing a regulatory role between the Rpb9- and Rad26-dependent pathways (S. Li & Smerdon 2002). The C-terminus of transcription elongation factor Spt5 and the RNAPII-associated factor 1 complex (Paf1C) have been shown to be able to suppress the Rad26-independent TC-NER (Ding et al. 2010; Tatum et al. 2011). The two sub-pathways of TC-NER seem to be preferred in different genes and different part of the gene, with the Rpb9-dependent sub-pathway playing a bigger role in highly-transcribed genes (S. Li & Smerdon 2002; S. Li 2004). However, the molecular details of the proposed Rbp9-dependent TC-NER pathway are still unclear.

1.4.3 The last resort pathway

If the TC-NER pathway is not capable of dealing with a DNA lesion and transcription cannot be successfully restarted, the stalled RNAPII has to be removed from the DNA strand due to the potentially detrimental effects to the cell, and possibly allowing access to general repair factors to repair the lesion. This is when the last resort pathway for the removal and degradation of RNAPII becomes activated. The last resort pathway consists of two sequential ubiquitylation steps of the largest RNAPII subunit, Rpb1, extraction of RNAPII from chromatin, and proteasomal degradation of Rpb1. Yeast proteins involved in the pathway are discussed in this section, however, the last resort pathway is highly conserved from yeast to humans (Table 1-2).

Table 1-2. Mammalian homologues of the proteins involved in the last resort pathway.

	S. cerevisiae	Mammals
E1	Uba1	Uba1
E2	Ubc4, Ubc5	UbcH5c, UbcH7
E3 (mono-ubiquitylation)	Rsp5	Nedd4
E3 (poly-ubiquitylation)	Elc1-Ela1-Cul3-Rbx1	Elongin A-Elongin BC-CUL5-Rbx2 VHL-ElonginBC-CUL2-Rbx1
Deubiquitylating enzymes	Ubp2 Ubp3-Bre5	Usp2 USP10-G3BP
Accessory factors	Def1 Rpb9	Functional Def1 homologue (Svejstrup lab, unpublished) RBP9
Degradation factors	Cdc48-Ubx4/5 26S Proteasome	p97 with adaptor proteins 26S Proteasome

The observed RNAPII ubiquitylation and degradation in response to DNA damage was first considered to be required for TC-NER (Bregman et al. 1996; Ratner et al. 1998). Later, it was noted that perturbation of the NER pathway, and TC-NER, resulted in increased levels of Rpb1 ubiquitylation and degradation (Bregman et al. 1996; Ratner et al. 1998), but that TC-NER was normal when such ubiquitylation/degradation was perturbed (Woudstra et al. 2002; X. Chen et al. 2007), and ubiquitylation and degradation of Rpb1 was attributed to a new, distinct pathway, which is initiated only when damage-stalled RNAPII cannot be dealt with through DNA repair. This pathway has been designated The Last Resort Pathway (Wilson, Harreman & Svejstrup 2013).

Importantly, Rpb1 poly-ubiquitylation is not a DNA damage response *per se*; it occurs in response to RNAPII arrest on a DNA strand regardless of what caused this persistent stalling – inhibition of transcription with α-amanitin, depletion of ribonucleotide pools with 6-azauracil, or blocking the transcript cleavage activity of RNAPII (Somesh et al. 2005; Anindya et al. 2007; Sigurdsson et al. 2010). However, there is some evidence to suggest that the pathways for DNA damage-dependently and independently stalled RNAPII fates might differ slightly (Karakasili et al. 2014). The TC-NER pathway obviously cannot rescue RNAPII when there is no DNA damage, but poly-ubiquitylated RNAPII is recognised and dealt with by the last resort pathway in a number of conditions. Hence, this pathway is not specific to DNA damage, but rather generally deals with the situations of transcription stress (Figure 1.12).

1.4.3.1 Mono-ubiquitylation of Rpb1

The first step in the last resort pathway is mono-ubiquitylation of Rpb1, which is catalysed by the ubiquitin ligase Rsp5 (Huibregtse et al. 1997). As discussed in previous sections (1.1.2), Rsp5 is a HECT ubiquitin ligase, involved in various cellular processes in yeast. Rps5 recognises the CTD repeats on Rpb1 via its WW domains (Chang et al. 2000; Somesh et al. 2005). The temperature-sensitive *rsp5-1* strain shows a defect in Rpb1 ubiquitylation and degradation in response to DNA damage (Beaudenon et al. 1999; Harreman et al. 2009). Further evidence for the

direct involvement of Rsp5 came from extract-based *in vitro* studies, where extracts with inactivated Rsp5 were shown to be deficient in Rpb1 ubiquitylation (Reid & Svejstrup 2006), but adding purified Rsp5 back to the system restored Rpb1 ubiquitylation (Harreman et al. 2009). Finally, the ubiquitylation of Rpb1 has been reconstituted *in vitro* by the addition of Uba1 (E1), Ubc5 (E2) and Rsp5 to RNAPII in the reaction (Somesh et al. 2005).

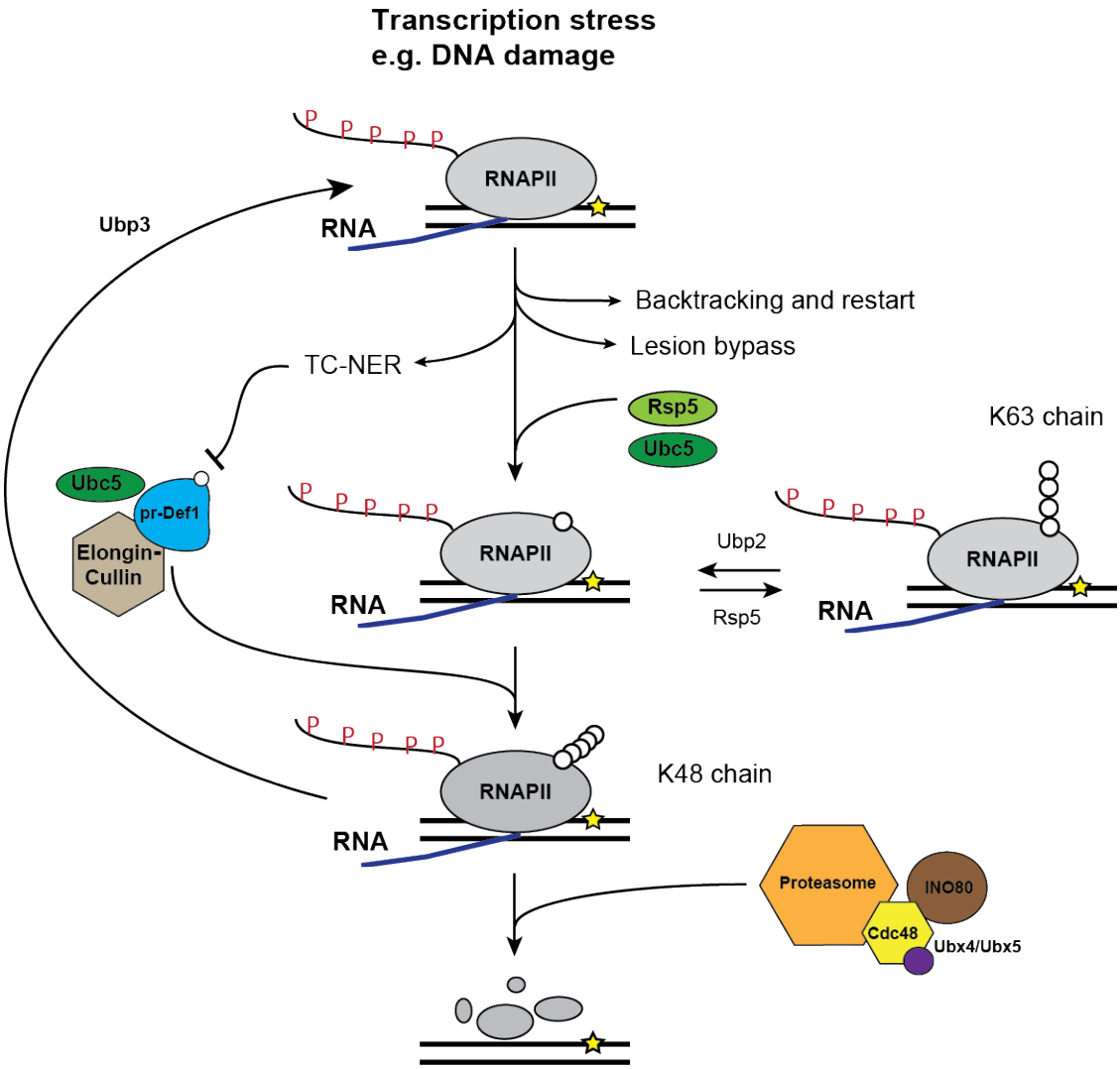

Figure 1.12. The last resort pathway.
Persistently stalled RNAPII is dealt with by the last resort pathway, leading to poly-ubiquitylation and degradation of the Rpb1 subunit, while all the other subunits are recycled. Backtracking and restart as well as lesion bypass lead to the continuation of transcription. See text for details.

Rsp5 has been reported to be able to both mono-ubiquitylate and assemble K63-linked ubiquitin chains, both *in vivo* and *in vitro* (Kee et al. 2005; Kee et al. 2006; H. C. Kim & Huibregtse 2009). However, neither of these Rsp5-generated ubiquitin signals is sufficient for proteasomal degradation. Moreover, K63-liked chain is not the main ubiquitin signal found on RNAPII in response to DNA damage *in vivo* in human cells (Jung & Lippard 2006). This suggested that although Rsp5 ubiquitylation is essential for the Rpb1 degradation, it is not the only ubiquitin ligase involved in the pathway. It has also been shown that Ubp2 deubiquitylase, which associates with Rsp5, is responsible for trimming down the K63-chains synthesised by Rsp5, resulting in mono-ubiquitylation of Rpb1 as Ubp2 is unable to remove the last ubiquitin mark (Harreman et al. 2009) (Figure 1.12). In fact, mono-ubiquitylated Rpb1 is found at low levels in cells even in the absence of external transcription stress (Woudstra et al. 2002; Sigurdsson et al. 2010). A plausible explanation for this observation might be the mono-ubiquitylation of RNAPII complexes that are temporarily stalled, but then successfully restarted without the need for the removal and degradation.

1.4.3.2 Poly-ubiquitylation of Rpb1

The second step of Rpb1 ubiquitylation has been demonstrated to be carried out by the Elongin-Cullin ubiquitin ligase, producing K48-linked ubiquitin chains (Ribar et al. 2006; Ribar et al. 2007; Harreman et al. 2009). The strains missing the components of this complex – Ela1, Elc1, Cul3, and Rbx1 – were not able to poly-ubiquitylate Rpb1 in response to treatment with DNA damaging agents, whilst mono-ubiquitylation was unperturbed (Ribar et al. 2006; Ribar et al. 2007; Harreman et al. 2009). The Elongin-Cullin complex was shown to require pre-mono-ubiquitylated Rpb1 for poly-ubiquitylating it (Harreman et al. 2009), highlighting the step-wise mechanism of ubiquitylation. The activated Def1 protein (discussed in detail below (1.4.3.6)) is required to target the Elongin-Cullin to mono-ubiquitylated Rpb1 (Wilson, Harreman, Taschner, et al. 2013). However, whether poly-ubiquitylation by the Elongin-Cullin complex extends the ubiquitin chain by adding subsequent ubiquitin moieties on the pre-existing Rsp5-initiated mono-ubiquitin signal, or whether it is only using the mono-ubiquitin for substrate

recognition and starts a *de novo* formation of the K48-linked ubiquitin chain at a different lysine, remains unknown. Rpb1 has been reported to be ubiquitylated on multiple lysine residues (Peng et al. 2003; Somesh et al. 2007). Ubiquitylation sites on Rpb1 seem to be involved in the DNA damage response, with the double mutant K330R/K695R being inviable (Somesh et al. 2007).

A non-essential RNAPII subunit, Rpb9, has also been implicated in the DNA damage-dependent ubiquitylation of Rpb1. Cells lacking the Rpb9 subunit were observed to be deficient in UV damage-dependent degradation of Rpb1 (X. Chen et al. 2007). It is worth noting, that one of the characterised sites for Rpb1 ubiquitylation, lysine 695 (Somesh et al. 2007; Peng et al. 2003), is found close to the Rpb1-Rpb9 interface. This raises a question whether Rpb9, implicated in transcription elongation regulation *in vivo* (Hemming et al. 2000), is required for the signalling from stalled RNAPII.

1.4.3.3 De-ubiquitylating enzymes in the last resort pathway

The degradation of RNAPII is a highly regulated process, and therefore it is not surprising that the fate of ubiquitylated Rpb1 can be changed by de-ubiquitylating enzymes (DUBs). With two distinct Rpb1 ubiquitylation steps in the last resort pathway, two DUBs have been implicated as well. As mentioned earlier, Ubp2 works in concert with Rsp5 to ensure the correct ubiquitylation state of Rpb1 after the first step (Harreman et al. 2009). The second DUB is Ubp3, capable of removing K48 chains and leading to complete rescue of Rpb1 from degradation (Kvint et al. 2008; Harreman et al. 2009). Ubp3 directly interacts with RNAPII and Def1, and, furthermore, cells lacking Ubp3 degrade Rpb1 at an elevated rate (Kvint et al. 2008). Even though degradation of Rpb1 is required in response to DNA damage, safeguard mechanisms must exist to prevent the degradation of RNAPII that is merely temporarily stalled and can be rescued by other means. Ubp3 is a good candidate for performing this function *in vivo*.

1.4.3.4 Removal of RNAPII from chromatin

Poly-ubiquitylation of Rpb1 typically leads to its degradation; however, the interaction between RNAPII and DNA is strong (Kireeva 2000), and thus the RNAPII complex has to be removed from DNA for degradation. It has been shown that ubiquitylation itself does not destabilise the RNAPII complex neither *in vivo*, nor *in vitro* (Ratner et al. 1998; K.-B. Lee et al. 2002). Moreover, high avidity association with chromatin has been demonstrated to prevent proteasomal degradation of ubiquitylated substrates (Coppotelli et al. 2011). Thus, an additional step for the extraction of RNAPII from chromatin seemed likely to exist before it is degraded by the proteasome.

Indeed, it has been discovered that Cdc48 (discussed in (1.3)) is required for the removal of ubiquitylated RNAPII from chromatin. Mutation of Cdc48 leads to the accumulation of ubiquitylated Rpb1 associated with the proteasome, but not degraded by it (Verma et al. 2011). For this role of Cdc48, the Ubx4 and Ubx5 adaptor proteins are required, and in their absence the degradation of Rpb1 is perturbed, and poly-ubiquitylated Rpb1 accumulates in the cell (Verma et al. 2011). Interestingly, it has recently been suggested that INO80 chromatin remodeler is also somehow required for this process (Lafon et al. 2015). The role of INO80 in the process is not entirely clear, but it has been observed to simultaneously associate with both Cdc48 and Rpb1 (Lafon et al. 2015).

The proteasome is associated with highly transcribed genes (Auld & Silver 2006), as well as the sites where RNAPII tends to accumulate (Gillette et al. 2004). Hence it is likely that the proteasome is directly targeted to the poly-ubiquitylated Rpb1 for degradation. In fact, certain ‘degradation centres’ have been observed on chromatin in *C. elegans* upon transcription inhibition, where the proteasome is thought to degrade the polymerase (Scharf et al. 2011). It is worth noting that only the Rpb1 subunit is degraded in response to DNA damage, while other RNAPII subunits are thought to be recycled (Malik et al. 2008).

1.4.3.5 Recognition of persistently stalled RNAPII

It is obviously important that only the persistently arrested RNAPII complexes enter the last resort pathway, so as to avoid the unwarranted degradation of transcribing or reversibly stalled RNAPII complexes. While the main steps and players in the last resort pathway are clear, it is still not fully understood how a persistently stalled RNAPII is recognised. Nevertheless, several features of the RNAPII have been described aiding the recognition of arrested RNAPII complexes.

The hyper-phosphorylated form of RNAPII has been observed to be targeted for destruction (Mitsui & Sharp 1999; Luo et al. 2001), indicating that only the actively transcribing polymerase complexes are being degraded. As mentioned earlier, the C-terminal domain of RNAPII is differentially phosphorylated depending on its position in the transcription cycle (1.4.1.2). After transcription termination, all phosphorylation marks are removed from the CTD (Heidemann et al. 2013).

In yeast, only serine-2 phosphorylated Rpb1 (indicative of the elongation stage in transcription) has been observed to become ubiquitylated (Somesh et al. 2005). *In vitro* studies have shown that the Rsp5 ubiquitin ligase does not associate with the CTD if it is phosphorylated on the Serine-5 residue (Somesh et al. 2005). Moreover, cells lacking the CTD phosphatase Ssu2 (and thus having higher levels of serine-5 phosphorylation) showed decreased Rpb1 degradation (Somesh et al. 2005). Thus, phosphorylation of CTD might play an important role in the recognition of arrested RNAPII complexes. Additionally, the conformational change in CTD might also be involved in the process. A proline isomerase, Rrd1, has been demonstrated to be able to release RNAPII from chromatin and may also be required for efficient degradation of Rpb1 (Jouvet et al. 2010; Jouvet et al. 2011).

Since CTD phosphorylation does not specifically label stalled RNAPII, additional signals must be present for correct recognition. Interestingly, *in vitro* experiments have demonstrated that RNAPII incorporated in an elongation complex is a much better ubiquitylation substrate than free RNAPII, and ubiquitylation levels are further increased by allowing the RNAPII complex to transcribe up to a stall point (Somesh et al. 2005). It has been suggested that the E2 enzyme Ubc5 participating

in mono-ubiquitylation of Rpb1 is directly involved in the recognition of its substrate, stalled RNAPII. This is mediated through Ubc5 binding to a domain in RNAPII, which only appears to be structured in the elongation complex (Somesh et al. 2007; Gnatt et al. 2001). Thus, Ubc5 may contribute to the specific recognition of the stalled/arrested RNAPII complex.

It is worth noting that RNAPII has been reported to also become SUMOylated in response to transcriptional stalling (X. Chen et al. 2009). However, this did not appear to have an effect on Rpb1 ubiquitylation or TC-NER rates. It seems reasonable to suggest that a combination of several different signals is required to correctly identify persistently stalled RNAPII.

Since low levels of mono-ubiquitylated RNAPII can be found in cells at all times (Woudstra et al. 2002; Sigurdsson et al. 2010), not only Rsp5 but also the second ubiquitylation complex, Elongin-Cullin, also has to be correctly targeted to mono-ubiquitylated RNAPII. The details of this process are not completely understood. Def1 was observed to specifically associate with RNAPII in response to DNA damage (Reid & Svejstrup 2006), and is important to bring the Elongin-Culling E3 ligase for poly-ubiquitylation of RNAPII, via a direct Def1-Elongin interaction (Wilson, Harreman, Taschner, et al. 2013). However, it is not clear what features of the stalled RNAPII enable this interaction. It is also important to consider the fact that the second ubiquitylation step, although reversible, might be the step differentiating between the last resort pathway and the alternative option, TC-NER. As the recruiter of Elongin-Cullin, Def1 might be playing an important role as a switch between the two pathways.

In yeast, the slow-growth *Δdef1* phenotype can be supressed by expressing the poorly understood *SMY2* gene from a high-copy plasmid (Corbett laboratory, unpublished). Smy2 was first identified as a high-copy suppressor of the conditional lethal *myo2-66* mutation of myosin gene in yeast (Lillie & Brown 1994). The only defined structural feature of the Smy2 protein is the glycine-tyrosine-phenylalanine (GYF) domain, which binds proline-rich sequences (Kofler et al. 2005). Interestingly, Smy2 is also able to suppress the UV sensitivity of *Δdef1Δ rad16* cells, and even the lethality of *Δdef1 rsp5-1* (Michelle Harreman, unpublished), and was also

shown to be interacting with the RNAPII Rpb8 subunit (Briand et al. 2001). Thus, Smy2 might also be involved in the last resort pathway, although its precise role in the pathway is not yet clear.

1.4.3.6 The role of Def1 protein in the last resort pathway

The *S. cerevisiae* protein Def1 (Degradation factor 1) is an abundant, constitutively expressed protein (estimated 3380 copies of Def1 per cell; (Ghaemmaghami et al. 2003)) and apart from its function in ubiquitylation and degradation of Rpb1 in response to DNA damage, it has been implicated in a number of other cellular processes as well. Indeed, Def1 has been reported to interact with both telomeric DNA and the telomere helicase, Rrm3, participating in telomere maintenance (Y.-B. Chen et al. 2005), and in other genome maintenance processes as well (Stundon & Zakian 2015). High-throughput genetic studies have suggested Def1 to be involved in meiotic cross-over recombination (Jordan et al. 2007), regulation of peptide transporter Ptr2 (Cai et al. 2006), glutathione production (Suzuki et al. 2011), and poly-glutamine aggregate formation (Manogaran et al. 2011). Recent data indicate that Def1 is also required for efficient stress-induced gene activation (Vanacloig-Pedros et al. 2015).The deletion of *DEF1* in yeast is not lethal, but the resulting phenotype is large and slow-growing cells (Woudstra et al. 2002; Jorgensen et al. 2002). Due to its unstructured poly-glutamine rich C-terminus, Def1 was also identified as one of several yeast prion proteins (Duennwald et al. 2006; Alberti et al. 2009; Nizhnikov et al. 2014), although the exact role of such proteins (and specifically Def1) in this context is not known.

Def1 was first identified through its interaction with Rad26 protein, the regulator of TC-NER pathway (Woudstra et al. 2002). However, Def1 is not involved in the TC-NER pathway. Instead, cells lacking Def1 are unable to properly degrade Rpb1 when challenged with transcription stress (Woudstra et al. 2002; Somesh et al. 2005). Moreover, Def1 associates with RNAPII and stimulates ubiquitylation of Rpb1 *in vivo* (Reid & Svejstrup 2004; Somesh et al. 2005), even though it is not absolutely required for Rpb1 ubiquitylation *in vitro* (Harreman et al. 2009).

One initially confusing aspect of the role of Def1 in the last resort pathway was its localisation primarily in the cytoplasm (Huh et al. 2003; Tkach et al. 2012). However, it was discovered that Def1 becomes activated in response to UV damage. As also mentioned earlier, the activation of Def1 *in vivo* requires Rsp5 ubiquitin ligase and a functional proteasome, and results in the production of a shorter form of the protein, processed Def1 (pr-Def1) that can accumulate in the nucleus (Wilson, Harreman, Taschner, et al. 2013). Consistent with the observation that *Δdef1* cells have a defect in poly- but not mono-ubiquitylation of Rpb1 (Woudstra et al. 2002), Def1 acts as a bridging factor, bringing Elongin-Culling E3 ligase complex to stalled RNAPII to bring about Rpb1 poly-ubiquitylation (Wilson, Harreman, Taschner, et al. 2013).

Interestingly, the function of Def1 in protein degradation is not limited to the last resort pathway. Def1 has also been reported to promote ubiquitylation and degradation of Pol3, the catalytic subunit of replicative polymerase δ in response to DNA damage (Daraba et al. 2014). This enables a switch to translesion synthesis polymerases (Daraba et al. 2014). An interesting parallel between the DNA polymerase switch and the last resort pathway was the finding that in response to the DNA damaging agent methyl methanesulfonate (MMS), Def1 interacts with Rad5, a factor, which governs error-free DNA damage bypass (Daraba et al. 2014). Just like Rad26 in relation to the last resort pathway, Rad5 is found in a parallel pathway to the one where Def1 works.

This parallel reveals a more general method whereby Def1 might be regulated. Rad26 and Rad5 may antagonise the function of Def1, ensuring that the degradation of respective polymerases (Rpb1 and Pol3) only starts when the alternative pathways fail or are not present. In that case Def1 can be released to initiate the degradation pathway. It is worth noting, that the activation of Def1 has to be highly regulated – when a constitutively active Def1 form is expressed, it leads to cell death (Wilson, Harreman, Taschner, et al. 2013). However, this hypothesis remains to be tested. Also, the nature of the signal that indicates that the alternative pathways did not succeed in solving the DNA damage-induced problem remains unclear.

Due to the obscure primary sequence, no mammalian homologues of Def1 could be found bioinformatically. To date, there are no published reports of Def1 homologues in other organisms. However, recent unpublished work from the Svejstrup lab suggests the presence of a functional homologue in human cells, involved in the last resort pathway. This finding highlights the importance of the protein and the extraordinary conservation of the very complex last resort pathway from yeast to human.

1.5 Aims of this thesis

As discussed above, although a great deal of molecular detail in the last resort pathway is understood and the main players in the system are known, there are still some important questions remaining. It is not completely known how the persistently stalled RNAPII is recognised and how the pathway is regulated. Moreover, insight into the switch between the TC-NER pathway and the last resort pathway is still missing. Def1, being a bridging factor between the RNAPII and the Elongin-Cullin ubiquitin ligase, responsible for poly-ubiquitylation of Rpb1 (Wilson, Harreman, Taschner, et al. 2013), might be playing an important role in the process. The fact that the protein becomes activated in response to DNA damage makes this hypothesis even more compelling.

The aim of this thesis was to understand how the processing of Def1 occurs in detail, both *in vivo* and *in vitro*. It was our hope that this would not only provide more insight into how the last resort pathway is regulated, but would also help to answer important questions from the field of partial proteasomal processing, especially the controversy surrounding the function of the ubiquitin-dependent segregase, Cdc48. The investigation of the partial proteasomal processing of the transcription factor, Spt23, in yeast has suggested that the proteasome is not the only factor involved in the reaction, and that Cdc48 is playing an important role in the process as well (Rape et al. 2001; Shcherbik & Haines 2007). Whether Cdc48 and its co-factors might play a role also in Def1 processing remained unclear. Moreover, to date there are no reported attempts to reconstitute partial proteasomal processing *in vitro.* After first having identified additional players

required for the processing of Def1 *in vivo*, I present an attempt to reconstitute the partial proteasomal processing reaction of Def1 with purified factors.

2 Materials & Methods

2.1 Buffers, Media and Solutions

Standard rich growth media for yeast and bacteria was obtained from the media and cells cervices unit at the Francis Crick Institute Clare Hall Laboratory.

2.1.1 Bacterial Growth Media

2.1.1.1 LB (rich medium)

1 % w/v bacto-tryptone (DIFCO)
0.5 % w/v yeast extract (DIFCO)
1 % w/v NaCl
pH adjusted to 7
+/- 100 µg/ml Ampicillin (Melford Biosciences)
+/- 35 µg/ml Chloramphenicol (Sigma-Aldrich)
+/- 50 µg/ml Kanamycin (Sigma-Aldrich)

2.1.1.2 SOC medium (rich medium)

2 % w/v bacto-tryptone (DIFCO)
0.5 % w/v yeast extract (DIFCO)
10 mM NaCl
2.5 mM KCl
10 mM $MgCl_2$
10 mM $MgSO_4$
20 mM glucose
pH adjusted to 7

2.1.2 Yeast Growth Media

2.1.2.1 YPD

1 % w/v yeast extract (DIFCO)
1 % w/v peptone (DIFCO)
2 % w/v glucose

+/- 200 µg/ml G418 sulfate (Sigma Aldrich)
+/- 50 µg/ml Hygromycin B (Invitrogen)
+/- 100 µg/ml Nourseothricin (NAT) (Jena Bioscience)

2.1.2.2 Selective drop-out media (SD media)

2 % sugar (glucose, raffinose or galactose)
6.7 mg/ml Yeast nitrogen base without amino acids (DIFCO)
1.4 mg/ml Yeast Synthetic Drop-Out Medium Supplement (Sigma-Aldrich)
12 µg/ml adenine
+/- 80 µg/ml leucine
+/- 40 µg/ml histidine
+/- 40 µg/ml uracil
+/- 40 µg/ml tryptophan
+/- 1 µg/ml 5-Fluoroorotic acid (5-FOA) (Sigma-Aldrich)

2.1.2.3 Sporulation media

50 mM Potassium acetate pH 7.0
6 µg/ml adenine
20 µg/ml uracil
40 µg/ml leucine
20 µg/ml tryptophan
20 µg/ml histidine

2.1.2.4 TE/LiOAc

Tris-EDTA pH 7.5
100 mM lithium acetate

2.1.2.5 PEG/TE/LiOAc

Tris-EDTA pH 7.5
100 mM lithium acetate
40 % Polyethylene glycol (PEG) 3350

2.1.3 General Solutions

2.1.3.1 Phosphate Buffered Saline (PBS)

137 mM NaCl
2.7 mM KCl
10 mM Na_2HPO_4
2 mM NaH_2PO_4
pH adjusted to 7.5

2.1.3.2 Phosphate buffer

700mM Na_2HPO_4
300 mM NaH_2PO_4
pH adjusted as required

2.1.3.3 PBST (PBS-Tween)

137 mM NaCl
2.7 mM KCl
10 mM Na_2HPO_4
2 mM NaH_2PO_4
0.025 % Tween 20

2.1.3.4 Tris-EDTA (TE)

10 mM Tris-Cl pH 7.5 or pH 8.0
1 mM EDTA pH 8.0

2.1.3.5 Borate Buffer

40 mM Sodium Borate
70 mM Boric Acid
pH ~9

2.1.3.6 Tris-Borate-EDTA (TBE)

89 mM Tris-Cl

89 mM Boric Acid

2 mM EDTA

A 10 x stock buffer was routinely used to prepare 1 x TBE.

2.1.3.7 5 x DNA loading buffer for agarose gels

20 mM EDTA pH 8.0

30 % glycerol

0.05 % bromophenol blue

2.1.3.8 1x SDS-PAGE loading buffer

65 mM Tris-Cl pH 6.8

10 % glycerol

2 % SDS

0.01 % bromophenol blue

100 mM *β*-Mercaptoethanol

2.1.3.9 1.5 x SDS-PAGE loading buffer

98 mM Tris-Cl pH 6.8

15 % glycerol

3 % SDS

0.015 % bromophenol blue

150 mM *β*-Mercaptoethanol

2.1.3.10 5 x SDS-PAGE loading buffer

325 mM Tris-Cl pH 6.8

50 % glycerol

10 % SDS

0.05 % bromophenol blue

500 mM *β*-Mercaptoethanol

2.1.3.11 SDS-PAGE running buffer

A 20x stock solution of MES or MOPS (BioRad or Invitrogen) buffer was diluted with dH_2O when running Bis-Tris gels, 20x Tricine buffer (BioRad) was used for

Tris-Acetate gels. Alternatively, 10x stock solution of TGS Buffer (BioRad) was used for TGX gels (BioRad).

2.1.3.12 Transfer buffer

25 mM Tris-base
192 mM Glycine
20 % Methanol
0.02 % SDS

2.1.3.13 100x Protease Inhibitor (PI) mix

28.4 µg/ml leupeptin
137 µg/ml pepstatin A
17 mg/ml phenylmethylsulfonyl fluoride
33 mg/ml benzamindine
Dissolved in ethanol

2.1.3.14 10x ATP regeneration system (ARS)

10 mM ATP
150 mM Creatine phosphatase
50 µg Creatine phosphokinase

2.1.3.15 Yeast Lysis Buffer

150 mM Tris-Acetate pH 7.8
50 mM potassium acetate
3 mM EDTA
5 mM DTT
20 % Glycerol
0.1 % Triton X-100
50 µM MG132
2 mM NEM
1 x PI

2.1.3.16 Yeast extraction buffer for NER and transcription competent extracts

0.2 M Tris pH 7.5
0.39 M Ammonium Sulfate
10 mM $MgSO_4$
20 % glycerol
1 mM EDTA
1 mM DTT
1x PI

2.1.3.17 Dialysis buffer for NER and transcription competent extracts

20 mM HEPES pH 7.5
20 % glycerol
10 mM $MgSO_4$
10 mM EGTA
5 mM DTT
1x PI

2.1.3.18 TLC running buffer

1 M formic acid
0.3 M LiCl

2.1.4 Protein Purification Buffers

2.1.4.1 STE buffer

10 mM Tris pH 8
1 mM EDTA
100 mM NaCl
1x PI

2.1.4.2 MultiDsk wash buffer 1

1x PBS
450 mM NaCl

10 % glycerol
0.1 mM EDTA
0.1 % Triton X-100
1x PI
2 mM DTT

2.1.4.3 MultiDsk wash buffer 2

50 mM Phosphate buffer pH 7.4
50 mM NaCl
10 % glycerol
1 mM *β*-Mercaptoethanol
1x PI
0.2 % Triton X-100

2.1.4.4 Ni lysis buffer (Def1 1-500 purification)

1x PBS
15 mM Phosphate buffer pH 7.5
150 mM NaCl
10 % glycerol
0.2 % Triton X-100
1x PI
2 mM *β*-Mercaptoethanol
15 mM Imidazole

2.1.4.5 Ni wash buffer (Def1 1-500 purification)

1x PBS
450 mM NaCl
10 % glycerol
0.1 % Triton X-100
1x PI
2 mM *β*-Mercaptoethanol
20 mM Imidazole

2.1.4.6 Ni elution buffer (Def1 1-500 purification)

1x PBS
15 mM Phosphate buffer pH 7.5
150 mM NaCl
10 % glycerol
0.2 % Triton X-100
1x PI
2 mM *β*-Mercaptoethanol
300 mM Imidazole
pH adjusted to ~7.5

2.1.4.7 GST wash buffer 1 (Def1 1-500 purification)

1x PBS
250 mM NaCl
10 % glycerol
0.1 % Triton X-100
1x PI
2 mM *β*-Mercaptoethanol

2.1.4.8 GST wash buffer 2 (Def1 1-500 purification)

50 mM Phosphate buffer pH 7.5
50 mM NaCl
10 % glycerol
0.3 % Triton X-100
1 mM *β*-Mercaptoethanol
1x PI

2.1.4.9 GST cleavage buffer (Def1 1-500 purification)

25 mM Phosphate buffer pH 7.5
300 mM NaCl
5 mM *β*-Mercaptoethanol
0.01 % Triton X-100

2.1.4.10 GST lysis buffer (GST-myc-Def1 purification)

1x PBS
5 % glycerol
0.01 % Triton X-100
2 mM *β*-Mercaptoethanol
1 mM EDTA
1x PI

2.1.4.11 GST wash buffer 1 (GST-myc-Def1 purification)

1x PBS
250 mM NaCl
10 % glycerol
0.1 % Triton X-100
1x PI
2 mM *β*-Mercaptoethanol
1 mM EDTA

2.1.4.12 GST wash buffer 2 (GST-myc-Def1 purification)

50 mM Phosphate buffer pH 7.5
50 mM NaCl
10 % glycerol
0.3 % Triton X-100
1x PI
1 mM *β*-Mercaptoethanol
1 mM EDTA

2.1.4.13 GST cleavage buffer (GST-myc-Def1 purification)

25 mM Phosphate buffer pH 7.5
150 mM NaCl
2 % glycerol
5 mM *β*-Mercaptoethanol
0.01 % Triton X-100

1 mM EDTA

2.1.4.14 Mono Q buffer A (GST-myc-Def1 purification)

25 mM Phosphate buffer pH 7.5
10 % glycerol
0.01 % Triton X-100
2 mM *β*-Mercaptoethanol
1x PI

2.1.4.15 Mono Q buffer B (GST-myc-Def1 purification)

25 mM Phosphate buffer pH 7.5
1 M NaCl
10 % glycerol
0.01 % Triton X-100
2 mM *β*-Mercaptoethanol
1x PI

2.1.4.16 Gel Filtration (GF) buffer (GST-myc-Def1 purification)

25 mM Phosphate buffer pH 7.5
300 mM NaCl
10 % glycerol
0.01 % Triton X-100
2 mM *β*-Mercaptoethanol

2.1.4.17 Gel Filtration buffer 2 (GST-myc-Def1 purification)

50 mM Phosphate buffer pH 7.5
300 mM NaCl

2.1.4.18 Flag buffer (Cdc48/Ubx1 purification)

150 mM Tris acetate pH 7.8
150 mM KoAc
20 % glycerol
0.01 % NP40

1 mM ATP

1 mM $MgCl_2$

1x PI

2.1.4.19 TEV cleavage buffer (Cdc48/Ubx1 purification)

50 mM Phosphate buffer pH 7.5

150 mM NaCl

1 mM *β*-Mercaptoethanol

10 % glycerol

0.01 % NP40

1 mM ATP

1 mM $MgCl_2$

2.1.4.20 Gel Filtration buffer (Cdc48 purification)

50 mM Tris acetate pH 7.8

150 mM KoAc

1 mM DTT

10 % glycerol

2.1.4.21 His-Sumo lysis buffer (His-Sumo-Smy2 purification)

50 mM Tris pH 7.0

200 mM NaCl

0.1 % Triton X-100

1 mM DTT

20 mM imidazole

1x PI

2.1.4.22 His-Sumo elution buffer (His-Sumo-Smy2 purification)

50 mM Tris pH 7.0

200 mM NaCl

0.1 % Triton X-100

1 mM DTT

500 mM imidazole

2.1.4.23 His-Sumo dialysis buffer (His-Sumo-Smy2 purification)

20 mM Tris pH 7.0
150 mM NaCl
0.01 % Triton X-100
1 mM DTT
10 % glycerol

2.1.4.24 Mono S buffer A (His-Sumo-Smy2 and HA-Smy2 purifications)

20 mM Tris pH 7.0
0.01 % Triton X-100
1 mM DTT
10 % glycerol

2.1.4.25 Mono S buffer B (His-Sumo-Smy2 and HA-Smy2 purifications)

20 mM Tris pH 7.0
1 M NaCl
0.01 % Triton X-100
1 mM DTT
10 % glycerol

2.1.4.26 Ni lysis buffer (Def1-His-Flag purification)

50 mM Tris pH 7.8
500 mM NaCl
0.01 % NP40
10 mM imidazole
40 µM MG132
1x PI

2.1.4.27 Ni elution buffer (Def1-His-Flag purification)

30 mM Tris pH 7.8
300 mM NaCl
0.006 % NP40

400 mM imidazole
1x PI

2.1.4.28 Flag buffer (Def1-His-Flag purification)

50 mM Tris acetate pH 7.8
150 mM KoAc
20 % glycerol
0.01 % NP40

2.1.4.29 Mono Q buffer A (Def1-His-Flag purifications)

50 mM Tris pH 7.5

2.1.4.30 Mono Q buffer B (Def1-His-Flag purifications)

50 mM Tris pH 7.5
1 M NaCl

2.1.4.31 Pre1 buffer (26S proteasome purification)

50 mM Tris pH 7.5
150 mM NaCl
10 % glycerol
5 mM $MgCl_2$
5 mM ATP
1x ARS

2.1.4.32 Pre1 wash buffer 1 (26S proteasome purification)

50 mM Tris pH 7.5
150 mM NaCl
10 % glycerol
5 mM $MgCl_2$
5 mM ATP
0.2 % Triton X-100

2.1.4.33 Pre1 wash buffer 2 (26S proteasome purification)

50 mM Tris pH 7.5
150 mM NaCl
10 % glycerol
5 mM $MgCl_2$
2 mM ATP

2.1.4.34 HA lysis buffer (Cdc48-3HA purification)

150 mM Tris acetate pH 7.8
150 mM KoAc
20 % glycerol
0.01 % NP40
1 mM ATP
1 mM $MgCl_2$
1x PI

2.1.4.35 HA wash buffer (Cdc48-3HA purification)

150 mM Tris acetate pH 7.8
500 mM KoAc
20 % glycerol
0.01 % NP40
1 mM ATP
1 mM $MgCl_2$
1x PI

2.1.4.36 HA lysis buffer (HA-smy2 purification)

150 mM Tris acetate pH 7.8
50 mM KoAc
1 mM EDTA
20 % glycerol
0.01 % NP40
1x PI

2.1.4.37 Def1 fragments Ni lysis buffer

1x PBS
0.01 % Triton X-100
10 mM imidazole
1x PI

2.1.4.38 Def1 fragments Ni elution buffer

1x PBS
0.01 % Triton X-100
300 mM imidazole

2.1.4.39 Def1 fragments wash buffer

1x PBS
0.01 % Triton X-100

2.1.4.40 Def1 fragments MBP elution buffer

1xPBS
0.01 % Triton X-100
10 mM maltose

2.1.4.41 Ni lysis buffer (His-Sumo-Ubx1 and His-Sumo-Ubx5 purifications)

50 mM Tris pH 7.0
200 mM NaCl
0.1 % Triton X-100
1 mM DTT
20 mM imidazole
1x PI

2.1.4.42 Ni elution buffer (His-Sumo-Ubx1 and His-Sumo-Ubx5 purifications)

50 mM Tris pH 7.0
200 mM NaCl
0.01 % Triton X-100
1 mM DTT
500 mM imidazole

2.1.4.43 Dialysis buffer (His-Sumo-Ubx1 and His-Sumo-Ubx5 purifications)

20 mM Tris pH 7.0
150 mM NaCl
0.01 % Triton X-100
1 mM DTT
10 % glycerol

2.1.4.44 Mono Q buffer A (His-Sumo-Ubx1 and His-Sumo-Ubx5 purifications)

20 mM Tris pH 7.0
0.01 % Triton X-100
1 mM DTT
10 % glycerol

2.1.4.45 Mono Q buffer B (His-Sumo-Ubx1 and His-Sumo-Ubx5 purifications)

20 mM Tris pH 7.0
1M NaCl
0.01 % Triton X-100
1 mM DTT
10 % glycerol

2.1.4.46 Flag lysis buffer (Cdc48-3xFlag purification)

150 mM Tris acetate pH 7.8

150 mM KoAc
20 % glycerol
0.01 % NP40
1 mM ATP
1 mM $MgCl_2$
1x PI

2.1.4.47 Mono Q buffer A (Cdc48-3xFlag purification)

50 mM Tris acetate pH 7.8
10 % glycerol
1 mM ATP
1 mM $MgCl_2$

2.1.4.48 Mono Q buffer B (Cdc48-3xFlag purification)

50 mM Tris acetate pH 7.8
2 M KoAc
10 % glycerol
1 mM ATP
1 mM $MgCl_2$

2.1.5 Assay Buffers

2.1.5.1 Def1 stability buffer

25 mM Tris pH 7.5
125 mM NaCl
10 % glycerol

2.1.5.2 Ubiquitylation buffer

25 mM Tris pH 7.5
125 mM NaCl
2 mM $MgCl_2$
1 mM DTT
3.75 mM ATP

2.1.5.3 Proteasomal processing buffer

25 mM Tris pH 7.5
100 mM NaCl
10 % glycerol
2 mM ATP
5 mM $MgCl_2$
1 mM DTT
0.25 mg/ml BSA
1x PI

2.1.5.4 Def1 Binding buffer

1x PBS
50 mM NaCl
1 mM βME
0.05 % Triton X-100
15 % glycerol
75 µg/ml BSA
1x PIs

2.1.5.5 ATPase buffer

50 mM Tris pH 7.5
20 mM KCl
6 mM $MgCl_2$
0.5 mM DTT
0.08 mg/ml BSA

2.1.5.6 Proteasome activity buffer

50 mM Tris pH 7.5
40 mM KCl
5 mM $MgCl_2$
0.5 mM ATP
1 mM DTT

50 µg/ml BSA

2.1.5.7 Smy2-Cdc48 interaction buffer

1x PBS
0.01 % Triton X-100

2.2 DNA techniques

2.2.1 Plasmids

Table 2-1. Plasmids used in this study

Name	Description	Source
pGEX-6p1_myc-Def1	AmpR, GST-1xMyc-DEF1, codon optimised for bacterial expression	KT
pGEX-6p1_Def1 1-506	AmpR, GST-DEF1 1-506-6xHis, codon optimised.	MDW
pGEX-6p1_Def1 1-506 CueM	As pGEX-6p1_Def1 1-506, but with CUE domain mutated (I54A, I55A, F33A, P34A)	MDW
pGEX-6P1_Def1-500-738-6xHis-FLAG	AmpR, GST-DEF1 500-738-6xHis-Flag, codon optimised.	KT
pRS414	AmpR, CEN, TRP1	(Sikorski & Hieter 1989)
pRS414_Def1-HA	AmpR, CEN, TRP1; DEF1-1xHA expressed from own promoter and terminator	KT
pRS414_Def1	AmpR, CEN, TRP1; DEF1 expressed from own promoter and terminator	JW
pRS414_MTH-Def1	AmpR, CEN, TRP1; as above, but 9xMyc-2xTEV-6xHis-DEF1	MDW
pRS414_MTH-Def1$_{Ubm}$	AmpR, CEN, TRP1; as above, but Def1 mutated at K281R, K288R, K328R, and K329R	KT

pRS426	AmpR, 2µ, URA3	(Sikorski and Hieter, 1989)
pRS426_Smy2	AmpR, 2µ, URA3, SMY2 expressed from its own promoter and terminator	MH
pRS426_Ubx1	AmpR, 2µ, URA3, UBX1 expressed from its own promoter and terminator	KT
pRS426_Cdc48	AmpR, 2µ, URA3, CDC48 expressed from its own promoter and terminator	KT
pRS426_Def1	AmpR, 2µ, URA3, DEF1 expressed from its own promoter and terminator	MH
pRS426_Spt23	AmpR, 2µ, URA3, SPT23 expressed from its own promoter and terminator	KT
pRS426_Npl4	AmpR, 2µ, URA3, NPL4 expressed from its own promoter and terminator	KT
pRS426_Ufd1	AmpR, 2µ, URA3, UFD1 expressed from its own promoter and terminator	KT
pRS424-dual-GAL_Cdc48	AmpR, 2µ, TRP1, GAL10-GAL1 promoter, expressing Cdc48-1xFlag	KT
pRS424-dual-GAL-Cdc48/Ubx1	AmpR, 2µ, TRP1, GAL10-GAL1 promoter, expressing Cdc48-1xFlag and 5xMyc-2xTEV-Ubx1	KT
pYES2	AmpR, 2µ, URA, GAL1 promoter	Invitrogen
pYES2_Def1 1-500-HA	AmpR, 2µ, URA, GAL1 promoter expressing Def1 1-500-3xHA	MH
pYES2_HA-Ubx1	AmpR, 2µ, URA, GAL1 promoter expressing HA-Ubx1	KT
pYES2_HA-Smy2	AmpR, 2µ, URA, GAL1 promoter expressing HA-Smy2	KT
pET28a_6xHis-Sumo-Smy2	KanR, bacterial expression of 6xHis-Sumo-Smy2	KT
pET28a_6xHis-Sumo-HA-Ubx1	KanR, bacterial expression of 6xHis-Sumo-1xHA-Ubx1	KT
pET28a_6xHis-Sumo-	KanR, bacterial expression of 6xHis-	KT

HA-Ubx5	Sumo-1xHA-Ubx5	
pET28a_6xHis-Sumo-Def1 1-230	KanR, bacterial expression of 6xHis-Sumo-Def1 1-230	KT
pET28a_6xHis-Sumo-Def1 230-380	KanR, bacterial expression of 6xHis-Sumo-Def1 230-380	KT
pET28a_6xHis-Sumo-Def1 380-550	KanR, bacterial expression of 6xHis-Sumo-Def1 380-550	KT
pET28a_6xHis-Sumo-Def1 550-738	KanR, bacterial expression of 6xHis-Sumo-Def1 550-738	KT
pET28a_6xHis-Sumo-Def1	KanR, bacterial expression of 6xHis-Sumo-Def1 full length	KT
pET28a_6xHis-Sumo-Def1 1-500	KanR, bacterial expression of 6xHis-Sumo-Def1 1-500	KT
pET21b_MBP	AmpR, MBP tag cloned into pET21b plasmid from Invitrogen	KT
pET21b_MBP-Def1 1-230	AmpR, bacterial expression of MBP-Def1 1-230	KT
pET21b_MBP-Def1 230-380	AmpR, bacterial expression of MBP-Def1 230-380	KT
pET21b_MBP-Def1 380-550	AmpR, bacterial expression of MBP-Def1 380-550	KT
pET21b_MBP-Def1 550-738	AmpR, bacterial expression of MBP-Def1 550-738	KT
pET21b_MBP-Def1	AmpR, bacterial expression of MBP-Def1 full length	KT
pET21b_MBP-Def1 1-500	AmpR, bacterial expression of MBP-Def1 1-500	KT
pRS303_ADH-AFB2	AmpR, HIS3, expression of AFB2 protein under ADH promoter	Ulrich lab, unpublished
pHyg-AID*-6FLAG	AmpR, AID*-6FLAg for c-term tagging, hphNT selection.	(Morawska & Ulrich 2013)
pGS-21a-MultiDSK	AmpR, GST-6xhis- 5x dsk2 UBD-6xhis with 8a/a polylinker between.	MDW

YC2	AmpR, URA3, CEN GAL1 promoter	MH
YC2_Def1	AmpR, URA3, CEN GAL1 promoter expressing full length Def1-3xHA	MH
YC2_Def1 1-500	AmpR, URA3, CEN GAL1 promoter expressing Def1 1-500-3xHA	MH
pYES_3xFlag-SPT23-HA	AmpR, URA3, 2μ, GAL1 promoter expressing 3xFlag-Spt23-HA	MH

Plasmids were created for this study by: KT = Kotryna Temcinaite; MDW = Marcus Wilson; JW = Jane Walker; MH = Michelle Harreman.

All plasmids were created via standard cloning techniques.

2.2.2 Polymerase chain reaction (PCR)

KOD Hot Start DNA polymerase kit (Novagen) was used for PCRs for cloning and yeast strain manipulation, as per manufacturer's instructions. GoTaq DNA polymerase (Promega) was used as per manufacturer's instructions for analytical experiments. Primers were synthesised by Sigma-Aldricht or DNA Technologies. Thermocycling conditions were optimised for each PCR.

2.2.3 DNA purification

DNA was purified from PCRs, restriction digests or agarose gels using either QIAquick PCR and gel purification kits from Qiagen or PCR and gel purification kits from Thermo Fischer Scientific, as per manufacturer's instructions.

2.2.4 Cloning

For restriction digests, DNA was incubated with enzymes of choice from New England Biolabs (NEB) for 1-4 hours at 37 °C in an appropriate buffer. Vectors were dephosphorylated using Calf intestinal phosphatase (NEB) after digestion. Digested DNA was purified using appropriate kits (2.2.3). Nanodrop spectrophotometer (Thermo Fisher Scientific) was used to quantify DNA. Ligations were set up with between 5:1 and 3:1 molar ratios of insert: vector. Roche T4 DNA ligase kit was used for the reactions. The reactions were incubated for 30 min at RT before transformation.

2.2.5 Sequencing

All sequencing reactions were performed by the Francis Crick Institute Lincoln Inn Fields Sequencing Facility.

2.2.6 Agarose gel electrophoresis

Appropriate percentage agarose gels were run in TBE buffer at 100 V to resolve DNA fragments. Gels were stained with SYBR Safe DNA stain (Thermo Fisher Scientific).

2.3 Bacterial techniques

2.3.1 Bacterial transformation

Top10 (Invitrogen) or XL-10 Gold (Stratagene) competent cells were used to transform newly made constructs. For recombinant protein expression, BL-21 DE3 (RIL) (Invitrogen) or Rossetta 2 (DE3) Singles (Novagen) were used for transformations when protein expression was intended. All transformations were carried out as per manufacturer's instructions. Transformants were selected on LB plates with appropriate antibiotics.

2.3.2 Extraction of plasmid DNA

Plasmid DNA was extracted as per manufacturer's specifications using either QIAprep miniprep (Qiagen) or GeneJET plasmid miniprep (Thermo Fisher Scientific) kits.

2.3.3 Overexpression of recombinant proteins

Starter cultures of transformed bacteria were grown overnight at 37 °C with appropriate selection. Usually 800 µl of a starter culture was used to inoculate 800 ml LB with appropriate antibiotics. Bacterial cultures were allowed to grow at 37 °C to OD_{600} 0.5-0.8 before inducing protein expression with 1 mM final concentration IPTG. The cultures were shifted to 30 °C for 4 h, if expressing a yeast protein. Cells were harvested by centrifugation for 30 min at 6000 g, 4 °C, washed in ice cold PBS and frozen in liquid nitrogen.

2.4 Yeast techniques

2.4.1 Yeast strains

Standard *Saccharomyces cerevisiae* growth and manipulation techniques were used. All strains are in W303 1A background, unless stated otherwise.

Table 2-2. Yeast strains used in this study

Strain name	Genotype	Source
W303-1a	*MATa ura3 leu2-3, 112 his3-11,15 trp1-1 ade2-1 can1-100*	R. Rothstein
Δdef1::URA3	*W303 MATa leu2-3,112 his3-11,15 trp1-1 ade2-1 can1-100 Δdef1::URA3*	(Woudstra et al. 2002)
Δdef1::TRP1	*W303 MATa ura3 leu2-3,112 his3-11,15 ade2-1 can1-100 Δdef1::TRP1*	(Woudstra et al. 2002)
9xMyc-TEV-6xhis-DEF1	*W303 MATa leu2-3,112 his3-11,15 trp1-1 ade2-1 can1-100 Δdef1::9xMyc-2xTEV-6xHis-DEF1*	MDW
DEF1-6xHA	*W303 MATa ura3 leu2-3,112 his3-11,15 ade2-1 can1-100 def1::pHAHIS304*	(Reid & Svejstrup 2004)
BY4742	*S288C MATa his3Δ1 leu2Δ0 lys2Δ0 ura3Δ0*	*Saccharomyces* genome deletion project
BY4742 ΔUBX1	*S288C MATa his3Δ1 leu2Δ0 lys2Δ0 ura3Δ0 Δubx1::KanMX*	*Saccharomyces* genome deletion project
BY4742 ΔUBX2	*S288C MATa his3Δ1 leu2Δ0 lys2Δ0 ura3Δ0 Δubx2::KanMX*	*Saccharomyces* genome deletion project
BY4742 ΔUBX3	*S288C MATa his3Δ1 leu2Δ0 lys2Δ0 ura3Δ0 Δubx3::KanMX*	*Saccharomyces* genome deletion project
BY4742	*S288C MATa his3Δ1 leu2Δ0 lys2Δ0*	*Saccharomyces*

ΔUBX4	*ura3Δ0 Δubx4::KanMX*	genome deletion project
BY4742 ΔUBX5	*S288C MATa his3Δ1 leu2Δ0 lys2Δ0 ura3Δ0 Δubx5::KanMX*	*Saccharomyces* genome deletion project
BY4742 ΔUBX6	*S288C MATa his3Δ1 leu2Δ0 lys2Δ0 ura3Δ0 Δubx6::KanMX*	*Saccharomyces* genome deletion project
BY4742 ΔUBX7	*S288C MATa his3Δ1 leu2Δ0 lys2Δ0 ura3Δ0 Δubx7::KanMX*	*Saccharomyces* genome deletion project
BY4742 ΔSmy2	*S288C MATa his3Δ1 leu2Δ0 lys2Δ0 ura3Δ0 Δsmy2::URA3*	MH
BY4742 ΔSmy2 ΔUbx1	*S288C MATa his3Δ1 leu2Δ0 lys2Δ0 ura3Δ0 Δsmy2::HIS3 Δubx1::KanMX*	KT
Cdc48-3HA::URA	*W303 MATa ura3 leu2-3,112 his3-11,15 ade2-1 can1-100 CDC48-3HA::URA*	KT
P_{GAL}-3HA-Ubx1	*W303 MATa ura3 leu2-3,112 his3-11,15 ade2-1 can1-100 integration of pFA6a- kanMX6-PGAL-3HA*	(Cheng & R.-H. Chen 2010)
Def1 1-500 with P_{GAL}-DEF1 TRP	*As WT, but lacking Def1 residues 501-738, covered with P_{GAL}-DEF1 plasmid, TRP selection*	MH
yJF1	*W303-1a pep4::KanMx4 bar1::Hph-NT1 ade2-1 ura3-1 his3-11 trp1-1 leu2-3*	(Frigola et al. 2013)
Pre1-FH	*MATa his3Δ200 leu2-3,112 lys2-801 trp1Δ63 ura3-52 $PRE1^{FH}$ΔYlplac211 (URA3)*	(Verma et al. 2000)
Cdc48-AID*-6xFlag	*W303 MATa ura3 leu2-3, 112 his3-11,15 trp1-1 ade2-1 can1-100 P_{ADH}-AFB2 (HIS) C-terminal degron tag on*	KT

	Cdc48 (hphNT)	
W303 ΔPdr5	*W303 MATa ura3 leu2-3, 112 his3-11,15 trp1-1 ade2-1 can1-100 pdr5::TRP1*	KT
P_{GAL}-3HA-Ubx1 ΔPDR5	*W303 MATa ura3 leu2-3,112 his3-11,15 ade2-1 can1-100 integration of pFA6a- kanMX6-PGAL-3HA pdr5::TRP1*	KT
Def1-HF	*W303 MATa ura3 leu2-3,112 his3-11,15 ade2-1 can1-100 Def1 C-terminally tagged with 1xhis 1xFlag (TRP)*	KT
Cdc48-3xFlag	*W303 MATa ura3 leu2-3,112 his3-11,15 ade2-1 can1-100 Cdc48 C-terminally tagged with 3xFlag (NATMX6)*	KT
6xUbm	*As WT, but 6 mutations in genomic DEF1 locus K281R, K288R, K328R, K329R, K269R, K270R*	MDW
Def1 1-530-3xHA	*As WT, but truncated version of Def1 with a C-terminal 3xHA tag*	MH
$Ubx1^{ts}$	*W303 MATa ura3 leu2-3,112 his3-11,15 ade2-1 can1-100 ΔUbx1::KanMX $Ubx1^{ts}$-TAP::TRP1*	(Cheng & R.-H. Chen 2015)
$Ubx1^{ts}$ ΔSmy2	*W303 MATa ura3 leu2-3,112 his3-11,15 ade2-1 can1-100 ΔUbx1::KanMX $Ubx1^{ts}$-TAP::TRP ΔSmy2::HIS3*	KT
Cdc48-3	*W303 Cdc48-3*	Chen lab
Cdc48-3 ΔSmy2	*W303 Cdc48-3 ΔSmy2::HIS3*	KT
Cdc48-3 ΔDef1	*W303 Cdc48-3 ΔDef1::TRP1*	KT
Npl4-1	*W303 Npl4-1*	Chen lab

Npl4-1 ΔSmy2	*W303 Npl4-1 ΔSmy2::HIS3*	KT
Npl4-1 ΔDef1	*W303 Npl4-1 ΔDef1::TRP1*	

Strains were created for this study by: KT = Kotryna Temcinaite; MDW = Marcus Wilson; MH = Michelle Harreman.

2.4.2 Generation of yeast strains

Yeast deletion strains or C-terminal tag strains were created by the PCR technique. For gene deletions, an auxotrophic marker was amplified with homology sequences for up- and down-stream of the gene of interest. For C-terminal tagging, a tag and a marker were amplified with homology sequences to the end of the gene and immediately downstream of the gene. The PCR product (1-3 µg) was used to transform yeast strains. Transformants were selected on appropriate selection plates. Successful integration was screened by PCR and western blots (for protein tags).

2.4.3 Yeast growth conditions

Yeast cultures were grown at 30 °C, unless indicated otherwise, in YPD (2.1.2.1) or SD (2.1.2.2) media. Yeast cell density was measured using the Z2 Coulter Particle Count and Size Analyzer (Beckman-Coulter), with particle gating from 2.5-7.5 µm. For all experiments logarithmically growing cultures between $0.5x10^7$ and $3x10^7$ cells/ml were used. When drug was used, they were added to the culture at an indicated time before experiment. 4-Nitroquinoline-1-oxide (4-NQO) (Sigma) dissolved in DMSO was used to induce DNA damage, at the final concentration of 10 µg/ml. When cultures were treated with MG132 (Calbiochem) to inhibit the proteasome, the drug was dissolved in DMSO, the final concentration of the drug was 50 µM.

2.4.4 Yeast cell transformations

A starter culture of yeast cells was grown overnight at 30 °C or 25 °C for temperature-sensitive (ts) strains. In the morning the culture was diluted to early logarithmic phase and allowed to grow to 1-$2.5x10^7$ cells/ml. Cells were harvested by centrifugation for 3 min at 2500 g, 4°C, washed 1x in sterile water followed by a

wash in TE/LiOAc (2.1.2.4) and resuspended in TE/LiOAc at 10^9 cells/ml. PCR product (1-3 µg) or plasmid (100 ng) was mixed with 70 µg of single stranded salmon sperm DNA prior to addition to 50 µl of cell suspension and 300 µl of PEG/TE/LiOAc (2.1.2.5). The mixture was incubated at 30 °C (or 25 °C for ts strains) for 30 min before the addition of 35 µl of DMSO and 15 min heat shock at 42 °C. Cells were washed once in sterile water and plated on appropriate selective media for auxotrophic selection or YPD for a subsequent drug selection. After 14 h on YPD yeast was replica-plated onto a drug plate, e.g. 5-FOA, G418, NAT. Plates were incubated at 30 °C or 25 °C until colonies appeared usually after 3-4 days. A negative control without PCR or plasmid DNA was always performed.

2.4.5 Spotting assays

Overnight starter yeast cultures were diluted to an early logarithmic phase and allowed to grow. Equal amounts of cells were taken from cultures and resuspended in sterile water. A ten times dilution series were performed from 10^6 to 10^0 and 2 µl of cell suspension was spotted on either YPD or selective plates. Plates were allowed to grow at an appropriate temperature and photographed using a GelDoc XR (BioRad).

2.4.6 Protein overexpression in yeast

For protein overexpression, the gene of interest was cloned into a vector containing GAL1 or GAL10-GAL1 promoter (see Table 2-1). Cultures were grown in selective media with glucose overnight. When the cultures reached appropriate density, they were washed 3 times in sterile water and released into media containing galactose to induce protein expression. Samples at an indicated timepoints were taken or cultures were harvested for protein purification.

2.4.7 Genomic DNA isolation

For genomic DNA extraction The MasterPure Yeast DNA purification kit (Epicentre) was used as per manufacturer's instructions. The RNase treatment step was included if subsequently DNA was to be used for KOD PCR reactions.

2.4.8 Yeast colony PCR

For colony PCRs a quick DNA extraction method was used. A colony was resuspended in 100 µl sterile water. Then it was spun down for 1 min at 14,000 g, supernatant was removed and cells were resuspended in 0.2% SDS. The suspension was boiled for 10 min at 95 °C. 1 µl of resulting supernatant was used for PCR as described (2.2.2).

2.4.9 UV treatment of yeast cultures

Logarithmically growing yeast cultures were treated with UV at a cell density ~1x10^7. Cultures were spun down for 3 min at 2,500 g, 4°C, and resuspended in 50 ml ice cold PBS (2.1.3.1). The suspension was poured into a large Pyrex dish before exposing to 400 J/m^2 of 254nm UV light, using a calibrated UV box. After UV treatment yeast cells were spun down again and released into the original media. Timepoints were taken as indicated.

2.4.10 Yeast whole cell extracts via manual grinding

Yeast cells were harvested at 2,600 g and washed in ice-cold PBS. The pellet was resuspended in one volume of yeast lysis buffer (2.1.3.15). Cell suspension was slowly dripped into a mortar filled up with liquid nitrogen. Frozen drops of yeast suspension were ground by hand and transferred to a microcentrifuge tube. An additional one volume of lysis buffer was added while defrosting ground cells. The extracts were spun 3 times for 10 min at 16,000 g, transferring the supernatant to a new tube each time. Total protein concentration was assessed by Bradford assay (2.5.3).

2.4.11 Yeast whole cell extracts via glass bead beating

Yeast cells were harvested by centrifugation for 3 min at 2,500 g, 4°C and washed in ice-cold PBS before freezing in liquid nitrogen. After defrosting on ice, pellet was resuspended in 700 µl of yeast lysis buffer (2.1.3.15) and the microcentrifuge tube was filled up almost to the top with 0.5mm diameter Glass beads (BioSpec Products). The cells were disrupted using a FastPrep-24 cell homogenizer (MP Biosystems) with 6 rounds of 30 s at 5.5 amplitude. There was one-minute pause

on ice after each round and a 10-minute pause on ice after round 3. The extracts were clarified by centrifugation 3x 10 min at 16,000 g 4 °C. Supernatant was transferred to a new tube after each spin. Protein concentration was measured by Bradford assay (2.5.3).

2.4.12 Quick sodium hydroxide extracts

The method was adapted from (Kushnirov 2000). Essentially, 1.5 ml of yeast culture at ~ $1x10^7$ cells/ml was spun down for 1 min at 14,000 g and resuspended in 100 µl dH_2O. Subsequently 100 µl of 0.2 M NaOH was added to cell suspension and incubated for 5 min at RT. Suspension was spun down for 1 min at 14,000 g, resuspended in 1.5x SDS loading dye (2.1.3.9) and boiled for 5 min at 95 °C before loading on SDS-PAGE gels.

2.4.13 Yeast extracts to visualise membrane-tethered Spt23

Cells were harvested by centrifugation for 3 min at 2,500 g, 4°C and washed in ice-cold PBS before freezing in liquid nitrogen. After defrosting on ice, the pellet was boiled for 3 min at 95 °C. Subsequently, 100 µl of 1x SDS loading buffer (2.1.3.8) supplemented with 5 mM N-ethylmaleimide was added, and the microcentrifuge tube was filled half-way with 0.5mm diameter Glass beads (BioSpec Products). FastPrep-24 cell homogenizer (MP Biosystems) was used at 6.5 amplitude for 1 minute to open up cells. The supernatant was boiled again for 3 min at 95 °C and was cleared by centrifugation for 5 min at 16,000 g before loading on SDS-PAGE gels.

2.4.14 Preparation of TC-NER competent extracts

The method for TC-NER competent extract preparation was modified from (Schultz et al. 1991). Yeast cultures were harvested at OD_{600} = 2 by chilling on ice water and subsequently centrifugating for 4 min at 4,000 g. The pellet was washed in 1/10 volume of ice-cold dH_2O followed by the same volume wash in extraction buffer (2.1.3.16). Cells were lysed by freezer mill at speed 15, 6 times 2 min with 2 min pauses. Extracts were thawed on ice, resuspended in 1 volume extraction buffer supplemented with PIs (2.1.3.13) and spun twice for 2 h at 120,000 g 4 °C to clear. Proteins were precipitated by slowly adding ammonium sulfate to final

concentration of 2.94 M and pelleted by centrifugation for 15 min at 40,000 g 4 °C. Protein pellet was resuspended in dialysis buffer (2.1.3.17) and dialysed in the same buffer overnight. Extract concentration was measured in Bradford assay (Protein quantification).

2.5 Protein techniques

2.5.1 SDS-PAGE

For protein separation precast gradient 4-12 % Bis-Tris Criterion, 4-15 % TGX or 3-8 % Tris-Acetate (BioRad) were commonly used. Gels were run in appropriate buffers (see 2.1.3.11) at 200 V for 4-12 % Bis-Tris and 4-15 % TGX, and 150 V for 3-8 % Tris-Acetate gels. Gels were stained with InstantBlue (Expedion) or SilverQuest silver staining kit (Invitrogen) as per manufacturer's instructions. Alternatively, proteins were transferred onto a membrane for Western blots.

2.5.2 Western blotting

The western blot apparatus was assembled as per manufacturer's specifications. H-bond C-extra Nitrocellulose membrane (Amersham) was used. Transfer was typically performed in transfer buffer (2.1.3.12) for 90 min at 500 mAmp for Bis-Tris and Tris-Acetate gels and 60 min at 500 mAmp for TGX gels. After transfer the membrane was stained with Ponceau S solution (Sigma-Aldrich) and the image was scanned. The membrane was blocked in PBST (2.1.3.3) buffer containing 5 % Milk powder (Sigma-Aldrich). The list of primary antibodies used in this study can be found in Table 2-3. Membrane incubation with the primary antibody was performed in PBST+ 5 % milk powder either overnight at 4 °C or for 2 h at RT followed by 3x wash in PBST before a two-hour incubation with the appropriate secondary antibody in PBST+ 5 % milk powder at RT. The secondary antibodies used in this study were anti-mouse HRP (GE Healthcare), 1:10,000; anti-mouse TrueBlot HRP (eBioscience), 1:1000; anti-rabbit HRP (GE Healthcare), 1:10,000, and anti-rabbit TrueBlot HRP (eBioscience), 1:1000. The membranes were then incubated with SuperSignal Pico or Dura ECL reagents (Thermo Scientific) and exposed to Amersham Hyperfilm ECL film. For quantitative westerns IRDye (LI-COR) secondary antibodies were incubated with the membrane in the dark and the image was taken using Odyssey imager (LI-COR).

Table 2-3. Primary antibodies used in this study

Antibody	Epitope	Source	Supplier	Dilution
8WG16	Rpb1 CTD	Mouse, m	In house	1 : 2,000
9E10	Myc tag	Mouse, m	In house	1 : 5,000
9E11	Myc tag	Mouse, m	In house	1 : 5,000
α-Pgk1	Pgk1	Mouse, m	Invitrogen	1 : 5,000
12CA5	HA tag	Mouse, m	In house	1 : 5,000
α-HA	HA tag	Rabbit, p	Abcam	1 : 4,000
P4D1	ubiquitin	Mouse, m	Enzo	1 : 1,000
α-MBP	MBP tag	Mouse, m	NEB	1 : 1,000
α-Flag	Flag-tag	Rabbit, p	Sigma-Aldrich	1 : 1,000
α-Cdc48	Cdc48	Rabbit, p	Jentsch lab	1 : 20,000
α-Def1	Def1 1-500	Rabbit, p	This study	1 : 10,000
TAT-1	tubulin	Mouse, m	In house	1 : 10,000
α-His	6xHis tag	Mouse, m	Novagen	1 : 1,000

m = monoclonal, p = polyclonal

2.5.3 Protein quantification

Proteins in whole cells extracts were quantified by Bradford protein assay (BioRad). Purified proteins were quantified by Nanodrop, using an appropriate extinction coefficient or by running them on a gel next to a BSA standard curve and performing band quantification with ImageQuant software on Gel Doc XR+ (BioRad). Purified 26S proteasome was quantified by Bradford.

2.5.4 Analysis of protein ubiquitylation in extracts

MultiDsk protein bound to GST beads (2.5.8) was used to deplete ubiquitylated proteins from extracts. Typically, 1 mg of yeast extracts in 700 µl yeast lysis buffer (2.1.3.15) was incubated with 5 µl (packed volume) of resin for 2-3 h at 4 °C. After incubation beads were washed 3x in yeast lysis buffer + 500 mM KoAc and 1x in PBS, resuspended in 60 µl 1.5x SDS loading dye (2.1.3.9), boiled for 10 min at

95 °C before loading on SDS-PAGE gels. Ubiquitylated proteins were visualised by western blots (2.5.2) using appropriate antibodies.

2.5.5 Analysis of Def1 processing in extracts

For visualising pr-Def1, the extracts were always prepared fresh by the quick NaOH method (2.4.12). pr-Def1 was visualised by western blots against Def1 or an appropriate tag.

2.5.6 Immunoprecipitations (IPs)

Extracts for IPs were prepared by either glass bead beating (2.4.11) or manual grinding (2.4.10). Typically 200 µg of extract was used with 10 µl (packed volume) of appropriate beads. IPs were incubated at 4 °C for 2 hours, then washed 3x in yeast lysis buffer (2.1.3.15), or yeast lysis buffer with increased salt concentration, before either elution or resuspension in 50 µl 1.5x SDS loading dye (2.1.3.9). IPs were typically visualised by western blotting. True Blot secondary antibodies were used when appropriate.

2.5.7 Antibody crosslinking to beads

Antibody crosslinking to beads was carried out as described in (Harlow & Lane 1999). Briefly, Protein A and Protein G agarose (Pierce) was mixed in equal amounts and incubated with 2-4 mg of antibody of choice per 1 ml of resin overnight at 4 °C. Beads were washed in PBS and Borate buffer (2.1.3.5) before coupling for 1 h at RT with dimethylpimelimidate. Coupling was stopped by addition of 1M Tris pH 9.0. The beads were washed in PBS and stored as 50 % slurry in PBS + 0.01 % sodium azide.

2.5.8 MultiDsk bead preparation

MultiDsk beads were prepared as described in (Wilson et al. 2012). In short, bacteria expressing MultiDsk protein (Table 2-1) were lysed in STE buffer (2.1.4.1) with lysozyme and incubated on ice for 15 min. Subsequently N-lauryl sarcosine was added to the final concentration of 1.5 % to denature proteins and the lysates were sonicated briefly. After centrifugation for 5 min at 10,000 g Triton X-100 was added to the supernatant to the final concentration of 3 %. The supernatant was

incubated for 2 h at 4 °C with pre-equilibrated glutathione agarose beads (GE healthcare). The beads were washed extensively in MultiDsk wash buffer 1 (2.1.4.2) and then MultiDsk wash buffer 2 (2.1.4.3) and final wash in PBS. The beads were stored as 50 % slurry in PBS + 0.01 % sodium azide.

2.5.9 Antibody production

Purified Def1 1-500 (2.6.3) and Smy2 (2.6.9) were sent out to Eurogentec to produce rabbit polyclonal antibodies via the 28-day speedy protocol.

2.5.10 Antibody purification

The antigen was coupled to appropriate beads in the same manner as described (2.5.7), followed by two alternating washes in 0.2 M glycine pH 2.5 and 1 M K_2HPO_4 and two washes in PBS. The final bleed from rabbit was diluted in half in PBS + 0.2 % Tween 20 and pre-cleared over an empty resin of the same kind as was subsequently used for purification. The flowthrough was incubated with the resin coupled to antigen for 4 h at 4 °C, washed with 4 CV of PBS + 0.2 % Tween 20 followed by a wash in 2 CV of PBS. Antibody was eluted in 0.75 ml of 0.2 M glycine pH 2.5 and collected in tubes containing 0.25 ml 1 M K_2HPO_4. Presence of the antibody in the elutions was tested by Bradford assay. All positive fractions were pooled together and dialysed in PBS:glycerol 1:1 mixture overnight.

2.6 Protein purification

2.6.1 Recombinant myc-Def1 purification

Recombinant myc-Def1 was purified from bacteria, from a plasmid with a codon-optimised sequence (Table 2-1). Bacterial pellet was resuspended in GST lysis buffer (2.1.4.10) and sonicated. The extract was cleared by centrifugation at 25,000 g 4 °C for 20 min. Polymin P was slowly added to the cleared extracts to the final concentration of 0.03 % to precipitate nucleic acids. The pellet was removed by centrifugation for 30 min at 25,000 g 4 °C. Then an ammonium sulfate precipitation was performed by adding saturated ammonium sulfate solution to the extract to the final ratio of 1:1 (v:v) extract: ammonium sulfate. Protein pellet was collected by repeating the spin as previously. The pellet was resuspended in 15 ml GST lysis buffer and incubated with 2 ml (packed volume) glutathione sepharose beads (GE

Healthcare) at 4 °C overnight. Subsequently beads were washed in 50 CV of GST wash buffer 1 (2.1.4.11), 10 CV of GST wash buffer 2 (2.1.4.12) and 10 CV in GST cleavage buffer (2.1.4.13). Beads were incubated in batch in GST cleavage buffer containing HRV3C protease for 5 h 30 min at 4 °C to cleave off the GST tag. Two 1CV elutions were collected after cleavage and were loaded on a Mono Q column (GE Healthcare). A 40 CV gradient going from 10 % to 100 % Mono Q buffer B (2.1.4.15) was performed on an AKTA HPLC machine. Fractions containing protein were pooled together.

2.6.2 Def1-His-Flag purification from yeast

Purification of Def1-His-Flag was performed from yeast cells expressing the construct from an endogenous promoter in DEF1 locus (Table 2-2). Cells were opened up by freezer milling for 6 rounds of 2 min at 15 pcs with 1 min pause. Freezer milled pellet was resuspended in 20 ml Ni lysis buffer (2.1.4.26). Extracts were cleared by centrifugation for 40 min at 50,000 g 4 °C. Resulting supernatant was incubated with 5 ml packed volume Ni NTA agarose (QIAGEN) for 1 h 30 min at 4 °C. 4 x 1 CV elutions were collected in Ni elution buffer (2.1.4.27). Elutions containing protein were pooled together and incubated with 0.5 ml (packed volume) anti-Flag M2 resin (Sigma-Aldrich) overnight at 4 °C. The beads were washed in 20 CV Flag buffer (2.1.4.28) and protein was eluted in 4x 1 CV fractions in Flag buffer + 0.5 mg/ml 3xFlag peptide (synthesised by peptide synthesis facility at the Francis Crick Institute). Elutions containing protein were pooled together and loaded on a Mono Q column (GE Healthcare). The column was run on AKTA HPLC system with a 20 CV gradient from 10 % to 100 % Mono Q buffer B (2.1.4.30). Fractions containing the protein were pooled together.

2.6.3 Recombinant Def1 1-500 purification

Codon optimised Def1 1-500 fragment was overexpressed in bacteria from a pGEX-6p1 plasmid (Table 2-2). Bacterial pellet from a 4 L culture was resuspended in 50 ml Ni lysis buffer (2.1.4.4), sonicated and centrifuged for 30 min at 25,000 g 4 °C. The extracts were incubated with 2 ml (packed volume) of Ni NTA agarose (QIAGEN) for 4 h at 4 °C. Beads were washed in 150 CV Ni wash buffer (2.1.4.5) prior to 5x 1 CV elutions in Ni elution buffer (2.1.4.6). Fractions containing protein

were pooled together and incubated with 1.5 ml (packed volume) glutathione sepharose (GE Healthcare) for 4 h at 4 °C. Beads were washed with 75 CV of GST wash buffer 1 (2.1.4.7), then 10 CV of GST wash buffer 2 (2.1.4.8) and finally 10 CV in GST cleavage buffer (2.1.4.9). GST tag was cleaved off by incubating beads with HRV3C protease in 1.5 CV GST cleavage buffer. Elution fractions containing protein were pooled together and concentrated on Ni beads.

2.6.4 Cd48/Ubx1 purification from yeast

Cdc48-1xFlag and 5xMyc-2xTEV-Ubx1 were co-expressed together from a dual GAL promoter (Table 2-1) in yeast. Yeast pellet was freezer milled and resuspended in Flag buffer (2.1.4.18). The extracts were cleared by centrifugation for 30 min at 40,000 g 4 °C and incubated for 2 h at 4 °C with 0.5 ml packed volume 9E11 beads (2.5.7). The beads were washed in 100 CV of Flag buffer and 40 CV of TEV cleavage buffer (2.1.4.19) before adding TEV protease and leaving to cleave overnight at 4 °C. Elutions containing cleaved protein were pooled together and incubated with 0.5 ml (packed volume) anti-Flag M2 resin (Sigma Aldrich). Beads were washed in 12 CV of TEV cleavage buffer and the protein was eluted in 4x 1 CV of TEV cleavage buffer + 0.2 mg/ml 3x Flag peptide (synthesised by peptide synthesis facility at the Francis Crick Institute). Fractions containing purified protein were pooled together.

2.6.5 Cdc48-3HA purification from yeast

Cdc48-3HA was purified from yeast expressing the tagged version of Cdc48 from the endogenous locus (Table 2-2). Yeast pellet was freezer milled, then resuspended in HA lysis buffer (2.1.4.34) and centrifuged fro 1 h at 40,000g 4 °C. Cleared extracts were incubated with 0.5 ml (packed volume) anti-HA affinity matrix (Roche) for 2 h at 4 °C. Beads were washed in 100 CV of HA wash buffer (2.1.4.35) followed by 30 CV of HA lysis buffer. Protein was eluted in binding buffer with increasing amounts of HA pep2 (synthesised by peptide synthesis facility at the Francis Crick Institute).

2.6.6 Cdc48-3xFlag purification from yeast

Purification of Cdc48-3xFlag was performed from yeast cells expressing the construct from an endogenous promoter in CDC48 locus (Table 2-2). Cells were opened up by freezer milling for 6 rounds of 2 min at 15 pcs with 1 min pause. Freezer milled pellet was resuspended in Flag buffer (2.1.4.46) spun 1 h at 25,000 g to clear the extract and incubated with 1 ml (packed volume) anti-Flag M2 resin (Sigma-Aldrich) for 2 h at 4 °C. Beads were washed in 50 CV Flag buffer and the protein was eluted in Flag buffer + 0.5 mg/ml 3xFlag peptide (synthesised by peptide synthesis facility at the Francis Crick Institute). Elutions containing protein were pooled together and loaded on a Mono Q column (GE Healthcare). The Mono Q column was run on the AKTA HPLC system with a 20 CV gradient going from 15 % to 100 % Mono Q buffer B (2.1.4.48). Fractions containing protein were pooled together.

2.6.7 Recombinant HA-Ubx1 and HA-Ubx5 purification

Recombinant Ubx1 and Ubx5 proteins were purified using the same protocol. Pellet resulting from an 800 ml bacterial culture was resuspended in 30 ml Ni lysis buffer (2.1.4.41). Bacteria were lysed by sonication and the extracts were cleared by centrifugation for 40 min at 20,000 g 4 °C. Resulting extracts were filtered through 0.22 µm syringe filter before 2 h 30 min incubation at 4 °C with 2 ml (packed volume) Ni NTA agarose (QIAGEN). Beads were washed in 50 CV lysis buffer and 4x 1.5 CV elutions were collected in elution buffer (2.1.4.42). Fractions containing protein were pooled together, mixed with Ulp1 protease to cleave off the His-Sumo tag and dialysed overnight in dialysis buffer (2.1.4.43). Protein solution was cleared by centrifugation before loading onto Mono Q column (GE Healthcare). The Mono Q column was run on AKTA HPLC system with a 20 CV gradient from 10 % to 100 % buffer B (2.1.4.45). Fractions containing protein were pooled together.

2.6.8 26S proteasome purification

26 S proteasome was purified from yeast expressing a tagged Pre1 subunit, Pre1-His-Flag, from an endogenous locus. Yeast pellet was freezer milled and resuspended in Pre1 buffer (2.1.4.31). Extracts were cleared by centrifugation at 35,000 g 4 °C for 20 min. Supernatant was supplemented with 5 mM ATP and 1x

ARS (2.1.3.14) before incubating for 3 h at 4 °C with 0.5 ml (packed volume) of anti-Flag M2 resin (Sigma-Aldrich). The beads were washed in 50 CV of Pre1 wash buffer 1 (2.1.4.32) and 40 CV of Pre1 wash buffer 2 (2.1.4.33). Protein was eluted in Pre1 wash buffer 2 + 0.2 mg/ml 3xFlag peptide (synthesised by peptide synthesis facility at the Francis Crick Institute). Five 1CV elution fractions were collected. All fractions containing protein were pooled together.

2.6.9 Recombinant Smy2 purification

Recombinant Smy2 was purified from bacteria expressing His-Sumo-Smy2 construct (Table 2-1). Pellet from 800 ml bacterial culture were lysed in Ni lysis buffer (2.1.4.21). Bacteria were lysed by sonication, the extracts were cleared by centrifugation for 40 min 20,000 g and incubated with 2 ml (packed volume) Ni-NTA agarose (QIAGEN) at 4 °C for 1 h 30 min. Beads were washed in 25 CV of lysis buffer and 3x 1.5 CV elutions were collected in elution buffer (2.1.4.22). Elutions containing protein were pooled together, mixed with Ulp1 sumo protease to cleave off the tag and dialysed overnight in dialysis buffer (2.1.4.23). The sample was cleared after dialysis by centrifugation and loaded onto a Mono S column (GE Healthcare) for concentration. The column was run on an AKTA HPLC system with 40 CV gradient going from 15 % to 100 % Mono S buffer B (2.1.4.25). Fractions containing the protein were pooled together.

2.6.10 Purification of HA-Smy2 from yeast

HA-Smy2 was overexpressed in yeast from a plasmid (Table 2-1). Pellet was freezer milled and resuspended in HA lysis buffer (2.1.4.36). The extracts were cleared by centrifugation for 1 h at 40,000 g 4 °C. Cleared extract was incubated with 0.5 ml (packed volume) of anti-HA affinity matrix (Roche) overnight at 4 °C. Beads were washed in 100 CV of HA lysis buffer and protein was eluted 5x 2 CV in HA lysis buffer + 5 µg/ml HA pep2 (synthesised by peptide synthesis facility at the Francis Crick Institute) at RT. Fractions containing protein were pooled together and loaded on Mono S column to concentrate. The column was run on AKTA HPLC system for 20 CV, gradient from 10 % to 100 % Mono S buffer B (2.1.4.25). Fractions containing purified protein were pooled together.

2.6.11 Purification of ubiquitylated Def1

Ubiquitylated Def1 was purified from ubiquitylation reaction. The reaction was performed using HA-tagged ubiquitin (Boston Biochem). The 800 µl reaction was incubated with 150 µl anti-HA affinity matrix (Roche) for 2 h at 4 °C. Beads were washed 3x in 800 µl PBS + 300 mM NaCl. The protein was eluted in proteasomal processing buffer (2.1.5.3) + 5 µg/ml HA pep2 (synthesised by peptide synthesis facility at the Francis Crick Institute) at RT. Fractions containing ubiquitylated Def1 were subsequently used in proteasomal processing reactions.

2.7 In vitro assays

2.7.1 Ubiquitylation assays

Def1 ubiquitylation assays were essentially performed as RNAPII ubiquitylation assays described in (Somesh et al. 2005). Briefly, Def1, ubiquitin, E1, E2, and E3 (Table 2-4) were mixed together in ubiquitylation buffer (2.1.5.2) and incubated at 30 °C. Timepoints were taken as appropriate. The reaction was either stopped by addition of 5x SDS loading buffer (2.1.3.10) and proteins were visualised by western blotting (2.5.2) or the assay was used to purify ubiquitylated Def1.

Table 2-4. Ubiquitylation reaction components

Component		Amount	Source
E1	rUba1	0.3 pmol	Boston Biochem
E2	yUbc5	2 pmol	MDW
E3	GST-Rsp5	50 nmol	MDW
Ubiquitin	yUbiquitin	250 pmol	Boston Biochem
	No K Ubiquitin	250 pmol	Boston Biochem
	HA-Ubiquitin	250 pmol	Boston Biochem
Substrate	Myc-Def1	titrated	KT
	Def1-HF	titrated	KT

KT = Kotryna Temcinaite, MDW = Marcus Wilson

2.7.2 Def1 processing assays

Def1 processing assays were performed at 30 °C in proteasomal processing buffer (2.1.5.3) with either recombinant myc-Def1 (2.6.1), Def1-HF (2.6.2), or ubiquitylated forms of Def1 in the presence of 26S (2.6.8) or 20S proteasome (Luke Selth). Additional proteins and yeast extracts were added to the assay and timepoints were taken as described in each individual case. The reactions were initiated by addition of Def1 protein and stopped by addition of 5x SDS loading buffer (2.1.3.10). They were typically run on 3-8 % Tris-Acetate gels (BioRad) and the outcome of the reactions was analysed by western blotting (2.5.2).

2.7.3 Def1 stability assays

The stability of purified myc-De1 protein was tested by incubating Def1 in Def1 stability buffer (2.1.5.1) at different temperatures or with different interaction partners, as described in each specific case.

2.7.4 ATPase assays

ATPase assays were performed on purified Cdc48 protein to establish if the protein is active and evaluate the effects of adaptor proteins on Cdc48 activity. The assays were carried out at 30 °C in ATPase buffer (2.1.5.5). The reactions were started by adding P^{32} labelled γ-ATP, and stopped by addition of EDTA. Timepoints were taken as indicated. Reaction products were visualised by thin layer chromatography (TLC) on PEI-impregnated cellulose TLC plate (CEL 300 PEI, Machery-Nagel). TLCs were run in TLC running buffer (2.1.3.18). TLC plates were exposed to a phospho-imager screen for 1h and overnight. The screen was scanned in Typhoon scanner, and the appearance of free, labelled phosphate was quantified using ImageJ software.

2.7.5 Proteasome activity assays

Proteasome activity assays were carried out to check the activity of purified 26S proteasome before using it in Def1 processing assays (2.7.2). Proteasome activity assay kit (Merck Millipore) was used as per manufacturer's specifications. The

release of fluorescent reaction product was measured using Pherastar FS spectrophotometer with excitation at 380 nm wavelength, and emission at 460 nm.

2.7.6 Binding assays

Binding assays with purified proteins were performed as described in individual case. Typically, two or more purified proteins were mixed in a variation of the binding buffer (2.1.5.4) and incubated with appropriate beads for 2 h at 4 °C. Beads were washed 3x in either binding buffer, or binding buffer with higher salt concentration. Subsequently, the proteins were either eluted (in case of Ni and anti-Flag resin) or beads were boiled in 1.5x SDS loading buffer (2.1.3.9). The outcome was visualised by SDS-PAGE (2.5.1) or western blotting (2.5.2).

2.7.7 Def1 fragment interaction

Def1 fragments carrying either MBP or His-Sumo tags (Table 2-1) were co-expressed in bacteria. Bacterial pellet from 100 ml cultures were resuspended in Def1 fragment Ni lysis buffer (2.1.4.37) and sonicated to open up cells. After clearing lysates at 20,000 g for 20 min, 700 µl of extracts were incubated with 20 µl (packed volume) Ni NTA agarose (QIAGEN) at 4 °C overnight. Beads were washed 3x in 700 µl of Ni lysis buffer and eluted in 150 µl of Ni elution buffer (2.1.4.38). Then 100 µl of Ni elutions were incubated for 3 h at 4 °C with 5 µl of amylose resin (NEB). The resin was washed 3x 700 µl of wash buffer (2.1.4.39) and eluted in 50 µl of MBP elution buffer (2.1.4.40). The results were analysed by SDS-PAGE (2.5.1)

3 Cdc48 and Ubx1 are involved in Def1 processing

As described in the introduction (1.4.1.3), RNAPII stalls upon encountering a DNA lesion. It leads to the initiation of the TC-NER pathway. If the lesion cannot be removed by TC-NER, the last resort pathway comes into play to disassemble the arrested RNAPII. Removing RNAPII complex from chromatin probably allows the general repair factors to access the lesion, so that it can be removed by general genome repair. The regulation of the switch between the TC-NER and the last resort pathways is not currently understood.

Def1 protein in its processed, activated form (pr-Def1) was shown to recruit the Elongin-Cullin complex responsible for the poly-ubiquitylation of Rpb1, leading to its degradation (Wilson, Harreman, Taschner, et al. 2013). Def1 was also proved to interact with the Rad26 protein (Woudstra et al. 2002), which is governing the TC-NER pathway. I hypothesised that due to its interaction with Rad26, and an important role in Rpb1 degradation, Def1 would be a good candidate for sensing when the TC-NER pathway cannot resolve the DNA lesion and restart the stalled RNAPII. Thus the activation of the Def1 protein might be an important event leading to the switch between TC-NER and the last resort pathway. My aim was therefore to investigate the molecular detail of Def1 processing, starting with *in vivo* experiments and defining the players involved in the process.

The requirement of Rsp5 and the proteasome for Def1 processing (Wilson, Harreman, Taschner, et al. 2013) highlighted a strong parallel with other examples of partially proteasomally processed proteins in yeast, such as Spt23 and Mga2 (1.2.3). Spt23 processing was shown to require a ubiquitin-dependent segregase, Cdc48, working with an ER-tethered adaptor protein Ubx2 (Hoppe et al. 2000; Rape et al. 2001; Kolawa et al. 2013). This result gave me the rationale to investigate whether there might be a role for Cdc48 and UBX adaptor proteins in the last resort pathway.

3.1 Are Cdc48 and Ubx1 involved in the last resort pathway?

Cdc48 already has an established role acting as a segregase and extracting proteins from chromatin in various pathways (Verma et al. 2011; Maric et al. 2014). Cdc48, with the Ubx4 and Ubx5 adaptor proteins (1.3.3.1), has also been previously shown to be required for the removal of RNAPII from chromatin in response to DNA damage (Verma et al. 2011). I wanted to replicate these results and further investigate the involvement of Cdc48 and UBX domain proteins in the last resort pathway.

3.1.1 Rpb1 degradation is perturbed in the absence of Cdc48

Since Cdc48 is an essential protein, the strategy was to create an auxin-inducible degron (Nishimura et al. 2009; Morawska & Ulrich 2013) of Cdc48 for rapid, inducible degradation of the protein. I reasoned that the degron system would allow for the most direct investigation into the effect of Cdc48 on the last resort pathway, as Cdc48 is involved in multiple pathways in the cell. The side effects arising from other functions of Cdc48 being perturbed for prolonged periods of time would also be minimised using the degron system. Additionally, the degron system offered a flexible activation and deactivation of the protein, unlike the temperature-sensitive mutant strains.

The Cdc48 degron strain was created by inserting an F-box protein Afb2 coding sequence into the HIS locus in the yeast genome and adding a truncated AID sequence followed by a Flag tag to the C-terminus of the endogenous Cdc48, as described in the literature (Morawska & Ulrich 2013). As can be seen from Figure 3.1 A, Cdc48 was rapidly degraded upon the addition of Indole-3-acetic acid (IAA), and this process did not influence the state of Def1 protein in yeast. Assessing the Def1 protein state in the presence of the IAA was important for subsequent experiments, where Def1 processing was used as a read-out.

To investigate the importance of Cdc48 in the last resort pathway, IAA was added 30 min before challenging yeast cultures with the UV-mimetic drug 4NQO. Under these conditions Rpb1 degradation in response to DNA damage was decreased in

the absence of Cdc48 (Figure 3.1 B). The longer exposure of 8WG16 blot also revealed an accumulation of poly-ubiquitylated form of Rpb1 in the absence of Cdc48 compared to the wild type. These results are indicative of slower Rpb1 degradation due to decreased processing of ubiquitylated Rpb1, and are in agreement with the observations published by Verma *et al.* who reported that Cdc48 is required to dissociate RNAPII from chromatin so that it can be degraded by the proteasome (Verma et al. 2011).

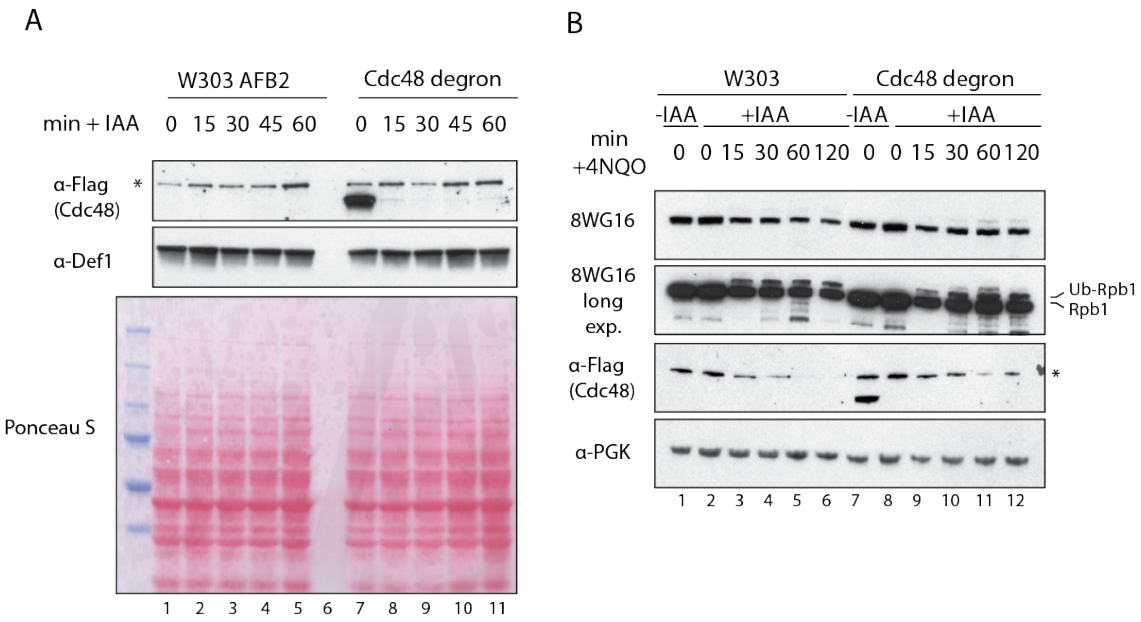

Figure 3.1. The Cdc48 degron strain and the effect of Cdc48 depletion on Rpb1 degradation in response to DNA damage.
A – The Cdc48 degron strain was grown for indicated time in the presence of the degradation inducer, IAA. The W303 AFB2 strain was used as a control. The state of Def1 protein was also assessed in the experiment. The results were visualised by Western blotting. Ponceau S staining was used to check for equal protein loading between the lanes. Note that the W303 strain does not show a signal for Cdc48 since Cdc48 is not tagged in this strain. ***B*** – the degradation of Rpb1 was assessed in the Cdc48 degron strain in response to DNA damage (4NQO treatment). The first sample was taken before the addition of the degradation inducer, IAA. After the addition of IAA the cultures were grown at 30 °C for 30 min before challenging them with 4NQO. The degradation of Rpb1 was followed using 8WG16 antibody, PGK was used as a loading control. The asterisk marks a non-specific band crossreacting with α-Flag antibody.

3.1.2 Rpb1 degradation is perturbed in a *Δubx1* strain

Investigating the effect of Cdc48 on the removal of RNAPII from chromatin in response to UV damage, Verma *et al.* made an interesting observation: like in the *Δubx4* and *Δubx5* mutants they focused on, Rpb1 was not properly degraded in *Δubx1* (Verma et al. 2011). However, while *Δubx4* and *Δubx5* showed an accumulation of poly-ubiquitylated Rbp1 in response to UV, such an accumulation was not observed in the *Δubx1* strain. The authors proposed that this might be due to a defect in UV signalling in the *Δubx1* strain. I instead hypothesised that the Ubx1 adaptor protein might be involved in the processes upstream of Rpb1 poly-ubiquitylation, such as in the activation of Def1.

I performed an Rpb1 degradation experiment by treating yeast cultures with 400 J/m^2 dose of UV irradiation and collecting timepoints for up to 2 h post UV. Yeast cultures were lysed by glass bead beating (2.4.11) and the degradation of Rpb1 was analysed by Western blotting. In response to UV damage the *Δubx1* strain showed a defect in Rpb1 degradation (Figure 3.2) (compare the 120 min timepoints between wild type and mutant strains; notice the decrease in Rpb1 signal relative to tubulin in the WT, but not the mutant strain). This initial observation is in agreement with Verma's data. The ubiquitylation differences between *Δubx1* and *Δubx5* mutants were determined next.

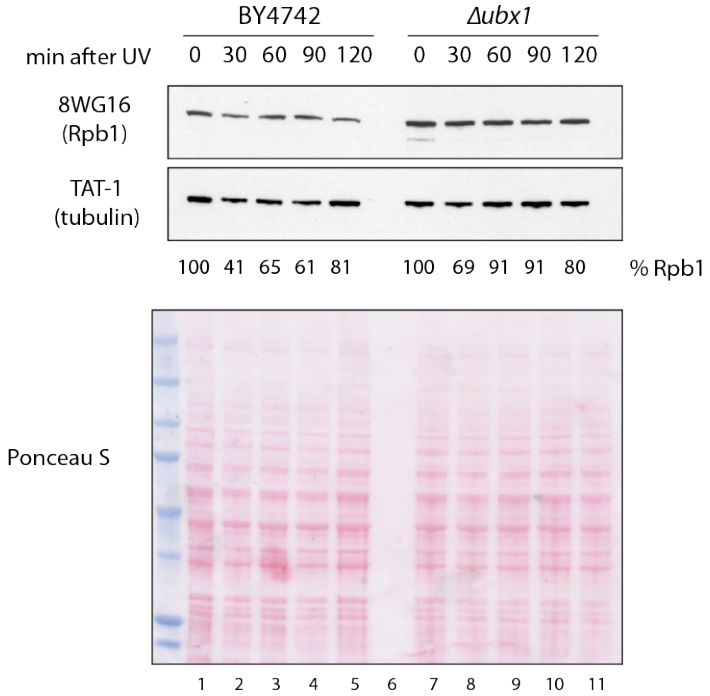

Figure 3.2. Rpb1 degradation in response to DNA damage in the Δubx1 strain. The degradation of Rpb1 in response to UV damage was followed in a Δubx1 strain. The logarithmically growing yeast cells were treated with 400 J/m2 dose of UV light and samples were collected at indicated timepoints post UV. The results were visualised by Western blotting. Tubulin and Ponceau S staining were used to ensure equal protein loading between the lanes. The Rpb1 bands were normalised to tubulin signal and quantified using Image J software.

3.1.3 Ubiquitylation defects of Rpb1 in a *Δubx1* strain

To investigate the ubiquitylation state of Rpb1 in response to UV damage, MultiDSK resin was utilised (Wilson et al. 2012). It has five UBDs from the Dsk2 protein, each separated by a flexible linker, and can efficiently deplete ubiquitylated proteins from extracts. This approach allowed me to easily analyse the changes in ubiquitylation of various proteins.

As in the previous experiments, yeast cultures were UV-irradiated and samples collected at timepoints for up to 2 h post UV. Cells were lysed by glass bead method (2.4.11). Extracts were normalised for total protein concentration and incubated with MultiDSK beads (2.5.8) to pull out all ubiquitylated proteins. The results were visualised by Western blot with 8WG16 antibody. The Ponceau S staining of MultiDSK protein was used to assess loading.

The differences between Rpb1 ubiquitylation states in wild type, *Δubx1,* and *Δubx5* strains in response to UV irradiation can be seen clearly (Figure 3.3). While in the wild type strain (lanes 1-5) a decrease in (the mono-ubiquitylated form of) Rpb1 in response to UV could be seen over time, the *Δubx5* mutant (lanes 13-17) showed a progressive accumulation of poly-ubiquitylated Rpb1, as expected since degradation of Rpb1 occurs in WT strain, while ubiquitylation, but no proteasomal degradation occurs in the *Δubx5* strain. Interestingly, the *Δubx1* strain (lanes 7-11) exhibited increased steady levels of mono-ubiquitylated Rpb1. This result suggests that in the *Δubx1* strain, the Rpb1 poly-ubiquitylation step is perturbed and that this leads to the accumulation of mono-ubiquitylated Rpb1, which cannot be efficiently degraded, as shown in the previous experiment (Figure 3.2). Since Def1 is required for poly-ubiquitylation, but not mono-ubiquitylation of Rpb1 (Wilson, Harreman, Taschner, et al. 2013), this observation led me to investigate whether Ubx1 and Cdc48 might be involved in the activation of Def1.

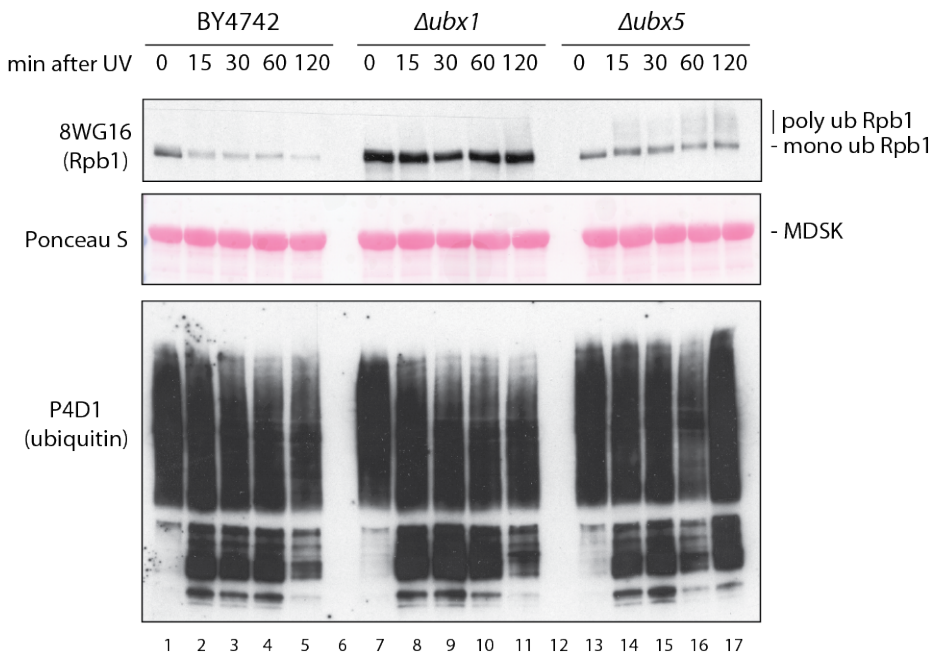

Figure 3.3. Ubiquitylation of Rpb1 in response to DNA damage in Δubx1 and Δubx5 strains.
Logarithmically growing yeast cells were treated with UV light (400 J/m2) and samples were collected at the indicated timepoints post UV. Extracts were measured so that equal amounts of total protein were incubated with MultiDSK beads for isolation of ubiquitylated proteins. The results were visualised by Western blotting, using 8WG16 antibody to detect Rpb1. Ponceau S staining of the MultiDSK beads indicated equal

loading. The total ubiquitin content on the beads was visualised by P4D1 (anti-ubiquitin) antibody. Note that the increase in Rpb1 signal in Δubx1 is specific; it is not due to a generally higher level of ubiquitylated proteins in these extract (lower panel).

3.2 Are Cdc48 and Ubx1 involved in Def1 processing?

A possible involvement of Cdc48 and Ubx1 in Def1 processing was not only suggested by the Rpb1 behaviour in response to DNA damage in the mutant strains, but also – indirectly – by an apparent similarity between Def1 and Spt23 activation mechanisms: both Spt23 and Def1 undergo mono-ubiquitylation by Rsp5 prior to the cleavage step carried out by the proteasome and the activated forms of these proteins accumulate in the nucleus. Spt23 processing was described to additionally require Cdc48 with the UBX domain protein, Ubx2 (Kolawa et al. 2013). Thus, it was important to investigate why and how Cdc48 and Ubx1 are involved in Def1 activation.

3.2.1 Def1 processing is delayed in a Cdc48 degron strain

Def1 becomes activated by partial proteasomal processing in response to DNA damage. However, the resulting active pr-Def1 form is very short-lived and cannot be detected in the extracts prepared by glass bead beating. A quick sodium hydroxide extraction method (2.4.12) was used to examine the effect of Cdc48 on Def1 processing, as it preserves the pr-Def1 form.

The Cdc48 degron strain described above (3.1.1) was used in this experiment. The Cdc48 degron strain was either treated with IAA or left untreated 30 min before the addition of 4NQO. Timepoints were taken for up to 2 h after the addition of the DNA damage-inducing drug, and the state of Def1 was assessed by Western blotting with a custom-made polyclonal α-Def1 antibody, raised against $Def1_{1\text{-}500}$ fragment.

As tested earlier, the degradation of Cdc48 did not itself result in processing of Def1 (Figure 3.1). However, when Cdc48 is degraded before inducing DNA damage, the processing of Def1 is delayed by an hour compared to the -IAA condition (Figure 3.4, compare lanes 3 and 9). This result is reproducible and

indicates that Cdc48 might be involved in Def1 processing, but is not essential for the processing to occur. For example, it might be playing a stimulatory role in Def1 activation.

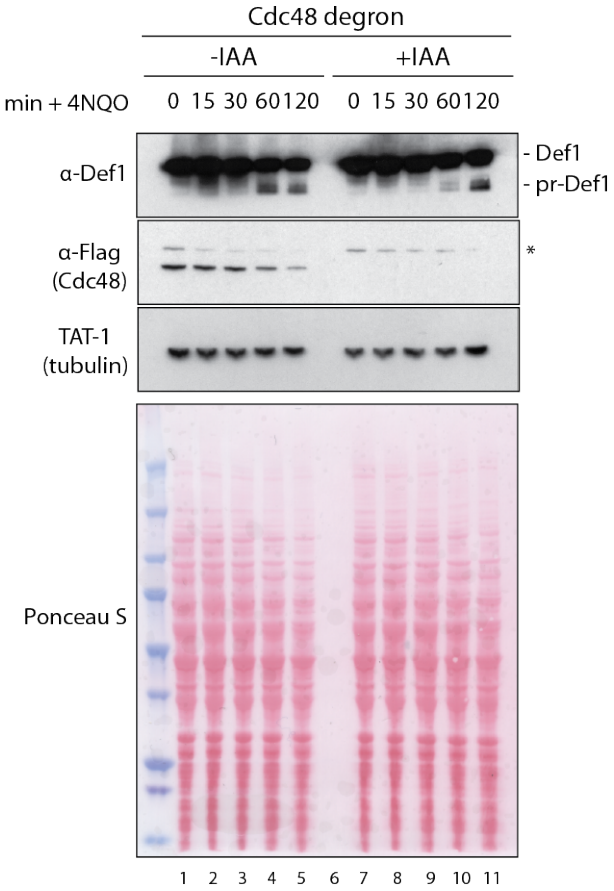

Figure 3.4. Def1 processing in the Cdc48 degron strain.
Logarithmically growing yeast cells were treated ±IAA 30 min before the addition of 4NQO. Extracts were prepared by quick sodium hydroxide extraction (2.4.12) at the indicated timepoints. The results were visualised by Western blotting using α-Def1 antibody. The levels of Cdc48 were monitored using α-Flag antibody. Tubulin and Ponceau S staining were used to assess protein loading between the lanes. Asterisk marks a non-specific band crossreacting with the α-Flag antibody.

Note that the levels of Cdc48 protein were also decreasing in response to the 4NQO treatment, even in the -IAA condition. This can be attributed to the upregulation of global protein degradation in response to DNA damage in yeast (Burgis & Samson 2007). Additionally, however, this effect might lead to the underestimation of the delay in Def1 processing in the absence of Cdc48.

Since Cdc48 is required for multiple pathways in the cell, the observed effect on Def1 processing may not be direct, even though Cdc48 is known to associate with the proteasome. A better way to look at the requirement of Cdc48 for Def1 processing is to use strains deleted for a gene encoding a Cdc48 adaptor protein. Removing a specific Cdc48 adaptor would thus only perturb the specific function of Cdc48 where that adaptor is needed. I adopted this approach to further investigate Cdc48 involvement in Def1 processing.

3.2.2 UBX protein screen shows a defect in Def1 processing in *Δubx1*

To address the question whether any of the UBX domain proteins (1.3.3.1) (and thus Cdc48 as well) play a role in Def1 processing, a screen using UBX deletion strains was performed. The strains were subjected to DNA damage by 4NQO, and their ability to activate Def1 was assessed by Western blotting, as in the previous experiments. Protein loading was assessed by Ponceau S staining of the membrane.

The extent of Def1 processing varied among the different strains, presumably at least partly due to differences in growth characteristic and indirect effects, but only in the *Δubx1* strain no pr-Def1 was detected in response to 4NQO treatment (Figure 3.5). This important result supports the hypothesis that the defect in poly-ubiquitylation and degradation of Rpb1 observed in the *Δubx1* mutant arises as a consequence of its inability to correctly activate Def1 in response to DNA damage. Next I wanted to determine whether Ubx1 works directly at the processing of Def1 or whether it is required upstream of Def1 activation, for example in the DNA damage signalling pathway.

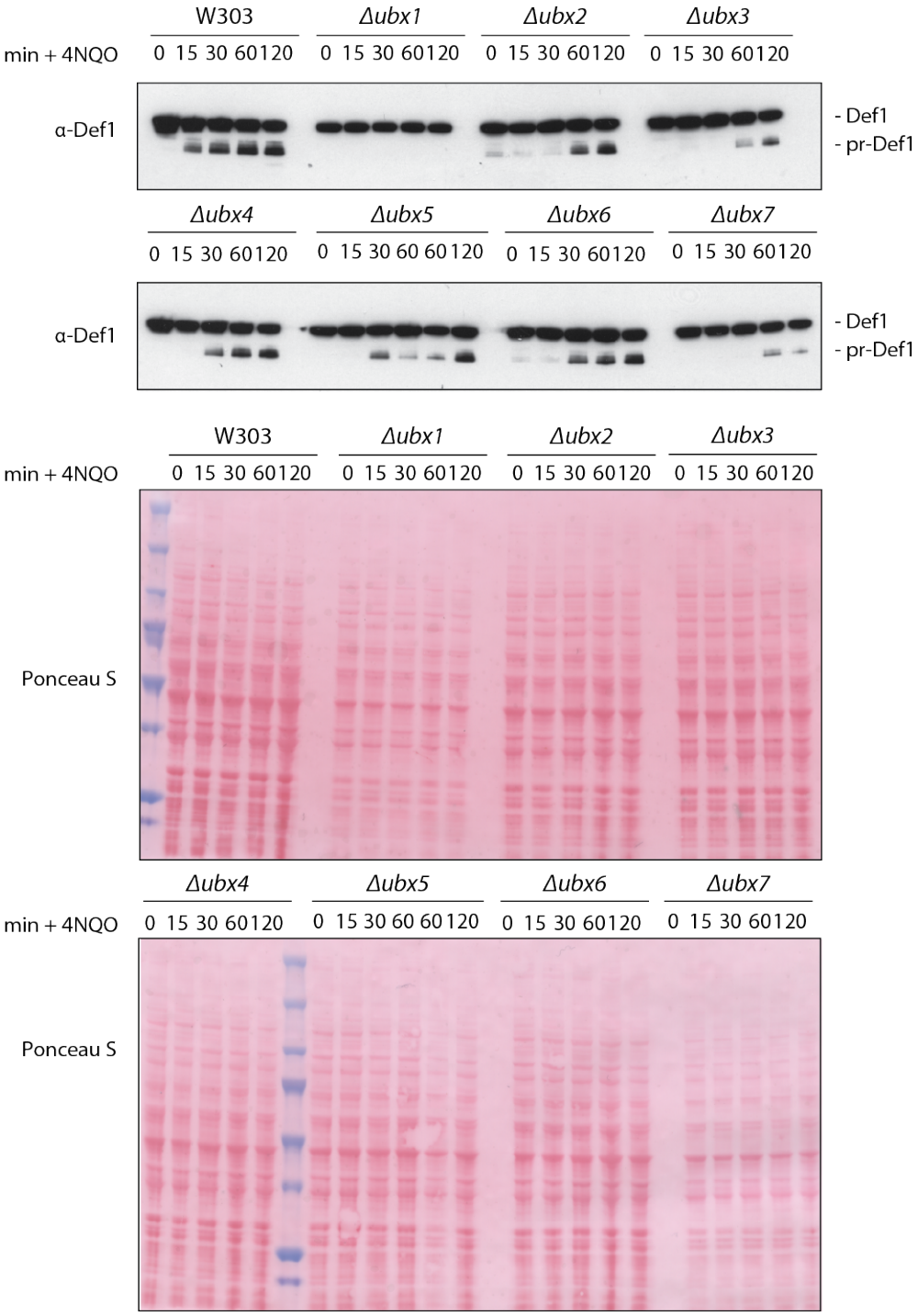

Figure 3.5. UBX protein screen for Def1 processing.
All seven Δubx strains from the yeast deletion collection were used in a Def1 processing screen. The logarithmically growing yeast cultures were challenged with 4NQO, extracts were prepared by quick sodium hydroxide method (2.4.12), and Def1 processing was assessed by Western blot with α-Def1 antibody. Protein loading between the lanes was compared by Ponceau S staining.

3.2.3 Ubiquitylation of Def1 is unperturbed in the *Δubx1* strain

DNA damage-dependent ubiquitylation of Def1 by the ubiquitin ligase Rsp5 was previously shown to be a prerequisite for the processing reaction (Wilson, Harreman, Taschner, et al. 2013). If Ubx1 were working upstream of Def1 processing in the DNA damage signalling pathway, one would thus expect the Def1 ubiquitylation step to be perturbed in the *Δubx1* strain. To investigate this possibility a MultiDSK experiment was performed. Yeast cultures were exposed to 400 J/m^2 UV irradiation and samples were collected for up to 2 hours after UV damage. Total ubiquitylated proteins were pulled out from the extract using MultiDSK beads, and Def1's ubiquitylation state was analysed by Western blotting. Ponceau S staining of MultiDSK protein served as an indication of equal loading between the lanes.

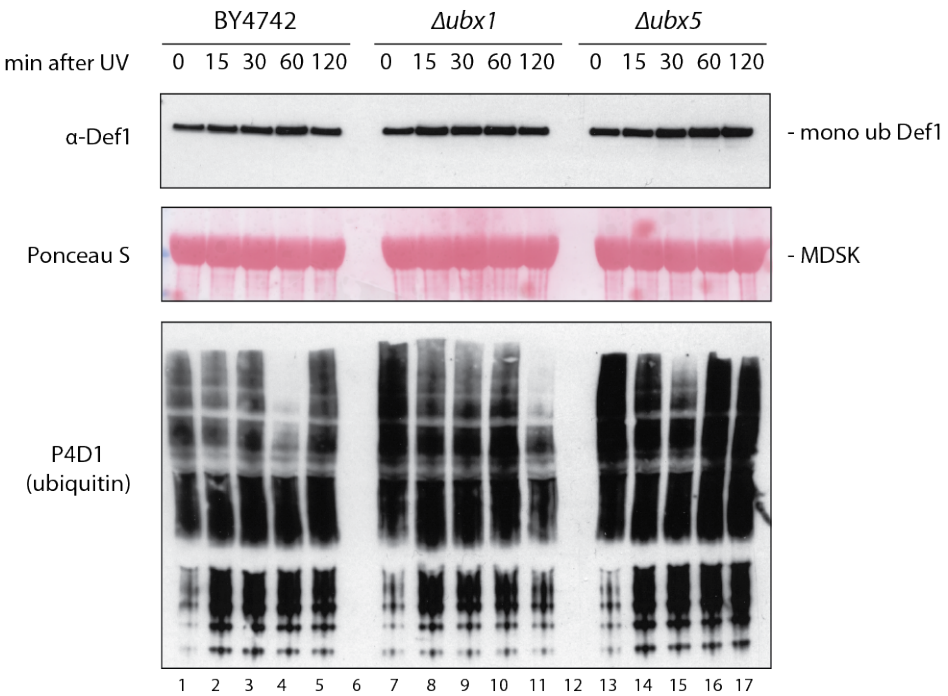

Figure 3.6. Def1 ubiquitylation in *Δubx1* and *Δubx5* strains.
A MultiDSK pulldown was used to assess Def1 ubiquitylation state in response to DNA damage in *Δubx1* and *Δubx5* strains. Logarithmically growing yeast cultures were treated with 400 J/m^2 dose of UV light. The extracts were prepared by glass bead beating (2.4.11) and equal amounts of total protein were incubated with the beads. The results were visualised by Western blotting using α-Def1 antibody. The Ponceau S staining of MultiDSK beads was used to compare loading between the lanes. Total ubiquitin content was visualised using P4D1 antibody.

Rsp5 targets a number of different sites in Def1 (Wilson, Harreman, Taschner, et al. 2013), some of which may be ubiquitylated already before UV-irradiation, but the ubiquitylation levels of Def1 increased in response to UV in all three strains tested, and was actually in this experiment more easily observed in the mutant strains than in wild type (Figure 3.6). So, the absence of Ubx1 does not prevent Def1 from being ubiquitylated. This result argues against the hypothesis that Ubx1 is involved in the DNA damage signalling upstream of Def1 processing, unless that signalling specifically feeds into other, unknown components of the pathway rather than ubiquitylation of Def1.

3.2.4 A Ubx1 degron strain

Cdc48 adaptor protein Ubx1 is also involved in several other important cellular processes. Indeed, Ubx1 deletion strain is lethal in the W303 background, which was otherwise used in all previous Svejstrup lab investigations of the last resort pathway. To overcome this issue, an attempt was made to construct a Ubx1 degron strain, which would allow to bypass the lethality by rapidly degrading the Ubx1 protein immediately prior to the experiment.

In a strain expressing the Afb2 F-box protein, an attempt was made to tag Ubx1 at the endogenous locus with either an N-terminal degron tag introducing a CUP1 promoter, or a C-terminal degron tag (Morawska & Ulrich 2013). None of these attempts gave the desired result. Ubx1 seemed to be resistant to induced degradation. The protein was only disappearing after culturing cells in IAA for prolonged periods of time (16 hours; Figure 3.7 A), which was most likely leading to cell death, judging by the tubulin blot and Ponceau S staining (Figure 3.7 B). Thus it was not possible to examine Def1 processing after Ubx1 degradation in this strain. An alternative, less optimal, approach was to look at the overexpression of the Ubx1 protein and how this might affect Def1 processing.

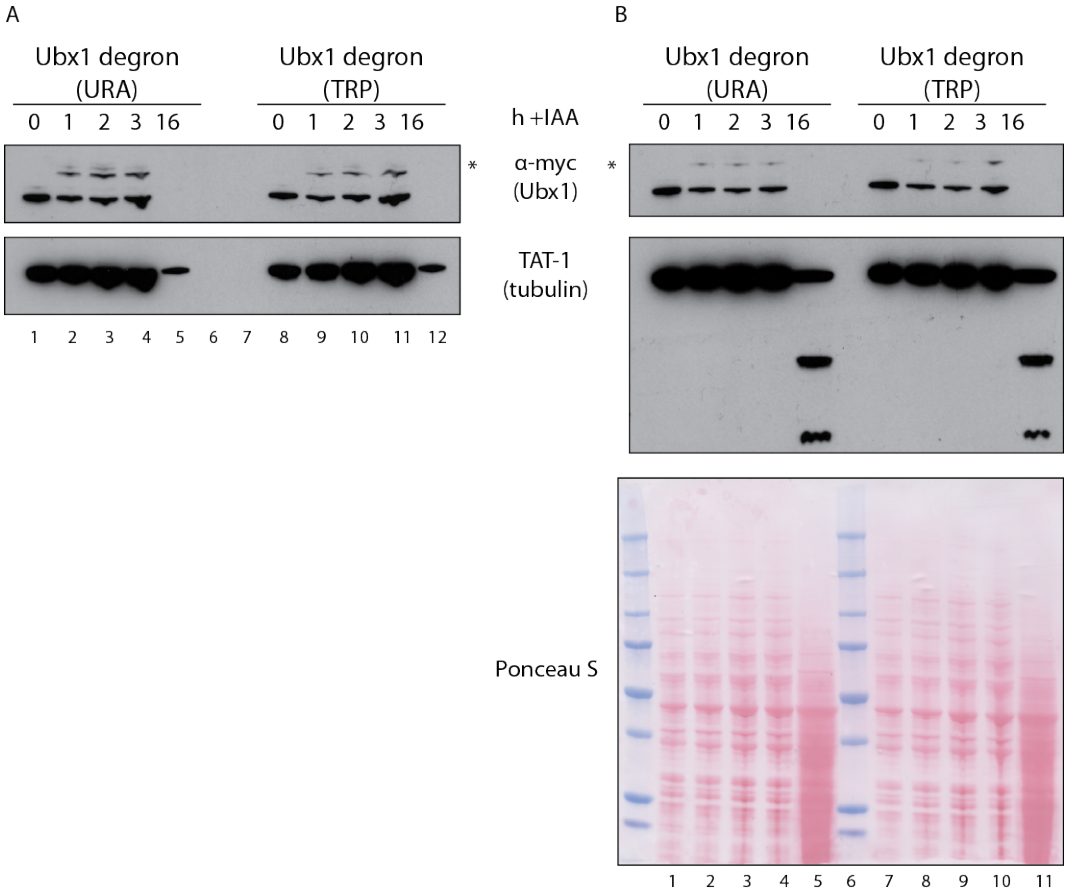

Figure 3.7. The Ubx1 degron strain.
Ubx1 degron strain was created by tagging the endogenous copy of Ubx1 with a C-terminal AID degron sequence and a Myc tag to detect Ubx1. Two different selection markers – TRP and URA were used for generating the strains. ***A*** – Ubx1 degradation was monitored via Western blot after the addition of IAA using α-myc antibody. Tubulin antibody was used to assess loading between the lanes. ***B*** – Samples from the same experiment were re-loaded to try to adjust the tubulin signal between different timepoints. The Ponceau S staining was used to assess the total protein content in each lane. Asterisk marks a non-specific band crossreacting with the α-myc antibody. Note the pronounced protein degradation in the dying cells at 16 hours.

3.2.5 Def1 processing is increased in response to Ubx1 overexpression

A strain expressing HA-tagged Ubx1 under control of the GAL promoter (Chen lab) was utilised to further assess the effect of Ubx1 on Def1 activation. All strains were grown in galactose media until 3 h before the addition of 4NQO. At this point the strains were either shifted to media containing glucose or left in galactose to over-express Ubx1. Timepoints were taken for up to 2 h after the addition of 4NQO, and Def1 processing was visualised by Western blotting.

Def1 processing was clearly increased after Ubx1 overexpression (Figure 3.8). However, it is not entirely clear whether the activation of Def1 was DNA damage-dependent, since pr-Def1 form was detectable even at the time of 4NQO addition. Pr-Def1 form was also observed at the timepoint 0 in *pGAL_Ubx1,* and in the *pGAL_Ubx1 Δmad2* strains grown in glucose. *MAD2* is a spindle checkpoint gene, deletion of which allows cells to overcome the metaphase arrest that is triggered by the absence of Ubx1 (Cheng & R.-H. Chen 2010), and was chosen as an additional control. The effect of the detectable pr-Def1 band at timepoint 0 could be explained if 3 h in glucose was not enough to decrease Ubx1 protein levels to wild type levels, and there still was an excess of Ubx1, even though it was not readily detectable by Western blot. Nevertheless, it is clear that Ubx1 levels affect Def1 processing and might even override DNA-damage dependency of Def1 activation.

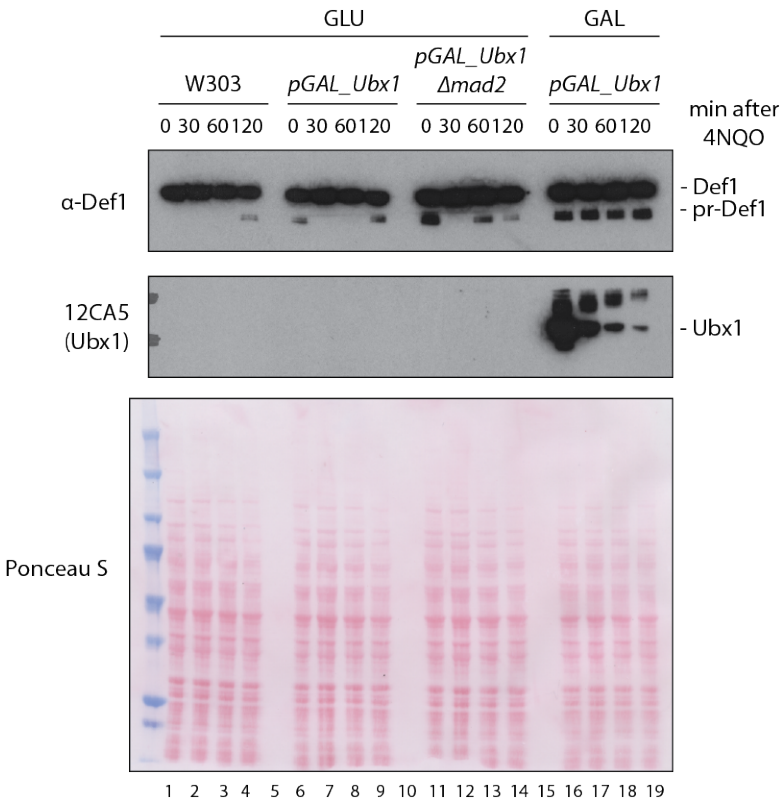

Figure 3.8. Def1 processing in the strain overexpressing Ubx1.
W303, *pGAL_Ubx1,* and *pGAL_Ubx1 Δmad2* strains were grown in either glucose or galactose for 3 h before the addition of 4NQO to damage DNA. The extracts were prepared by quick sodium hydroxide extraction (2.4.12) and Def1 processing was visualised by Western blot, using α-Def1 antibody. The levels of overexpressed Ubx1

were monitored with 12CA5 antibody. Protein loading between the lanes was monitored by Ponceau S staining.

3.2.6 Genetic interactions of Def1, Ubx1, and Cdc48

To further examine the involvement of Ubx1 in the last resort pathway, I investigated potential genetic interactions between Def1, Cdc48, Ubx1, and the well-described Cdc48 adaptor Npl4 (see Introduction (1.3.3)). Genetic interactions were assessed by spotting assays as described in the Materials and Methods (2.4.5).

Neither Ubx1, nor Cdc48 overexpression was able supress the slow growth phenotype of *Δdef1* strain (Figure 3.9 A). This result might be expected for Ubx1, given its potential role in Def1 processing: Ubx1 acts on the fl-Def1 protein to activate it and thus cannot compensate for its absence. However, Cdc48 is thought to work at two places in the last resort pathway – Def1 processing and the removal of RNAPII from chromatin, and thus its overexpression might conceivably stimulate the removal of RNAPII enough to somewhat suppress the negative effects of lacking Def1. Nevertheless, Cdc48 overexpression failed to compensate for the loss of Def1. Interestingly, however, overexpression of *SMY2* was able to supress *Δdef1* phenotype (first observed by Michelle Harreman), and this relationship is further investigated later in this thesis (4).

A multi-copy plasmid carrying the *CDC48* gene (or the *UBX1* gene itself) can compensate for the loss of Ubx1 (Figure 3.9 B). Interestingly, however, the expression of *DEF1* from the native promoter on a high-copy plasmid was also able to somewhat compensate for the loss of Ubx1. This result supports the involvement of Ubx1 in Def1 activation in that the overproduction of Def1 might be expected to partially compensate for the slower Def1 processing kinetics when Ubx1 is lost.

Taken together, these results suggest that Ubx1 and Cdc48 are involved in Def1 activation in response to DNA damage. To prove that the involvement is direct, I set out to look for a physical association between these proteins and Def1.

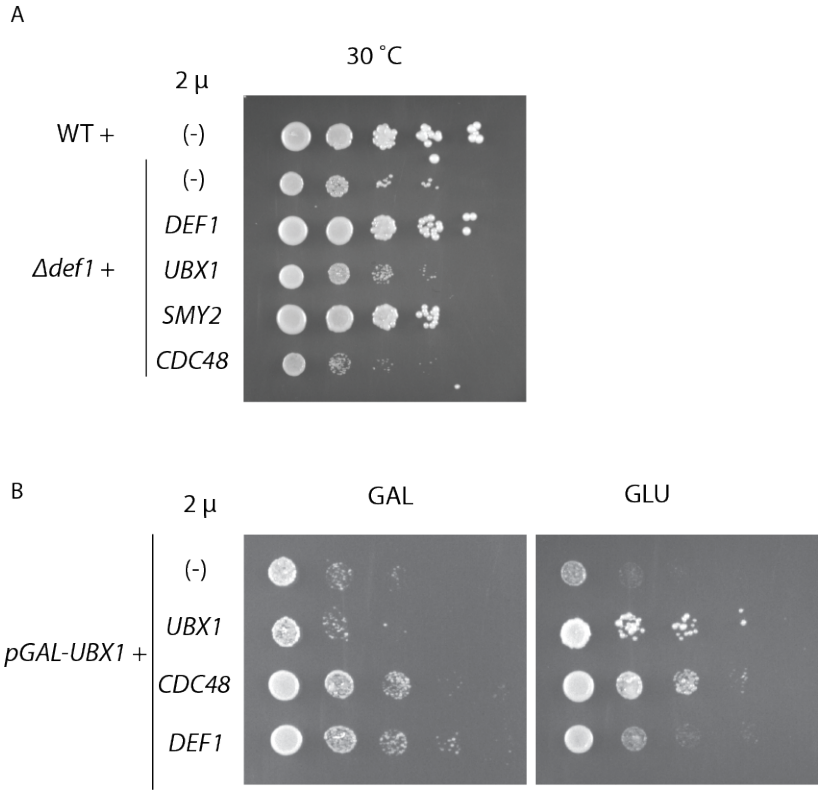

Figure 3.9. Genetic interactions between *DEF1, CDC48,* and *UBX1.*
Genetic interactions between these genes were assessed in yeast spotting assays (2.4.5). ***A*** – Attempt to rescue the slow growth phenotype of *Δdef1* strain via overexpression of *CDC48* and *UBX1* via *2 μ* plasmids expressing the gene in question from its own promoter. 1:10 serial dilutions were performed and the cells were grown on selective plates at 30 °C for 4 days. ***B*** – the ability of *DEF1* to rescue consequences of loss of Ubx1 protein was assessed in *pGAL_UBX1* strain. *CDC48, UBX1,* and *DEF1* were expressed from their native promoter on a *2 μ* plasmid. 1:10 serial dilutions were performed and the cells were grown on selective plates on either glucose or galactose at 30 °C for 3 days as indicated.

3.3 Does Def1 physically associate with Ubx1 and Cdc48?

A series of protein pulldowns were performed under different conditions to investigate the potential physical interactions between Def1 and Cdc48 together with Ubx1. An interaction of Def1 with either of them would indicate that Cdc48 and Ubx1 are directly involved in Def1 activation.

3.3.1 Cdc48 does not seem to associate with Def1

Multiple attempts were made to capture the physical interaction between Def1 and Cdc48. Yeast cells expressing Cdc48-3xHA from the endogenous promoter were grown to around $1x10^7$ cells/ml. Half of the culture was spun down, washed in ice-cold PBS and frozen in LN. The other half of the culture was treated with a 400 J/m^2 dose of UV light and allowed to recover for 15 min at 30 °C before washing and freezing. The 15 min timepoint was chosen expecting the interaction between the two proteins to occur at the very early stages of Def1 processing. Extracts were prepared by glass bead beating and anti-HA affinity matrix (Roche) was used for the IPs. IgG agarose was used as a negative control for the IPs. The results were visualised by Western blot.

No specific interaction was observed between Cdc48 and Def1 either before or after UV treatment (Figure 3.10, right hand side), even though low stringency binding and wash buffers were used. Somewhat disturbingly, Def1 interacted much more with the IgG control beads than with beads containing Cdc48. Def1 is a 'sticky protein' (most likely due to the disordered C-terminal poly-Q domain), which might explain this unusual result. To be able to draw strong conclusions from this sub-optimal experiment, it should be repeated at different times after UV irradiation and using more stringent binding and wash conditions to avoid the non-specific interaction between Def1 and IgG agarose.

Indeed, the fact that I was unable to detect an interaction between Def1 and Cdc48 does not mean it does not occur. The interaction might be temporary and Cdc48 is involved in many different cellular processes. Thus it is possible that only a very small subset of Cdc48 molecules inside the cell interact with Def1 at any given time. Therefore, I next investigated if I could detect an interaction between the Cdc48 adaptor Ubx1 and Def1.

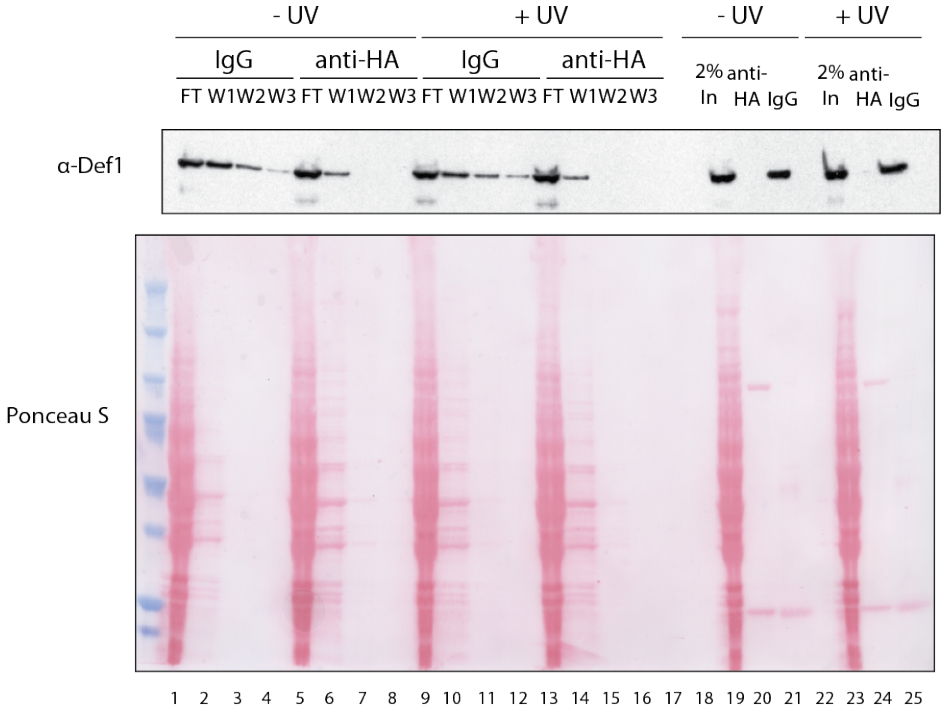

Figure 3.10. Cdc48 IP from yeast extracts.
Cdc48-3HA IPs were performed using extracts prepared by glass bead beating (2.4.11) from yeast cultures ± UV. UV-treated cultures were allowed to recover for 15 min before the IP. IPs and washes were performed in yeast lysis buffer (2.1.3.15). The extracts were incubated with anti-HA beads for 2 h at 4 °C to precipitate Cdc48. IgG agarose was used as a negative control. The results were visualised by Western blotting and Ponceau S staining. FT – flowthrough, W1-3 – washes 1 to 3, IPs are on the right (lanes 19-25).

3.3.2 Ubx1 interacts with Def1

In order to have a higher chance of detecting an interaction between Ubx1 and Def1, the yeast strain overexpressing Ubx1 was utilised to investigate the binding. An analogous experiment to the Cdc48 IP above was performed, probing the interaction in both -UV and +UV conditions, but shifting the UV recovery to a later timepoint. Yeast extracts were prepared in by grinding yeast in liquid nitrogen. Anti-HA affinity matrix was used to IP HA-tagged Ubx1, and a non-tagged wild type strain was used as a negative control.

The Ubx1 protein was able to pull down Def1 in a UV-dependent manner (Figure 3.11 A, compare lanes 6 and 8). Even though larger amounts of Ubx1 were precipitated in the absence of DNA damage, much more Def1 was detected in the

precipitates upon UV-irradiation. This result supports the idea that Ubx1 is directly involved in the DNA damage-dependent activation of Def1. The interaction of Ubx1 with Def1, specifically after DNA damage, might guide Def1 to Cdc48 and the proteasome for processing, thus ensuring that Def1 is only activated at the right time.

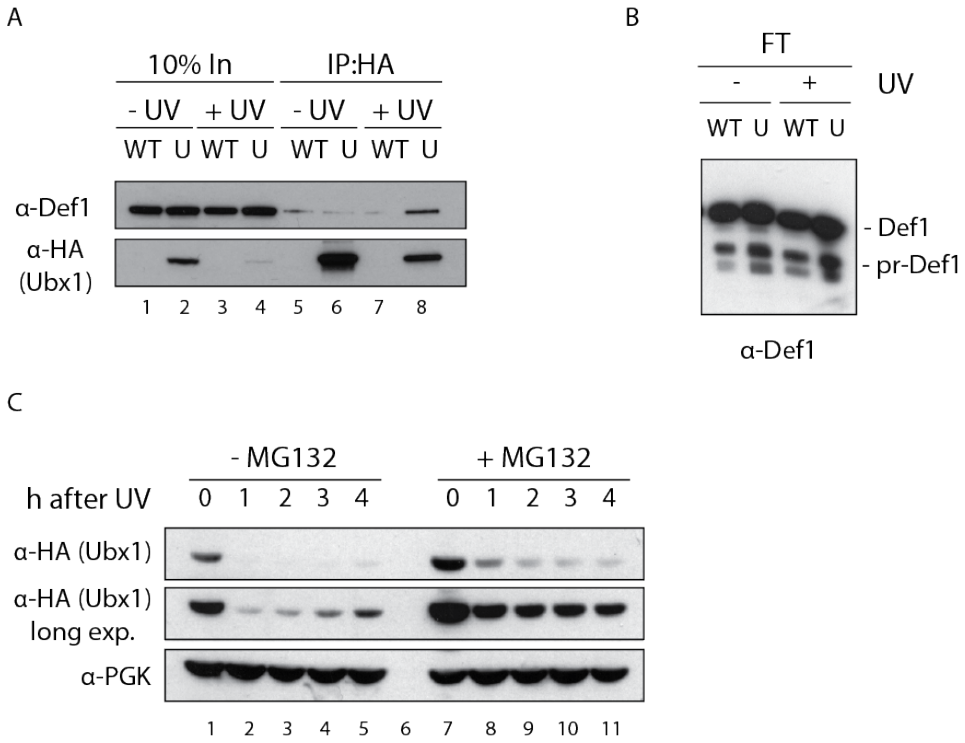

Figure 3.11. Ubx1 has a UV-dependent interaction Def1 and is proteasomally degraded upon UV treatment.
A – HA-Ubx1 IP from the *pGAL_HA-Ubx1* strain in ±UV conditions. Yeast cultures were treated with UV (400 J/m^2) and allowed to recover for 1 h at 30 °C. Yeast extracts were prepared by grinding in LN (2.4.10). IPs were performed in yeast lysis buffer (2.1.3.15) by incubating equal amounts of extract with anti-HA agarose for 1 h at 4 °C to precipitate Ubx1. Beads were washed 3 times in 20 mM Tris pH 7.0, 200 mM NaCl, 0.01 % Triton X-100, 10 % glycerol. WT – W303 strain; U - *pGAL_HA-Ubx1* strain. ***B*** – The flowthrough fractions from ***A*** were visualised by Western blotting with α-Def1 antibody. ***C*** – Investigation of the decrease of Ubx1 levels in response to DNA damage. The *PDR5* gene was deleted in the *pGAL_HA-Ubx1* strain to increase its sensitivity to the proteasomal inhibitor MG132 (40 μM). MG132 was added 30 min before UV irradiation. The extracts were prepared at the indicated timepoints post UV by quick sodium hydroxide extraction (2.4.12). The results were visualised by Western blotting, using the indicated antibodies. PGK was used as a loading control.

It is worth noting that Ubx1 did not seem to interact with the processed form of Def1, as the flowthrough fractions from this experiment contained all the pr-Def1 (Figure

3.11 B). However, it is difficult to ensure that the processed form of Def1 did not appear as a consequence of sample handling. If the processed form of Def1 does indeed not bind to Ubx1 as seems reasonable to hypothesize, this result would point to the role of Ubx1 protein being upstream from the actual digestion step performed by the proteasome, as might also be expected.

Interestingly, the levels of Ubx1 appeared to drop significantly in response to UV treatment (Figure 3.11 A compare lanes 2 and 4). To investigate whether this was due to proteasomal degradation, an analogous experiment was performed in a *pGAL_UBX1 ΔPDR5* strain. This strain lacks a plasma membrane multidrug transporter, Pdr5, allowing better uptake of the proteasome inhibitor MG132 (Collins et al. 2010). In response to UV treatment, 3HA-Ubx1 expressed from a GAL promoter rapidly disappears (Figure 3.11 C). This effect was less pronounced in the presence of MG132, arguing that the degradation of Ubx1 is happening via the proteasome. Since in these experiments Ubx1 is overexpressed from a GAL promoter, it is possible that the degradation in response to UV treatment is nonspecific and falls under the general protein degradation response (Burgis & Samson 2007).

3.3.3 Ubx1 does not interact with Def1 lacking its ubiquitylation sites

Apart from the UBX domain, which is necessary for the interaction with Cdc48, Ubx1 also has a ubiquitin-binding UBA domain (1.1.4). Mechanistically, it seemed plausible that Ubx1 would bind the ubiquitylated form of Def1. Def1 ubiquitylation increases in response to UV. This could lead to the increased interaction with Ubx1 and Cdc48, subsequently helping the proteasome to activate Def1 by processing. A yeast strain expressing Def1 mutated at all known ubiquitylation sites – K281R, K288R, K328R, K329R, K269R, and K270R – was used to test this hypothesis.

The experiment was essentially performed as above, except that the strains used were either WT or $Def1_{6Ubm}$, and expressing the HA-tagged version of Ubx1 under the control of a GAL promoter from a plasmid. Strains carrying an empty plasmid were used as negative controls in this experiment. Again, the experiment was

performed both in the presence and absence of UV irradiation. Extracts were prepared by grinding yeast in LN, and the IP was carried out using anti-HA antibody.

Like in the previous experiments, the levels of Ubx1 seem to be decreased after UV treatment (Figure 3.12) Somewhat frustratingly, the interaction between Ubx1 and wild type Def1 in this experiment can be seen both in untreated and UV-treated conditions (lanes 7 and 15). More importantly, however, in both cases the interaction with wild type Def1 was clearly stronger than the interaction with $Def1_{6Ubm}$ (compare lane 7 with 8, and lane 16 with 17). This result suggests that the ubiquitylation of Def1 is required for the interaction with the Ubx1 protein.

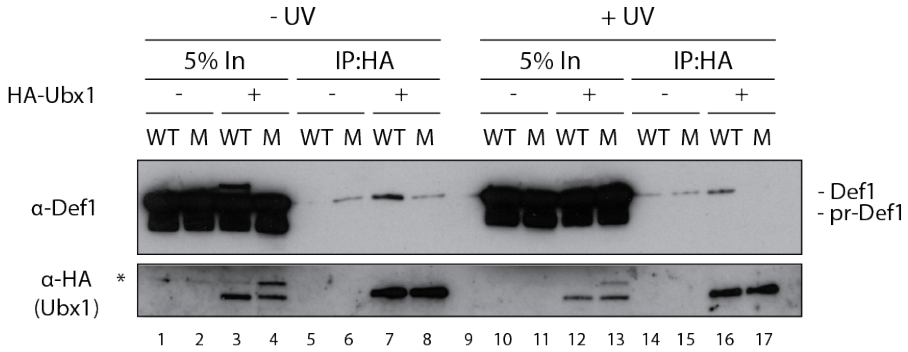

Figure 3.12. The interaction between Ubx1 and Def1 is decreased when ubiquitylation sites on Def1 are mutated.
W303 (WT) or *$Def1_{6Ubm}$* (M) strains were expressing HA-Ubx1 from a plasmid. The cells were either treated with UV (400 J/m^2) and allowed to recover for 1 h after UV, or left untreated. Extracts were prepared by grinding in LN (2.4.10). HA-IPs were performed in yeast lysis buffer (2.1.3.15) for 1 h at 4 °C. The anti-HA agarose beads were washed 3 times in 20 mM Tris pH 7.0, 200 mM NaCl, 0.01 % Triton X-100, 10 % glycerol. The results were visualised by Western blotting, using the indicated antibodies. WT – strain expressing wild type Def1; M – strain expressing the ubiquitylation site mutant of Def1.

3.3.4 Def1-Def1 interaction in Cdc48 degron strain

The role proposed for Cdc48 protein in Spt23 processing was that of a segregase. In other words, since Spt23 is normally dimeric and tethered to the ER membrane, the cleaved, active monomeric form of Spt23 (lacking the membrane-association domain) has to be released by Cdc48, from its unprocessed, membrane-associated partner to enter the nucleus (Rape et al. 2001). If Def1 and Spt23 processing were

to follow the same pattern and Def1 also acts as a dimer, a reaction intermediate – fl-Def1 bound to pr-Def1 – might form in the absence of Cdc48. An IP experiment was performed in the hope of capturing this intermediate and validating the function of Cdc48 in the processing reaction.

The previously discussed Cdc48 degron strain (3.1.1) was utilised for the experiment. It was either expressing Def1 with a C-terminal HA tag, or the wild type untagged copy of Def1 from a plasmid. For this experiment it was essential to have a C-terminal tag on Def1 to ensure that only the full-length form, but not the C-terminally truncated form (pr-Def1) was directly pulled down. The cultures were either treated with IAA or left untreated for 30 min before splitting each culture into two and exposing one of them to UV light.

An interaction between fl-Def1 and pr-Def1 could be observed, but only in the absence of Cdc48, and only after UV (Figure 3.13, last lane). Even though the co-precipitated pr-Def1 band was faint, the result was reproducible. It suggests that the function of Cdc48 is indeed in the separation of the activated (truncated) form of the protein from the inactive full-length Def1 form. This result also highlights the similarity between the processing of Def1 and Spt23, supporting the hypothesis for the existence of a general mechanism in partial proteasomal processing.

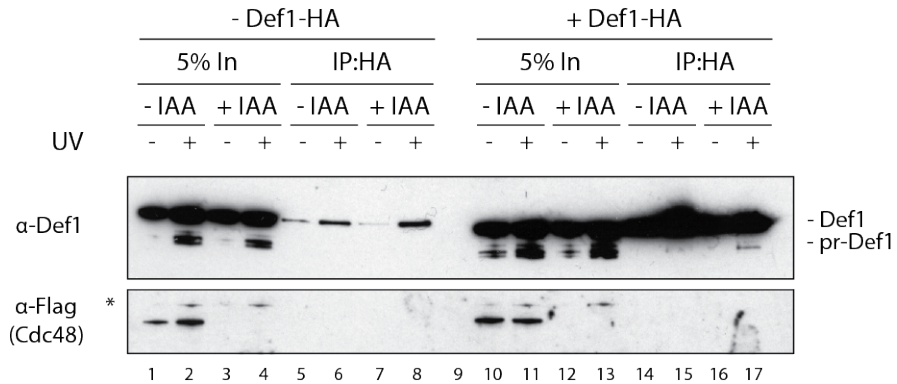

Figure 3.13. Capture of the fl-Def1/pr-Def1 intermediate in the absence of Cdc48. Yeast cultures were treated ± degradation inducer IAA 30 min before the ±UV treatment (400 J/m^2). Yeast cultures were immediately processed by grinding in LN. IPs were performed in yeast lysis buffer (2.1.3.15) for 1 h at 4 °C with anti-HA agarose to IP fl-Def1. The beads were washed 4 times in 20 mM Tris pH 7.0, 500 mM NaCl, 0.01 % Triton X-100, 10 % glycerol. The results were visualised by Western blotting, using the indicated antibodies.

3.4 Model for Def1 processing

All the experiments described in this chapter point to the involvement of Cdc48 and the UBX domain adaptor protein, Ubx1, in Def1 processing. Combining this information and drawing a parallel between Def1 and Spt23 partial proteasomal processing, a model of Def1 processing emerges (Figure 3.14).

Def1-Def1 interaction was captured in fl-Def1/pr-Def1 form in the absence of Cdc48 and after UV damage. Whether it is arising in response to DNA damage and in the presence of specific PTMs remains to be tested. Additionally, there is some evidence indirectly pointing to the fact that such an interaction should exist: toxicity of $Def1_{1\text{-}500}$ can be overcome by co-expressing it with fl-Def1. For these reasons, Def1 is depicted as a dimer, although multimerisation cannot be refuted.

As it has been shown previously, in response to UV damage Def1 becomes mono-ubiquitylated by Rsp5 (Wilson, Harreman, Taschner, et al. 2013). My data indicate that subsequently, this ubiquitylation signal is recognised by the UBA domain in Ubx1, and Ubx1 recruits Cdc48. The proteasome performs the Def1 processing reaction, removing the C-terminus, and Cdc48 then dissolves the fl-Def1/pr-Def1 species, freeing pr-Def1 to accumulate in the nucleus, where it can perform its function.

Interestingly, for the processing of Spt23 it has been proposed that Cdc48 is not only required for the resolution of Spt23 dimer, but that it also helps the proteasome with the actual cleavage step (Hitchcock et al. 2001; Kolawa et al. 2013). However, the processing of Spt23 was only investigated *in vivo* and in crude yeast extracts, meaning that the controversy over the exact function of Cdc48 has not been resolved. In an attempt to address the numerous outstanding questions about the biochemistry of Def1 processing, I set out to establish a reconstituted *in vitro* system using purified proteins (5). However, to ensure that I knew as many of the proteins required for Def1 processing as possible before starting work on this complex system, I decided to first investigate the relationship between Def1 and a high-copy suppressor of *Δdef1*, named Smy2.

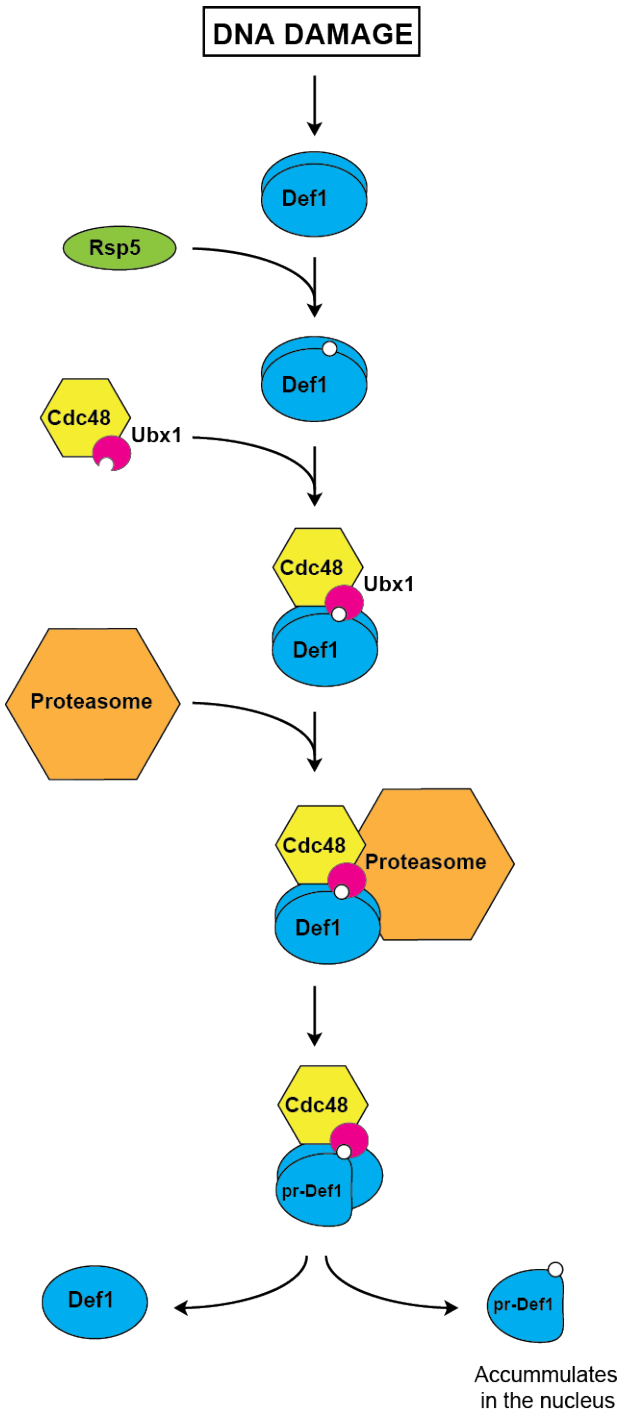

Figure 3.14. Def1 processing model.
A schematic representing the Def1 processing model. The processing requires the action of Rsp5, the proteasome the and Cdc48/Ubx1 complex. It remains unclear if Cdc48/Ubx1 is acting together with the proteasome or at a separate step. Little white circles on the Def1 protein represent ubiquitin.

4 The *Δdef1* phenotype suppressor *SMY2* is involved in the last resort pathway

Expression of *SMY2* from a high-copy plasmid was able to supress the slow growth *Δdef1* phenotype (3.2.6). This observation implies that increased levels of the Smy2 protein can compensate for the lack of Def1 function. We hypothesised that Smy2 is involved in the last resort pathway downstream of Def1 or in a parallel pathway for the removal of arrested RNAPII from chromatin and thus went on to further investigate the function of Smy2.

Very little is known about the Smy2 protein in yeast. It is a non-essential protein, which has previously been implicated in disparate processes such mRNA splicing, COPII vesicle formation, and transcriptional regulation of certain mRNAs (Ash et al. 2010; Sezen et al. 2009). The only defined domain in the protein sequence is the glycine-tyrosine-phenylalanine (GYF) domain, which was shown to bind proline-rich sequences (Kofler et al. 2005). With no obvious connection to Def1 or the last resort pathway, we started our investigations from an expanded set of genetic interaction tests. I note that this part of my project was a close collaboration with Michelle Harreman, and that several figures in this chapter were produced by her. When this is the case, the (sub)figure in question has been labelled accordingly.

4.1 *SMY2* is a high-copy suppressor of *Δdef1* phenotype

Further studies of *SMY2* ability to supress *Δdef1* phenotype lead to the discovery that the GYF domain was potentially involved in the process (Figure 4.1 A). A yeast spotting assay (2.4.5) was performed with the *Δdef1* strain, expressing *SMY2* from a plasmid. Since the *Δdef1* phenotype is exacerbated at higher temperatures, three temperatures were compared – 25, 30, and 37 °C. Only *SMY2* expressed from a *2μ* plasmid showed a full suppression of the *Δdef1* slow growth phenotype. Wild type *SMY2* expressed from a *CEN* plasmid exhibited only a partial suppression, indicating that the levels of Smy2 have to be increased to be able to compensate for the lack of Def1 in the cell. The GYF domain mutant, carrying a Y234A mutation which disrupts binding to proline-rich sequence (Kofler et al. 2009), expressed from

a *2μ* plasmid also showed only partial suppression. We also observed that a C-terminal tag on Smy2 decreased its ability to suppress the *Δdef1* phenotype, indicating that tagging the C-terminus of Smy2 is detrimental for its function, and for all subsequent experiments Smy2 protein was therefore N-terminally tagged.

High-throughput proteomics screen has previously reported that Smy2 could be found in a complex with Cdc48 (Krogan et al. 2006). I examined how deletion of *SMY2* affected *cdc48-3, npl4-1,* and *ubx1-ts* temperature sensitive strains (Figure 4.1 B). Deletion of *SMY2* did not have a significant effect on the temperature sensitivity of *cdc48-3* and *ubx1-ts*, but showed a slight suppression of the *npl4-1* temperature sensitivity at 30, but not 37 °C. Expression of *SMY2* from a high-copy plasmid failed to rescue cells depleted for Ubx1, and in fact decreased the growth (Figure 4.1 C), while a *Δubx1 Δsmy2* double mutant in the BY4742 background seemed to be slightly more slow-growing compared to *Δubx1* alone, indicating that *SMY2* deletion has a slightly negative effect on the *Δubx1* strain.

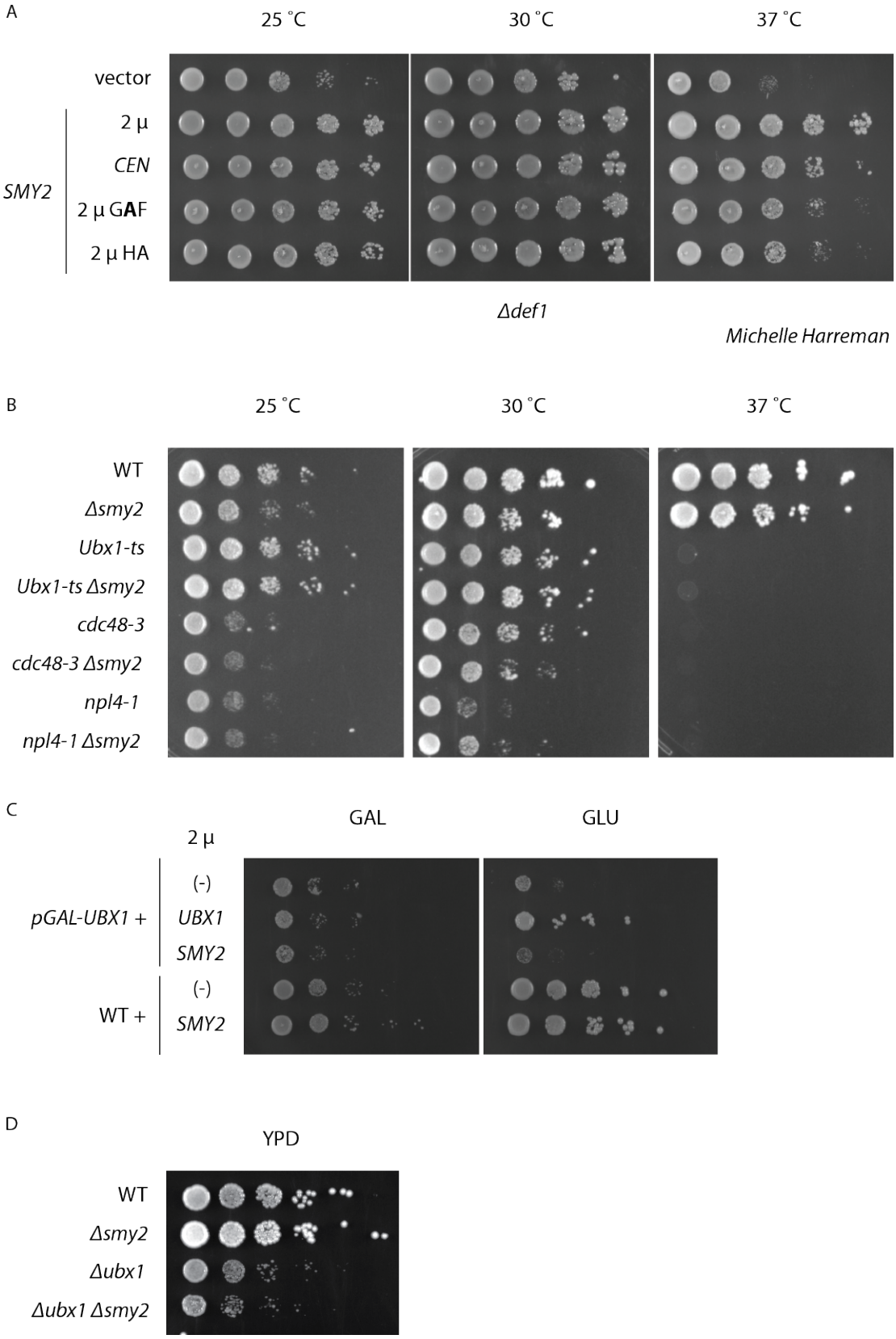

Figure 4.1. Smy2 genetic interactions.
A – a spotting assay of 1:10 dilution series of the *Δdef1* strain expressing wild type copy of *SMY2* from its own promoter in *CEN* and *2 µ* plasmids, as well as the Smy2

GYF domain mutant (GAF) and Smy2 with a C-terminal tag, both also from a *2 μ* plasmid. Grown on selective plates at 25, 30 and 37 °C, as indicated. ***B*** – The effect of *SMY2* deletion in *cdc48-3, Ubx1-ts,* and *Npl4-1* temperature-sensitive strains. The strains were grown on YPD plates for 3 days at the indicated temperatures. 1:10 dilution series are shown. ***C*** – Expression of *SMY2* and *UBX1* from their own promoter on *2 μ* plasmids in *pGAL_Ubx1* strain. The strains were grown in galactose and then plated on selective plates with either glucose or galactose, and grown at 30 °C for 3 days. 1:10 dilution series are shown. ***D*** – Deletion of *SMY2* in the *Δubx1* strain, in the BY4742 background. Grown at 30 °C on a YPD plate for 3 days. 1:10 dilution series were performed

4.2 Def1 processing is perturbed in the absence of Smy2

While the connection between Smy2 and Cdc48 has been previously suggested in high-throughput interaction and genetic screens (Krogan et al. 2006; Magtanong et al. 2011), and my data from (3.2.1) demonstrated that Cdc48 might be involved in Def1 activation, the next step was to look whether the absence of Smy2 affected Def1 ubiquitylation and processing *in vivo.* Def1 ubiquitylation state was assessed in a MultiDSK experiment (2.5.8). As can be seen in Figure 4.2 A, the *Δsmy2* strain had elevated levels of ubiquitylated Def1 (ub-Def1) even at timepoint 0, without DNA damage, and did not show an increase in response to 4NQO treatment (compare lanes 1 and 2 with lanes 6 and 7). This result indicated that Smy2 might be involved in the ubiquitin signalling system, or processes affecting Def1 upstream of its ubiquitylation.

Next, Def1 processing was investigated in the *Δsmy2* strain. An *in vivo* Def1 processing assay was performed with two independent clones of *Δsmy2* (Figure 4.2 B). The *SMY2* genomic copy was either replaced with a HIS (left panel) or a TRP marker (right panel). Both strains were behaving similarly in terms of Def1 processing. In response to 4NQO treatment, Def1 processing was delayed in the *Δsmy2* strain. Since Def1 ubiquitylation in this strain was elevated (Figure 4.2 A), it is reasonable to hypothesise that higher levels of ub-Def1 accumulate when Def1 cannot be processed effectively and that Smy2 might be directly involved in Def1 processing.

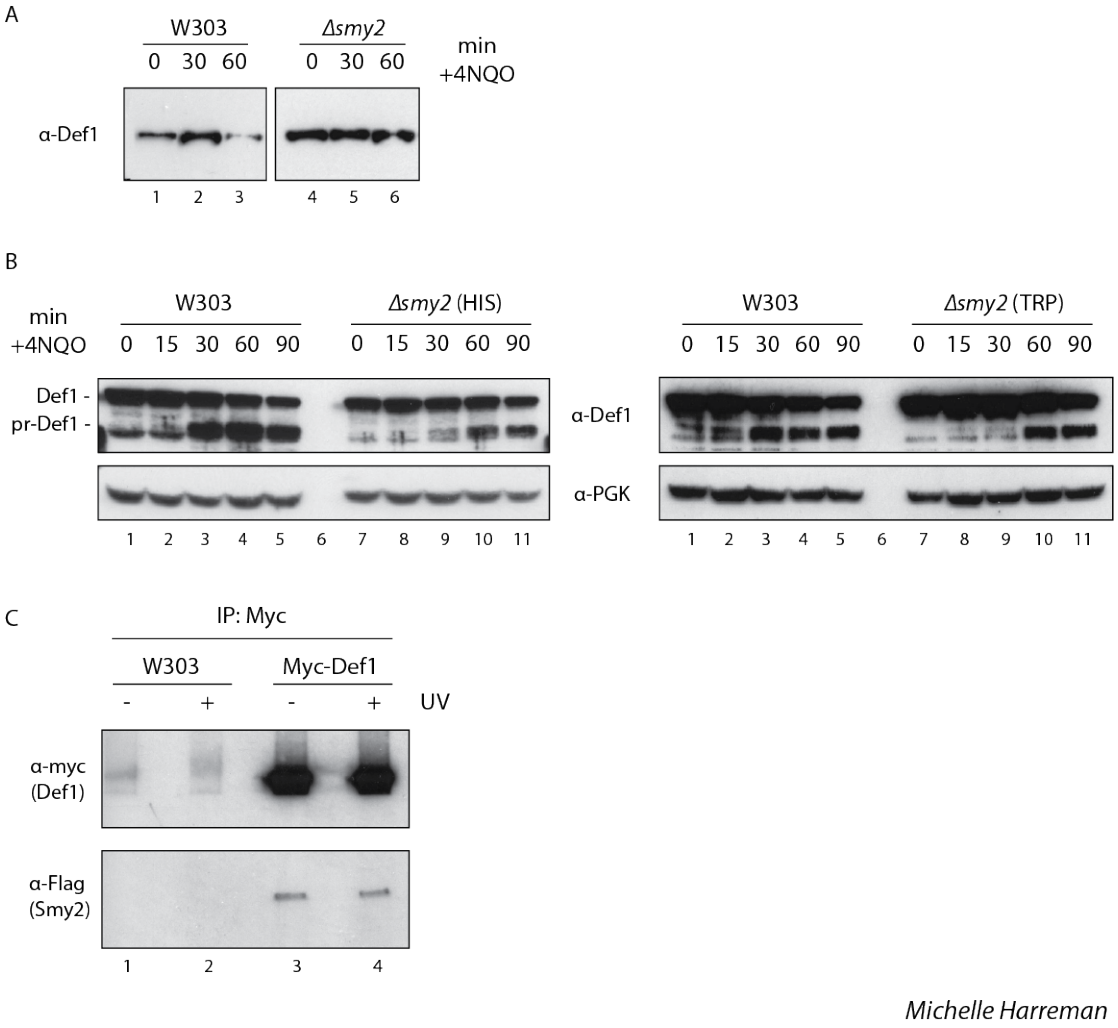

Figure 4.2. Involvement of Smy2 in Def1 activation.
A – Def1 ubiquitylation state in *Δsmy2*. Yeast strains were treated with 4NQO and cell extracts made at the indicated timepoints. A MultiDSK pulldown was performed and ub-Def1 was visualised by Western blotting with the α-Def1 antibody. ***B*** – Def1 processing in response to 4NQO treatment in the *Δsmy2* strain. Two independent *Δsmy2* strains were used for the experiment. Def1 processing in extracts was visualised by Western blotting using α-Def1 antibody. PGK was used as a loading control. ***C*** – Myc-Def1 IP from yeast extracts ±UV. After UV damage cultures were recovered for 1 h before performing the IP. A strain expressing wild type Def1 was used as negative control. The results were visualised by Western blotting.

To investigate the hypothesis that Smy2 is directly involved in Def1 processing, the putative interaction between these proteins was investigated (Figure 4.2 C). Cells were either treated with UV, or not, and allowed to recover for 1 hour. Myc-Def1 IP was then performed from the cell extracts. A control IP was done from extracts of cells expressing Def1 without a tag. Def1 clearly co-precipitated Smy2 (compare lanes 1 and 2 with 3 and 4), but UV treatment did not appear to change the interaction (compare lanes 3 and 4). This interaction gave me a rationale to include

Smy2 into the *in vitro* Def1 processing assays (5) and to further investigate its role in Def1 processing.

4.3 Smy2 association with Cdc48

Smy2 was previously found in a complex with Cdc48 in a high-throughput screen (Krogan et al. 2006), and, as mentioned above, it was also detected as a high-copy suppressor of *cdc48-3* temperature sensitive phenotype at 30, but not 37 °C in a genetic screen (Magtanong et al. 2011). These results were also independently confirmed in the Svejstrup lab (Michelle Harreman). Thus the relationship between Smy2 and Cdc48, and their involvement together in the last resort pathway, was further investigated.

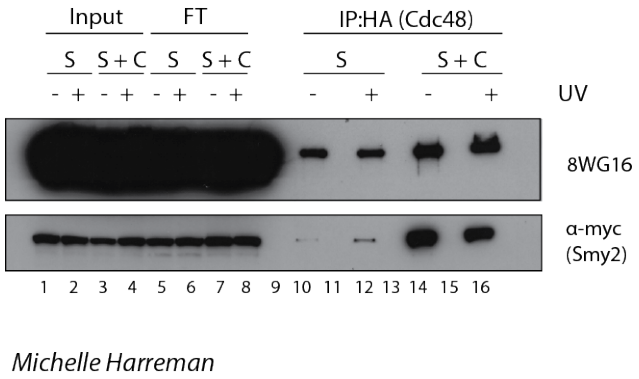

Michelle Harreman

Figure 4.3. Smy2 interacts with Cdc48 *in vivo.*
Cdc48 IP from yeast extracts ±UV. After UV damage cultures were recovered for 1 h before performing the IP. A strain lacking a tagged version of Cdc48 was used as a negative control, labelled S (for Myc-Smy2 only), the strain also expressing Cdc48-3HA is labelled S+C (for Myc-Smy2 + Cdc48-3HA). The result was visualised by western blotting using 8WG16 antibody to detect Rpb1 and α-myc for Smy2.

The interaction of Cdc48 with Rpb1 and Smy2 was investigated by co-IP in yeast cells either treated with UV, or not, and allowed to recover for 1 h at 30 °C (Figure 4.3). While Rpb1 showed non-specific interaction with the anti-HA agarose even in the absence of Cdc48 (lanes 10 and 12 top panel), Cdc48 was able to co-precipitate a small fraction of Rpb1 both in the presence and absence of UV treatment (lanes 14 and 16 top panel). The very modest level of interaction was expected, since Cdc48 was hypothesised to only interact with arrested RNAPII (Verma et al. 2011). More importantly, Cdc48 was able to efficiently pull down the

Smy2 protein, both in the absence and presence of UV treatment (compare bottom panel lanes 10 and 12 with lanes 14 and 16). Overall, these results further supported the hypothesis that Smy2 is involved in the last resort pathway and suggested that it might be working together with Cdc48.

To examine this hypothesis further, the interaction between Cdc48 and Smy2 was investigated *in vitro* using purified proteins. Cdc48-3HA protein bound to anti-HA agarose (Figure 4.4 A) was incubated for 1 h at 4 °C with Smy2 protein purified from *E. coli* (2.6.9). Given that Cdc48 is an ATPase, the incubation was performed both in the presence and absence of ATP. In the reaction where ATP was added, the ATP-regenerating system (ARS, 2.1.3.14) was also present. As can be seen from Figure 4.4 B lanes 4, 5, and 6, fl-Smy2 did not seem to bind Cdc48-3HA much above the background level. Given the results above, this was unexpected. One possibility is that for the binding to occur, post-translational modifications on Smy2 are needed, so that Smy2 purified from a recombinant source is unable to bind. It is also possible that the interaction between the two proteins is very weak and transient, and that a higher concentration of proteins is needed to detect the interaction.

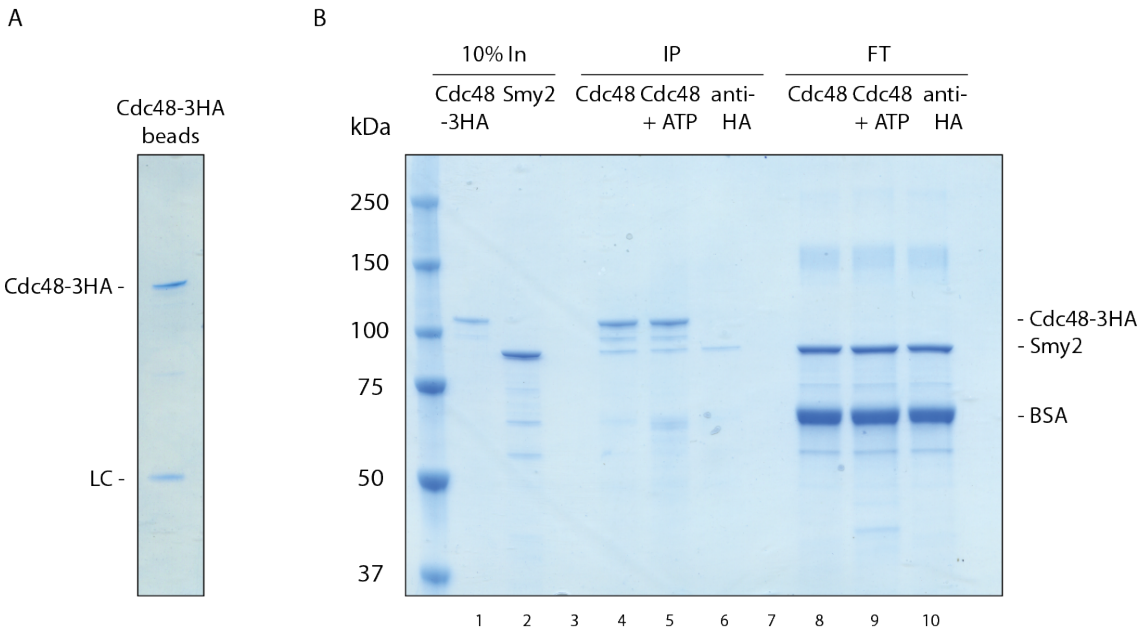

Figure 4.4. The interaction between purified fl-Cdc48 and fl-Smy2.
A – Cdc48-3HA beads used in the *in vitro* reactions. LC – light antibody chain.

B – fl-Smy2 purified from *E. coli* (2.6.9) was incubated with Cdc48-3HA beads ± ATP. ATP regeneration mix (ARS, 2.1.3.14) was added to the reaction with ATP. The results were visualised by SDS-PAGE. Anti-HA agarose was used as a negative control.

Much higher concentrations could be achieved from the purification of the Smy2 GYF domain (Smy2 amino acids 205-261). The interaction between the GYF domain and full-length Cdc48 was tested *in vitro* with purified proteins. The GST, GST-GYF, and GST-GAF domains were purified from bacteria (Michelle Harreman), and I purified Cdc48-Flag as well as Cdc48-3HA from yeast (2.6.6, 2.6.5, 5.1.3). As can be seen from (Figure 4.5 A), both GST-GYF and GST-GAF, but not GST alone, were able to interact with Cdc48 (compare lanes 13 and 16 with lane 10). Interestingly, the mutation of the tyrosine residue implicated in poly-proline binding did not markedly affect the interaction with Cdc48 (compare lanes 13 and 16).

To confirm these results, the reverse pulldown was performed, with Cdc48-3HA immobilised on beads and free GST and GST-GYF constructs (Figure 4.5 B). This experiment gave the same result – both GYF and the GYF domain mutant were able to interact with Cdc48, while no interaction was detected between Cdc48 and GST alone. Nevertheless, more experiments are needed to establish the suitable conditions for the interaction between the full-length proteins.

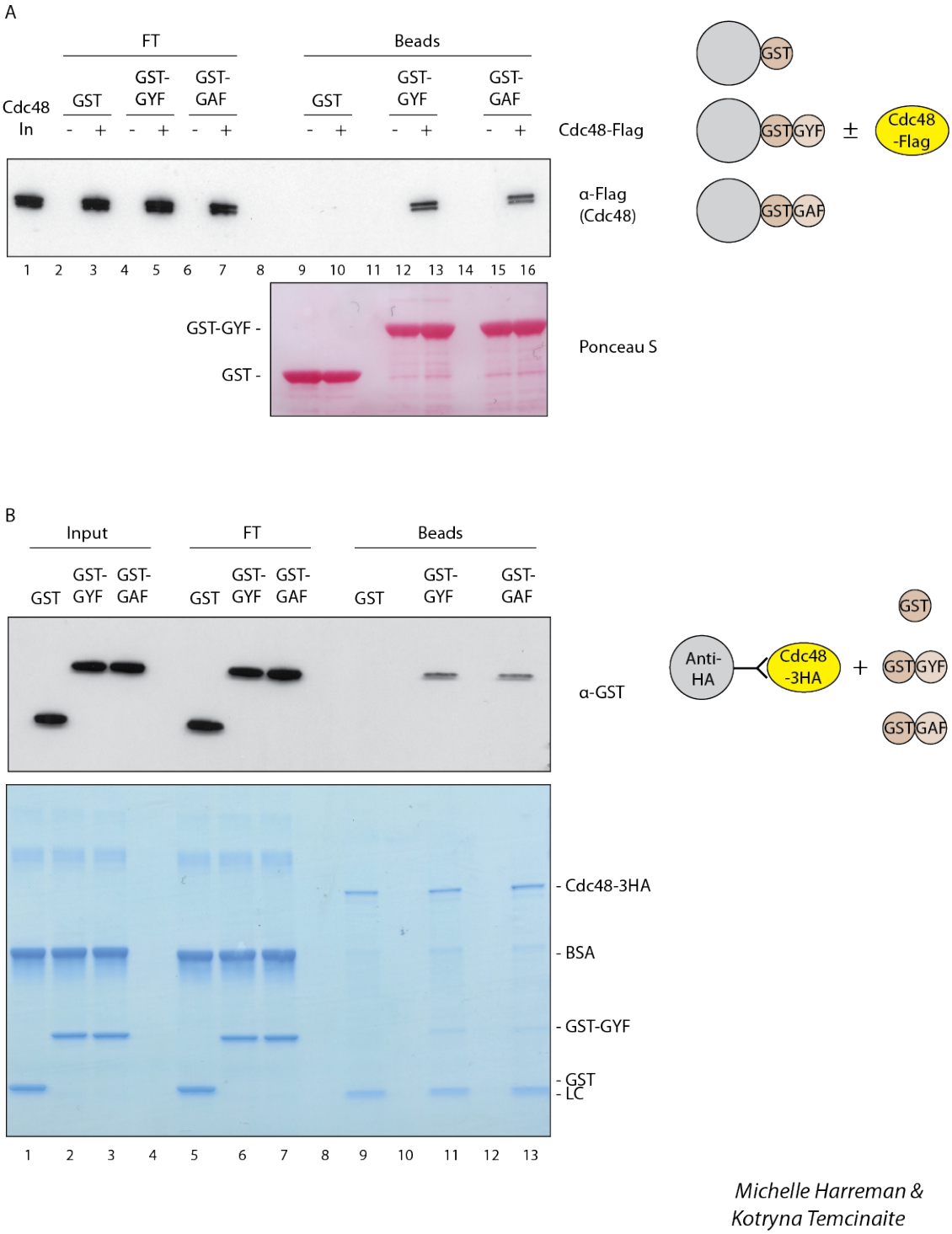

Figure 4.5. The interaction between the purified Smy2 GYF domain and the Cdc48 protein.
A – The beads with either GST alone, GTS-GYF or GST-GAF were incubated with purified Cdc48-Flag protein, before washes and visualisation of the result by Western blotting. Ponceau S staining was used to visualise the beads. Experimental strategy is depicted in the right panel. Cdc48-Flag was purified from yeast with overexpression (5.1.3), while GST, GST-GYF, and GST-GAF were purified from *E. coli*. ***B*** – A reverse interaction between Cdc48 and GST-GYF constructs. Cdc48-3HA (2.6.5) bound to

beads was incubated with GST alone, GST-GYF and GST-GAF before washes and visualisation of the result by both Western blot (upper panel) and SDS-PAGE (lower panel). The experimental strategy is also outlined on the right. LC – light antibody chain.

4.4 Smy2 as a general Cdc48 cofactor

Even if the interaction between Smy2 and Cdc48 is transient and difficult to detect in pulldown assays, Smy2 might still be able to influence the function of Cdc48. Therefore, the ability of Smy2 to influence the ATPase activity of Cdc48 was investigated. The first experiment was done by performing an ATPase assay (2.7.4) with Cdc48 and Smy2 that I had purified from yeast (5.1.3) (Figure 4.6 A). Increasing amounts of Smy2 were added to the reaction immediately prior to the start of the reaction by the addition of ATP. Smy2 did not have a measurable effect on the ability of Cdc48 to hydrolyse ATP.

The effect of Smy2 was further investigated in a timecourse experiment. This experiment was performed to test if Smy2 might change the kinetics of the ATPase reaction. This time Cdc48 was pre-incubated with Smy2 for 30 min on ice prior to the start of the reaction (Figure 4.6 B). Since Smy2 and Cdc48 proteins were in different buffers, the salt concentration was carefully adjusted between the samples. Interestingly, the presence of Smy2 in the reaction seemed to stimulate the Cdc48 ATPase activity and doubled the amount of Pi released over the 15 min period.

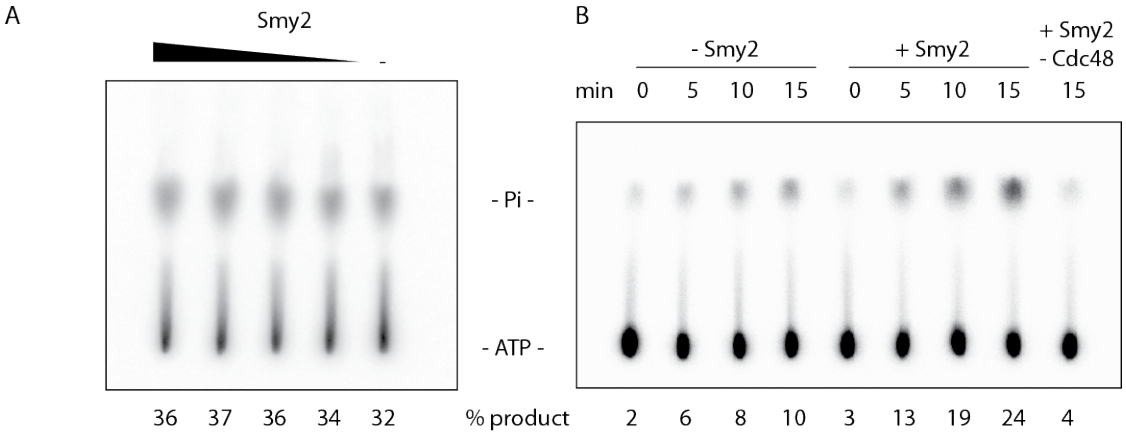

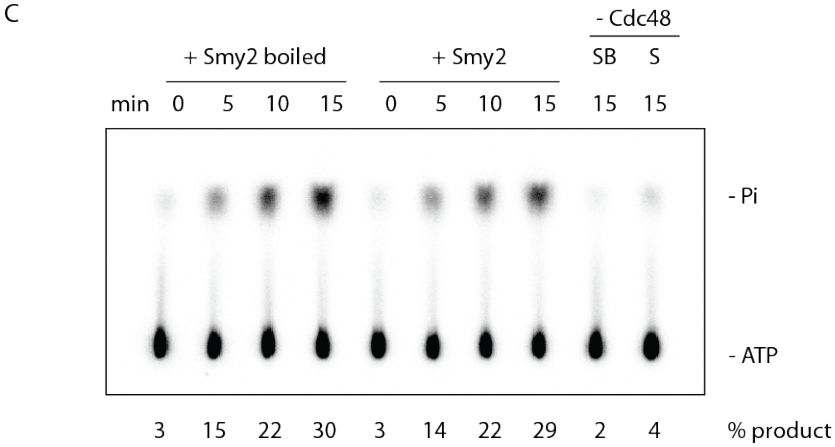

Michelle Harreman

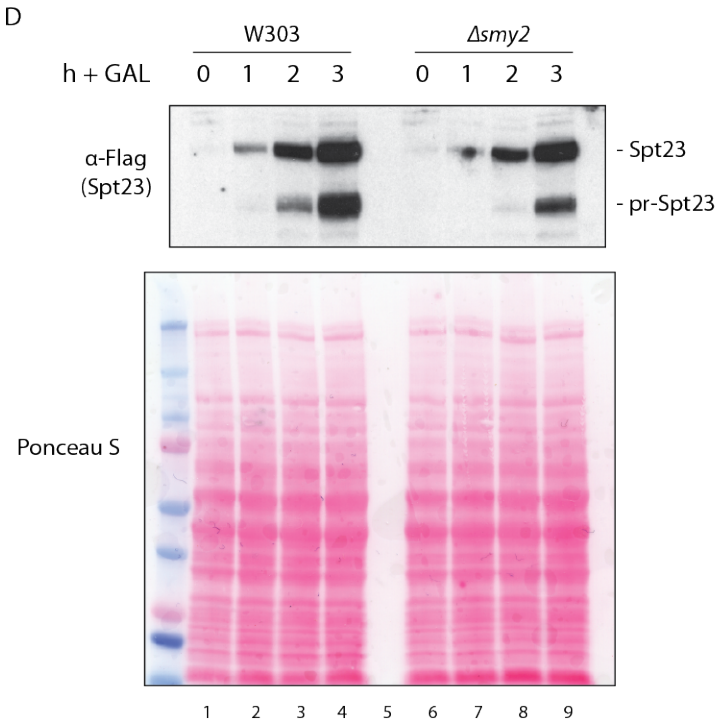

Figure 4.6. Smy2 as a general Cdc48 cofactor.
A – Smy2 purified from *E. coli* was added to the Cdc48-3xFlag ATPase reaction (2.7.4). The reactions were performed with 33.5 nM Cdc48-3xFlag and Smy2 concentrations from left to right: 1.04 μM, 0.52 μM, 0.26 μM, and 0.13 μM. The reaction was performed at 30 °C. Results were visualised by thin layer chromatography (TLC) and radiography. ***B*** – The ATPase assay was performed by pre-incubating Cdc48 and Smy2 for 30 min on ice before the addition of the ATP mix. Cdc48-3xFlag was used at 33.5 nM concentration and Smy2 at 1 μM. The reaction was performed at 30 °C. ***C*** – the reaction was performed in the same manner as ***B***, except Smy2 was boiled for 5 min at 95 °C before the incubation with Cdc48. SB – Smy2 boiled, S – Smy2. ***D*** – The function of Smy2 as a general Cdc48 cofactor. 3xFlag-Spt23 was expressed from a plasmid under a GAL promoter in wild type and the *Δsmy2* strain. Processing of Spt23 happens spontaneously after the induction of protein expression. Extracts were prepared as described (2.4.13). Spt23 processing was visualised by Western blotting using α-Flag antibody. Ponceau S staining was used to assess equal extract loading. Note that SMY2 deletion has little effect on Spt23 expression, but a clear effect on its processing.

To additionally control for the fact that the Smy2 protein was in a different buffer compared to Cdc48 and validate the previous result, an experiment was performed where Smy2 was boiled for 5 min at 95 °C before the addition to the reaction (Figure 4.6 C). Disappointingly, there was no difference between the boiled Smy2 and native Smy2. This result implied that the protein was either able to re-nature after boiling, or that an unknown component in the Smy2 buffer was contributing to the increased ATPase activity of Cdc48 in Figure 4.6 B. Recently, upon further investigation we noted that others have suggested that Triton X-100 may stimulate p97 activity by helping it to release bound ADP or by decreasing aggregation/non-specific adhesion (Chou et al. 2014), and my Smy2 preparation contained 0.01 % Triton X-100. However, the final Triton X-100 concentration in our reaction was lower than that tested by Chou *et al*. In order to investigate the effect of Smy2 on Cd48 ATPase activity, the experiments will need to be repeated with a Triton-free preparation of the Smy2 protein.

Although much still need to be done, the experiments above open the possibility that Smy2 is a novel Cdc48 co-factor. Thus, it was relevant to investigate if Smy2 working together with Cdc48 was specific to the last resort pathway, or if it was also needed for other processes where Cdc48 is involved. For this purpose, the partial proteasomal processing of the Spt23 protein was investigated in the *Δsmy2* strain. In the absence of oleic acid in the medium, Spt23 is constantly processed in yeast cells. It was previously shown that Cdc48 is involved in Spt23 processing (Rape et

al. 2001). To investigate whether Smy2 is also required for this process, I expressed Flag-tagged Spt23 from a galactose-inducible promoter on a plasmid. Upon addition of galactose in the growth media Flag-Spt23 is expressed and processed to pr-Spt23 in wild type cells (Figure 4.6 D, lanes 1-4). Importantly, however, such processing was clearly delayed in the *Δsmy2* strain (lanes 6-9), suggesting that Smy2 is a general Cdc48 co-factor, and not specific for the last resort pathway.

4.5 The role of Smy2 in the last resort pathway

Although more experiments are needed to fully define the function of Smy2 in the last resort pathway, its role is slowly emerging. The ability of *SMY2* to supress the *Δdef1* phenotype and its involvement in Def1 processing, as well as other data in the Svejstrup lab, lead to the hypothesis that Smy2 might be involved at a two distinct steps in the last resort pathway. Interestingly, the ubiquitin-dependent segregase Cdc48 is also implicated in two independent steps in the pathway (Figure 4.7). Our further experiments suggested that Smy2 is able to interact with Cdc48, although the molecular detail is still missing.

The ability of Smy2 over-expression to suppress the *Δdef1* phenotype indicates that Smy2 works downstream of Def1, possibly by stimulating the activity of Cdc48. On the other hand, Def1 processing was delayed in the absence of Smy2, implicating the Smy2 protein in processes upstream of or at the activation of Def1. Importantly, we were able to show that Smy2 is not specific to the last resort pathway, but is also required for the partial proteasomal processing of the transcription factor, Spt23. This observation suggests a more general role for Smy2. We also found that Smy2 associates with Cdc48, irrespective of DNA damage, in agreement with the hypothesis of Smy2 having a role in Cdc48 function. Nevertheless further experiments are needed to understand what the exact function of Smy2 is as well as if and how Smy2 modulates the activity of Cdc48, before classifying Smy2 as a novel Cdc48 co-factor.

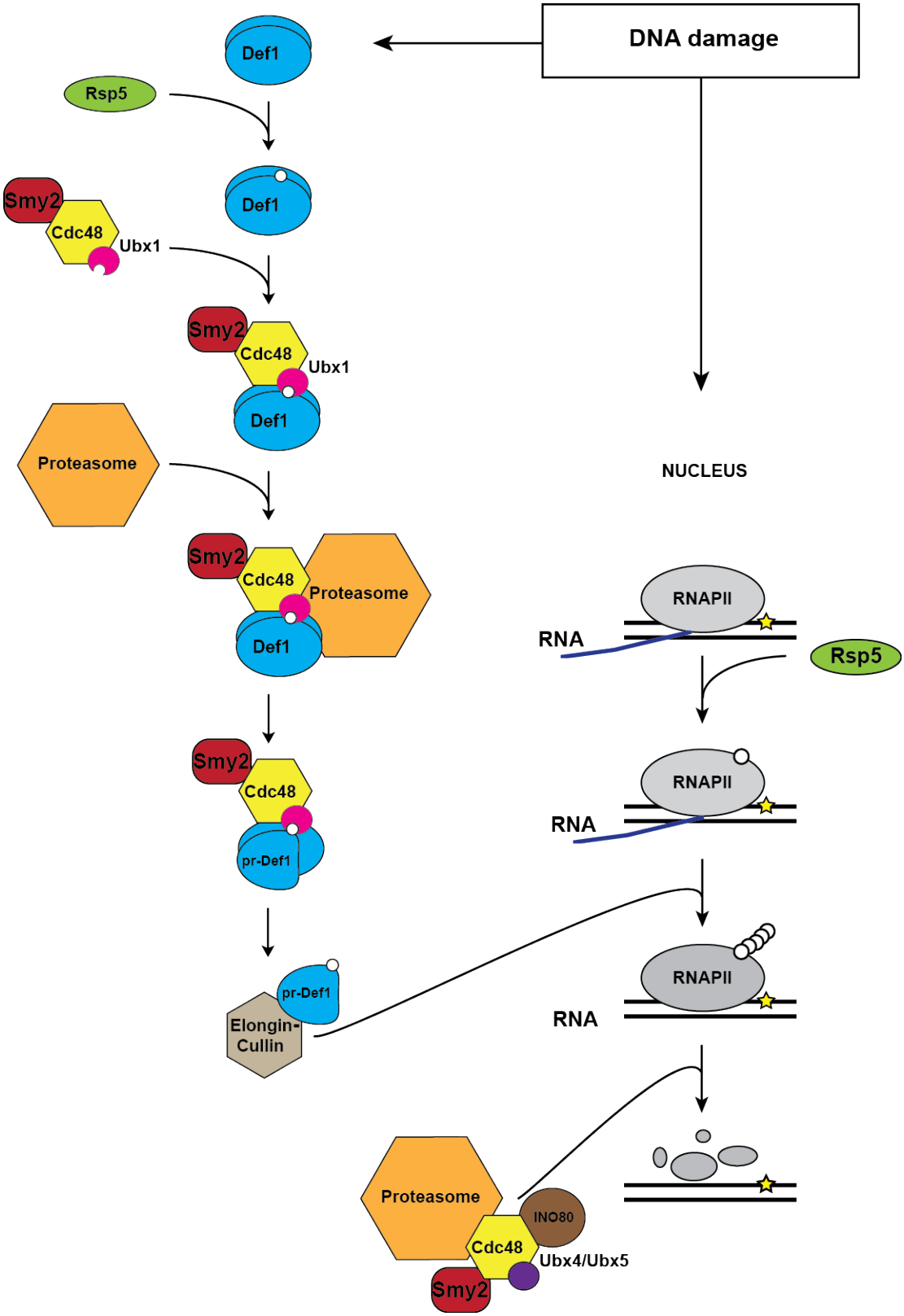

Figure 4.7. The model of Smy2 role in the last resort pathway.
A schematic representation of the last resort pathway. Smy2 protein (red) might be involved in both steps requiring Cdc48. In response to DNA damage Def1 becomes

ubiquitylated by Rsp5. This modification allows Ubx1 to bring Cdc48 and Smy2 to Def1 and the 26S proteasome follows. After the cleavage step is complete Cdc48 acts as a segregase to separate pr-Def1 from fl-Def1. As a result, pr-Def1 can accumulate in the nucleus and bring Elongin-Cullin complex to a stalled mono-ubiquitylated RNAPII to poly-ubiquitylate it. This results in the disassembly of the complex performed with Cdc48 and Ubx4 or Ubx5 adaptors, and Smy2 might also be involved in this step and the degradation of the largest RNAPII subunit Rpb1 by the proteasome.

5 Reconstitution of Def1 processing *in vitro*

In spite of the interesting and very unusual nature of proteasomal protein processing, there is currently no reconstituted *in vitro* assay for studying the process, even for such well-described examples as the Spt23 protein. I aimed to develop a novel *in vitro* assay for partial proteasomal processing using highly purified proteins, with Def1 as the processing substrate, in order to delineate the molecular detail of the reaction and assign an exact function to each of the components involved. Reconstitution of Def1 processing *in vitro* would also allow me to answer a long-standing question of the Cdc48 function in partial proteasomal processing. Since the discovery of the involvement of Cdc48 in the processing of Spt23 (Rape et al. 2001) it has remained unclear whether Cdc48 is required only *after* processing by the proteasome, or if it is needed before processing, e.g. to guide and stimulate the proteasome.

Another advantage of *in vitro* studies with pure proteins would be the determination of the protein sequence and structure requirements for the partial proteasomal processing. Even though some elements, such as an unstructured region in proximity to ubiquitylation sites and a strongly-folded domain have been suggested as being necessary for the proteasomal action on Ci and NF-κB (Tian et al. 2005; Piwko & Jentsch 2006), more information is needed to be able to predict if a protein would be susceptible to regulation by partial proteasomal processing. For example, being able to perform the *in vitro* processing reaction on Def1 point mutants and truncated versions would facilitate further understanding of the sequence and structure specificity for Def1 processing.

In vivo studies helped me to identify several proteins that are involved in Def1 processing. However, these experiments were not sufficient to elucidate the role of each player. For example, the involvement of Cdc48, Rsp5, and Smy2 proteins at two independent steps in the last resort pathway hindered the investigation of their direct function in Def1 processing *in vivo*, due to the difficulty in functionally separating the two steps in the pathway.

The information gathered from *in vivo* experiments and combined with insights from published material would potentially allow us to draw conclusions on both the processing of the Def1 protein and the general mechanism of partial proteasomal processing.

5.1 Purification of reaction components

The first step in reconstituting Def1 processing was purification of all the known components. The functional competency of the components also had to be assessed. Different approaches as required were taken for purifications of Def1, Cdc48, the 26S proteasome, Ubx1, Ubx5, and Smy2 proteins. Not all the proteins needed for the assay had previously been purified, or purified to the standard required; hence a substantial effort was put into optimising these purifications. Purification strategies and their outcomes are described in the subsequent sections.

5.1.1 Def1 purification

A good preparation of the Def1 protein was central to reconstituting the processing reaction *in vitro*. Thus a lot of effort was put into Def1 purification and ensuring that the reaction was not carried out on a suboptimal sample.

The initial strategy for Def1 purification was purifying Def1 from yeast. As Def1 is an abundant protein, overexpression was not necessary. The main challenge of this approach was isolating the full-length protein from any pr-Def1 and degradation species that invariably arise in cells over the course of sample preparation. In order to minimise the likelihood of other Def1 forms co-purifying with fl-Def1, the protein was tagged with a C-terminal 6xHis-2xTev-9xMyc tag at the endogenous locus. The tagged strain (Def1-HTM, Figure 5.1 A) did not show the growth defect associated with the loss of Def1 (*Δdef1*, Figure 5.1 A), and the C-terminally tagged Def1 protein was previously used in the Svejstrup laboratory for Rpb1 ubiquitylation studies; thus the tagged protein was deemed functional.

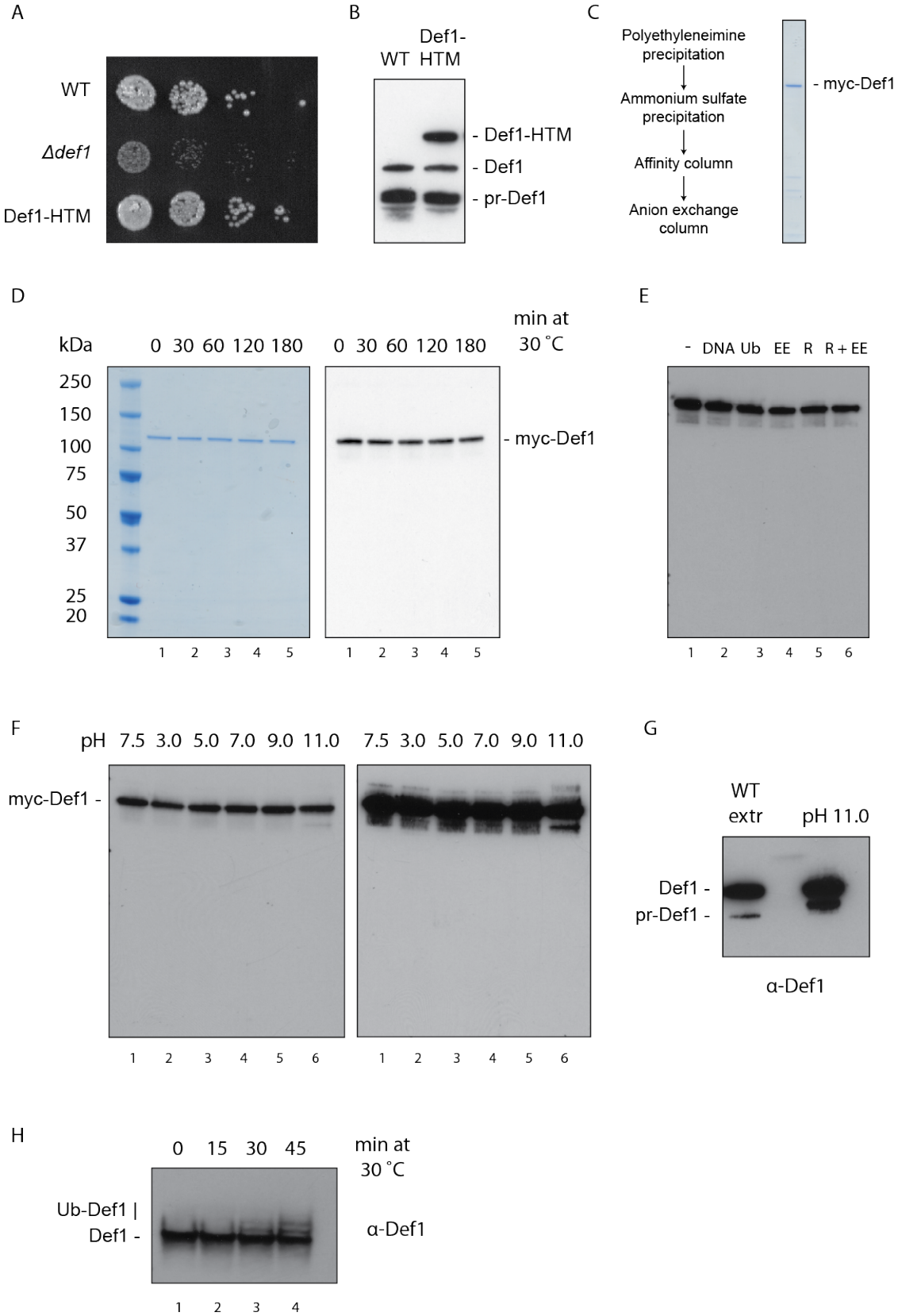

Figure 5.1. Recombinant Def1 purification and functionality tests.
A – Spotting assay of Def1-HTM strain. The strains were spotted and grown on YPD plates for 3 days at 30 °C. 1:10 dilutions were used. ***B*** – Western blot comparison of

Def1 species from wild type and Def1-HTM strains. Extracts were prepared by quick sodium hydroxide extraction (2.4.12). Results were visualised by Western blotting using α-Def1 antibody. ***C*** – Purification strategy for recombinant Myc-Def1 (on the left) and the purified sample visualised by SDS-PAGE. ***D*** – Myc-Def1 stability assay. Myc-Def1 was incubated for up to 180 min at 30 °C. Samples were taken at the indicated timepoints and the results were analysed by SDS-PAGE (left panel) and Western blot using α-Def1 antibody (right panel). ***E*** – Def1 stability assay in the presence of known interactors of Def1. Ub – free ubiquitin; EE – Ela1/Elc1 complex; R – RNAPII, R+EE – RNAPII together with Ela1/Elc1. Proteins were incubated for 17 h at 30 °C. Results were visualised by Western blotting using α-Def1 antibody. ***F*** – Myc-Def1 stability at different pHs. Def1 was incubated for 17 h at 30 °C in glycine buffer (pH 3.0), phthalate buffer (pH 5.0), Tris buffer (pH 7.0 and pH 9.0), and sodium bicarbonate buffer (pH 11.0). The results were visualised by Western blotting using α-Def1 antibody. Short exposure on the left, long exposure on the right. ***G*** – a comparison between Def1 species arising at pH 11 and pr-Def1 from yeast extract by Western blot using α-Def1 antibody. ***H*** – Ubiquitylation of Myc-Def1 *in vitro* using purified ubiquitylation factors. The reactions were incubated at 30 °C for the indicated periods of time. Results were visualised by Western blotting using α-Def1 antibody.

DEF1-HTM was the only source of Def1 in the cells, however, Def1-HTM protein was discovered to be losing the tag (Figure 5.1 B). As can be seen from the figure, when detected by an anti-Def1 antibody, the Def1-HTM strain (on the right) had three species of the Def1 protein – the tagged copy, the untagged copy, and the processed form. When compared to the wild type strain (on the left), there was no size difference between the untagged species in Def1-HTM strain and the wild type Def1. The apparent loss of the tag in a sizeable fraction of Def1 molecules was a concern, as it might conceivably only be the tag-less versions of Def1 that retained the functionality indicated by the data in Figure 5.1 A. It is worth noting that the identical size of pr-Def1 from both strains was expected, as for the generation of this Def1 form the C-terminus of the protein is removed by the proteasome. Overall, it was impossible to tell whether the loss of the tag was happening before or after the opening of the cells. It was therefore decided not to pursue purification from this strain due to the uncertainty surrounding functionality, and a different approach was taken.

The next approach was overexpression and purification of recombinant Def1 from *Escherichia coli* (2.6.1). The challenge of separating pr-Def1 and fl-Def1 was eliminated by the fact that bacteria do not have the proteasome. Thus the use of bacterial expression system allowed for the utilization of an N-terminal tag on Def1, which had previously been found to not affect function in yeast (Wilson, Harreman,

Taschner, et al. 2013). Having an N-terminal tag also decreased the risk of the interference with the processing reaction, since it is the C-terminus of the protein that gets degraded during the processing reaction. Purification of recombinant Def1 also meant that the protein would not carry any PTMs, potentially providing us with an opportunity to investigate the role of PTMs in Def1 processing. On the other hand, it was obviously harder to ascertain whether the recombinant protein actually retains full function, as no *in vitro* assay for Def1 function currently exists.

The Def1 sequence was codon-optimised for better expression in *E. coli*. The protein was expressed as a GST-Myc-Def1 construct from a T7 promoter in pGEX_6p1 vector. The precision protease site after the GST tag allowed for easy removal of the big GST tag, which is also prone to dimerise. After several rounds of optimisation, the purification strategy outlined in Figure 5.1 C was devised (2.6.1). In short, after the lysis of bacteria and extract clarification by centrifugation, a polyethyleneimine precipitation was performed to remove nucleic acids from the extract. It was followed by an ammonium sulfate (AS) precipitation. The AS pellet was solubilised and bound to glutathione sepharose beads. After bead washes, cleavage of the GST tag was performed on the column and the Myc-Def1 protein was eluted. The protein was further cleaned up and concentrated on a MonoQ column. The purification resulted in a fairly homogeneous Myc-Def1 sample (Figure 5.1 C).

Before starting the *in vitro* processing assays, the quality of the sample had to be ensured and potential experimental conditions for the assay investigated. The initial experiments were performed to investigate whether Myc-Def1 was stable at different conditions and did not spontaneously process into the pr-Def1 form. The possibility of auto-cleavage could not be ruled out, with examples of proteins capable of self-cleavage, such as the bacterial transcriptional repressor, LexA (Butala et al. 2009). The stability of Myc-Def1 was examined by incubation of either the Myc-Def1 protein alone (Figure 5.1 D) or with known interactors (Figure 5.1 E), reasoning that these might bind Def1 and allow it to adopt a conformation that is more favourable for self-cleavage. As can be seen from the figures, however, Def1 failed to be processed under any of these conditions.

Since auto-cleavage of the LexA protein can also be affected by pH (Lin & Little 1989), it was important to see the effect of different pH buffers on Def1 stability (Figure 5.1 F). Knowing Def1 stability at different pH buffers would also provide valuable information for the development of the *in vitro* processing assay. Myc-Def1 remained stable at all the pH values tested, except for the pH 11 buffer. At pH 11 a distinct faster migrating band crossreacting with the Def1 antibody appeared (last lane Figure 5.1 F). Incubating a protein in basic conditions may result in spontaneous hydrolysis at an exposed amide bond, thus this result might not have a physiological relevance.

A comparison between the faster migrating Def1 band resulting from the incubation at pH 11 and 'real' pr-Def1 resulting from Def1 processing *in vivo* was necessary to determine the physiological relevance of the band appearing at high pH (Figure 5.1 G). As the figure shows, pr-Def1 and the faster migrating Def1 species from pH 11 sample did not migrate identically. pH 11 is not a physiologically relevant condition, and the observed change was attributed to general base hydrolysis of Def1 at an exposed peptide bond.

Further experiments were performed to assess the ability of Myc-Def1 to become ubiquitylated. Since ubiquitylation by the Rsp5 ligase is a prerequisite for the processing reaction *in vivo* (Wilson, Harreman, Taschner, et al. 2013), a ubiquitylation assay (2.7.1) was performed. As Figure 5.1 H demonstrates, Myc-Def1 was successfully ubiquitylated by Rsp5. Several mono-ubiquitylation bands started to appear after 30 min at 30 °C in the ubiquitylation mix and continued to accumulate during the incubation period. This result confirmed that Myc-Def1 could be recognised and ubiquitylated by Rsp5 *in vitro*, similar to what has previously been observed with purified yeast Def1 (Wilson, Harreman, Taschner, et al. 2013).

However, problems arose with the recombinant Myc-Def1 protein when an attempt was made to compare the recombinant Myc-Def1 with Def1 purified from yeast on a size exclusion column (Figure 5.2 A). Recombinant Myc-Def1 (blue trace in the figure) eluted from the size exclusion column in a broad peak fairly late in the elution profile. The comparison with standard proteins (pink trace) indicated that the size of recombinant Myc-Def1 ranged between a monomer and a dimer. However,

Def1 purified from yeast (black trace) eluted much earlier from the same column under the same conditions, suggesting a much higher molecular weight, presumably a large multimer. This result did not on its own indicate a problem with the bacterially expressed Myc-Def1 protein, since I could not know whether the purified yeast Def1 was forming aggregates, for example due to the different purification procedure used. However, this result prompted me to carry out additional control experiments.

A

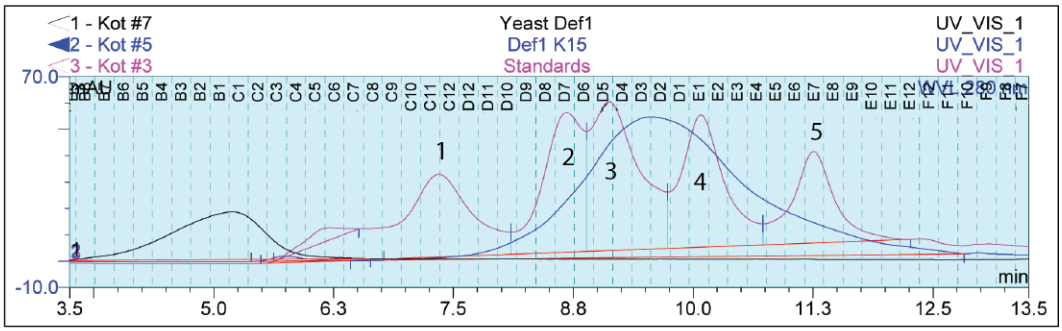

1 - Thyroglobulin, 669 kDa; 2 - Apoferritin, 443 kDa; 3 - β-amylase, 200 kDa; 4 - Albumin, 66 kDa; 5 - Carbonic anhydrase, 29 kDa.

B

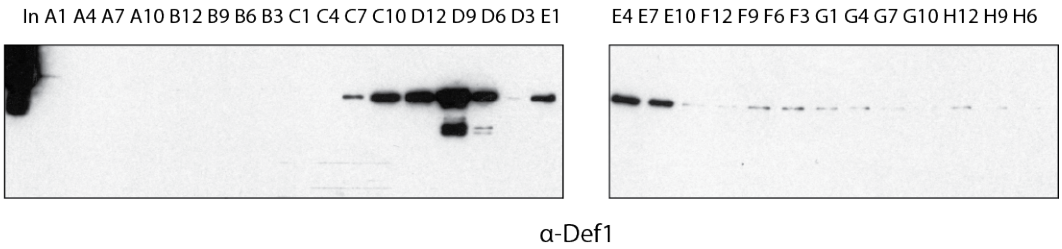

Figure 5.2. Comparison between the recombinant Myc-Def1 and yeast Def1.
A – Analysis of myc-Def1 and Def1 purified from yeast on MAbPac SEC-1 sizing column. Protein standard trace - magenta, Myc-Def1 – blue, Def1 purified from yeast – black. Protein standard sizes are listed below the trace. ***B*** – analysis of Def1 migration on the MAbPac SEC-1 sizing column in yeast extracts. Def1 was traced by Western blotting using α-Def1 antibody. Fraction numbers are listed above the blot.

An investigation into how yeast Def1 behaves in crude whole cell extracts was carried out. Yeast extracts were prepared by glass bead beating (2.4.11) and treated with benzonase to digest nucleic acids and minimise the potential interference of proteins interacting with DNA or RNA. The extracts were run on the same size exclusion column under the same conditions as before. Def1 was

tracked in the elution fractions by Western blotting. As can be seen from Figure 5.2 B, Def1 eluted in two broad peaks. Nevertheless, none of them corresponded to the profile observed with recombinant Myc-Def1 (compare fraction numbers between Figure 5.2 A and B). In the crude yeast extracts, Def1 might conceivably be interacting with other proteins, giving rise to the early eluting protein species, but the second Def1 peak from the extract eluted later than recombinant Myc-Def1, indicating that this Def1 species is smaller (i.e. likely a monomer). Again, this gave rise to concern about the usability of the recombinant Def1 protein, and compelled me to again look for an alternative strategy for Def1 production and purification.

After careful considerations, purification of Def1 from the endogenous source was chosen. However, given the results from the previous attempts, the tagging strategy was revised. Having previously discovered that a large C-terminal tag on Def1 was unstable, a smaller C-terminal tag was chosen. A yeast strain expressing Def1-6xHis-1xFlag from the endogenous locus was therefore generated, and a simple purification strategy (2.6.2) was devised (Figure 5.3 A). In short, first Def1-HF was isolated from the extracts with anti-Flag agarose. This step was followed by the elution with Flag peptide, and finally the protein was cleaned up on MonoQ column (Figure 5.3 B). The first two fractions of MonoQ column containing the Def1 protein did seem to have faster migrating Def1 species, potentially being able to interfere with the *in vitro* processing reaction. Those fractions were pooled separately from the later fractions containing a more homogeneous Def1 population.

The stability and the presence of unseparated pr-Def1 in the new Def1-HF samples were assessed by Western blotting (Figure 5.3 C). Pool 2 (P2 sample in the figure, lane 4) containing the later fractions from MonoQ column resulted in a better sample, as expected. In pool 1 (P1 sample, lane 3) containing the earlier fractions a faint lower band of Def1 was present, and the sample was deemed unsuitable for the *in vitro* processing assays. The protein in pool 2 remained stable when incubated for 1 h both at 4 and 30 °C (lanes 1 and 2), behaving as expected.

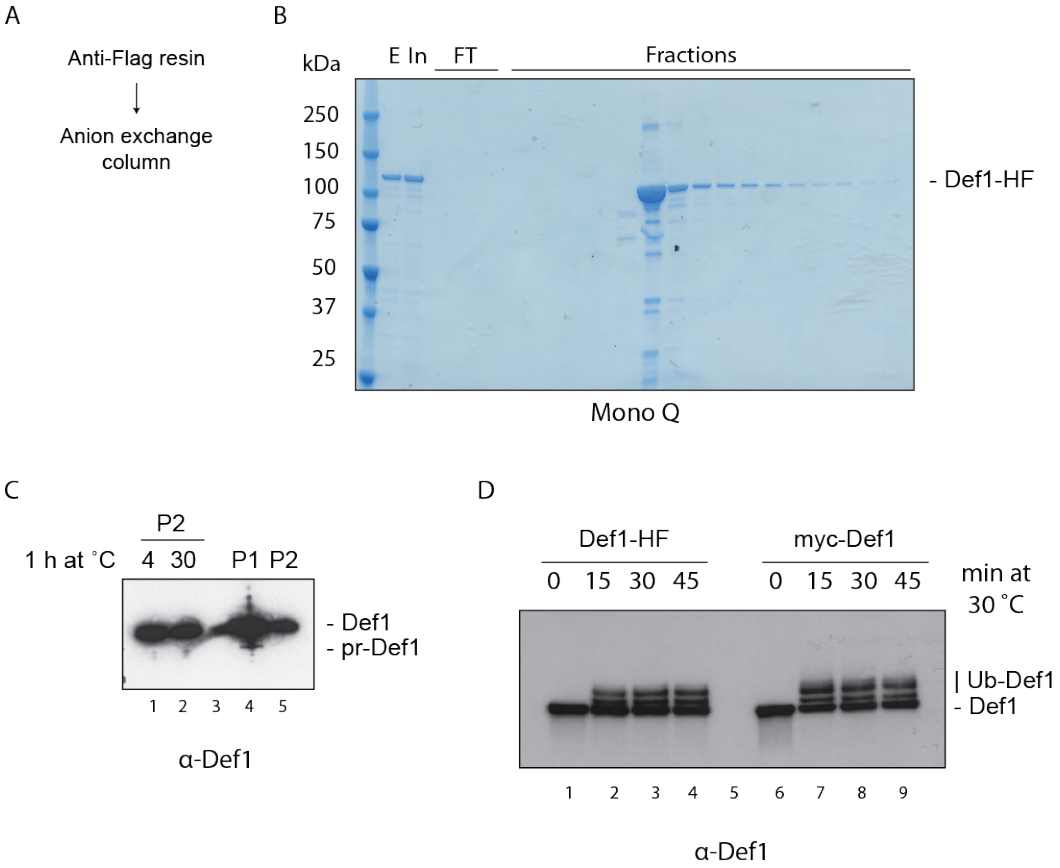

Figure 5.3. Purification of Def1-His-Flag.
A – purification strategy for Def1-HF, purified from the endogenous source. ***B*** – analysis of Def1-HF purification on MonoQ column by SDS-PAGE. E – elution from Flag resin, In – MonoQ column input, FT – flowthrough fractions. ***C*** - analysis of Def1-HF purification by Western blot and Def1 stability test. P1 – pool 1, the first two MonoQ fractions containing Def1-HF; P2 – pool 2, all other Def1-HF fractions. P2 was incubated for 1 h at 4 and 30 °C. Results were visualised by Western blotting using α-Def1 antibody. ***D*** – *In vitro* ubiquitylation of Def1-HF and recombinant myc-Def1. The ubiquitylation assay was performed using purified ubiquitylation factors and incubated at 30 °C for indicated amounts of time. The results were visualised by Western blotting using α-Def1 antibody.

The ability of Def1-HF to be ubiquitylated by Rsp5 *in vitro* was also assessed (Figure 5.3 D). Def1-HF (lanes 1-4) was successfully ubiquitylated by Rsp5. Since Def1-HF was behaving as expected – could be successfully ubiquitylated, and did not have faster migrating forms of Def1 present after purification – it was subsequently used for the *in vitro* studies.

5.1.2 Purification of the 26S proteasome

The next necessary component for the *in vitro* processing assay was the 26S proteasome. The proteasome was purified from a yeast strain expressing a tagged subunit, Pre1. Purification was carried out essentially as described in the literature (Verma et al. 2000) (2.6.8) and the strategy is briefly outlined in Figure 5.4 A. The resulting 26S proteasome complex can be seen in Figure 5.4 B. The 19S and 20S components of the proteasome seemed to be present in stoichiometric amounts and only one high molecular weight band (marked by asterisk) was co-purified as a contaminant.

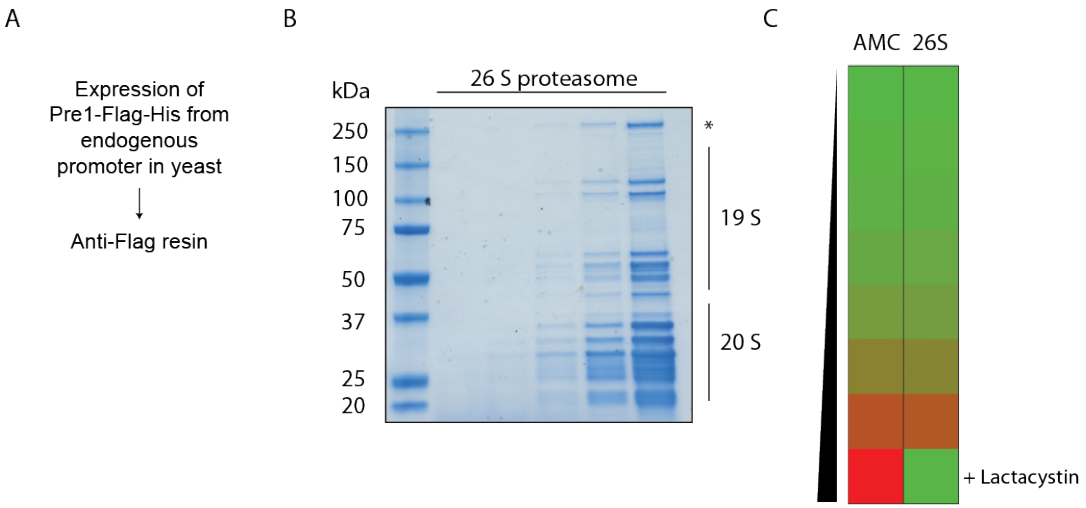

Figure 5.4. Purification and activity of the 26 S proteasome.
A – Purification strategy for the 26S proteasome. ***B*** – Purified 26 S proteasome, factor 2 dilution series visualised by SDS-PAGE. ***C*** – The 26S proteasome activity test. Green – no activity, red – high activity. Left lane – AMC product titration going from top to bottom: 0, 0.2, 0.4, 0.8, 0.16, 3.1, 6.25, and 12.5 μM AMC. Right lane - factor 2 dilution series of the purified 26S proteasome starting with 2 fM, at the bottom. The bottom square in the proteasome dilution series contained the proteasome inhibitor lactacystin. The proteasome activity was measured spectroscopically and depicted as a heatmap.

The activity of the 26S proteasome was tested using a proteasome activity assay kit (2.7.5). The activity was quantified spectroscopically by measuring the fluorescence of the reaction product. During the cleavage of a fluorogenic substrate LLVY-AMC, AMC is released. AMC can be excited at 380 nm and emits at 460 nm. Increasing amounts of AMC standard were used to visualise the standard

fluorescence and the 26S proteasome titration was performed using 2-times dilution series (Figure 5.4 C). The reaction with the highest amount of the proteasome was also inhibited with lactacystin, to show the specificity of the proteasomal activity. The purified 26S proteasome was able to cleave the fluorogenic substrate and thus deemed suitable for the reconstitution of Def1 processing *in vitro*.

5.1.3 Cdc48 purification

Given the evidence that Cdc48 might play a role in Def1 processing, I wanted to use this protein in the *in vitro* Def1 processing reaction. Since the evidence points towards Cdc48 working together with Ubx1, the first attempt was to purify Cdc48 together with Ubx1 from yeast, as a complex.

The genes encoding these proteins were cloned into the same plasmid, with a dual GAL1-GAL10 promoter. Cdc48 was expressed with a single C-terminal Flag tag, and Ubx1 had an N-terminal cleavable 5xMyc-2xTEV tag. The purification strategy is outlined in Figure 5.5 A. Essentially, the first step of purification was pulling on the Ubx1 protein via its Myc-tag. Subsequently the tag was cleaved off. The second step of the purification involved pulling on Cdc48-Flag to ensure the right stoichiometry between the Cdc48 and Ubx1 proteins. However, the resulting complex was of different stoichiometry, compared to what has been previously reported in literature for p97 and p47, mammalian homologues of Cdc48 and Ubx1 (Figure 5.5 B lanes 7-9).

Different stoichiometries have been reported for the mammalian homologues of Cdc48 and Ubx1, named p97 and p47. The p97 protein was first described to interact with p47 in a 1:2 stoichiometry with three molecules of p47 interacting with a p97 hexamer (Kondo et al. 1997) and later observed by (Beuron et al. 2006). Alternatively, a stoichiometry of 1:1, with 6 molecules of p47 binding to a p97 hexamer, was reported (Rouiller et al. 2000) in the presence of ATP in a cryo-EM study. To date, the issue of stoichiometry has not been completely resolved, with suggestions that different stoichiometries between p97 and p47 may influence the ATPase activity of the former (Xiaoyi Zhang et al. 2015).

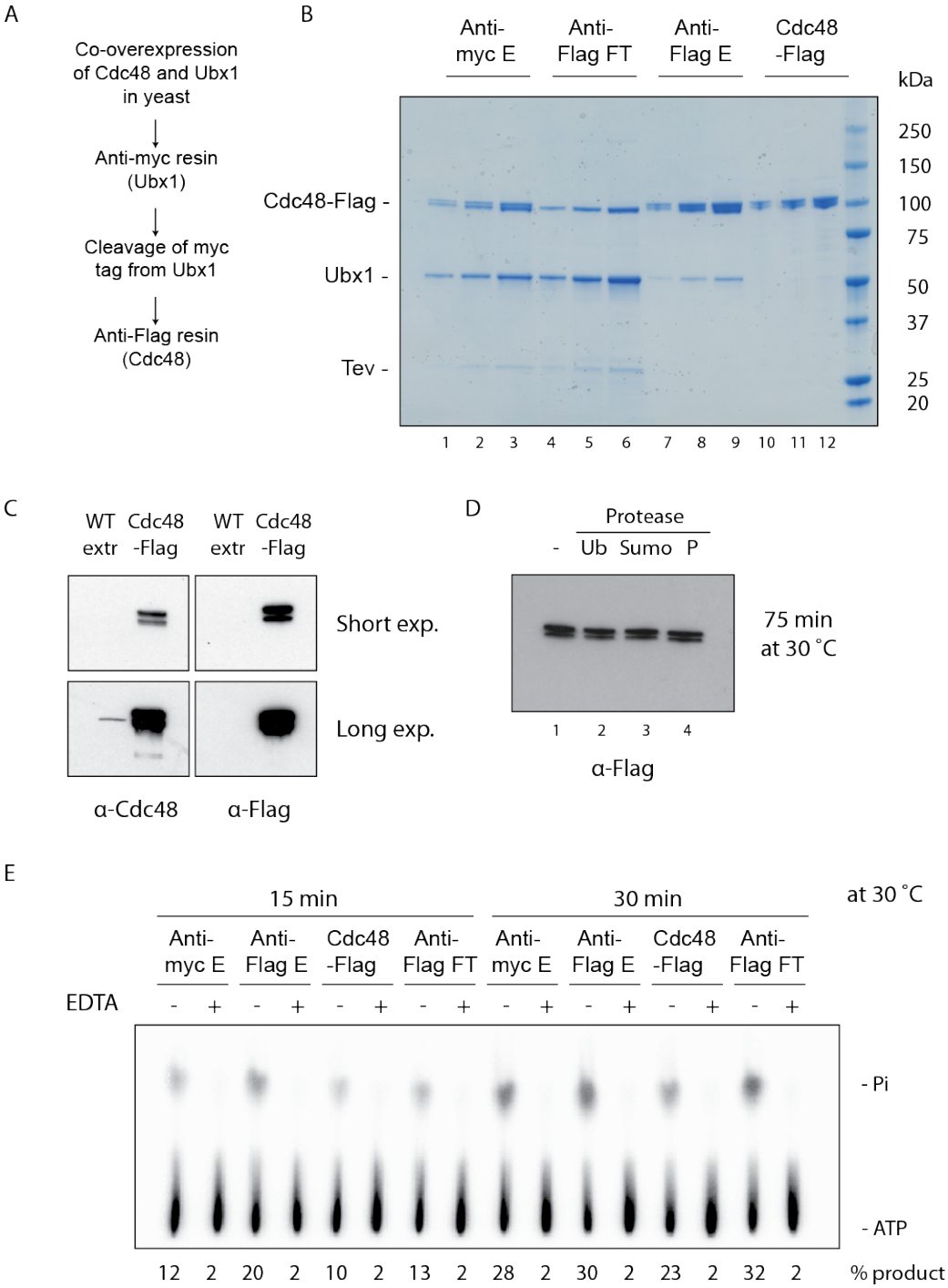

Figure 5.5. Purification and activity test of Cdc48-Flag.
A – Purification strategy for the Cdc48/Ubx1 complex purified from yeast with overexpression. ***B*** – Various forms of Cdc48/Ubx1 resulting from different steps in the purification visualised by SDS-PAGE. Three dilutions of each sample were loaded on the gel. E – elution, FT – flowthrough. ***C*** – A comparison between the purified Cdc48 and the Cdc48 species in wild type yeast extracts by Western blotting using α-Flag (right) and α-Cdc48 (left) antibodies. ***D*** – Investigation into the nature of Cdc48-Flag modification. Cdc48-Flag was incubated with ubiquitin protease (ubi), SUMO protease (Sumo), and λ phosphatase (P) for 75 min at 30 °C. Results were visualised by

Western blotting using α-Flag antibody. ***E*** - Cdc48 ATPase assay. ATPase assay (2.7.4) was performed on different fractions of Cdc48/Ubx1 from (***B***). The assay was performed for either 15 or 30 min at 30 °C with the same amount of Cdc48 protein and visualised by TLC and autoradiography.

I observed different stoichiometries between Cdc48 and Ubx1 in different steps of the purification (Figure 5.5 B). After the first step, isolation of Myc-tagged Ubx1, Cdc48 and Ubx1 seemed to be stoichiometric (1:1) (first three lanes, Figure 5.5 B). During the second step, however, a lot of Ubx1 was found in the flowthrough (lanes 4-6 Figure 5.5 B). Some of the Cdc48 protein was lost there as well. This was possible due to the fact that Cdc48-Flag was expressed in a yeast strain already carrying a wild type copy of Cdc48. After the final step of the purification, much more Cdc48 was present compared to Ubx1 (lanes 7-9, Figure 5.5 B). Given the previously reported stoichiometries for p97/p47 complex, this result was not ideal for the Def1 processing assay.

Another issue this purification approach produced was the doublet band of the Cdc48 protein. This effect was not only seen when Cdc48 was co-expressed with Ubx1, but also when Cdc48 was expressed alone from the same dual GAL expression plasmid (Figure 5.5 B, lanes 10-12). The purified protein was compared to Cdc48 in the extracts (Figure 5.5 C). First of all, it is worth noting that both bands in the purified sample were recognised by the Flag antibody (right panel), arguing against the possibility that Cdc48 lost its tag or that a significant amounts of un-tagged protein was co-purifying in the sample.

These data opened the possibility that a fraction of Cdc48 might be modified when over-expressed. If so, it might be possible to remove this modification utilising different de-modifying enzymes (Figure 5.5 D). The purified Cdc48-Flag protein was incubated either with a SUMO protease, Ulp1 (lane 2), a ubiquitin protease, Usp2 (lane 3), or λ phosphatase (lane 4) in the appropriate buffers as per manufacturer's instructions for 75 min at 30 °C. However, none of the enzymes made a difference to the appearance of the doublet band. Antibodies against SUMO and ubiquitin were also tried with this Cdc48 sample, yielding negative results (data not shown).

The activity of similar amounts of the different Cdc48/Ubx1 complexes was assessed in an ATPase assay (2.7.4) (Figure 5.5 D). Even though Cdc48 was heterogeneous (partially modified or degraded) and each sample contained different ratios between Ubx1 and Cdc48, all the samples showed ATPase activity. The activity was readily inhibited by the addition of EDTA in the reaction (every second lane). However, not having an unmodified sample of Cdc48, it was impossible to ascertain whether the ATPase activity was affected.

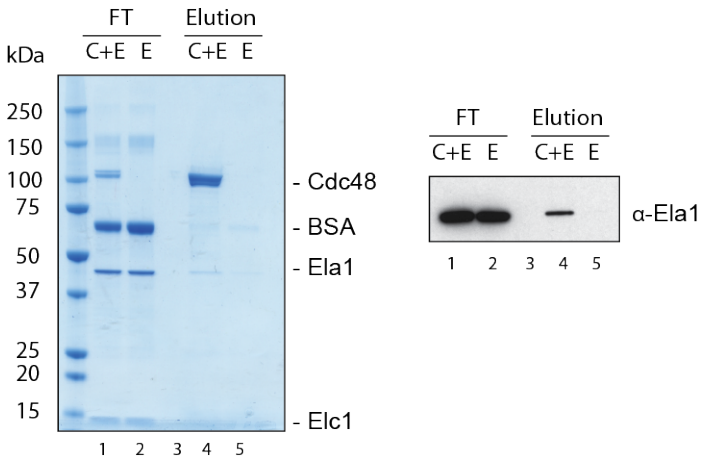

Figure 5.6. The interaction between Cdc48 and Ela1/Elc1.
In vitro interaction between purified Cdc48 and Ela1/Elc1 complex. C – Cdc48-Flag, E – Ela1/Elc1. A Flag IP was performed followed by elution in a buffer containing Flag peptide. Left panel – SDS-PAGE gel, right panel – Western blot using α-Ela1 antibody.

In preparation for the *in vitro* Def1 processing assays, some interaction studies with the purified Cdc48 protein were performed. Prompted by evidence in the literature that Cdc48 is capable of interacting with some ubiquitin ligases in high-throughput screens (Carvalho et al. 2006; Carvalho et al. 2010; Krogan et al. 2006), the ability of Cdc48 to interact with the Ela1/Elc1 adaptor proteins of the Cul3 Ub ligase (Marcus Wilson) was tested. Interestingly, an *in vitro* binding assay using highly purified proteins (Figure 5.6) showed an interaction between Cdc48 and Ela1/Elc1. The interaction can be seen especially clearly by Western blot analysis (right panel). The Ela1/Elc1/Cul3 complex might act with Cdc48 to stimulate ubiquitylation and removal of arrested RNAPII from chromatin. Since Def1 acts as an adaptor protein bringing Ela1/Elc1 to the arrested RNAPII, the Ela1/Elc1 complex might also be involved in Def1 activation. Indeed, Def1 activation may well occur in the nucleus, leading to its retention there (Wilson, Harreman, Taschner, et al. 2013).

Since Cdc48 became modified or proteolysed upon overexpression and was not representing the predominant Cdc48 form normally found in extracts, a new purification strategy was needed. A strain expressing a C-terminally tagged Cdc48 from the endogenous locus was created. The purification approach was very straightforward (Figure 5.7 A) – affinity purification followed by a clean-up step on MonoQ. The resulting Cdc48-3xFlag sample was homogeneous (Figure 5.7 B), and the purified protein had ATPase activity (Figure 5.7 C). This purified protein sample was chosen as the preferred sample for the processing assays.

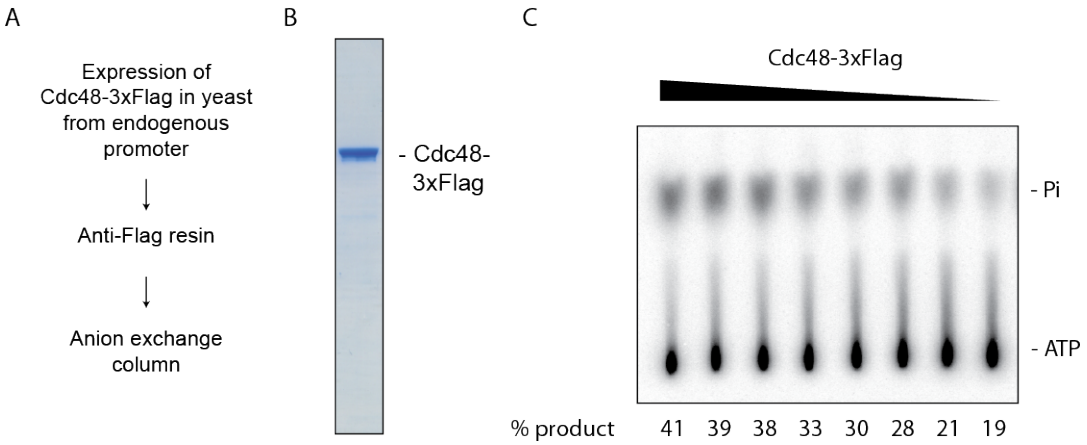

Figure 5.7. Purification and activity test of Cdc48-3xFlag.
A – Purification strategy for the Cdc48-3xFlag protein expressed in yeast from the endogenous promoter. ***B*** – Purified Cdc48-3xFlag sample visualised by SDS-PAGE. ***C*** – ATPase assay (2.7.4) of Cdc48-3xFlag was carried out for 15 min at 30 °C. A Factor 2 dilution series was performed going from left to right starting from 0.26 μM. The result was visualised by TLC and autoradiography.

5.1.4 Purification of Ubx1, Ubx5, and Smy2 proteins

The evidence that Smy2 might be involved in Def1 processing (4.2) encouraged me to test its function in the *in vitro* processing assay. Thus, purified Smy2 protein was needed. First, recombinant Smy2 was purified from *E. coli*. A His-SUMO tag was used for the purification. The purification strategy is outlined in Figure 5.8 A (2.6.9). The purification resulted in a reasonably homogeneous Smy2 sample (right panel). This sample was used for the investigation of the possible Smy2 association with Cdc48, which was described in the previous chapter (4.3).

As binding between Cdc48 and recombinant Smy2 was not observed, an attempt to purify Smy2 from yeast, potentially carrying all the required PTMs, was also made. For Smy2 purification from yeast, HA-Smy2 was expressed under a GAL promoter from a pYES2 plasmid. The purification strategy is outlined in Figure 5.8 B (2.6.10). The resulting sample was reasonably pure (right panel). However, the yield was much lower compared to the recombinant protein. Since this sample was purified from the endogenous source, it was nevertheless the preferred sample for Def1 processing assays. However, to investigate if any Smy2 PTMs are required for the processing reaction, it was potentially beneficial to also have the Smy2 protein purified from *E. coli.*

To investigate the action of Cdc48 in Def1 processing, the Ubx1 adaptor protein was also needed. The Ubx5 protein was chosen as a negative control for Ubx1 action. Ubx5 is involved in the last resort pathway together with Cdc48, but acts at a later step (for the removal of RNAPII from chromatin (Verma et al. 2011)) and thus carries out a different function from Ubx1. Ubx5 whould thus be exected to have a different substrate specificity and act as a good negative control. For this reason, Ubx1 and Ubx5 proteins were purified under the same conditions.

The Ubx1 and Ubx5 proteins were purified from a recombinant source (Figure 5.8 C) (2.6.7), in a very similar manner to the Smy2 protein. The main difference between the purifications was the final ion exchange column. In the case of Smy2, MonoS was chosen, while both Ubx1 and Ubx5 were purified on MonoQ. The purifications resulted in reasonably homogenous protein samples (Figure 5.8 C).

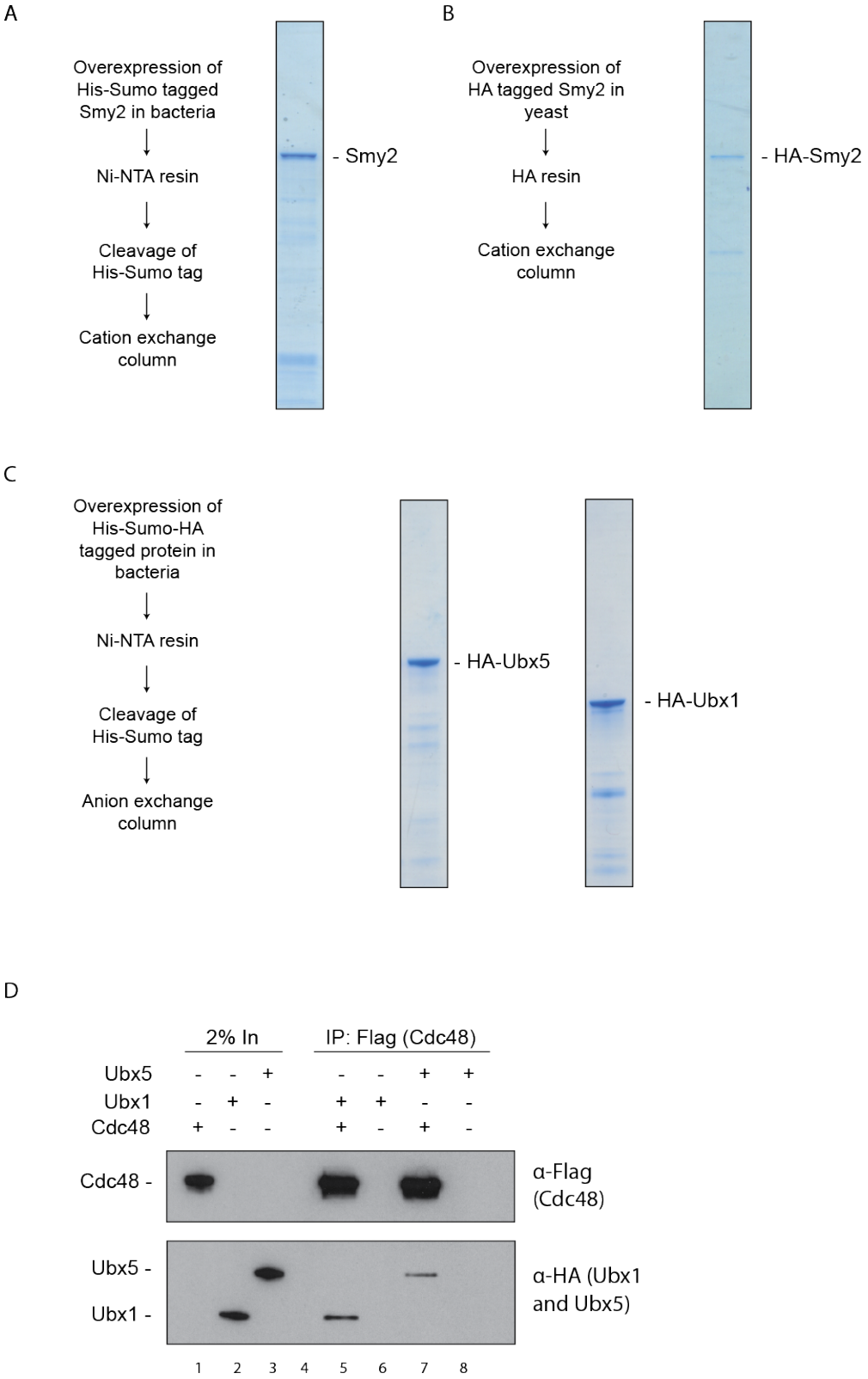

Figure 5.8. Purification of Smy2, Ubx1, and Ubx5 proteins.
A – Purification strategy for the Smy2 protein expressed in *E. coli* (left panel). Right panel – purified Smy2 protein visualised by SDS-PAGE. ***B*** – Purification strategy for

the HA-Smy2 protein from yeast (left panel). Right panel – purified HA-Smy2 protein visualised by SDS-PAGE. ***C*** – Purification strategy for Ubx1 and Ubx5 proteins from *E. coli* (left panel). Right panels – purified HA-Ubx1 and HA-Ubx5 visualised by SDS-PAGE. ***D*** – *In vitro* interaction between purified Cdc48-3xFlag and HA-Ubx1 and HA-Ubx5 proteins. Flag IP (Cdc48) and elution with Flag peptide were performed. Results were visualised by Western blotting using α-Flag (Cdc48) and α-HA (Ubx1 and Ubx5) antibodies.

Ubx1 and Ubx5 proteins were tested for their ability to bind Cdc48. An *in vitro* interaction assay was performed by incubating the purified proteins together with Cdc48 in the presence of ATP, and then utilising the C-terminal Flag tag on Cdc48 for an IP. Proteins were eluted from anti-Flag beads with the Flag peptide. The result was visualised by Western blot (Figure 5.8 D). As expected, both Ubx1 (lane 4) and Ubx5 (lane 6) were able to bind Cdc48 and were subsequently used in Def1 processing assays.

5.2 26S proteasome is sufficient for Def1 processing

Due to time constraints and the fact that several attempts were made to purify each of the Def1 processing reaction components, some initial assays were done with samples from earliest available purifications. It is made clear in figure legends which protein purification sample was used.

The first step in assembling the Def1 processing assay *in vitro* was to find the minimal set of conditions under which Def1 became processed. An important question was whether ubiquitylation of Def1 was needed to initiate the minimal processing reaction and if any accessory proteins were required to terminate the processing reaction and release the pr-Def1 form.

5.2.1 Processing of recombinant Myc-Def1

Initial studies of Def1 processing were done using the recombinant Myc-Def1. This approach offered one strong advantage of Myc-Def1 not carrying any PTMs and allowed me to determine whether Def1 sequence and structure alone are sufficient for the processing reaction to occur.

Looking at whether ubiquitylation of Def1 was required for the processing, two Def1 ubiquitylation reactions were set up – one with functional Rsp5 protein and the other one with catalytically dead Rsp5 mutant, carrying a C777A mutation at the catalytic cysteine (kind gift from Marcus Wilson). After allowing the ubiquitylation reaction to proceed for 1 h at 30 °C, the 26S proteasome was added to the reaction and a timecourse experiment was performed (Figure 5.9 A). The presence of ubiquitylated myc-Def1 in the reaction did not seem to make a significant difference. In both cases, the pr-Def1 form started to appear after 15 min with the 26S proteasome (lanes 3 and 9). Interestingly, the pr-Def1 forms resulting from ubiquitylated and non-ubiquitylated samples, did not differ in size. It is worth noting, that despite the fact that the pr-Def1 bands are weak, they specifically appear upon the incubation with the proteasome and is the product of the partial proteasomal processing reaction, since the incubation of Def1 alone does not change its appearance (5.1.1), and thus is not a result of non-specific degradation. This finding would suggest that either in both cases only the non-ubiquitylated Def1 in the sample was processed, or that the ubiquitin moiety was removed from Def1 during the processing reaction, since all ubiquitylation sites identified so far in Def1 sequence are shared between the fl- and pr-Def1 (Wilson, Harreman, Taschner, et al. 2013). In any case, this experiment suggested that Def1 sequence and structure carry all the necessary information for the processing reaction to occur in the presence of the 26S proteasome. However, the processing reaction did not seem to be very efficient – there was very little pr-Def1 generated after the incubation with the proteasome for 60 min (Figure 5.9 A, lanes 5 and 11). This observation could have arisen for many reasons. One possibility was that a conformational change in Def1 was needed to allow for more favourable processing kinetics. To investigate this possibility, Myc-Def1 processing was assessed in the presence of several known Def1 interactors.

In this experiment, the effect of Rsp5, RNAPII, and free ubiquitin was tested (Figure 5.9 B). Myc-Def1 was either pre-incubated with these proteins for 30 min at 30 °C before the addition of the 26S proteasome (lanes 3-8), or the proteasome was added at the same time as the interactors (lanes 10-15). The addition of proteasome resulted in processing, but there did not seem to be a significant stimulation of proteasome-dependent Def1 processing in the presence of RNAPII,

Rsp5, and ubiquitin in either of the conditions. This result lead me to hypothesise that it might be the 26S proteasome needing accessory proteins, such as Cdc48, to make the reaction more efficient.

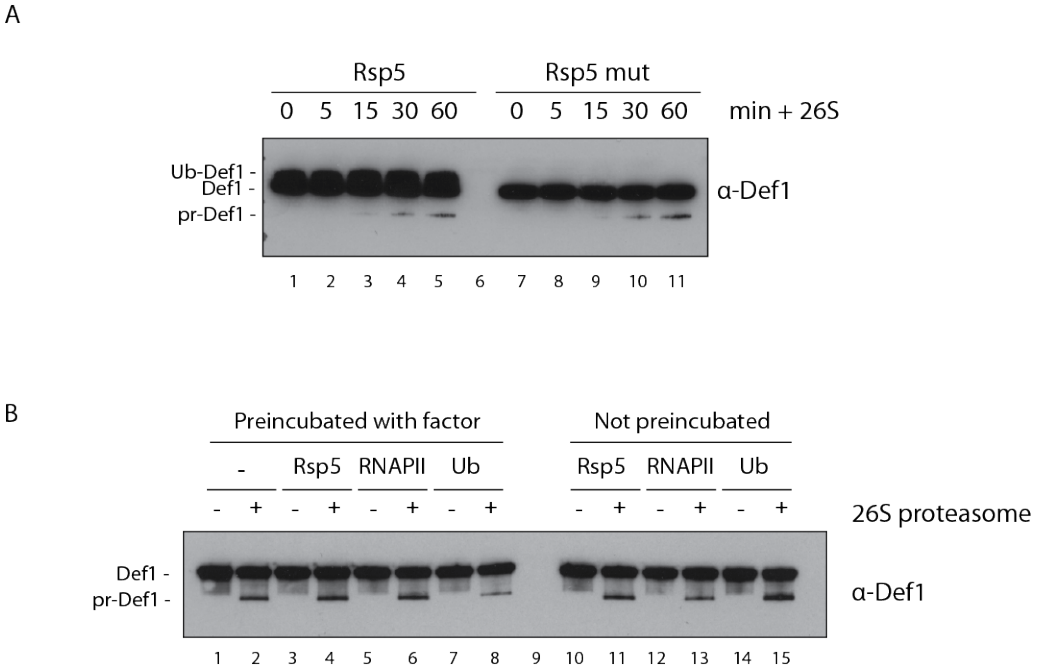

Figure 5.9. Myc-Def1 *in vitro* processing reactions.
A – a comparison between Def1 and ub-Def1 processing. The 26S proteasome was added directly into *in vitro* ubiquitylation reactions (2.7.1) performed either with wild type (Rsp5) or a catalytically dead mutant (Rsp5 mut) of Rsp5 ligase. Indicated timepoints after the addition of the 26S proteasome were taken. The reaction was performed at 30 °C and results were visualised by Western blotting using α-Def1 antibody. ***B*** – Myc-Def1 processing in the presence of known Def1 interactors: Rsp5, RNAPII and free ubiquitin. Myc-Def1 was either pre-incubated with the indicated factors for 1 h at 30 °C before the addition of the 26S proteasome (left) or the factors were added just before the addition of the proteasome (right). The reaction was performed for 1 h at 30 °C and visualised by Western blotting using α-Def1 antibody.

Taking into consideration the low efficiency of the processing reaction, there was also a possibility that only a small sub-population of the recombinant Myc-Def1 was processing-competent. Hence all the subsequent Def1 processing reactions were performed using Def1-HF purified from yeast as a substrate.

5.2.2 The effect of Cdc48 on Def1 processing *in vitro*

When Def1-HF processing reactions were set up, the first goal was to find out whether the recombinant Myc-Def1 and Def1-HF purified from yeast behaved similarly.

The 26S proteasome titration was performed to find the optimal conditions for subsequent reactions (Figure 5.10 A). An immediate difference between the recombinant Myc-Def1 and Def1-HF was observed – the addition of the proteasome not only resulted in the appearance of pr-Def1 form, there was also a significant decrease in fl-Def1 species that could not be accounted for by the formation of pr-Def1 (compare Figure 5.10 A and Figure 5.9 A). This finding suggested that when using Def1-HF as a substrate two processes are happening at the same time – processing *and* degradation of Def1. Since the Def1 antibody was raised against $Def1_{1-500}$ fragment, it would recognise both fl-Def1 and pr-Def1 the same. This experiment raised an interesting question of whether the degradation was happening independently or via the pr-Def1 form.

A timecourse experiment (Figure 5.10 B) revealed that Def1 processing reached a saturation point at 45 min after the addition of the 26S proteasome (lane 6). Interestingly, the level of pr-Def1 did not seem to change markedly with longer incubation times from the 30 min point onwards. However, the levels of fl-Def1 were continuously decreasing over the course of the experiment. As mentioned before, in this type of experiment it was impossible to differentiate whether fl-Def1 degradation occurred via the pr-Def1 form. This finding raised the question if any of the 26S proteasome accessory proteins would be able to change the equilibrium between the degradation and processing reactions, shifting it towards the processing of Def1. Another possibility would be that the Def1 processing reaction is in fact rather efficient, but that the pr-Def1 protein is afterwards readily degraded by the proteasome. This possibility was much harder to investigate, but in agreement with the results from previous *in vivo* experiments, in which it was found that the genetically truncated form of Def1 is highly unstable (Michelle Harreman, unpublished data).

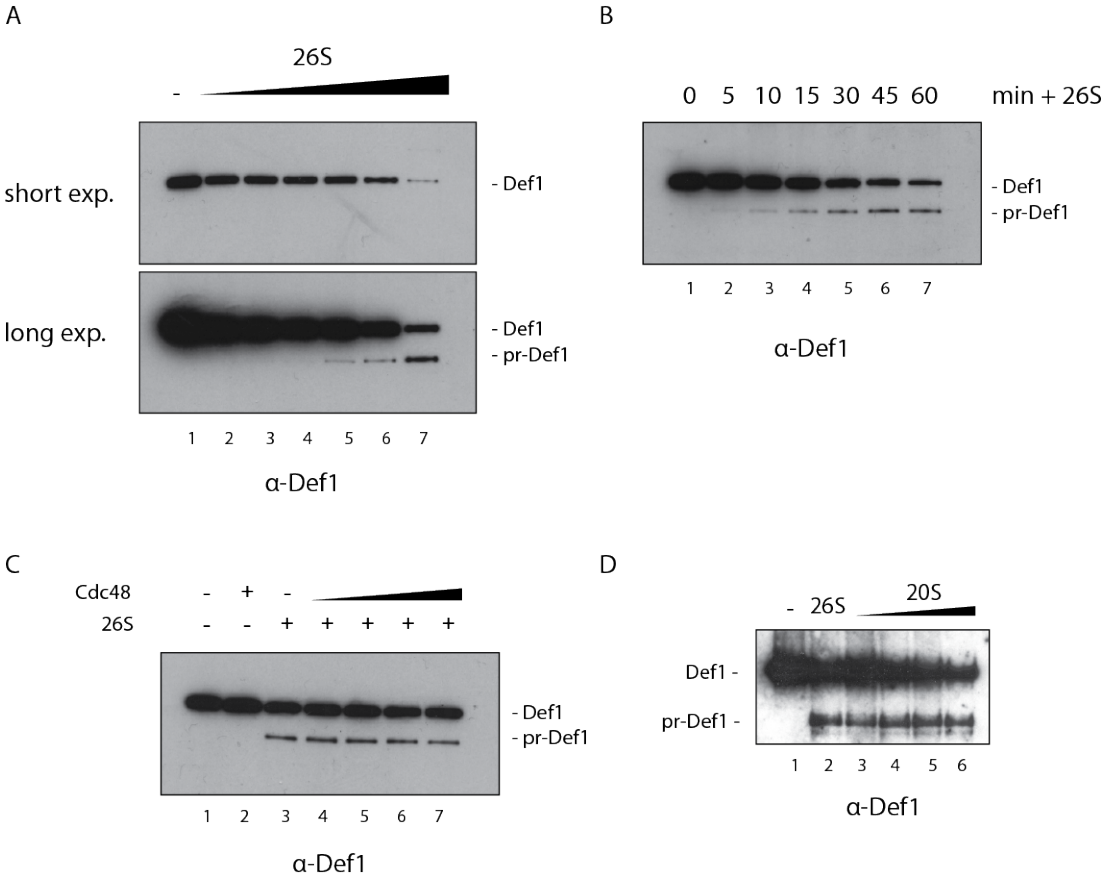

Figure 5.10. *In vitro* processing of Def1-HF.
A – Titration of the 26S proteasome in Def1-HF processing reaction (2.7.2). Factor 2 dilution series of the 26S proteasome were performed starting from 5.1 fM. The reaction was performed at 30 °C for 1 h and visualised by Western blotting using α-Def1 antibody. ***B*** – Timecourse processing reaction for Def1. The 26S proteasome was used at the concentration of 5.1 fM. Samples were taken at the indicated timepoints. The results were visualised by Western blotting using α-Def1 antibody. ***C*** – Def1-HF processing in the presence of Cdc48-Flag. Cdc48-Flag was purified from yeast with overexpression as shown (5.1.3). The 26S proteasome was used at the final concentration of 5.1 fM. Excess of Cdc48-Flag was added to the reaction going from left to right: 40 nM, 80 nM, 160 nM, and 320 nM. The reaction was carried out for 1 h at 30 °C and visualised by Western blotting using α-Def1 antibody. ***D*** – Def1 processing by the 20S proteasome. The reaction was carried out for 1 h at 30 °C in the same buffer either with the 26S proteasome or with increasing amounts of the 20S proteasome. The samples were run on a 8-12% Tris Acetate gel. The result was visualised by Western blotting using α-Def1 antibody.

Since Cdc48 has been implicated in the partial proteasomal processing of Spt23 and has been suggested to be required for both the efficient processing and the dissolution of the processing intermediate (Rape et al. 2001; Kolawa et al. 2013; Hitchcock et al. 2001), and was required for Def1 processing *in vivo* (3.2.1), it was the immediate choice of protein to investigate in the *in vitro* Def1 processing

reaction. A reaction was set up with increasing amounts of Cdc48 added to the Def1 processing reaction (Figure 5.10 C). Disappointingly, there was no significant difference observed upon the addition of Cdc48. It did not make the processing more efficient, nor did it prevent the degradation of fl-Def1. One possible explanation for the lack of the effect upon Cdc48 addition is that it needs to interact with Def1. However, this interaction may only be possible via an adaptor protein, such as Ubx1, and Def1 ubiquitylation might also be a necessary pre-requisite for such interaction. Moreover, Cdc48 has been reported to be able to replace the 19S cap on the proteasome in archaea (Barthelme & Sauer 2012); thus it is formally possible that Cdc48 requires the 20S rather than the 26S proteasome to exert its action. However, this hypothesis could not be tested due to the time constraints.

Another important experiment was looking at the processing in the presence of the 20S proteasome. Interestingly, the 20S proteasome (Luke Selth) was fully able to process Def1 (Figure 5.10 D). It is the 19S regulatory subunit of the proteasome that contains ubiquitin binding sites (Elsasser et al. 2002; Elsasser et al. 2004). It is thus possible that the difference between the 26S and 20S proteasome processing could be revealed only if ubiquitylated Def1 was used as a substrate. All these observations taken together lead me to re-investigate the effect of Def1 ubiquitylation on the processing reaction, this time using the yeast protein.

5.2.3 The effect of Def1 ubiquitylation on the processing reaction

To see how ubiquitylation affected processing of yeast Def1-HF in the *in vitro* assay, a Def1 ubiquitylation reaction was set up, either with or without the addition of ubiquitin. The reaction was allowed to proceed for 1 h at 30 °C before the addition of the 26S proteasome. As can be seen in Figure 5.11 A, ubiquitylation of Def1 did not dramatically affect its degradation (compare lanes 1 and 5 with lanes 7 and 11). It is worth noting, however, that more pr-Def1 was accumulating in the case of non-ubiquitylated Def1. This result could be explained by ubiquitin interacting with the 26S proteasome and slowing down the movement of the substrate into the proteasome chamber, thus delaying the reaction.

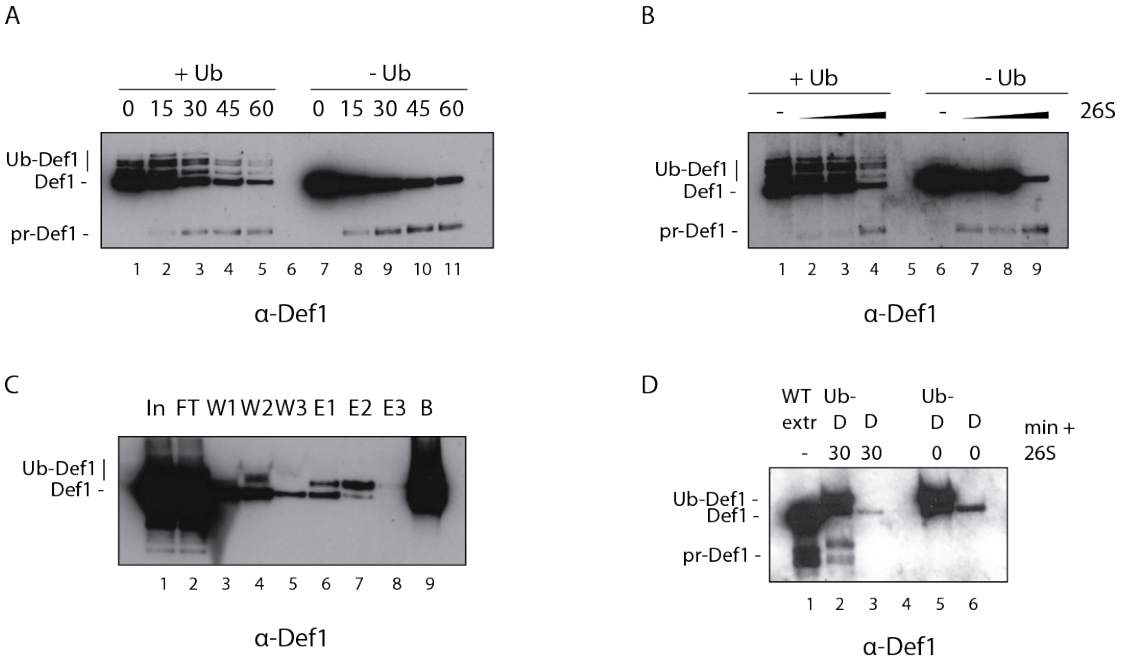

Figure 5.11. *In vitro* processing of ubiquitylated Def1-HF.
A – The 26S proteasome was added directly to the *in vitro* ubiquitylation reactions (2.7.1) performed ± ubiquitin. Samples were taken at the indicated timepoints after the addition of the 26S proteasome. The reaction was carried out at 30 °C and the results were visualised by Western blotting using α-Def1 antibody. ***B*** – Titration of the 26S proteasome in the ub-Def1 processing reaction. Three different concentrations of the 26S proteasome were used in the *in vitro* processing assay: 5.1 fM, 2.55 fM, and 0.5 fM. The reaction was carried out at 30 °C for 1h and visualised by Western blotting using α-Def1 antibody. ***C*** – Purification of ubiquitylated Def1-HF. HA-ubiquitin was used in an *in vitro* ubiquitylation reaction to ubiquitylate Def1. Then ubiquitylated Def1 was purified from the reaction (2.6.11) via the HA-tagged ubiquitin. In – input; FT – flowthrough; W1, W2, W3 – washes 1, 2, and 3; E1, E2, E3 – elutions 1, 2, and 3; B – beads. The results were visualised using α-Def1 antibody in a Western blot. ***D*** – A comparison between pr-Def1 resulting from an *in vitro* reaction and a pr-Def1 from yeast extracts by Western blot using α-Def1 antibody. WT extr – wild type extract; Ub-D – purified ubiquitylated Def1; D – purified Def1 protein.

It is also likely that the concentration of the 26S proteasome in the reaction is high enough for ubiquitin not to be essential for the reaction between Def1 and the proteasome. As in the similar experiment performed on Myc-Def1 (5.2.1), ubiquitylation of Def1 did not reach completion before the addition of the 26S proteasome and it was impossible to tell whether the pr-Def1 form had been generated from the ubiquitylated or non-ubiquitylated Def1. However, there was no difference in the pr-Def1 species resulting from both samples.

As the proteasome concentration in the reaction might have been too high to see the stimulating effect of ubiquitin, the next experiment attempted to decrease the concentration of the proteasome in the reaction, potentially unmasking the effect of ubiquitin (Figure 5.11 B). The results showed the same pattern as the timecourse experiment (Figure 5.11 A): more pr-Def1 appeared in the reaction containing only non-ubiquitylated Def1. A better system was needed where most of Def1 population would be ubiquitylated to determine what effect ubiquitylation has on Def1 processing.

The approach taken to enrich for the ubiquitylated form of Def1 in the reaction was purification of the ubiquitylated Def1 from the ubiquitylation mix. HA-tagged ubiquitin (Boston Biochem) was used to ubiquitylate Def1 *in vitro* (2.7.1). Subsequently, ubi-Def1 was purified from the reaction utilising the HA tag on ubiquitin (2.6.11). During the purification a lot of material was lost (Figure 5.11 C lane 2), but a better ratio between ubiquitylated and non-ubiquitylated Def1 was achieved (Figure 5.11 C lane 7). Although it was not impossible to completely separate ubiquitylated Def1 from the non-ubiquitylated form, elution fraction E2 primarily contained ubiquitylated Def1. It could be argued that there is a possibility that the ub-Def1 species from the *in vitro* reaction may not be ubiquitylated at the same sites as *in vivo*, further complicating the *in vitro* processing experiments.

Nevertheless, having a more homogeneous sample of ub-Def1, I was able to investigate how the processed forms of Def1 generated *in vitro* corresponded to pr-Def1 generated *in vivo*. As can be seen in Figure 5.11 D, when the purified ub-Def1 was used for processing, two main species of pr-Def1 now appeared (lane 2). Both of them seemed to be of higher molecular weight compared to the pr-Def1 species in yeast extracts (lane 1). This difference could not be explained by the tag on the Def1 protein, since the C-terminal 1xHis-1xFlag tag is degraded during the processing reaction. Importantly, however, Def1 was ubiquitylated with the HA-tagged ubiquitin, which could in theory account for the higher molecular weight of the pr-Def1 species obtained *in vitro* (lane 2).

Overall, these experiments suggest that the ubiquitylation of Def1 is not an absolute requirement for the processing reaction *in vitro*. Nevertheless, it might be

an important signal increasing the affinity of the proteasome for Def1 *in vivo*. And another potential function of the ubiquitin on Def1 is the recruitment of Cdc48 via its adaptor protein. This was the focus for further experiments.

5.3 The effect of accessory factors on Def1 processing

It is clear from the results presented thus far that Def1 sequence and structure has all the necessary information for Def1 processing to occur in the presence of the 26S proteasome. However, the processing reaction was not efficient or was outcompeted or masked by the (subsequent) complete degradation of Def1. Knowing that Def1 processing is regulated inside the cell, I investigated how other factors associated with the last resort pathway affect the *in vitro* reaction.

5.3.1 The effect of purified factors on Def1 processing *in vitro*

The initial experiment to evaluate the effect of accessory proteins on the processing of Def1 included Cdc48 alone, Cdc48/Ubx1 complex co-purified together (2.6.4, 5.1.3), and Ela1/Elc1 complex (Marcus Wilson), due to its ability to interact with Cdc48 (5.1.3) and previously described association with Def1 (Wilson, Harreman, Taschner, et al. 2013). Different combinations of these factors were examined in the Def1 processing assay (Figure 5.12 A). All the factors were added to the reaction immediately before the addition of the 26S proteasome. The factors alone did not induce Def1 processing (lanes 1-6) and none of them seemed to significantly affect the processing reaction (compare lane 7 and lanes 8-12). However, in this first attempt, the suboptimal preparations of Cdc48 and Cdc48/Ubx1 proteins were used, as discussed earlier (5.1.3).

Once better purification strategies for Cdc48 and Ubx1 were developed, and the Smy2 protein was purified, their influence on the *in vitro* processing of Def1 was revisited. This time Cdc48, Ubx1, Smy2, and Ela1/Elc1 complex were all added together to the Def1 processing assay and a timecourse experiment was performed. This type of experiment was chosen with the reasoning that the end-point of both reactions (with and without accessory poroteins) might be the same, but that the reaction rates might differ.

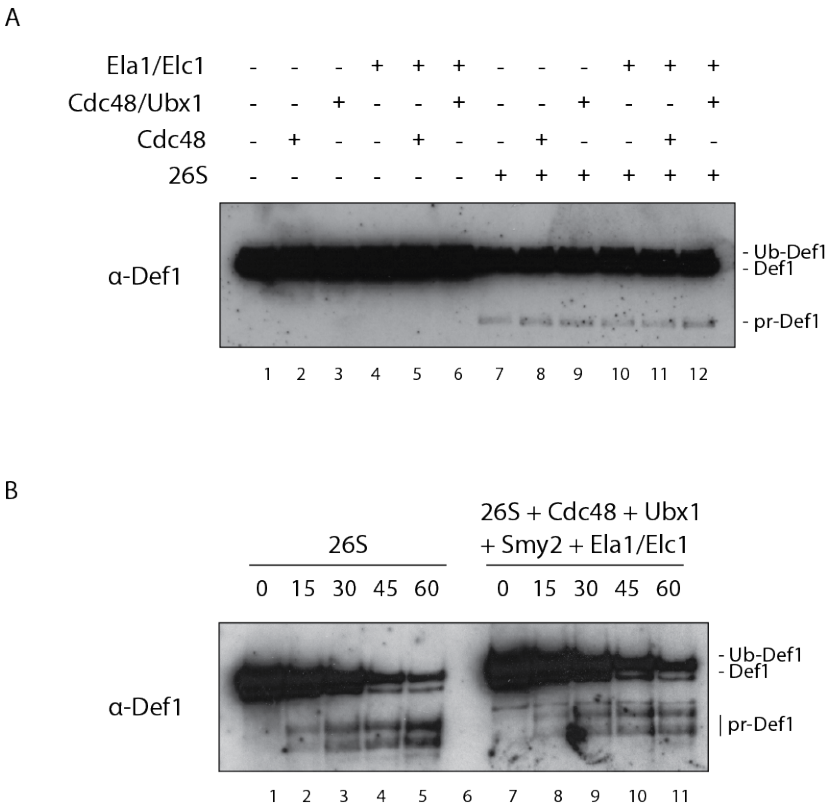

Figure 5.12. The influence of Def1 interactors on the processing reaction.
A – Def1 processing reaction was carried out in the presence of Ela1/Elc1 (20 nM), Cdc48/Ubx1 (20 nM) co-expressed and purified from yeast, and Cdc48 alone (20 nM) overexpressed and purified from yeast (5.1.3) as well as their combinations for 1 h at 30 °C. Results were visualised by Western blotting using α-Def1 antibody. ***B*** – Processing of ubiquitylated Def1 in the presence of Cdc48 (purified from yeast from the endogenous promoter, (2.6.6), Ubx1 (purified from *E. coli* (2.6.7)), Smy2 (purified from yeast, (2.6.10)), and Ela1/Elc1 (Marcus Wilson) factors all together for indicated times at 30 °C. The concentration of each factor in the reaction was 20 nM. The 26S proteasome-alone reaction contained 80 nM BSA to control for any molecular crowding effects in the reaction. Results were visualised by Western blotting using α-Def1 antibody.

To compensate for any molecular crowding effects, BSA was added to the proteasome-only reaction to the same final molar concentration as all the factors in the experimental reaction (Figure 5.12 B). The reaction was performed on the purified fraction of ub-Def1, as described above (5.2.3). The addition of all these factors together did make a slight difference to the reaction, when compared to the proteasome-only condition. Both Def1 processing and degradation seemed to be decreased in the presence of all the factors together (compare lanes 5 and 11). However, the difference is reasonably small and the possibility that one or some of

the factors might be targets for the proteasome (to a higher degree than BSA) and thus titrated the proteasome away from Def1 could not be ruled out. Being unable to solve this issue I decided to examine whether the addition of crude yeast extracts, presumably containing all the necessary factors for Def1 degradation, would have an effect on Def1 processing *in vitro*.

5.3.2 The effect of yeast extracts on Def1 processing *in vitro*

Addition of yeast extracts to the processing reaction would help me to evaluate whether I have already discovered all the factors required for Def1 activation, and if not, adjust the reaction components accordingly.

Since the proteasome is an abundant protein inside the cell, the first effort was to see if extracts alone were able to process purified non-ubiquitylated Def1-HF. The extracts were prepared in a manner previously shown to be compatible with TC-NER and transcription experiments (Schultz et al. 1991; Harreman et al. 2009) (2.4.14), as this preparation yields extracts with high protein concentration. Before the extract preparation, yeast cultures were either exposed to UV light and left for an hour to recover, or left untreated. The accessory proteins from the experiment in Figure 5.12 A were used to supplement the extracts in case their concentration in the extracts was limiting.

As expected, UV treated extracts were better at processing Def1 than untreated extracts (Figure 5.13 A). However, the addition of Cdc48 alone, Cdc48/Ubx1 complex, Ela1/Elc1 or free ubiquitin did not seemed to change the ability of the extracts to process Def1. Intriguingly, however, the degradation effect of fl-Def1 was not pronounced in this experiment.

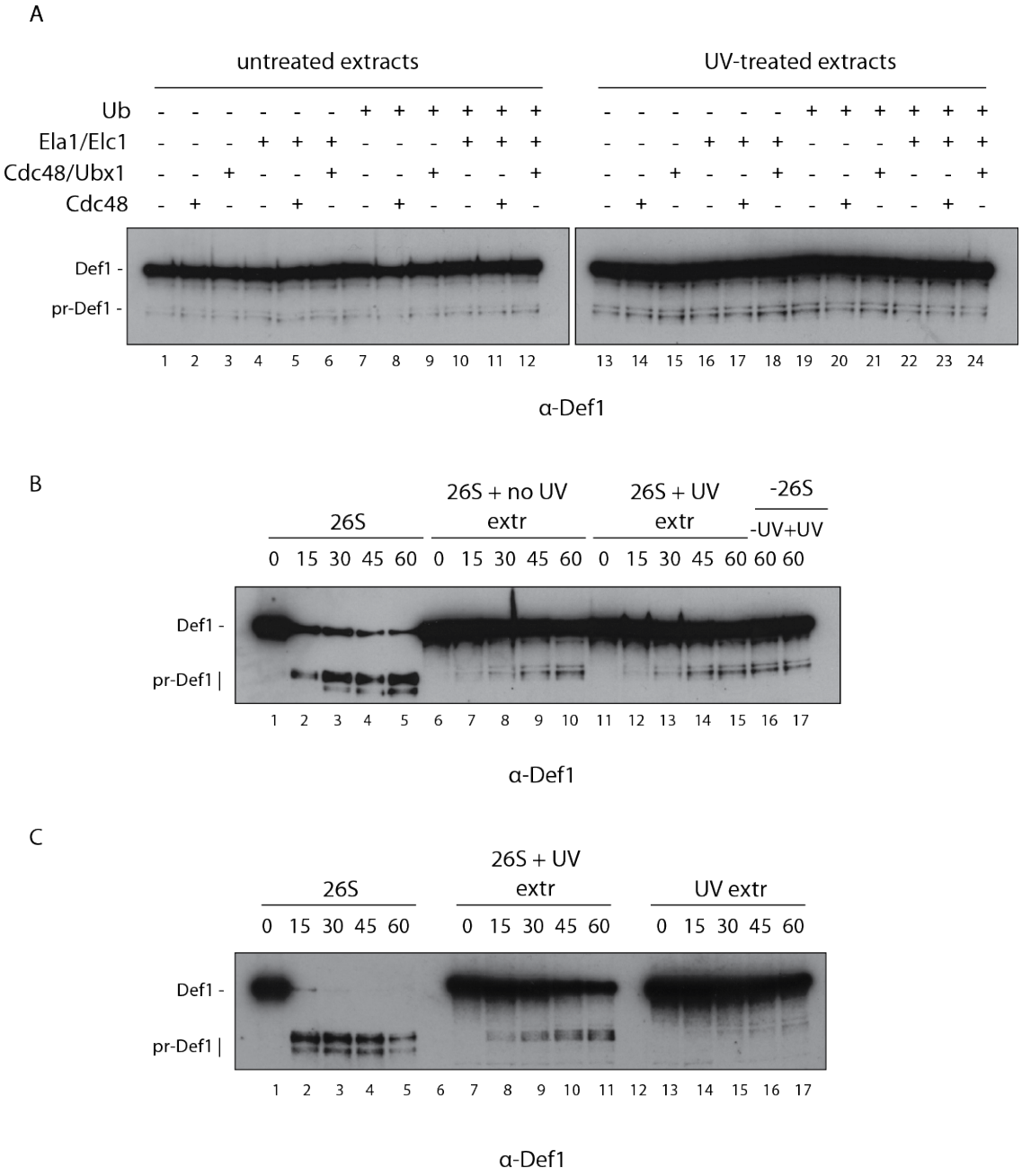

Figure 5.13. Def1 processing in extracts.
A – Def1 processing was performed using non-ubiquitylated Def1 in the presence of 100 ng extracts ± UV and no 26S proteasome for 1h at 30 °C. Half of the reactions were supplemented with free ubiquitin. Ela1/Elc1, Cdc48 alone, and Cdc48/Ubx1 (same as in Figure 5.12 A) were added to the reactions to the final concentration of 20 nM each. Results were visualised by Western blotting using α-Def1 antibody. ***B*** – Effect of extracts on Def1 processing in the presence of the 26S proteasome. *In vitro* processing reactions were supplemented with 100 ng extracts ± UV. The reaction was carried out for the indicated times at 30 °C. Results were visualised by Western blotting using α-Def1 antibody. ***C*** - Effect of extracts in the presence of the 10x the concentration of the 26S proteasome compared to ***B***. The experiment was performed as in ***B***.

The next step was to explore if the extracts were able to stimulate the processing of Def1 if purified 26S proteasome was added to the reaction (Figure 5.13 B). Unexpectedly, in the reactions supplemented with extracts (lanes 6-15), Def1 processing, as well as degradation (which was normally seen in the processing reactions), were decreased. The level of pr-Def1 generated in the reaction was comparable between the 26S proteasome reactions supplemented with extracts (lanes 10 and 15) and extract alone samples at 60 min timepoint (lanes 16 and 17). Moreover, no difference was observed between the UV treated and untreated extracts (compare lanes 6-10 and 11-15). One possibility is that in the presence of extracts the 26S proteasome had many more substrates thus was actively being titrated away from the Def1 protein.

Another result from this experiment was the altered migration of pr-Def1 bands resulting from the proteasome-alone reaction and processing reaction in the presence of extracts (compare lanes 1-5 to the rest of the lanes). Pr-Def1 resulting from 26S proteasome processing was migrating faster, suggesting a smaller protein size. Even though no fl-Def1 modification was observed in the reactions where extracts were added, it could not be refuted that pr-Def1 might be additionally modified in the extract, which would account for the size difference. Another possibility is that a small proportion of fl-Def1 got modified in the extracts and only the modified fl-Def1 was processed by the proteasome.

The reduction of the 26S proteasome activity towards Def1 in the presence of extracts could have masked any stimulatory effect extracts might have had on the reaction. This issue was solved by the addition of more of the 26S proteasome to the reaction. In this experiment, the concentration of the 26S proteasome was increased 10 times compared to the previous reactions (Figure 5.13 C). As expected, the amount of pr-Def1 resulting from the 26S proteasome with the extract reaction was increased as well (lanes 7-11). Nevertheless, it was still less compared to the proteasome-alone sample (lanes 1-5) and the size of the pr-Def1 species from the two reactions remained different.

The reaction with proteasome alone in this experiment gave some additional insight into the processing reaction. Almost all of the fl-Def1 was either degraded or

converted into pr-Def1 by the proteasome in the first 15 minutes (lane 2). But it is worth noting, that after 60 minutes there was also a decrease in the intensity of pr-Def1 band (lane 5), suggesting that this species was also being degraded by the proteasome. However, it was disappearing slower compared to the fl-Def1, indicating that fl-Def1 might be the preferred substrate.

Overall, several attempts were made to delineate Def1 processing *in vitro*. Even though I was unable to fully reconstitute the reaction and investigate the exact role of each protein, some valuable insights can be taken from these studies. First of all, the minimal requirement for the processing reaction is Def1 and the proteasome, implying that all the necessary information is already present in Def1's sequence and structure. Secondly, ubiquitylation did not seem to have an effect *in vitro*, and it may not be absolutely required for the reaction, even though it undoubtedly plays an important role *in vivo*. And finally, more efforts are needed to conclusively evaluate the effect of Cdc48, Ubx1 and other accessory proteins in the reaction. One possibilty for the efficiency of the processing reaction is a requirement of a scafold, such as chromatin. All these points are discussed more in depth in the Discusssion section (6).

6 Discussion

6.1 Molecular requirements for partial proteasomal processing

Previous *in vivo* experiments have demonstrated that the ubiquitin ligase Rsp5 and the proteasome are involved in Def1 activation by partial proteasomal processing (Wilson, Harreman, Taschner, et al. 2013). The work presented in this thesis has expanded the list of factors involved in the process. Both the ubiquitin-dependent segregase Cdc48 and its adaptor protein Ubx1 were shown to be required for Def1 processing. While Cdc48 has been implicated in similar processes before, this is the first time a role in partial proteasomal processing has been suggested for the Ubx1 protein. Smy2, a high-copy suppressor of *Δdef1* phenotypes, was also shown to be needed for the Def1 processing reaction *in vivo.* While Cdc48 and Ubx1 are most likely to be involved in the resolution of a reaction intermediate, such as the pr-Def1/fl-Def1 dimer, in the same manner as Cdc48 and another UBX family member, Ubx2, act in the processing of the transcription factor Spt23 (Kolawa et al. 2013), the role of Smy2 remains elusive, although initial studies suggest it might also be working with Cdc48.

Unfortunately, the Def1 processing reconstitution reaction *in vitro* using purified proteins requires further optimisation. One of the biggest obstacles in the assay is the dual action of the proteasome – it was both processing Def1 and degrading it. Due to the fact that the requirements for proteasomal processing and degradation are very similar, it is virtually impossible to separate the two processes. Bearing in mind that pr-Def1 is a very short-lived form *in vivo* and can only be visualised in extracts prepared either by gentle (yeast pellet grinding in liquid nitrogen) or quick (quick sodium hydroxide extraction and immediate SDS-PAGE) methods, it is highly likely that the pr-Def1 form is also rapidly degraded *in vitro.* Nevertheless, there is a possibility that it could be stabilised *in vivo* under the right conditions, e.g. while interacting with stalled ubiquitylated RNAPII. One possibility for separating the two proteasomal activities on Def1 would be the identification of the sequence or structure elements leading to the rapid degradation of pr-Def1 and eliminating them by mutation, so that they would not interfere with the processing reaction.

Such experiments would allow measurements of the true accumulation of the pr-Def1 product, provided the same sequence or structural elements are not required for the processing reaction to occur. If the separation of function of the proteasome is possible, it would also give valuable insight into how the proteasome works and could be used to study other partially proteasomally processed substrates. It should be mentioned that preliminary results obtained by Marcus Wilson in the Svejstrup lab suggested that partial proteasomal processing is difficult to address by mutation and deletion (unpublished observations), in all likelihood because there is both some flexibility in structural element use, and several such elements.

There is also a possibility that a substantial proportion of Def1 is degraded, rather than processed, due to an incorrect arrangement of the proteasomal stop signal in a large proportion of molecules. Although the minimal requirements for the processing reaction of Def1 have been identified, the immediate molecular environment of Def1 might also play an important role. For example, Def1 interacting partners could be required to induce subtle allosteric changes, arranging the protein in a processing-favourable conformation. An intriguing requirement for efficient Def1 processing would be the interaction with the transcription-coupled nucleotide excision repair (TC-NER) factor Rad26. Actually, Def1 was first identified due to its interaction with Rad26 (Woudstra et al. 2002), and only later discovered not to be directly involved in the TC-NER pathway, but rather in RNAPII ubiquitylation/degradation. One could imagine a scenario where, for example, only Def1 molecules bound to Rad26 can become processed, ensuring the coordination between the TC-NER and the last resort pathways. Alternatively, it is possible that Rad26 could be preventing the processing of Def1 by masking the processing signal and that the activation can only occur when Def1 is released. In apparent agreement with the latter, degradation of RNAPII in response to UV damage occurs faster in the *Δrad26* strain (Woudstra et al. 2002).

A limiting factor in the Def1 *in vitro* assay was the mono-ubiquitylated Def1 species. Unfortunately, the purification efficiency of mono-ubiquitylated Def1 from the *in vitro* ubiquitylation reaction was not satisfactory. Even though this purification underwent several optimisation steps, the yields were low. And due to the limiting amounts of mono-ubiquitylated Def1 substrate, a satisfying in-depth analysis of the processing

reaction of this substrate could not be carried out. First of all, it is likely that the *in vitro* Def1 ubiquitylation reaction produced multi-ubiquitylated Def1 (poly-ubiquitin chain formation was prevented by using the no-lysine ubiquitin mutant in the reaction). Since the purification strategy was based on the immunoprecipitation via the tag on ubiquitin moiety, the elution step was not efficient, most likely due to the many epitopes associated with a single molecule of Def1. Chemical ubiquitin conjugation (van Tilburg et al. 2016) to specific residues in Def1 would be a good strategy to overcome this problem. Since Def1 does not have any cysteine residues, it could be easily achieved by specifically mutating a target lysine residue to a cysteine, which is subsequently used in the conjugation reaction. Time constrains prevented the implementation of this strategy, but it is a potential future direction to pursue. This approach would potentially allow investigating the importance of the position of ubiquitin signal in partial proteasomal processing of Def1.

The purification of full-length Def1 also posed difficulties, most likely due to the compositional bias of the protein – the C-terminal part of Def1 is extraordinarily glutamine-rich (46% of Def1 sequence is defined as glutamine-rich and glutamines constitute 23% of the total amino acid composition). Indeed, this feature has lead to the classification of Def1 as one of the prion-like proteins in yeast (Duennwald et al. 2006; Alberti et al. 2009; Nizhnikov et al. 2014). Although this feature makes Def1 an interesting substrate, it may not be an ideal substrate to study the general proteasomal processing, since it has inherent problems that make *in vitro* studies difficult. Needless to say, however, Def1 cannot be substituted for the studies of the last resort pathway.

Despite the challenges of the *in vitro* system, several important observations were made. First of all, that all the necessary information guiding the proteasome during the partial proteasomal processing reaction must already be present in the Def1 primary sequence and structure. The current consensus for structural features for partial proteasomal processing includes a mono-ubiquitylation signal for proteasomal targeting, an unstructured region for the initiation of the cleavage, and a stop signal, which seems to differ for proteins from higher eukaryotes and yeast. Most likely due to differences in processivity of the respective proteasomes (Kraut

et al. 2012), a tightly folded domain or a dimerisation domain is a good stop signal in yeast; however, higher eukaryotes require an additional nearby 'slippery' sequence (Nassif et al. 2014), helping to decrease the coupling efficiency between ATP hydrolysis and the work performed on the substrate (Hoyt et al. 2006).

Def1 becomes ubiquitylated by the Rps5 ubiquitin ligase in response to DNA damage, and this ubiquitylation activity has been shown to be required for Def1 processing *in vivo* (Wilson, Harreman, Taschner, et al. 2013). Interestingly, it is not an absolute requirement for the processing reactions *in vitro*, although it can change the rate of the reaction. It is possible, however, that the concentration of the proteasome in the *in vitro* reactions is high enough for the proteasome to efficiently associate with the Def1 protein and process it, while *in vivo* Def1 has to be actively targeted to the proteasome. When the *in vitro* processing reactions were performed in the presence of yeast extracts, the activity of the proteasome towards Def1 was indeed decreased (Figure 5.13). This effect was most likely due to the fact that the proteasome was titrated away by the presence of other substrates. However, the reactions in the presence of extracts would need to be repeated on the ubiquitylated Def1 sample to draw any strong conclusions, since the extracts used did not seem to support Def1 ubiquitylation when supplemented with ubiquitin. This result might be explained by the limiting availability of other ubiquitylation factors in the extracts.

There is also a possibility that Def1 ubiquitylated *in vitro* does not carry the ubiquitin signal at the same (combination of) sites that are important *in vivo*, so that the difference between Def1 and ub-Def1 could not be observed in the *in vitro* assays. When the ubiquitylation sites identified from a ubiquitylation reaction *in vitro* were mutated in Def1 and the effect tested *in vivo,* a decrease in ubiquitylation was observed; however, ubiquitylation was not completely abolished (Wilson, Harreman, Taschner, et al. 2013). It is worth noting that the proteasomal targeting signal and the proteasomal initiation site do not have to be in close proximity (Schrader et al. 2009; Inobe et al. 2011). This implies that if the ubiquitylation of Def1 is required for direct targeting to the proteasome, most likely ubiquitylation at more than one exposed site, or perhaps *any* site, would suffice.

As already mentioned, mono-ubiquitylation is enough to target a protein for partial proteasomal processing (Kravtsova-Ivantsiv et al. 2009; Rape et al. 2001), while poly-ubiquitin chains are required to target a protein for degradation. This opens the possibility that the mono-ubiquitin signal may not be directly recognised by the proteasome, but rather by some other proteins, which might in turn present the substrate to the proteasome for processing. It is also possible that if the ubiquitin signal is not cleaved off during the processing reaction from the processed form of the substrate, having only one ubiquitin moiety allows the release of the processed form from the proteasome. Both the Ubx2 protein involved in the processing of Spt23 (Kolawa et al. 2013) and the Ubx1 protein involved in the processing of Def1 carry N-terminal ubiquitin-binding UBA domains. And indeed, results from this thesis showed that Ubx1 preferentially interacts with wild-type Def1 compared to the ubiquitin-site mutant *in vivo*. Such targeting factors are likely to be required for the processing in higher eukaryotes as well, although it remains to be demonstrated. It would be interesting to directly investigate if the UBA domain of Ubx1 is required for Def1 processing, even if the experiment can only presently be conducted *in vivo*.

Additional ubiquitin-related observation in this thesis was the size similarity between the pr-Def1 originating from ubiquitylated and non-ubiquitylated Def1 samples. Further experiments would be needed to determine if the ubiquitin signal on Def1 is removed during the processing reaction by the proteasome-associated de-ubiquitylating enzymes, since all Def1 ubiquitylation sites identified so far are placed on the N-terminus of the protein, which actually remains intact after the processing reaction. Interestingly, initially ubiquitin was still found on the processed forms of Spt23 and Mga2 (Rape et al. 2001), however, later studies suggested only the full-length Spt23 to be ubiquitylated (Shcherbik & Haines 2007). If the ubiquitin signal is removed from Def1 during the processing reaction, it could suggest that this is also true for the Spt23, since they follow a similar processing mechanism. If it is, however, present on the processed proteins, it could suggest that ubiquitin also plays additional roles in the downstream activities of the processed proteins.

Although it seems that both Def1 and Spt23 are processed in the same general manner, there are some additional subtle differences. The most notable of them is

the different Cdc48 complexes involved in the reactions. Spt23 processing was shown to require Ufd1-Npl4 and Ubx2 adaptors, while Def1 processing instead requires the Ubx1 adaptor. In this context it is worth noting, that Ufd1-Npl4 and Ubx1 interaction with Cdc48 is mutually exclusive (Meyer et al. 2000). Similarly to Spt23, Ubx2 is tethered to the ER membrane in a perfect position to recognise the substrate and target it for proteasomal processing. However, it is an intriguing possibility that Ufd1-Npl4 plays an additional role in the process, even though they might simply be required to stabilise the interaction between Cdc48 and Ubx2 (Hänzelmann et al. 2011). If Ufd1-Npl4 plays a distinct role in the process, it would suggest that the general partial processing mechanism has subtly adjusted to deal differently with various substrates.

The 20S proteasome was also able to process Def1 *in vitro*, just like the 26S proteasome. At first glance, this is a surprising result, but it is not completely unexpected if one keeps the Def1 structure in mind. Most of this unusual protein, especially the C-terminal part, is structurally disordered. Hence, for partial proteasomal processing to occur, the unwinding activity of the regulatory 19S particle might be dispensable, at least at the rather high concentration of proteasome used *in vitro*. The 19S regulatory particle also carries substrate- and ubiquitin- binding domains. However, again it is possible that the concentration of both Def1 and the proteasome in the *in vitro* reactions were high enough for the proteasome to initiate at an internal unstructured site without any additional tethering.

Both direct and indirect evidence leads to the conclusion that Def1 is capable of dimerisation ((Wilson, Harreman, Taschner, et al. 2013) and this thesis). For the processing of Spt23, the IPT (Immunoglobulin-like, plexins, transcription factors) dimerisation domain plays an important role in preventing complete degradation of the protein (Rape et al. 2001). In contrast, the putative dimerisation domain of Def1 remains elusive, and it is not known if Def1 is in a dimeric configuration at all times, or if dimerisation is specifically induced in response to UV damage or other signals. There is a coiled-coil domain predicted in Def1 structure in proximity to the processing site, which could fit the requirement for a stop signal. The dimerization via IPT domains in Spt23 is resistant to 2.5 M NaCl washes (Rape et al. 2001), so it

is an interesting question whether, for example, the interaction between coiled coils in different Def1 monomers would be strong enough to withstand proteasomal action. Another exciting possibility would be if Def1 dimerises via the N-terminal ubiquitin-binding CUE domain. Dimerisation via a CUE domain has been demonstrated for the Vps9 protein, with the CUE domain dimer additionally capable of binding a single ubiquitin moiety with increased affinity (Prag et al. 2003). Structurally, the CUE domain on Def1 might be too far away from the processing site to be directly involved in the processing reaction. Nevertheless, one can imagine a regulatory model, in which Def1 binds its Elongin substrate via the dimerised CUE domain, which in turn results in dimerization at the downstream coiled-coil region. The CUE domain of Def1 was demonstrated to interact with the Ela1 component of the Elongin-Cullin E3 ligase, which carries a ubiquitin homology domain (Wilson, Harreman, Taschner, et al. 2013). It is not known if CUE domain dimerization can occur if ubiquitin is substituted for a ubiquitin homology domain. For practical reasons, it was not possible to consistently include the Elongin complex in the processing reactions in vitro, but experiments on the effect of the Elongin complex would certainly be warranted.

It is worth noting that due to its glutamine-rich (poly-Q) C-terminus, Def1 resembles the partially proteasomally processed Sp1 protein (Roos et al. 1997), which seems to lack the canonical structures involved in partial proteasomal processing, like a strongly folded (or a dimerisation) domain acting as a stop signal for the proteasome. However, low complexity regions have been shown to significantly reduce the processivity of the proteasome (Kraut et al. 2012), and potentially suggests that the dimerisation may not be absolutely required for the processing reaction. Nevertheless, this hypothesis would not explain why Cdc48 is required for the processing of Def1.

The full-length Def1 protein is thought to constantly shuttle between the nucleus and the cytoplasm; however, upon processing, a nuclear export signal present in the C-terminus is removed, allowing Def1 to accumulate in the nucleus (Wilson, Harreman, Taschner, et al. 2013). An important question on the location of the processing reaction still remains: does it occur in the nucleus or the cytoplasm? Since Def1 is involved in the highly regulated last resort pathway, where the

elevated degradation of transcribing RNA polymerases might have severe consequences in the cell, one could imagine that the right environment is needed for Def1 processing to occur. The factors involved in the processing reaction can be found both in the nucleus and the cytoplasm, making both scenarios possible. Well-designed microscopy experiments would be required to fully answer this question.

The aims of reconstituting the partial proteasomal processing *in vitro* were both to understand the molecular detail of this type of reaction, and to gain more insight into the regulation of Def1 and its implications for the last resort pathway. However, for the study of the general mechanism of partial proteasomal processing, a different substrate might be beneficial, one that is easier to purify, modify, and handle. Nevertheless, for further investigation of the role of Def1 in the last resort pathway, the optimised version of the Def1 processing assay could be expanded further with the assembly of stalled transcription complexes to investigate if Def1 is able to specifically recognise stalled RNAPII and decide its fate. Additionally, as mentioned previously, Def1 appears to be involved not only in the last resort pathway, but also in a variety of other cellular processes (discussed in the introduction (1.4.3.6)) (Jordan et al. 2007; Manogaran et al. 2011; Y.-B. Chen et al. 2005; Suzuki et al. 2011; Cai et al. 2006). It would be interesting to investigate if partial proteasomal processing is required for Def1 to faithfully perform its function in these processes as well, or if the unstructured C-terminus of the protein has a role in those processes.

6.2 Role of Cdc48 in the partial proteasomal processing

Unfortunately, it was not possible to develop the Def1 processing assay to a level where it was feasible to unambiguously answer the question of whether Cdc48 is required only for the dissolution of pr-Def1/fl-Def1 reaction intermediate (which was only observed in the absence of Cdc48 in response to UV *in vivo* (Figure 3.13)), or if it is also capable of stimulating the cleavage step performed by the proteasome. The finding that Def1 processing is delayed in the absence of Cdc48 *in vivo* suggests that Cdc48 might play a stimulatory role in partial proteasomal processing.

If Cdc48 adaptor proteins (such as Ubx2 and Ubx1) are the major factors recognising mono-ubiquitylation on the substrate protein as the processing signal, Cdc48 might in fact be involved in the targeting of the substrate to the proteasome rather than direct stimulation of the proteasomal activity. This consideration is especially interesting in the light of the Cdc48-20S proteasome complex discovered in archaea (Barthelme et al. 2014). However, the existence of such a complex is still to be determined in eukaryotes. Further studies of a combination of Cdc48 with a 20S proteasome in the *in vitro* Def1 processing reaction might yield interesting mechanistic results.

Cdc48 adaptor proteins are known to influence the ATPase activity of Cdc48 (Kondo et al. 1997; Meyer et al. 1998; Xiaoyi Zhang et al. 2015). It would be interesting to compare the Cdc48 ATPase rate between the complexes with Ubx1 and/or Ubx2, both involved in the processing reaction, and Ubx5, involved in the disassembly of the RNAPII complex in response to DNA damage. Such experiments could also be expanded by the addition of the relevant ubiquitylated substrates, and measurement of the segregase activity of the respective Cdc48-Ubx complexes. Since it is likely that Cdc48 is present during the cleavage step by the proteasome, it is important that the Cdc48 complex involved does not exert too much force unfolding the substrate, because this might result in complete unfolding and degradation rather than partial processing. It is theoretically possible that Cdc48 adaptors are involved in the partial proteasomal processing to modulate the Cdc48 segregase activity, preventing the complete unfolding and thus degradation. Alternatively, there might be a switch activating Cdc48 for the dissolution of the processing reaction intermediate specifically after the proteasome has released the substrate. However, it is not entirely clear what component of the reaction could carry out such function, but adaptors and specificity factors of Cdc48 are still being identified, and their roles are still being defined.

6.3 Role of Ubx1 in partial proteasomal processing

The Cdc48 adaptor protein Ubx1 (also known as Shp1) was first identified as a mutant capable of supressing the toxic effects of overexpression of the catalytic

subunit of the protein serine/threonine phosphatase 1 (PP1), Glc7, in yeast (S Zhang et al. 1995). It is thought to act by promoting the nuclear localisation of Glc7 (Cheng & R.-H. Chen 2010) and through ensuring the correct folding of PP1 (Cheng & R.-H. Chen 2015). It has also been suggested to promote cell cycle progression via its effect on Glc7 (Böhm & Buchberger 2013). Ubx1 has also been implicated in autophagosome biogenesis via its interaction with ubiquitin-fold autophagy protein Atg8 (Krick et al. 2010). Additionally, it has been implicated in the proteasomal degradation pathway of a Cdc48 model substrate (Schuberth et al. 2004). The loss of Ubx1 has severe consequences for the cell – the *UBX1* null mutant is inviable in the *S. cerevisiae* W303 background (Cheng & R.-H. Chen 2010). Work presented in this thesis now indicates that Ubx1 is also involved in partial proteasomal processing and activation of Def1 in response to DNA damage. This raises an interesting question of how UBX proteins differentiate between a variety of substrates. Proteomics studies have indicated that the absence of different UBX domain proteins leads to distinct effects on the ubiquitin conjugate proteome (Kolawa et al. 2013), although how this effect is achieved remains unknown.

Although the requirement for the Ufd1-Npl4 complex, also known to act as a Cdc48 adaptor, was not tested in this thesis, it is unlikely that Ufd1-Npl4 plays a role in Def1 processing, if Ubx1 is involved. It has been previously demonstrated, that binding of Ubx1 and Ufd1-Npl4 to Cdc48 is mutually exclusive (Schuberth & Buchberger 2008). On the other hand, showing that Ufd1-Npl4 complex is not required for the partial proteasomal processing of Def1, would support the results of Ubx1 involvement in the process.

6.4 Def1 as a regulator of the last resort pathway

The last resort pathway becomes activated when a persistently stalled RNA polymerase II (RNAPII) cannot be rescued. It consists of two sequential ubiquitylation steps. The first one is performed by Rsp5 and leads to mono-ubiquitylation of the largest subunit of RNAPII, Rpb1 (Huibregtse et al. 1995). This is followed by poly-ubiquitylation of the same subunit by the Elongin-Cullin complex (Ribar et al. 2006; Ribar et al. 2007; Harreman et al. 2009). Def1 is involved in this

poly-ubiquitylation step by recruiting the Elongin-Cullin complex to the RNAPII (Wilson, Harreman, Taschner, et al. 2013) and promoting its poly-ubiquitylation. However, there are two important unresolved questions remaining – how is permanently arrested RNAPII recognised and what acts as a switch between the pathway trying to rescue the stalled RNAPII, such as the TC-NER, and the last resort pathway?

Def1 processing is induced by the same triggers as those resulting in stalling of RNAPII, such as DNA damage. It would be interesting to investigate if the environment of stalled RNAPII is important for efficient processing of Def1 protein, e.g. if Def1 processing can only occur when it associates with a stalled RNAPII complex. Another unifying observation is that both Def1 and Rpb1 become mono-ubiquitylated by the same E3 ligase, Rsp5, suggesting that the activation of this ubiquitin ligase ensures that the two processes are concurrent. However, irrespective of DNA damage or other cellular stresses, there is always a sub-population of mono-ubiquitylated Rpb1 (Woudstra et al. 2002; Sigurdsson et al. 2010), the substrate for Def1 activity, while stress conditions are required for efficient Def1 processing (Wilson, Harreman, Taschner, et al. 2013). Even though the processing of Def1 removes the C-terminal nuclear export signal allowing it to accumulate in the nucleus (Wilson, Harreman, Taschner, et al. 2013), it might have additional effects on Def1 function, e.g. unmasking new interaction motifs. Mass spectrometry experiments with the $Def1_{1\text{-}500}$ form (mimicking the processed form) might help to identify if it has different interactors compared to the full-length protein.

Def1 also seems to be a suitable factor to regulate the switch between TC-NER and the last resort pathway. It is worth noting, however, that it appeared to only be the full-length, and not the processed form of Def1, that co-purifies with the TC-NER factor Rad26 from chromatin (Woudstra et al. 2002). As mentioned earlier, an attracting hypothesis would be if, for example, Def1 dissociates from Rad26 only if the TC-NER pathway fails to rescue the stalled RNAPII, allowing for processing to occur and the last-resort pathway to kick in. It would be interesting to investigate whether the interaction with Rad26 is able to protect Def1 from the activation by proteasomal processing, and the *in vitro* assay established here would provide a good platform for such experiments. It would also be interesting to investigate if

Rad26 is able to bind the pr-Def1 form and to identify the interaction motifs in both proteins. This direction of experiments would also potentially provide valuable information about the role of Def1 in (and the regulation of) the last resort pathway.

Another piece of evidence supporting the role of Def1 as a regulator between two parallel pathways comes from its role in the degradation of the Pol3 subunit of the replicative polymerase δ in response to DNA damage (Daraba et al. 2014). In a similar way to the last resort pathway, Def1 was found to interact with Rad5 protein, governing the error-free DNA damage bypass. Rad5 is thought to mediate template switching and utilise the newly synthesised strand of sister duplex as a template, bypassing the lesion ((H Zhang & C. W. Lawrence 2005) and leaving the damage on the original template to be repaired post-replicatively. The degradation of Pol3 aids the exchange between the replicative polymerase δ and an error-prone translesion synthesis polymerase Rev1, which is capable of replicating over the lesion (Daraba et al. 2014). Such regulation between the two pathways closely resembles the situation between TC-NER and the last resort pathway, where Def1 is involved in one branch, but is found to interact with a member of the alternative branch, namely Rad26.

6.5 Smy2 in the last resort pathway and as a general Cdc48 co-factor

Smy2 was identified as a high-copy suppressor of the slow growth phenotype of the *Δdef1* strain (Corbett laboratory, unpublished data), suggesting that elevated levels of Smy2 are able to at least partially compensate for the lack of Def1. This observation prompted further investigation into the role of Smy2 in the last resort pathway. Unexpectedly, we observed that the activation of Def1 is delayed in the absence of Smy2, and Smy2 was also able to interact with Def1 in a UV damage-independent manner (Figure 4.2). This raises the interesting question of how Smy2 can supress the *Δdef1* phenotype and be directly involved in Def1 processing as well? One possible explanation for these observations could be the involvement of Smy2 in two distinct steps in the last resort pathway. Indeed, Smy2 has previously been associated with the Rpb8 subunit of RNAPII in a low-throughput genetic study (Briand et al. 2001). Additional unpublished data from the Svejstrup laboratory also

supports this hypothesis of a dual role of Smy2 in that Smy2 on a high-copy plasmid was able to supress both the UV sensitivity of the *Δdef1Δrad16* mutant and the lethality of the *Δdef1 rsp5-1* strain. However, it was initially unclear why Smy2 is required at two different steps in the pathway and what its exact function is. The dual role of Smy2 in the pathway also complicated the *in vivo* experiments, since the separation of the two steps was required to elucidate its function.

An interesting observation was the accumulation of the ubiquitylated form of Def1 in the *Δsmy2* strain in response to DNA damage. It might simply be explained by processing of Def1 being perturbed in this strain, with accumulation of ub-Def1 as a direct consequence. However, the *Gyf* (homologue of Smy2) null mutants in *Drosophila melanogaster* were observed to accumulate ubiquitylated proteins without any external stress (M. Kim et al. 2015). Unpublished experiments from the Svejstrup lab (Michelle Harreman) have replicated this finding with the yeast *Δsmy2* mutant – indeed, under stress-free conditions this strain accumulates ubiquitin conjugates. Importantly, a similar effect has been observed for the Cdc48 and its UBX domain adaptor proteins (Kolawa et al. 2013), implying a more general function of Smy2 in the ubiquitin system, which is perfectly compatible with its role in the last resort pathway and Def1 processing.

An important result of this thesis was defining Smy2 as a general factor, rather than a factor specific to the last resort pathway, via the observation that the processing of Spt23 is also delayed in the *Δsmy2* strain (Figure 4.6 D). Further experiments are needed to understand the role of Smy2 in this process. However, since Cdc48 is also involved in both the processing of Def1 (this thesis) and Spt23 (Rape et al. 2001), we hypothesised that Smy2 might act as a general Cdc48 co-factor. Moreover, Cdc48 has already been implicated in two places in the last resort pathway - the removal of arrested RNAPII from chromatin (Verma et al. 2011) and Def1 processing (this thesis) – and Smy2 seems to have a dual role in the pathway as well.

Interestingly, previous reports on a high-throughput proteomics screen had actually already placed Smy2 in the vicinity of Cdc48 (Krogan et al. 2006), and genetic screens had classified Smy2 as a high-copy suppressor of a temperature-sensitive

cdc48-3 S. cerevisiae strain (Magtanong et al. 2011). Although we were not able to observe the interaction between purified full-length Cdc48 and Smy2 *in vitro* (potentially due to the lack of post-translational modifications on the Smy2 protein, or correct nucleotide state of Cdc48), the GYF domain of the Smy2 protein directly interacted with full-length Cdc48, and the proteins could also be co-immunoprecipitated from yeast extracts, suggesting that they do indeed interact.

GYF domains are known to bind proline-rich sequences with proline-proline-glycine (PPG) being a general recognition motif (Kofler et al. 2005). Interestingly, such a motif can be found in the Cdc48 protein in both the D1 and D2 ATPase domains - P254, P255, G256 and P529, P530, G531, respectively. Intriguingly, these residues constitute a part of the Walker A motif (also known as a phosphate binding loop, or P-loop), which, as the name suggests, is involved in nucleotide binding. The P-loop is a highly conserved feature, important for the ATPase activity, hence it at first glance seems unlikely to act as a binding site. Nevertheless, this scenario might be possible, since the P-loop of a bacterial serine/threonine protein kinase, HipA, has been observed in several different confirmations, one of which was accessible for auto-phosphorylation, hereby regulating the kinase activity (Schumacher et al. 2012). This observation opens up the new and exciting possibility of Smy2 interacting with Cdc48 molecules that are exhibiting the ejected P-loop confirmation, and hereby modulates Cdc48 ATPase activity. Such a scenario would constitute a novel class of Cdc48 regulators. It would be very exciting if Smy2 is indeed able to modulate the ATPase activity of Cdc48, as it might have high relevance to potential therapeutic strategies for Cdc48-related diseases. Several Cdc48 inhibitors are already being used for cancer treatment (Chapman et al. 2015). The work presented in this thesis is still at an early stage and further biochemical characterisation of the interaction between Cdc48 and Smy2 and the effect of Smy2 on Cdc48 activity is presently in progress, which will hopefully lead to interesting discoveries.

6.6 Relevance to higher eukaryotes

The last resort pathway is highly conserved from yeast to humans. The low complexity regions in Def1 have prevented the identification of a homologue by sequence or structure alignment methods. However, a recent unpublished work from the Svejstrup laboratory has suggested the presence of the functional homologue of Def1 in humans, named UBAP2L. It would be interesting to see if this functional homologue undergoes similar activation reactions as the yeast Def1. Intriguingly, faster migrating bands of the functional homologue of Def1 appear in response to UV damage, and this protein also interacts with CSB (human homologue of the Rad26 protein).

Another interesting aspect of the Def1 protein is the fact that during its activation it loses the majority of its poly-glutamine region. Due to this region, Def1 has also been identified as one of the yeast prion proteins (Duennwald et al. 2006; Alberti et al. 2009; Nizhnikov et al. 2014). In humans, several different neurodegenerative disorders are caused by poly-glutamine expansions, resulting from the CAG trinucleotide amplifications. Nine human proteins with poly-glutamine expansions have been implicated in different neurodegerative conditions (Schöls et al. 2004). Proteolytic cleavage of these proteins is thought to release the poly-glutamine fragment (Tarlac & Storey 2003), which is able to resist efficient degradation by the proteasome (Kraut et al. 2012). The current model suggests that the toxicity is generated via disregulation of transcription or ion channel formation (Tarlac & Storey 2003). It would be interesting to see whether new functions/phenotypes are triggered via poly-glutamine expansions of Def1 and if they in any way relate to the mechanism of the neurodegenerative disease in humans.

The human homologue of Smy2 protein is the GIGYF2 protein (also known as PERQ2). It has been implicated in splicing and COPII vesicle formation (Ash et al. 2010), as well as post-translational gene silencing (Kryszke et al. 2016). It would be interesting to investigate if, as we would propose, the function of GIGYF2 in these processes is dependent on, or related to, the p97 protein (human homologue of Cdc48). Current work in the Svejstrup laboratory is focused on creating CRISPR mutants of the GIGYF2 protein and further investigating its function in the ubiquitin system, e.g. whether elevated levels of ubiquitin conjugates are observed in the

absence of the protein, in a manner similar to the studies in *D. melanogaster* (M. Kim et al. 2015).

Interestingly, GIGYF2 has also been implicated in Parkinson's disease with the N56S and N457T mutations suggested to be associated with the increased risk of Parkinson's disease in Caucasians (Yuan Zhang et al. 2015). It would be interesting to know what effect the equivalent mutations have in Smy2 protein, whether they affect the last resort pathway and if the increased risk of Parkinson's is in any way related to the function of Cdc48.

6.7 Summary

The work presented in this thesis has demonstrated that in addition to the E3 ubiquitin ligase Rsp5 and the proteasome, Cdc48 together with a UBX family adaptor protein, Ubx1, are required for the activation of Def1 in response to DNA damage. The partial proteasomal processing of Def1 is likely to be very similar to that of the transcription factor Spt23, where Cdc48 and Ubx2 proteins are required, suggesting a general partial proteasomal processing mechanism in yeast.

Although the *in vitro* Def1 partial proteasomal processing reaction requires further optimisation, the minimal requirements for Def1 processing have been uncovered, suggesting that the primary sequence and structure of Def1 is sufficient to guide the proteasome in the *in vitro* reaction. The *in vitro* processing reaction forms a base for further *in vitro* studies of both the general proteasomal processing mechanism, and specifically the last resort pathway. The immediate direction of further investigations could be the relationship between Rad26 and Def1, potentially governing the switch between the TC-NER and the last resort pathways.

Additionally, the preliminary results presented in this thesis suggest that the GYF domain protein Smy2, which is both involved in Def1 processing and the last resort pathway, may act as a novel Cdc48 co-factor. Smy2 was observed to associate with Cdc48 in immunoprecipitation experiments and a direct binding between the Smy2 GYF domain and Cdc48 was demonstrated using purified proteins. In

addition to its roles in the last resort pathway, Smy2 is required for the efficient processing of Spt23 *in vivo*. Further experiments investigating the relationship between Smy2 and Cdc48 might yield interesting results regarding the regulation of Cdc48.

7 Reference List

Acconcia, F., Sigismund, S. & Polo, S., 2009. Ubiquitin in trafficking: The network at work. *Experimental cell research*, 315(9), pp.1610–1618.

Acharya, U. et al., 1995. The formation of Golgi stacks from vesiculated Golgi membranes requires two distinct fusion events. *Cell*, 82(6), pp.895–904.

Al-Moghrabi, N.M., Al-Sharif, I.S. & Aboussekhra, A., 2003. UV-induced de novo protein synthesis enhances nucleotide excision repair efficiency in a transcription-dependent manner in S. cerevisiae. *DNA repair*, 2(11), pp.1185–1197.

Alberti, S. et al., 2009. A systematic survey identifies prions and illuminates sequence features of prionogenic proteins. *Cell*, 137(1), pp.146–158.

Anindya, R., Aygün, O. & Svejstrup, J.Q., 2007. Damage-induced ubiquitylation of human RNA polymerase II by the ubiquitin ligase Nedd4, but not Cockayne syndrome proteins or BRCA1. *Molecular cell*, 28(3), pp.386–397.

Armache, K.-J., Kettenberger, H. & Cramer, P., 2003. Architecture of initiation-competent 12-subunit RNA polymerase II. *Proceedings of the National Academy of Sciences of the United States of America*, 100(12), pp.6964–6968.

Arnason, T.G. et al., 2005. Novel interaction between Apc5p and Rsp5p in an intracellular signaling pathway in Saccharomyces cerevisiae. *Eukaryotic cell*, 4(1), pp.134–146.

Ash, M.-R. et al., 2010. Conserved beta-hairpin recognition by the GYF domains of Smy2 and GIGYF2 in mRNA surveillance and vesicular transport complexes. *Structure*, 18(8), pp.944–954.

Aubin-Tam, M.-E. et al., 2011. Single-molecule protein unfolding and translocation by an ATP-fueled proteolytic machine. *Cell*, 145(2), pp.257–267.

Aufderheide, A. et al., 2015. Structural characterization of the interaction of Ubp6 with the 26S proteasome. *Proceedings of the National Academy of Sciences of the United States of America*, 112(28), pp.8626–8631.

Auld, K.L. & Silver, P.A., 2006. Transcriptional regulation by the proteasome as a mechanism for cellular protein homeostasis. *Cell cycle*, 5(14), pp.1503–1505.

Aza-Blanc, P. et al., 1997. Proteolysis that is inhibited by hedgehog targets Cubitus interruptus protein to the nucleus and converts it to a repressor. *Cell*, 89(7), pp.1043–1053.

Bachmair, A., Finley, D. & Varshavsky, A., 1986. In vivo half-life of a protein is a function of its amino-terminal residue. *Science*, 234(4773), pp.179–186.

Baek, G.H. et al., 2013. Cdc48: A Swiss Army Knife of Cell Biology. *Journal of*

Amino Acids, 2013(4), pp.1–12.

Bagola, K. et al., 2013. Ubiquitin binding by a CUE domain regulates ubiquitin chain formation by ERAD E3 ligases. *Molecular cell*, 50(4), pp.528–539.

Banerjee, S. et al., 2016. 2.3 Å resolution cryo-EM structure of human p97 and mechanism of allosteric inhibition. *Science*, 351(6275), pp.871–875.

Bar-Nahum, G. et al., 2005. A ratchet mechanism of transcription elongation and its control. *Cell*, 120(2), pp.183–193.

Bartel, B., Wünning, I. & Varshavsky, A., 1990. The recognition component of the N-end rule pathway. *The EMBO journal*, 9(10), pp.3179–3189.

Barthelme, D. & Sauer, R.T., 2012. Identification of the Cdc48•20S proteasome as an ancient AAA+ proteolytic machine. *Science*, 337(6096), pp.843–846.

Barthelme, D. et al., 2014. Architecture and assembly of the archaeal Cdc48*20S proteasome. *Proceedings of the National Academy of Sciences of the United States of America*, 111(17), pp.E1687–94.

Barthelme, D., Jauregui, R. & Sauer, R.T., 2015. An ALS disease mutation in Cdc48/p97 impairs 20S proteasome binding and proteolytic communication. *Protein Science*, 24(9), pp.1521–1527.

Bashore, C. et al., 2015. Ubp6 deubiquitinase controls conformational dynamics and substrate degradation of the 26S proteasome. *Nature structural & molecular biology*, 22(9), pp.712–719.

Beaudenon, S.L. et al., 1999. Rsp5 ubiquitin-protein ligase mediates DNA damage-induced degradation of the large subunit of RNA polymerase II in Saccharomyces cerevisiae. *Molecular and cellular biology*, 19(10), pp.6972–6979.

Beck, F. et al., 2012. Near-atomic resolution structural model of the yeast 26S proteasome. *Proceedings of the National Academy of Sciences of the United States of America*, 109(37), pp.14870–14875.

Belotserkovskaya, R. et al., 2003. FACT facilitates transcription-dependent nucleosome alteration. *Science*, 301(5636), pp.1090–1093.

Berndsen, C.E. & Wolberger, C., 2014. New insights into ubiquitin E3 ligase mechanism. *Nature structural & molecular biology*, 21(4), pp.301–307.

Bernier-Villamor, V. et al., 2002. Structural basis for E2-mediated SUMO conjugation revealed by a complex between ubiquitin-conjugating enzyme Ubc9 and RanGAP1. *Cell*, 108(3), pp.345–356.

Besche, H.C. et al., 2014. Autoubiquitination of the 26S proteasome on Rpn13 regulates breakdown of ubiquitin conjugates. *The EMBO journal*, 33(10), pp.1159–1176.

Beskow, A. et al., 2009. A conserved unfoldase activity for the p97 AAA-ATPase in proteasomal degradation. *Journal of Molecular Biology*, 394(4), pp.732–746.

Beuron, F. et al., 2006. Conformational changes in the AAA ATPase p97-p47 adaptor complex. *The EMBO journal*, 25(9), pp.1967–1976.

Bintu, L. et al., 2011. The elongation rate of RNA polymerase determines the fate of transcribed nucleosomes. *Nature structural & molecular biology*, 18(12), pp.1394–1399.

Boeddrich, A. et al., 2006. An arginine/lysine-rich motif is crucial for VCP/p97-mediated modulation of ataxin-3 fibrillogenesis. *The EMBO journal*, 25(7), pp.1547–1558.

Bohr, V., 1985. DNA repair in an active gene: Removal of pyrimidine dimers from the DHFR gene of CHO cells is much more efficient than in the genome overall. *Cell*, 40(2), pp.359–369.

Böhm, S. & Buchberger, A., 2013. The budding yeast Cdc48(Shp1) complex promotes cell cycle progression by positive regulation of protein phosphatase 1 (Glc7). *PloS one*, 8(2), p.e56486.

Braun, S. et al., 2002. Role of the ubiquitin-selective CDC48(UFD1/NPL4)chaperone (segregase) in ERAD of OLE1 and other substrates. *The EMBO journal*, 21(4), pp.615–621.

Bregman, D.B. et al., 1996. UV-induced ubiquitination of RNA polymerase II: a novel modification deficient in Cockayne syndrome cells. *Proceedings of the National Academy of Sciences of the United States of America*, 93(21), pp.11586–11590.

Briand, J.-F. et al., 2001. Partners of Rpb8p, a Small Subunit Shared by Yeast RNA Polymerases I, II, and III. *Molecular and cellular biology*, 21(17), pp.6056–6065.

Bruderer, R.M., Brasseur, C. & Meyer, H.H., 2004. The AAA ATPase p97/VCP Interacts with Its Alternative Co-factors, Ufd1-Npl4 and p47, through a Common Bipartite Binding Mechanism. *Journal of Biological Chemistry*, 279(48), pp.49609–49616.

Brueckner, F. et al., 2007. CPD damage recognition by transcribing RNA polymerase II. *Science*, 315(5813), pp.859–862.

Buchberger, A. et al., 2001. The UBX domain: a widespread ubiquitin-like module. *Journal of Molecular Biology*, 307(1), pp.17–24.

Bucheli, M. & Sweder, K., 2004. In UV-irradiated Saccharomyces cerevisiae, overexpression of Swi2/Snf2 family member Rad26 increases transcription-coupled repair and repair of the non-transcribed strand. *Molecular microbiology*, 52(6), pp.1653–1663.

Burgis, N.E. & Samson, L.D., 2007. The Protein Degradation Response of

Saccharomyces cerevisiaeto Classical DNA-Damaging Agents. *Chemical Research in Toxicology*, 20(12), pp.1843–1853.

Bushnell, D.A. & Kornberg, R.D., 2003. Complete, 12-subunit RNA polymerase II at 4.1-A resolution: implications for the initiation of transcription. *Proceedings of the National Academy of Sciences of the United States of America*, 100(12), pp.6969–6973.

Butala, M., Zgur-Bertok, D. & Busby, S.J.W., 2009. The bacterial LexA transcriptional repressor. *Cellular and molecular life sciences : CMLS*, 66(1), pp.82–93.

Cai, H. et al., 2006. Genomewide screen reveals a wide regulatory network for di/tripeptide utilization in Saccharomyces cerevisiae. *Genetics*, 172(3), pp.1459–1476.

Carey, M., Li, B. & Workman, J.L., 2006. RSC exploits histone acetylation to abrogate the nucleosomal block to RNA polymerase II elongation. *Molecular cell*, 24(3), pp.481–487.

Carvalho, P., Goder, V. & Rapoport, T.A., 2006. Distinct ubiquitin-ligase complexes define convergent pathways for the degradation of ER proteins. *Cell*, 126(2), pp.361–373.

Carvalho, P., Stanley, A.M. & Rapoport, T.A., 2010. Retrotranslocation of a misfolded luminal ER protein by the ubiquitin-ligase Hrd1p. *Cell*, 143(4), pp.579–591.

Chang, A. et al., 2000. Rsp5 WW domains interact directly with the carboxyl-terminal domain of RNA polymerase II. *The Journal of biological chemistry*, 275(27), pp.20562–20571.

Chapman, E. et al., 2015. Inhibitors of the AAA+ chaperone p97. *Molecules*, 20(2), pp.3027–3049.

Charlet-Berguerand, N. et al., 2006. RNA polymerase II bypass of oxidative DNA damage is regulated by transcription elongation factors. *The EMBO journal*, 25(23), pp.5481–5491.

Chen, C.H. et al., 1999. Nuclear trafficking of Cubitus interruptus in the transcriptional regulation of Hedgehog target gene expression. *Cell*, 98(3), pp.305–316.

Chen, X. et al., 2009. Rpb1 sumoylation in response to UV radiation or transcriptional impairment in yeast. *PloS one*, 4(4), p.e5267.

Chen, X., Ruggiero, C. & Li, S., 2007. Yeast Rpb9 plays an important role in ubiquitylation and degradation of Rpb1 in response to UV-induced DNA damage. *Molecular and cellular biology*, 27(13), pp.4617–4625.

Chen, Y.-B. et al., 2005. Def1p is involved in telomere maintenance in budding yeast. *The Journal of biological chemistry*, 280(26), pp.24784–24791.

Cheng, Y.-L. & Chen, R.-H., 2015. Assembly and quality control of the protein phosphatase 1 holoenzyme involves the Cdc48-Shp1 chaperone. *Journal of cell science*, 128(6), pp.1180–1192.

Cheng, Y.-L. & Chen, R.-H., 2010. The AAA-ATPase Cdc48 and cofactor Shp1 promote chromosome bi-orientation by balancing Aurora B activity. *Journal of cell science*, 123(Pt 12), pp.2025–2034.

Cheung, A.C.M. & Cramer, P., 2011. Structural basis of RNA polymerase II backtracking, arrest and reactivation. *Nature*, 471(7337), pp.249–253.

Choi, W.S. et al., 2010. Structural basis for the recognition of N-end rule substrates by the UBR box of ubiquitin ligases. *Nature structural & molecular biology*, 17(10), pp.1175–1181.

Cholbinski, P. et al., 2011. Yeast ubiquitin ligase Rsp5 contains nuclear localization and export signals. *European journal of cell biology*, 90(10), pp.834–843.

Chou, T.-F. et al., 2014. Specific Inhibition of p97/VCP ATPase and Kinetic Analysis Demonstrate Interaction between D1 and D2 ATPase Domains. *Journal of Molecular Biology*, 426(15), pp.2886–2899.

Chubb, J.R. et al., 2006. Transcriptional pulsing of a developmental gene. *Current biology*, 16(10), pp.1018–1025.

Churchman, L.S. & Weissman, J.S., 2011. Nascent transcript sequencing visualizes transcription at nucleotide resolution. *Nature*, 469(7330), pp.368–373.

Ciechanover, A. et al., 1980. Characterization of the heat-stable polypeptide of the ATP-dependent proteolytic system from reticulocytes. *The Journal of biological chemistry*, 255(16), pp.7525–7528.

Cloutier, P. et al., 2013. A newly uncovered group of distantly related lysine methyltransferases preferentially interact with molecular chaperones to regulate their activity. *PLoS genetics*, 9(1), p.e1003210.

Cohen, M., Stutz, F. & Dargemont, C., 2003. Deubiquitination, a new player in Golgi to endoplasmic reticulum retrograde transport. *The Journal of biological chemistry*, 278(52), pp.51989–51992.

Collins, G.A. et al., 2010. Combined chemical and genetic approach to inhibit proteolysis by the proteasome. *Yeast*, 27(11), pp.965–974.

Coppotelli, G. et al., 2011. High avidity binding to DNA protects ubiquitylated substrates from proteasomal degradation. *Journal of Biological Chemistry*, 286(22), pp.19565–19575.

Cramer, P., Bushnell, D.A. & Kornberg, R.D., 2001. Structural basis of transcription: RNA polymerase II at 2.8 angstrom resolution. *Science*, 292(5523), pp.1863–1876.

Crosas, B. et al., 2006. Ubiquitin chains are remodeled at the proteasome by opposing ubiquitin ligase and deubiquitinating activities. *Cell*, 127(7), pp.1401–1413.

Dai, R.M. & Li, C.C., 2001. Valosin-containing protein is a multi-ubiquitin chain-targeting factor required in ubiquitin-proteasome degradation. *Nature cell biology*, 3(8), pp.740–744.

Dalal, R.V. et al., 2006. Pulling on the nascent RNA during transcription does not alter kinetics of elongation or ubiquitous pausing. *Molecular cell*, 23(2), pp.231–239.

Damsma, G.E. et al., 2007. Mechanism of transcriptional stalling at cisplatin-damaged DNA. *Nature structural & molecular biology*, 14(12), pp.1127–1133.

Daraba, A. et al., 2014. Def1 Promotes the Degradation of Pol3 for Polymerase Exchange to Occur During DNA-Damage-Induced Mutagenesis in Saccharomyces cerevisiae. *PLoS biology*, 12(1), p.e1001771.

Daulny, A. et al., 2008. Modulation of RNA polymerase II subunit composition by ubiquitylation. *Proceedings of the National Academy of Sciences of the United States of America*, 105(50), pp.19649–19654.

DeLaBarre, B. & Brunger, A.T., 2005. Nucleotide dependent motion and mechanism of action of p97/VCP. *Journal of Molecular Biology*, 347(2), pp.437–452.

DeLaBarre, B. et al., 2006. Central pore residues mediate the p97/VCP activity required for ERAD. *Molecular cell*, 22(4), pp.451–462.

Depken, M., Galburt, E.A. & Grill, S.W., 2009. The origin of short transcriptional pauses. *Biophysical journal*, 96(6), pp.2189–2193.

Derheimer, F.A. et al., 2007. RPA and ATR link transcriptional stress to p53. *Proceedings of the National Academy of Sciences of the United States of America*, 104(31), pp.12778–12783.

Ding, B., Lejeune, D. & Li, S., 2010. The C-terminal repeat domain of Spt5 plays an important role in suppression of Rad26-independent transcription coupled repair. *Journal of Biological Chemistry*, 285(8), pp.5317–5326.

Domanska, A. & Kaminska, J., 2015. Role of Rsp5 ubiquitin ligase in biogenesis of rRNA, mRNA and tRNA in yeast. *RNA biology*, 12(12), pp.1265–1274.

Donahue, B.A. et al., 1994. Transcript cleavage by RNA polymerase II arrested by a cyclobutane pyrimidine dimer in the DNA template. *Proceedings of the National Academy of Sciences of the United States of America*, 91(18), pp.8502–8506.

Donaldson, K.M. et al., 2003. Ubiquitin signals protein trafficking via interaction with a novel ubiquitin binding domain in the membrane fusion regulator, Vps9p. *Current biology*, 13(3), pp.258–262.

Dreveny, I. et al., 2004. Structural basis of the interaction between the AAA ATPase p97/VCP and its adaptor protein p47. *The EMBO journal*, 23(5), pp.1030–1039.

Duda, D.M. et al., 2008. Structural insights into NEDD8 activation of cullin-RING ligases: conformational control of conjugation. *Cell*, 134(6), pp.995–1006.

Duennwald, M.L. et al., 2006. A network of protein interactions determines polyglutamine toxicity. *Proceedings of the National Academy of Sciences of the United States of America*, 103(29), pp.11051–11056.

Dunn, R. et al., 2004. The C2 domain of the Rsp5 ubiquitin ligase binds membrane phosphoinositides and directs ubiquitination of endosomal cargo. *The Journal of cell biology*, 165(1), pp.135–144.

Durcan, T.M. et al., 2014. USP8 regulates mitophagy by removing K6-linked ubiquitin conjugates from parkin. *The EMBO journal*, 33(21), pp.2473–2491.

Eddins, M.J. et al., 2006. Mms2-Ubc13 covalently bound to ubiquitin reveals the structural basis of linkage-specific polyubiquitin chain formation. *Nature structural & molecular biology*, 13(10), pp.915–920.

Elia, A.E.H. et al., 2015. Quantitative Proteomic Atlas of Ubiquitination and Acetylation in the DNA Damage Response. *Molecular cell*, 59(5), pp.867–881.

Elsasser, S. et al., 2002. Proteasome subunit Rpn1 binds ubiquitin-like protein domains. *Nature cell biology*, 4(9), pp.725–730.

Elsasser, S. et al., 2004. Rad23 and Rpn10 serve as alternative ubiquitin receptors for the proteasome. *The Journal of biological chemistry*, 279(26), pp.26817–26822.

Epshtein, V. & Nudler, E., 2003. Cooperation between RNA polymerase molecules in transcription elongation. *Science*, 300(5620), pp.801–805.

Esaki, M. & Ogura, T., 2010. ATP-bound form of the D1 AAA domain inhibits an essential function of Cdc48p/p97. *Biochemistry and cell biology = Biochimie et biologie cellulaire*, 88(1), pp.109–117.

Ewens, C.A. et al., 2010. Structural and functional implications of phosphorylation and acetylation in the regulation of the AAA+ protein p97. *Biochemistry and cell biology = Biochimie et biologie cellulaire*, 88(1), pp.41–48.

Fan, C.M. & Maniatis, T., 1991. Generation of p50 subunit of NF-kappa B by processing of p105 through an ATP-dependent pathway. *Nature*, 354(6352), pp.395–398.

Fehlker, M. et al., 2003. Blm3 is part of nascent proteasomes and is involved in a late stage of nuclear proteasome assembly. *EMBO reports*, 4(10), pp.959–963.

Feldman, R.M. et al., 1997. A complex of Cdc4p, Skp1p, and Cdc53p/cullin catalyzes ubiquitination of the phosphorylated CDK inhibitor Sic1p. *Cell*, 91(2),

pp.221–230.

Fierz, B. et al., 2011. Histone H2B ubiquitylation disrupts local and higher-order chromatin compaction. *Nature chemical biology*, 7(2), pp.113–119.

Finley, D., 2009. Recognition and processing of ubiquitin-protein conjugates by the proteasome. *Annual Review of Biochemistry*, 78, pp.477–513.

Finley, D. et al., 2012. The ubiquitin-proteasome system of Saccharomyces cerevisiae. *Genetics*, 192(2), pp.319–360.

Finley, D., Chen, X. & Walters, K.J., 2016. Gates, Channels, and Switches: Elements of the Proteasome Machine. *Trends in biochemical sciences*, 41(1), pp.77–93.

Fousteri, M. et al., 2006. Cockayne syndrome A and B proteins differentially regulate recruitment of chromatin remodeling and repair factors to stalled RNA polymerase II in vivo. *Molecular cell*, 23(4), pp.471–482.

Fradet-Turcotte, A. et al., 2013. 53BP1 is a reader of the DNA-damage-induced H2A Lys 15 ubiquitin mark. *Nature*, 499(7456), pp.50–54.

Fredrickson, E.K. et al., 2011. Exposed hydrophobicity is a key determinant of nuclear quality control degradation. *Molecular biology of the cell*, 22(13), pp.2384–2395.

Frigola, J. et al., 2013. ATPase-dependent quality control of DNA replication origin licensing. *Nature*, 495(7441), pp.339–343.

Fröhlich, K.-U. et al., 1995. The ATPase activity of purified CDC48p from Saccharomyces cerevisiae shows complex dependence on ATP-, ADP-, and NADH-concentrations and is completely inhibited by NEM. *Biochimica et Biophysica Acta (BBA) - Protein Structure and Molecular Enzymology*, 1253(1), pp.25–32.

Galburt, E.A. et al., 2007. Backtracking determines the force sensitivity of RNAP II in a factor-dependent manner. *Nature*, 446(7137), pp.820–823.

Galisson, F. et al., 2011. A novel proteomics approach to identify SUMOylated proteins and their modification sites in human cells. *Molecular & cellular proteomics*, 10(2), p.M110.004796.

García-Rubio, M.L. & Aguilera, A., 2012. Topological constraints impair RNA polymerase II transcription and causes instability of plasmid-borne convergent genes. *Nucleic Acids Research*, 40(3), pp.1050–1064.

Gatti, M. et al., 2015. RNF168 promotes noncanonical K27 ubiquitination to signal DNA damage. *Cell reports*, 10(2), pp.226–238.

Ghaemmaghami, S. et al., 2003. Global analysis of protein expression in yeast. *Nature*, 425(6959), pp.737–741.

Ghosh, A., Shuman, S. & Lima, C.D., 2011. Structural insights to how mammalian capping enzyme reads the CTD code. *Molecular cell*, 43(2), pp.299–310.

Gillette, T.G. et al., 2006. Distinct functions of the ubiquitin–proteasome pathway influence nucleotide excision repair | The EMBO Journal. *The EMBO ….*

Gillette, T.G. et al., 2004. Physical and functional association of RNA polymerase II and the proteasome. *Proceedings of the National Academy of Sciences of the United States of America*, 101(16), pp.5904–5909.

Glickman, M.H. et al., 1998. A subcomplex of the proteasome regulatory particle required for ubiquitin-conjugate degradation and related to the COP9-signalosome and eIF3. *Cell*, 94(5), pp.615–623.

Gnatt, A.L. et al., 2001. Structural basis of transcription: an RNA polymerase II elongation complex at 3.3 A resolution. *Science*, 292(5523), pp.1876–1882.

Grice, G.L. et al., 2015. The Proteasome Distinguishes between Heterotypic and Homotypic Lysine-11-Linked Polyubiquitin Chains. *Cell reports*, 12(4), pp.545–553.

Groll, M. et al., 2000. A gated channel into the proteasome core particle. *Nature Structural Biology*, 7(11), pp.1062–1067.

Gu, W. & Reines, D., 1995. Identification of a decay in transcription potential that results in elongation factor dependence of RNA polymerase II. *The Journal of biological chemistry*, 270(19), pp.11238–11244.

Guharoy, M. et al., 2016. Tripartite degrons confer diversity and specificity on regulated protein degradation in the ubiquitin-proteasome system. *Nature communications*, 7, p.10239.

Gupta, R. et al., 2007. Ubiquitination screen using protein microarrays for comprehensive identification of Rsp5 substrates in yeast. *Molecular systems biology*, 3, p.116.

Guterman, A. & Glickman, M.H., 2004. Complementary roles for Rpn11 and Ubp6 in deubiquitination and proteolysis by the proteasome. *The Journal of biological chemistry*, 279(3), pp.1729–1738.

Guzder, S.N. et al., 1996. RAD26, the yeast homolog of human Cockayne's syndrome group B gene, encodes a DNA-dependent ATPase. *The Journal of biological chemistry*, 271(31), pp.18314–18317.

Gwizdek, C. et al., 2005. The mRNA nuclear export factor Hpr1 is regulated by Rsp5-mediated ubiquitylation. *The Journal of biological chemistry*, 280(14), pp.13401–13405.

Hagai, T. & Levy, Y., 2010. Ubiquitin not only serves as a tag but also assists degradation by inducing protein unfolding. *Proceedings of the National Academy of Sciences of the United States of America*, 107(5), pp.2001–2006.

Hahn, S., 2004. Structure and mechanism of the RNA polymerase II transcription machinery. *Nature structural & molecular biology*, 11(5), pp.394–403.

Hanna, J. et al., 2007. A ubiquitin stress response induces altered proteasome composition. *Cell*, 129(4), pp.747–759.

Hannich, J.T. et al., 2005. Defining the SUMO-modified proteome by multiple approaches in Saccharomyces cerevisiae. *The Journal of biological chemistry*, 280(6), pp.4102–4110.

Harlow, E. & Lane, D., 1999. *Antibody-antigen interactions*, Using Antibodies: A Laboratory Manual.

Harreman, M. et al., 2009. Distinct ubiquitin ligases act sequentially for RNA polymerase II polyubiquitylation. *Proceedings of the National Academy of Sciences of the United States of America*, 106(49), pp.20705–20710.

Hänzelmann, P., Buchberger, A. & Schindelin, H., 2011. Hierarchical binding of cofactors to the AAA ATPase p97. *Structure*, 19(6), pp.833–843.

Heidemann, M. et al., 2013. Dynamic phosphorylation patterns of RNA polymerase II CTD during transcription. *Biochimica et Biophysica Acta (BBA) - Gene Regulatory Mechanisms*, 1829(1), pp.55–62.

Heine, G.F., Horwitz, A.A. & Parvin, J.D., 2008. Multiple Mechanisms Contribute to Inhibit Transcription in Response to DNA Damage. *Journal of Biological Chemistry*, 283(15), pp.9555–9561.

Heinemeyer, W. et al., 1997. The active sites of the eukaryotic 20 S proteasome and their involvement in subunit precursor processing. *The Journal of biological chemistry*, 272(40), pp.25200–25209.

Hemming, S.A. et al., 2000. RNA polymerase II subunit Rpb9 regulates transcription elongation in vivo. *The Journal of biological chemistry*, 275(45), pp.35506–35511.

Hendriks, I.A. et al., 2014. Uncovering global SUMOylation signaling networks in a site-specific manner. *Nature structural & molecular biology*, 21(10), pp.927–936.

Herbert, K.M. et al., 2006. Sequence-resolved detection of pausing by single RNA polymerase molecules. *Cell*, 125(6), pp.1083–1094.

Herrador, A. et al., 2013. A mechanism for protein monoubiquitination dependent on a trans-acting ubiquitin-binding domain. *Journal of Biological Chemistry*, 288(23), pp.16206–16211.

Heusch, M. et al., 1999. The generation of nfkb2 p52: mechanism and efficiency. *Oncogene*, 18(46), pp.6201–6208.

Hicke, L., Schubert, H.L. & Hill, C.P., 2005. Ubiquitin-binding domains. *Nature reviews. Molecular cell biology*, 6(8), pp.610–621.

Hitchcock, A.L. et al., 2001. The conserved npl4 protein complex mediates proteasome-dependent membrane-bound transcription factor activation. *Molecular biology of the cell*, 12(10), pp.3226–3241.

Hobson, D.J. et al., 2012. RNA polymerase II collision interrupts convergent transcription. *Molecular cell*, 48(3), pp.365–374.

Hoege, C. et al., 2002. RAD6-dependent DNA repair is linked to modification of PCNA by ubiquitin and SUMO. *Nature*, 419(6903), pp.135–141.

Hoeller, D. et al., 2007. E3-independent monoubiquitination of ubiquitin-binding proteins. *Molecular cell*, 26(6), pp.891–898.

Hofmann, K., 2009. Ubiquitin-binding domains and their role in the DNA damage response. *DNA repair*, 8(4), pp.544–556.

Hoppe, T. et al., 2000. Activation of a Membrane-Bound Transcription Factor by Regulated Ubiquitin/Proteasome-Dependent Processing. *Cell*, 102(5), pp.577–586.

Hoyt, M.A. et al., 2006. Glycine-alanine repeats impair proper substrate unfolding by the proteasome. *The EMBO journal*, 25(8), pp.1720–1729.

Huang, C., Li, G. & Lennarz, W.J., 2012. Dynamic flexibility of the ATPase p97 is important for its interprotomer motion transmission. *Proceedings of the National Academy of Sciences of the United States of America*, 109(25), pp.9792–9797.

Huang, L. et al., 1999. Structure of an E6AP-UbcH7 complex: insights into ubiquitination by the E2-E3 enzyme cascade. *Science*, 286(5443), pp.1321–1326.

Huh, W.-K. et al., 2003. Global analysis of protein localization in budding yeast. *Nature*, 425(6959), pp.686–691.

Huibregtse, J.M. et al., 1995. A family of proteins structurally and functionally related to the E6-AP ubiquitin-protein ligase. *Proceedings of the National Academy of Sciences of the United States of America*, 92(11), pp.5249–2567.

Huibregtse, J.M., Yang, J.C. & Beaudenon, S.L., 1997. The large subunit of RNA polymerase II is a substrate of the Rsp5 ubiquitin-protein ligase. *Proceedings of the National Academy of Sciences of the United States of America*, 94(8), pp.3656–3661.

Hurley, J.H., Lee, S. & Prag, G., 2006. Ubiquitin-binding domains. *The Biochemical journal*, 399(3), pp.361–372.

Husnjak, K. & Dikic, I., 2012. Ubiquitin-binding proteins: decoders of ubiquitin-mediated cellular functions. *Annual Review of Biochemistry*, 81, pp.291–322.

Husnjak, K. et al., 2008. Proteasome subunit Rpn13 is a novel ubiquitin receptor. *Nature*, 453(7194), pp.481–488.

Hutchins, A.P. et al., 2013. The repertoires of ubiquitinating and deubiquitinating enzymes in eukaryotic genomes. *Molecular biology and evolution*, 30(5), pp.1172–1187.

Inobe, T. et al., 2011. Defining the geometry of the two-component proteasome degron. *Nature chemical biology*, 7(3), pp.161–167.

Isaacson, R.L. et al., 2007. Detailed structural insights into the p97-Npl4-Ufd1 interface. *The Journal of biological chemistry*, 282(29), pp.21361–21369.

Izban, M.G. & Luse, D.S., 1992a. Factor-stimulated RNA polymerase II transcribes at physiological elongation rates on naked DNA but very poorly on chromatin templates. *The Journal of biological chemistry*, 267(19), pp.13647–13655.

Izban, M.G. & Luse, D.S., 1992b. The RNA polymerase II ternary complex cleaves the nascent transcript in a 3“----5” direction in the presence of elongation factor SII. *Genes & development*, 6(7), pp.1342–1356.

Jacobson, A.D. et al., 2014. Autoregulation of the 26S proteasome by in situ ubiquitination. *Molecular biology of the cell*, 25(12), pp.1824–1835.

Jarosch, E. et al., 2002. Protein dislocation from the ER requires polyubiquitination and the AAA-ATPase Cdc48. *Nature cell biology*, 4(2), pp.134–139.

Jentsch, S. & Rumpf, S., 2007. Cdc48 (p97): a “molecular gearbox” in the ubiquitin pathway? *Trends in biochemical sciences*, 32(1), pp.6–11.

Jordan, P.W., Klein, F. & Leach, D.R.F., 2007. Novel roles for selected genes in meiotic DNA processing. *PLoS genetics*, 3(12), p.e222.

Jorgensen, P. et al., 2002. Systematic identification of pathways that couple cell growth and division in yeast. *Science*, 297(5580), pp.395–400.

Jouvet, N. et al., 2011. RNA polymerase II degradation in response to rapamycin is not mediated through ubiquitylation. *Biochemical and biophysical research communications*, 413(2), pp.248–253.

Jouvet, N. et al., 2010. Rrd1 isomerizes RNA polymerase II in response to rapamycin. *BMC molecular biology*, 11, p.92.

Jung, Y. & Lippard, S.J., 2006. RNA Polymerase II Blockage by Cisplatin-damaged DNA. *Journal of Biological Chemistry*, 281(3), pp.1361–1370.

Kaliszewski, P. & Zoładek, T., 2008. The role of Rsp5 ubiquitin ligase in regulation of diverse processes in yeast cells. *Acta biochimica Polonica*, 55(4), pp.649–662.

Kang, R.S. et al., 2003. Solution Structure of a CUE-Ubiquitin Complex Reveals a Conserved Mode of Ubiquitin Binding. *Cell*, 113(5), pp.621–630.

Karakasili, E. et al., 2014. Degradation of DNA damage-independently stalled RNA polymerase II is independent of the E3 ligase Elc1. *Nucleic Acids Research*,

42(16), pp.10503–10515.

Kathe, S.D., Shen, G.-P. & Wallace, S.S., 2004. Single-stranded breaks in DNA but not oxidative DNA base damages block transcriptional elongation by RNA polymerase II in HeLa cell nuclear extracts. *The Journal of biological chemistry*, 279(18), pp.18511–18520.

Kee, Y. et al., 2006. The deubiquitinating enzyme Ubp2 modulates Rsp5-dependent Lys63-linked polyubiquitin conjugates in Saccharomyces cerevisiae. *The Journal of biological chemistry*, 281(48), pp.36724–36731.

Kee, Y., Lyon, N. & Huibregtse, J.M., 2005. The Rsp5 ubiquitin ligase is coupled to and antagonized by the Ubp2 deubiquitinating enzyme. *The EMBO journal*, 24(13), pp.2414–2424.

Kelsall, I.R. et al., 2013. TRIAD1 and HHARI bind to and are activated by distinct neddylated Cullin-RING ligase complexes. *The EMBO journal*, 32(21), pp.2848–2860.

Kernstock, S. et al., 2012. Lysine methylation of VCP by a member of a novel human protein methyltransferase family. *Nature communications*, 3, p.1038.

Kim, H.-K. et al., 2014. The N-terminal methionine of cellular proteins as a degradation signal. *Cell*, 156(1-2), pp.158–169.

Kim, H.C. & Huibregtse, J.M., 2009. Polyubiquitination by HECT E3s and the Determinants of Chain Type Specificity. *Molecular and cellular biology*, 29(12), pp.3307–3318.

Kim, H.T. et al., 2007. Certain pairs of ubiquitin-conjugating enzymes (E2s) and ubiquitin-protein ligases (E3s) synthesize nondegradable forked ubiquitin chains containing all possible isopeptide linkages. *The Journal of biological chemistry*, 282(24), pp.17375–17386.

Kim, I., Mi, K. & Rao, H., 2004. Multiple interactions of rad23 suggest a mechanism for ubiquitylated substrate delivery important in proteolysis. *Molecular biology of the cell*, 15(7), pp.3357–3365.

Kim, M. et al., 2015. Drosophila Gyf/GRB10 interacting GYF protein is an autophagy regulator that controls neuron and muscle homeostasis. *Autophagy*, 11(8), pp.1358–1372.

Kireeva, M.L., 2000. The 8-Nucleotide-long RNA:DNA Hybrid Is a Primary Stability Determinant of the RNA Polymerase II Elongation Complex. *Journal of Biological Chemistry*, 275(9), pp.6530–6536.

Kireeva, M.L. et al., 2005. Nature of the nucleosomal barrier to RNA polymerase II. *Molecular cell*, 18(1), pp.97–108.

Kleiger, G. et al., 2009. Rapid E2-E3 assembly and disassembly enable processive ubiquitylation of cullin-RING ubiquitin ligase substrates. *Cell*, 139(5), pp.957–968.

Koegl, M. et al., 1999. A novel ubiquitination factor, E4, is involved in multiubiquitin chain assembly. *Cell*, 96(5), pp.635–644.

Kofler, M. et al., 2009. Proline-rich Sequence Recognition: I. MARKING GYF AND WW DOMAIN ASSEMBLY SITES IN EARLY SPLICEOSOMAL COMPLEXES. *Molecular & Cellular Proteomics*, 8(11), pp.2461–2473.

Kofler, M., Motzny, K. & Freund, C., 2005. GYF Domain Proteomics Reveals Interaction Sites in Known and Novel Target Proteins. *Molecular & cellular proteomics*, 4(11), pp.1797–1811.

Kolawa, N. et al., 2013. Perturbations to the ubiquitin conjugate proteome in yeast δubx mutants identify Ubx2 as a regulator of membrane lipid composition. *Molecular & cellular proteomics*, 12(10), pp.2791–2803.

Komarnitsky, P., Cho, E.J. & Buratowski, S., 2000. Different phosphorylated forms of RNA polymerase II and associated mRNA processing factors during transcription. *Genes & development*, 14(19), pp.2452–2460.

Kondo, H. et al., 1997. p47 is a cofactor for p97-mediated membrane fusion. *Nature*, 388(6637), pp.75–78.

Kraut, D.A. & Matouschek, A., 2011. Proteasomal degradation from internal sites favors partial proteolysis via remote domain stabilization. *ACS chemical biology*, 6(10), pp.1087–1095.

Kraut, D.A. et al., 2012. Sequence- and species-dependence of proteasomal processivity. *ACS chemical biology*, 7(8), pp.1444–1453.

Kravtsova-Ivantsiv, Y., Cohen, S. & Ciechanover, A., 2009. Modification by single ubiquitin moieties rather than polyubiquitination is sufficient for proteasomal processing of the p105 NF-kappaB precursor. *Molecular cell*, 33(4), pp.496–504.

Krick, R. et al., 2010. Cdc48/p97 and Shp1/p47 regulate autophagosome biogenesis in concert with ubiquitin-like Atg8. *The Journal of cell biology*, 190(6), pp.965–973.

Kristjuhan, A. & Svejstrup, J.Q., 2004. Evidence for distinct mechanisms facilitating transcript elongation through chromatin in vivo. *The EMBO journal*, 23(21), pp.4243–4252.

Krogan, N.J. et al., 2006. Global landscape of protein complexes in the yeast Saccharomyces cerevisiae. *Nature*, 440(7084), pp.637–643.

Krummel, B. & Chamberlin, M.J., 1992. Structural analysis of ternary complexes of Escherichia coli RNA polymerase. Deoxyribonuclease I footprinting of defined complexes. *Journal of Molecular Biology*, 225(2), pp.239–250.

Kryszke, M.-H. et al., 2016. Post-transcriptional gene silencing activity of human GIGYF2. *Biochemical and biophysical research communications*, 475(3), pp.289–294.

Kushnirov, V.V., 2000. Rapid and reliable protein extraction from yeast. *Yeast*, 16(9), pp.857–860.

Kvint, K. et al., 2008. Reversal of RNA polymerase II ubiquitylation by the ubiquitin protease Ubp3. *Molecular cell*, 30(4), pp.498–506.

Lafon, A. et al., 2015. INO80 Chromatin Remodeler Facilitates Release of RNA Polymerase II from Chromatin for Ubiquitin-Mediated Proteasomal Degradation. *Molecular cell*, 60(5), pp.784–796.

Lainé, J.-P. & Egly, J.-M., 2006. Initiation of DNA repair mediated by a stalled RNA polymerase IIO. *The EMBO journal*, 25(2), pp.387–397.

Lamoliatte, F. et al., 2013. Targeted Identification of SUMOylation Sites in Human Proteins Using Affinity Enrichment and Paralog-specific Reporter Ions. *Molecular & cellular proteomics*, 12(9), pp.2536–2550.

Lander, G.C. et al., 2012. Complete subunit architecture of the proteasome regulatory particle. *Nature*, 482(7384), pp.186–191.

Larson, M.H. et al., 2012. Trigger loop dynamics mediate the balance between the transcriptional fidelity and speed of RNA polymerase II. *Proceedings of the National Academy of Sciences of the United States of America*, 109(17), pp.6555–6560.

Lasker, K. et al., 2012. Molecular architecture of the 26S proteasome holocomplex determined by an integrative approach. *Proceedings of the National Academy of Sciences of the United States of America*, 109(5), pp.1380–1387.

Latterich, M., Fröhlich, K.U. & Schekman, R., 1995. Membrane fusion and the cell cycle: Cdc48p participates in the fusion of ER membranes. *Cell*, 82(6), pp.885–893.

Leadon, S.A. & Lawrence, D.A., 1992. Strand-selective repair of DNA damage in the yeast GAL7 gene requires RNA polymerase II. *The Journal of biological chemistry*, 267(32), pp.23175–23182.

Lee, B.-H. et al., 2016. USP14 deubiquitinates proteasome-bound substrates that are ubiquitinated at multiple sites. *Nature*, 532(7599), pp.398–401.

Lee, C. et al., 2001. ATP-dependent proteases degrade their substrates by processively unraveling them from the degradation signal. *Molecular cell*, 7(3), pp.627–637.

Lee, C., Prakash, S. & Matouschek, A., 2002. Concurrent translocation of multiple polypeptide chains through the proteasomal degradation channel. *The Journal of biological chemistry*, 277(38), pp.34760–34765.

Lee, K.-B. et al., 2002. Transcription-coupled and DNA damage-dependent ubiquitination of RNA polymerase II in vitro. *Proceedings of the National Academy of Sciences of the United States of America*, 99(7), pp.4239–4244.

Lee, S.-K. et al., 2002. Yeast RAD26, a homolog of the human CSB gene, functions independently of nucleotide excision repair and base excision repair in promoting transcription through damaged bases. *Molecular and cellular biology*, 22(12), pp.4383–4389.

Lee, S.K. et al., 2001. Requirement for Yeast RAD26, a Homolog of the Human CSB Gene, in Elongation by RNA Polymerase II. *Molecular and cellular biology*, 21(24), pp.8651–8656.

Levinger, L. & Varshavsky, A., 1982. Selective arrangement of ubiquitinated and D1 protein-containing nucleosomes within the drosophila genome. *Cell*, 28(2), pp.375–385.

Li, G. et al., 2012. Interprotomer motion-transmission mechanism for the hexameric AAA ATPase p97. *Proceedings of the National Academy of Sciences of the United States of America*, 109(10), pp.3737–3741.

Li, S., 2004. Dissecting Transcription-coupled and Global Genomic Repair in the Chromatin of Yeast GAL1-10 Genes. *Journal of Biological Chemistry*, 279(14), pp.14418–14426.

Li, S., 2015. Transcription coupled nucleotide excision repair in the yeast Saccharomyces cerevisiae: The ambiguous role of Rad26. *DNA repair*, 36, pp.43–48.

Li, S. & Smerdon, M.J., 2002. Rpb4 and Rpb9 mediate subpathways of transcription-coupled DNA repair in Saccharomyces cerevisiae. *The EMBO journal*, 21(21), pp.5921–5929.

Li, S. et al., 2007. The roles of Rad16 and Rad26 in repairing repressed and actively transcribed genes in yeast. *DNA repair*, 6(11), pp.1596–1606.

Lillie, S.H. & Brown, S.S., 1994. Immunofluorescence localization of the unconventional myosin, Myo2p, and the putative kinesin-related protein, Smy1p, to the same regions of polarized growth in Saccharomyces cerevisiae. *The Journal of cell biology*, 125(4), pp.825–842.

Lin, L. & Ghosh, S., 1996. A glycine-rich region in NF-kappaB p105 functions as a processing signal for the generation of the p50 subunit. *Molecular and cellular biology*, 16(5), pp.2248–2254.

Lin, L.L. & Little, J.W., 1989. Autodigestion and RecA-dependent cleavage of Ind- mutant LexA proteins. *Journal of Molecular Biology*, 210(3), pp.439–452.

Liu, C.-W. et al., 2003. Endoproteolytic activity of the proteasome. *Science*, 299(5605), pp.408–411.

Liu, P. et al., 2010. Genetic organization, length conservation, and evolution of RNA polymerase II carboxyl-terminal domain. *Molecular biology and evolution*, 27(11), pp.2628–2641.

Liu, X., Bushnell, D.A. & Kornberg, R.D., 2013. RNA polymerase II transcription:

Structure and mechanism. *Biochimica et Biophysica Acta (BBA) - Gene Regulatory Mechanisms*, 1829(1), pp.2–8.

Livingstone, M. et al., 2005. Valosin-containing protein phosphorylation at Ser784 in response to DNA damage. *Cancer research*, 65(17), pp.7533–7540.

Lopez, A.D. et al., 2011. Proteasomal degradation of Sfp1 contributes to the repression of ribosome biogenesis during starvation and is mediated by the proteasome activator Blm10. *Molecular biology of the cell*, 22(5), pp.528–540.

Lorick, K.L. et al., 1999. RING fingers mediate ubiquitin-conjugating enzyme (E2)-dependent ubiquitination. *Proceedings of the National Academy of Sciences of the United States of America*, 96(20), pp.11364–11369.

Lu, Y. et al., 2015. Substrate degradation by the proteasome: A single-molecule kinetic analysis. *Science*, 348(6231), p.1250834.

Luo, Z. et al., 2001. Ultraviolet radiation alters the phosphorylation of RNA polymerase II large subunit and accelerates its proteasome-dependent degradation. *Mutation research*, 486(4), pp.259–274.

Madeo, F. et al., 1998. Tyrosine phosphorylation regulates cell cycle-dependent nuclear localization of Cdc48p. *Molecular biology of the cell*, 9(1), pp.131–141.

Madsen, L. et al., 2009. New ATPase regulators--p97 goes to the PUB. *The international journal of biochemistry & cell biology*, 41(12), pp.2380–2388.

Magtanong, L. et al., 2011. Dosage suppression genetic interaction networks enhance functional wiring diagrams of the cell. *Nature biotechnology*, 29(6), pp.505–511.

Malik, S. & Bhaumik, S.R., 2012. Rad26p, a transcription-coupled repair factor, promotes the eviction and prevents the reassociation of histone H2A-H2B dimer during transcriptional elongation in vivo. *Biochemistry*, 51(30), pp.5873–5875.

Malik, S. et al., 2008. Elongating RNA polymerase II is disassembled through specific degradation of its largest but not other subunits in response to DNA damage in vivo. *The Journal of biological chemistry*, 283(11), pp.6897–6905.

Malik, S. et al., 2012. Rad26p regulates the occupancy of histone H2A-H2B dimer at the active genes in vivo. *Nucleic Acids Research*, 40(8), pp.3348–3363.

Malik, S. et al., 2010. Rad26p, a transcription-coupled repair factor, is recruited to the site of DNA lesion in an elongating RNA polymerase II-dependent manner in vivo. *Nucleic Acids Research*, 38(5), pp.1461–1477.

Manogaran, A.L. et al., 2011. Prion formation and polyglutamine aggregation are controlled by two classes of genes. *PLoS genetics*, 7(5), p.e1001386.

Maric, M. et al., 2014. Cdc48 and a ubiquitin ligase drive disassembly of the CMG helicase at the end of DNA replication. *Science*, 346(6208), p.1253596.

Maspero, E. et al., 2013. Structure of a ubiquitin-loaded HECT ligase reveals the molecular basis for catalytic priming. *Nature structural & molecular biology*, 20(6), pp.696–701.

Matyskiela, M.E., Lander, G.C. & Martin, A., 2013. Conformational switching of the 26S proteasome enables substrate degradation. *Nature structural & molecular biology*, 20(7), pp.781–788.

Mayer, A. et al., 2010. Uniform transitions of the general RNA polymerase II transcription complex. *Nature structural & molecular biology*, 17(10), pp.1272–1278.

Mayne, L.V. & Lehmann, A.R., 1982. Failure of RNA synthesis to recover after UV irradiation: an early defect in cells from individuals with Cockayne's syndrome and xeroderma pigmentosum. *Cancer research*, 42(4), pp.1473–1478.

Mevissen, T.E.T. et al., 2013. OTU deubiquitinases reveal mechanisms of linkage specificity and enable ubiquitin chain restriction analysis. *Cell*, 154(1), pp.169–184.

Meyer, H.H., 2002. Direct binding of ubiquitin conjugates by the mammalian p97 adaptor complexes, p47 and Ufd1-Npl4. *The EMBO journal*, 21(21), pp.5645–5652.

Meyer, H.H. et al., 2000. A complex of mammalian ufd1 and npl4 links the AAA-ATPase, p97, to ubiquitin and nuclear transport pathways. *The EMBO journal*, 19(10), pp.2181–2192.

Meyer, H.H., Kondo, H. & Warren, G., 1998. The p47 co-factor regulates the ATPase activity of the membrane fusion protein, p97. *FEBS letters*, 437(3), pp.255–257.

Mimnaugh, E.G. et al., 1997. Rapid Deubiquitination of Nucleosomal Histones in Human Tumor Cells Caused by Proteasome Inhibitors and Stress Response Inducers: Effects on Replication, Transcription, Translation, and the Cellular Stress Response †. *Biochemistry*, 36(47), pp.14418–14429.

Min, J.-H. & Pavletich, N.P., 2007. Recognition of DNA damage by the Rad4 nucleotide excision repair protein. *Nature*, 449(7162), pp.570–575.

Min, M. et al., 2015. Efficient APC/C substrate degradation in cells undergoing mitotic exit depends on K11 ubiquitin linkages. *Molecular biology of the cell*, 26(24), pp.4325–4332.

Mischo, H.E. & Proudfoot, N.J., 2013. Disengaging polymerase: terminating RNA polymerase II transcription in budding yeast. *Biochimica et biophysica acta*, 1829(1), pp.174–185.

Mitsui, A. & Sharp, P.A., 1999. Ubiquitination of RNA polymerase II large subunit signaled by phosphorylation of carboxyl-terminal domain. *Proceedings of the National Academy of Sciences of the United States of America*, 96(11),

pp.6054–6059.

Moir, D. et al., 1982. Cold-sensitive cell-division-cycle mutants of yeast: isolation, properties, and pseudoreversion studies. *Genetics*, 100(4), pp.547–563.

Moorthy, A.K. et al., 2006. The 20S proteasome processes NF-κB1 p105 into p50 in a translation-independent manner. *The EMBO journal*, 25(9), pp.1945–1956.

Morawska, M. & Ulrich, H.D., 2013. An expanded tool kit for the auxin-inducible degron system in budding yeast. *Yeast*, 30(9), pp.341–351.

Mori-Konya, C. et al., 2009. p97/valosin-containing protein (VCP) is highly modulated by phosphorylation and acetylation. *Genes to cells : devoted to molecular & cellular mechanisms*, 14(4), pp.483–497.

Morreale, G. et al., 2009. Evolutionary divergence of valosin-containing protein/cell division cycle protein 48 binding interactions among endoplasmic reticulum-associated degradation proteins. *FEBS Journal*, 276(5), pp.1208–1220.

Murakami, K. et al., 2013. Architecture of an RNA polymerase II transcription pre-initiation complex. *Science*, 342(6159), p.1238724.

Murakami, Y. et al., 1992. Ornithine decarboxylase is degraded by the 26S proteasome without ubiquitination. *Nature*, 360(6404), pp.597–599.

Nassif, N.D., Cambray, S.E. & Kraut, D.A., 2014. Slipping up: partial substrate degradation by ATP-dependent proteases. *IUBMB life*, 66(5), pp.309–317.

Navon, A. & Goldberg, A.L., 2001. Proteins are unfolded on the surface of the ATPase ring before transport into the proteasome. *Molecular cell*, 8(6), pp.1339–1349.

Neuman, K.C. et al., 2003. Ubiquitous transcriptional pausing is independent of RNA polymerase backtracking. *Cell*, 115(4), pp.437–447.

Nishikori, S. et al., 2011. Positive cooperativity of the p97 AAA ATPase is critical for essential functions. *Journal of Biological Chemistry*, 286(18), pp.15815–15820.

Nishimura, K. et al., 2009. An auxin-based degron system for the rapid depletion of proteins in nonplant cells. *Nature chemical biology*, 6(12), pp.917–922.

Nizhnikov, A.A. et al., 2014. Proteomic Screening for Amyloid Proteins. *PloS one*, 9(12), p.e116003.

Nudler, E. et al., 1997. The RNA-DNA hybrid maintains the register of transcription by preventing backtracking of RNA polymerase. *Cell*, 89(1), pp.33–41.

Ohtake, F. et al., 2015. Ubiquitin acetylation inhibits polyubiquitin chain elongation. *EMBO reports*, 16(2), pp.192–201.

Olsen, S.K. & Lima, C.D., 2013. Structure of a Ubiquitin E1-E2 Complex: Insights to E1-E2 Thioester Transfer. *Molecular cell*, 49(5), pp.884–896.

Orian, A. et al., 1999. Structural Motifs Involved in Ubiquitin-Mediated Processing of the NF-κB Precursor p105: Roles of the Glycine-Rich Region and a Downstream Ubiquitination Domain. *Molecular and cellular biology*, 19(5), pp.3664–3673.

Orphanides, G. et al., 1998. FACT, a factor that facilitates transcript elongation through nucleosomes. *Cell*, 92(1), pp.105–116.

Ozkan, E., Yu, H. & Deisenhofer, J., 2005. Mechanistic insight into the allosteric activation of a ubiquitin-conjugating enzyme by RING-type ubiquitin ligases. *Proceedings of the National Academy of Sciences of the United States of America*, 102(52), pp.18890–18895.

Palombella, V.J. et al., 1994. The ubiquitin-proteasome pathway is required for processing the NF-κB1 precursor protein and the activation of NF-κB. *Cell*, 78(5), pp.773–785.

Pan, Y. & Wang, B., 2007. A novel protein-processing domain in Gli2 and Gli3 differentially blocks complete protein degradation by the proteasome. *The Journal of biological chemistry*, 282(15), pp.10846–10852.

Pan, Y. et al., 2006. Sonic hedgehog signaling regulates Gli2 transcriptional activity by suppressing its processing and degradation. *Molecular and cellular biology*, 26(9), pp.3365–3377.

Park, J.-S., Marr, M.T. & Roberts, J.W., 2002. E. coli Transcription repair coupling factor (Mfd protein) rescues arrested complexes by promoting forward translocation. *Cell*, 109(6), pp.757–767.

Parker, J.L. & Ulrich, H.D., 2009. Mechanistic analysis of PCNA poly-ubiquitylation by the ubiquitin protein ligases Rad18 and Rad5. *The EMBO journal*, 28(23), pp.3657–3666.

Parker, J.L. et al., 2007. Contributions of ubiquitin- and PCNA-binding domains to the activity of Polymerase eta in Saccharomyces cerevisiae. *Nucleic Acids Research*, 35(3), pp.881–889.

Pavri, R. et al., 2006. Histone H2B monoubiquitination functions cooperatively with FACT to regulate elongation by RNA polymerase II. *Cell*, 125(4), pp.703–717.

Peng, J. et al., 2003. A proteomics approach to understanding protein ubiquitination. *Nature biotechnology*, 21(8), pp.921–926.

Peters, J.M. et al., 1993. Structural features of the 26 S proteasome complex. *Journal of Molecular Biology*, 234(4), pp.932–937.

Piwko, W. & Jentsch, S., 2006. Proteasome-mediated protein processing by bidirectional degradation initiated from an internal site. *Nature structural & molecular biology*, 13(8), pp.691–697.

Plechanovová, A. et al., 2012. Structure of a RING E3 ligase and ubiquitin-loaded E2 primed for catalysis. *Nature*, 489(7414), pp.115–120.

Prag, G. et al., 2003. Mechanism of ubiquitin recognition by the CUE domain of Vps9p. *Cell*, 113(5), pp.609–620.

Prakash, S. et al., 2004. An unstructured initiation site is required for efficient proteasome-mediated degradation. *Nature structural & molecular biology*, 11(9), pp.830–837.

Prakash, S. et al., 2008. Substrate selection by the proteasome during degradation of protein complexes. *Nature chemical biology*, 5(1), pp.29–36.

Pye, V.E. et al., 2006. Going through the motions: the ATPase cycle of p97. *Journal of structural biology*, 156(1), pp.12–28.

Pye, V.E. et al., 2007. Structural insights into the p97-Ufd1-Npl4 complex. *Proceedings of the National Academy of Sciences of the United States of America*, 104(2), pp.467–472.

Raasi, S. et al., 2005. Diverse polyubiquitin interaction properties of ubiquitin-associated domains. *Nature structural & molecular biology*, 12(8), pp.708–714.

Rabinovich, E. et al., 2002. AAA-ATPase p97/Cdc48p, a cytosolic chaperone required for endoplasmic reticulum-associated protein degradation. *Molecular and cellular biology*, 22(2), pp.626–634.

Rape, M. et al., 2001. Mobilization of processed, membrane-tethered SPT23 transcription factor by CDC48(UFD1/NPL4), a ubiquitin-selective chaperone. *Cell*, 107(5), pp.667–677.

Ratner, J.N. et al., 1998. Ultraviolet radiation-induced ubiquitination and proteasomal degradation of the large subunit of RNA polymerase II. Implications for transcription-coupled DNA repair. *The Journal of biological chemistry*, 273(9), pp.5184–5189.

Reid, J. & Svejstrup, J.Q., 2006. An assay for studying ubiquitylation of RNA polymerase II and other proteins in crude yeast extracts. *Methods in enzymology*, 408, pp.264–273.

Reid, J. & Svejstrup, J.Q., 2004. DNA damage-induced Def1-RNA polymerase II interaction and Def1 requirement for polymerase ubiquitylation in vitro. *The Journal of biological chemistry*, 279(29), pp.29875–29878.

Reiley, W. et al., 2005. Regulation of the deubiquitinating enzyme CYLD by IkappaB kinase gamma-dependent phosphorylation. *Molecular and cellular biology*, 25(10), pp.3886–3895.

Reines, D. & Mote, J., 1993. Elongation factor SII-dependent transcription by RNA polymerase II through a sequence-specific DNA-binding protein. *Proceedings of the National Academy of Sciences of the United States of America*, 90(5), pp.1917–1921.

Ribar, B., Prakash, L. & Prakash, S., 2007. ELA1 and CUL3 are required along with ELC1 for RNA polymerase II polyubiquitylation and degradation in DNA-

damaged yeast cells. *Molecular and cellular biology*, 27(8), pp.3211–3216.

Ribar, B., Prakash, L. & Prakash, S., 2006. Requirement of ELC1 for RNA polymerase II polyubiquitylation and degradation in response to DNA damage in Saccharomyces cerevisiae. *Molecular and cellular biology*, 26(11), pp.3999–4005.

Richard, P. & Manley, J.L., 2009. Transcription termination by nuclear RNA polymerases. *Genes & development*, 23(11), pp.1247–1269.

Richly, H. et al., 2005. A Series of Ubiquitin Binding Factors Connects CDC48/p97 to Substrate Multiubiquitylation and Proteasomal Targeting. *Cell*, 120(1), pp.73–84.

Rockx, D.A. et al., 2000. UV-induced inhibition of transcription involves repression of transcription initiation and phosphorylation of RNA polymerase II. *Proceedings of the National Academy of Sciences of the United States of America*, 97(19), pp.10503–10508.

Rodrigo-Brenni, M.C. & Morgan, D.O., 2007. Sequential E2s drive polyubiquitin chain assembly on APC targets. *Cell*, 130(1), pp.127–139.

Roos, M.D. et al., 1997. O glycosylation of an Sp1-derived peptide blocks known Sp1 protein interactions. *Molecular and cellular biology*, 17(11), pp.6472–6480.

Rosenbaum, J.C. et al., 2011. Disorder targets misorder in nuclear quality control degradation: a disordered ubiquitin ligase directly recognizes its misfolded substrates. *Molecular cell*, 41(1), pp.93–106.

Rosenzweig, R. et al., 2012. Rpn1 and Rpn2 Coordinate Ubiquitin Processing Factors at Proteasome. *Journal of Biological Chemistry*, 287(18), pp.14659–14671.

Rouiller, I. et al., 2000. A major conformational change in p97 AAA ATPase upon ATP binding. *Molecular cell*, 6(6), pp.1485–1490.

Rouiller, I. et al., 2002. Conformational changes of the multifunction p97 AAA ATPase during its ATPase cycle. *Nature Structural Biology*, 9(12), pp.950–957.

Rumpf, S. & Jentsch, S., 2006. Functional Division of Substrate Processing Cofactors of the Ubiquitin-Selective Cdc48 Chaperone. *Molecular cell*, 21(2), pp.261–269.

Ruschak, A.M. et al., 2010. The proteasome antechamber maintains substrates in an unfolded state. *Nature*, 467(7317), pp.868–871.

Sadre-Bazzaz, K. et al., 2010. Structure of a Blm10 complex reveals common mechanisms for proteasome binding and gate opening. *Molecular cell*, 37(5), pp.728–735.

Saeki, H. & Svejstrup, J.Q., 2009. Stability, flexibility, and dynamic interactions of colliding RNA polymerase II elongation complexes. *Molecular cell*, 35(2),

pp.191–205.

Sakata, E. et al., 2012. Localization of the proteasomal ubiquitin receptors Rpn10 and Rpn13 by electron cryomicroscopy. *Proceedings of the National Academy of Sciences of the United States of America*, 109(5), pp.1479–1484.

Salghetti, S.E. et al., 2000. Functional overlap of sequences that activate transcription and signal ubiquitin-mediated proteolysis. *Proceedings of the National Academy of Sciences of the United States of America*, 97(7), pp.3118–3123.

Salghetti, S.E. et al., 2001. Regulation of transcriptional activation domain function by ubiquitin. *Science*, 293(5535), pp.1651–1653.

Sato, B.K. & Hampton, R.Y., 2006. Yeast Derlin Dfm1 interacts with Cdc48 and functions in ER homeostasis. *Yeast*, 23(14-15), pp.1053–1064.

Schaefer, J.B. & Morgan, D.O., 2011. Protein-linked ubiquitin chain structure restricts activity of deubiquitinating enzymes. *Journal of Biological Chemistry*, 286(52), pp.45186–45196.

Scharf, A. et al., 2011. Distant positioning of proteasomal proteolysis relative to actively transcribed genes. *Nucleic Acids Research*, 39(11), pp.4612–4627.

Schmidt, M. et al., 2005. The HEAT repeat protein Blm10 regulates the yeast proteasome by capping the core particle. *Nature structural & molecular biology*, 12(4), pp.294–303.

Schöls, L. et al., 2004. Autosomal dominant cerebellar ataxias: clinical features, genetics, and pathogenesis. *The Lancet. Neurology*, 3(5), pp.291–304.

Schrader, E.K. et al., 2011. A three-part signal governs differential processing of Gli1 and Gli3 proteins by the proteasome. *Journal of Biological Chemistry*, 286(45), pp.39051–39058.

Schrader, E.K., Harstad, K.G. & Matouschek, A., 2009. Targeting proteins for degradation. *Nature chemical biology*, 5(11), pp.815–822.

Schreiner, P. et al., 2008. Ubiquitin docking at the proteasome through a novel pleckstrin-homology domain interaction. *Nature*, 453(7194), pp.548–552.

Schuberth, C. & Buchberger, A., 2008. UBX domain proteins: major regulators of the AAA ATPase Cdc48/p97. *Cellular and molecular life sciences : CMLS*, 65(15), pp.2360–2371.

Schuberth, C. et al., 2004. Shp1 and Ubx2 are adaptors of Cdc48 involved in ubiquitin-dependent protein degradation. *EMBO reports*, 5(8), pp.818–824.

Schulman, B.A. & Harper, J.W., 2009. Ubiquitin-like protein activation by E1 enzymes: the apex for downstream signalling pathways. *Nature reviews. Molecular cell biology*, 10(5), pp.319–331.

Schultz, M.C., Choe, S.Y. & Reeder, R.H., 1991. Specific initiation by RNA polymerase I in a whole-cell extract from yeast. *Proceedings of the National Academy of Sciences of the United States of America*, 88(3), pp.1004–1008.

Schumacher, M.A. et al., 2012. Role of unusual P loop ejection and autophosphorylation in HipA-mediated persistence and multidrug tolerance. *Cell reports*, 2(3), pp.518–525.

Scott, D.C. et al., 2016. Two Distinct Types of E3 Ligases Work in Unison to Regulate Substrate Ubiquitylation. *Cell*, 166(5), pp.1198–1214.e24.

Selby, C.P. et al., 1997. RNA polymerase II stalled at a thymine dimer: footprint and effect on excision repair. *Nucleic Acids Research*, 25(4), pp.787–793.

Selth, L.A., Sigurdsson, S. & Svejstrup, J.Q., 2010. Transcript Elongation by RNA Polymerase II. *Annual Review of Biochemistry*, 79(1), pp.271–293.

Sezen, B., Seedorf, M. & Schiebel, E., 2009. The SESA network links duplication of the yeast centrosome with the protein translation machinery. *Genes & development*, 23(13), pp.1559–1570.

Sharon, M. et al., 2006. 20S proteasomes have the potential to keep substrates in store for continual degradation. *The Journal of biological chemistry*, 281(14), pp.9569–9575.

Shcherbik, N. & Haines, D.S., 2007. Cdc48p(Npl4p/Ufd1p) binds and segregates membrane-anchored/tethered complexes via a polyubiquitin signal present on the anchors. *Molecular cell*, 25(3), pp.385–397.

Shcherbik, N. et al., 2004. A single PXY motif located within the carboxyl terminus of Spt23p and Mga2p mediates a physical and functional interaction with ubiquitin ligase Rsp5p. *The Journal of biological chemistry*, 279(51), pp.53892–53898.

Shih, S.C. et al., 2003. A ubiquitin-binding motif required for intramolecular monoubiquitylation, the CUE domain. *The EMBO journal*, 22(6), pp.1273–1281.

Sigurdsson, S., Dirac-Svejstrup, A.B. & Svejstrup, J.Q., 2010. Evidence that transcript cleavage is essential for RNA polymerase II transcription and cell viability. *Molecular cell*, 38(2), pp.202–210.

Sikorski, R.S. & Hieter, P., 1989. A system of shuttle vectors and yeast host strains designed for efficient manipulation of DNA in Saccharomyces cerevisiae. *Genetics*, 122(1), pp.19–27.

Sims, J.J. & Cohen, R.E., 2009. Linkage-specific avidity defines the lysine 63-linked polyubiquitin-binding preference of rap80. *Molecular cell*, 33(6), pp.775–783.

Singh, J. & Padgett, R.A., 2009. Rates of in situ transcription and splicing in large human genes. *Nature structural & molecular biology*, 16(11), pp.1128–1133.

Skowyra, D. et al., 1997. F-box proteins are receptors that recruit phosphorylated substrates to the SCF ubiquitin-ligase complex. *Cell*, 91(2), pp.209–219.

Sledz, P. et al., 2013. Structure of the 26S proteasome with ATP-{gamma}S bound provides insights into the mechanism of nucleotide-dependent substrate translocation. *PNAS*, 110(18), pp.7264–7269.

Smith, D.M. et al., 2005. ATP binding to PAN or the 26S ATPases causes association with the 20S proteasome, gate opening, and translocation of unfolded proteins. *Molecular cell*, 20(5), pp.687–698.

Smith, D.M. et al., 2007. Docking of the proteasomal ATPases“ carboxyl termini in the 20S proteasome”s alpha ring opens the gate for substrate entry. *Molecular cell*, 27(5), pp.731–744.

Solé, C. et al., 2011. Control of Ubp3 ubiquitin protease activity by the Hog1 SAPK modulates transcription upon osmostress. *The EMBO journal*, 30(16), pp.3274–3284.

Somesh, B.P. et al., 2007. Communication between distant sites in RNA polymerase II through ubiquitylation factors and the polymerase CTD. *Cell*, 129(1), pp.57–68.

Somesh, B.P. et al., 2005. Multiple mechanisms confining RNA polymerase II ubiquitylation to polymerases undergoing transcriptional arrest. *Cell*, 121(6), pp.913–923.

Song, C., Wang, Q. & Li, C.-C.H., 2003. ATPase activity of p97-valosin-containing protein (VCP). D2 mediates the major enzyme activity, and D1 contributes to the heat-induced activity. *The Journal of biological chemistry*, 278(6), pp.3648–3655.

Stolz, A. et al., 2011. Cdc48: a power machine in protein degradation. *Trends in biochemical sciences*, 36(10), pp.515–523.

Stundon, J.L. & Zakian, V.A., 2015. Identification of Saccharomyces cerevisiae Genes Whose Deletion Causes Synthetic Effects in Cells with Reduced Levels of the Nuclear Pif1 DNA Helicase. *G3 (Bethesda, Md.)*, 5(12), pp.2913–2918.

Su, K. et al., 1999. An N-terminal region of Sp1 targets its proteasome-dependent degradation in vitro. *The Journal of biological chemistry*, 274(21), pp.15194–15202.

Sullivan, J.A. et al., 2007. Multiple interactions drive adaptor-mediated recruitment of the ubiquitin ligase rsp5 to membrane proteins in vivo and in vitro. *Molecular biology of the cell*, 18(7), pp.2429–2440.

Sun, Z.-W. & Allis, C.D., 2002. Ubiquitination of histone H2B regulates H3 methylation and gene silencing in yeast. *Nature*, 418(6893), pp.104–108.

Suryadinata, R. et al., 2013. Molecular and structural insight into lysine selection on substrate and ubiquitin lysine 48 by the ubiquitin-conjugating enzyme Cdc34.

Cell cycle, 12(11), pp.1732–1744.

Suzuki, T. et al., 2011. Identification and characterization of genes involved in glutathione production in yeast. *Journal of bioscience and bioengineering*, 112(2), pp.107–113.

Svejstrup, J.Q., 2007. Contending with transcriptional arrest during RNAPII transcript elongation. *Trends in biochemical sciences*, 32(4), pp.165–171.

Swatek, K.N. & Komander, D., 2016. Ubiquitin modifications. *Cell research*, 26(4), pp.399–422.

Sweder, K.S. & Hanawalt, P.C., 1992. Preferential repair of cyclobutane pyrimidine dimers in the transcribed strand of a gene in yeast chromosomes and plasmids is dependent on transcription. *Proceedings of the National Academy of Sciences of the United States of America*, 89(22), pp.10696–10700.

Takeuchi, J., Chen, H. & Coffino, P., 2007. Proteasome substrate degradation requires association plus extended peptide. *The EMBO journal*, 26(1), pp.123–131.

Tarlac, V. & Storey, E., 2003. Role of proteolysis in polyglutamine disorders. *Journal of Neuroscience Research*, 74(3), pp.406–416.

Taschner, M. et al., 2010. A role for checkpoint kinase-dependent Rad26 phosphorylation in transcription-coupled DNA repair in Saccharomyces cerevisiae. *Molecular and cellular biology*, 30(2), pp.436–446.

Tatum, D. et al., 2011. Diverse Roles of RNA Polymerase II-associated Factor 1 Complex in Different Subpathways of Nucleotide Excision Repair. *Journal of Biological Chemistry*, 286(35), pp.30304–30313.

Tennyson, C.N., Klamut, H.J. & Worton, R.G., 1995. The human dystrophin gene requires 16 hours to be transcribed and is cotranscriptionally spliced. *Nature genetics*, 9(2), pp.184–190.

Terleth, C., van Sluis, C.A. & van de Putte, P., 1989. Differential repair of UV damage in Saccharomyces cerevisiae. *Nucleic Acids Research*, 17(12), pp.4433–4439.

Thrower, J.S. et al., 2000. Recognition of the polyubiquitin proteolytic signal. *The EMBO journal*, 19(1), pp.94–102.

Tian, L. & Matouschek, A., 2006. Where to start and when to stop. *Nature structural & molecular biology*, 13(8), pp.668–670.

Tian, L., Holmgren, R.A. & Matouschek, A., 2005. A conserved processing mechanism regulates the activity of transcription factors Cubitus interruptus and NF-kappaB. *Nature structural & molecular biology*, 12(12), pp.1045–1053.

Tijsterman, M. et al., 1997. Transitions in the coupling of transcription and nucleotide excision repair within RNA polymerase II-transcribed genes of

Saccharomyces cerevisiae. *Proceedings of the National Academy of Sciences of the United States of America*, 94(15), pp.8027–8032.

Tkach, J.M. et al., 2012. Dissecting DNA damage response pathways by analysing protein localization and abundance changes during DNA replication stress. *Nature cell biology*, 14(9), pp.966–976.

Todi, S.V. et al., 2009. Ubiquitination directly enhances activity of the deubiquitinating enzyme ataxin-3. *The EMBO journal*, 28(4), pp.372–382.

Tonddast-Navaei, S. & Stan, G., 2013. Mechanism of transient binding and release of substrate protein during the allosteric cycle of the p97 nanomachine. *Journal of the American Chemical Society*, 135(39), pp.14627–14636.

Tornaletti, S., Park-Snyder, S. & Hanawalt, P.C., 2008. G4-forming sequences in the non-transcribed DNA strand pose blocks to T7 RNA polymerase and mammalian RNA polymerase II. *The Journal of biological chemistry*, 283(19), pp.12756–12762.

Unverdorben, P. et al., 2014. Deep classification of a large cryo-EM dataset defines the conformational landscape of the 26S proteasome. *Proceedings of the National Academy of Sciences of the United States of America*, 111(15), pp.5544–5549.

Valimberti, I. et al., 2015. E2 superfamily of ubiquitin-conjugating enzymes: constitutively active or activated through phosphorylation in the catalytic cleft. *Scientific reports*, 5, p.14849.

van Tilburg, G.B., Elhebieshy, A.F. & Ovaa, H., 2016. Synthetic and semi-synthetic strategies to study ubiquitin signaling. *Current opinion in structural biology*, 38, pp.92–101.

Vanacloig-Pedros, E. et al., 2015. Coordinated Gene Regulation in the Initial Phase of Salt Stress Adaptation. *Journal of Biological Chemistry*.

Varadan, R. et al., 2005. Structural determinants for selective recognition of a Lys48-linked polyubiquitin chain by a UBA domain. *Molecular cell*, 18(6), pp.687–698.

Varshavsky, A., 2011. The N-end rule pathway and regulation by proteolysis. *Protein Science*, 20(8), pp.1298–1345.

Verdecia, M.A. et al., 2003. Conformational flexibility underlies ubiquitin ligation mediated by the WWP1 HECT domain E3 ligase. *Molecular cell*, 11(1), pp.249–259.

Verhage, R.A., van de Putte, P. & Brouwer, J., 1996. Repair of rDNA in Saccharomyces cerevisiae: RAD4-independent strand-specific nucleotide excision repair of RNA polymerase I transcribed genes. *Nucleic Acids Research*, 24(6), pp.1020–1025.

Verhoef, L.G.G.C. et al., 2009. Minimal length requirement for proteasomal

degradation of ubiquitin-dependent substrates. *FASEB journal : official publication of the Federation of American Societies for Experimental Biology*, 23(1), pp.123–133.

Verma, R. et al., 2011. Cdc48/p97 mediates UV-dependent turnover of RNA Pol II. *Molecular cell*, 41(1), pp.82–92.

Verma, R. et al., 2000. Proteasomal proteomics: identification of nucleotide-sensitive proteasome-interacting proteins by mass spectrometric analysis of affinity-purified proteasomes. *Molecular biology of the cell*, 11(10), pp.3425–3439.

Verma, R. et al., 2002. Role of Rpn11 metalloprotease in deubiquitination and degradation by the 26S proteasome. *Science*, 298(5593), pp.611–615.

Vijay-Kumar, S., Bugg, C.E. & Cook, W.J., 1987. Structure of ubiquitin refined at 1.8 A resolution. *Journal of Molecular Biology*, 194(3), pp.531–544.

Walmacq, C. et al., 2012. Mechanism of translesion transcription by RNA polymerase II and its role in cellular resistance to DNA damage. *Molecular cell*, 46(1), pp.18–29.

Wang, B., Fallon, J.F. & Beachy, P.A., 2000. Hedgehog-regulated processing of Gli3 produces an anterior/posterior repressor gradient in the developing vertebrate limb. *Cell*, 100(4), pp.423–434.

Wang, Q. et al., 2003. D1 ring is stable and nucleotide-independent, whereas D2 ring undergoes major conformational changes during the ATPase cycle of p97-VCP. *The Journal of biological chemistry*, 278(35), pp.32784–32793.

Wang, Q., Song, C. & Li, C.-C.H., 2004. Molecular perspectives on p97-VCP: progress in understanding its structure and diverse biological functions. *Journal of structural biology*, 146(1-2), pp.44–57.

Watts, G.D.J. et al., 2004. Inclusion body myopathy associated with Paget disease of bone and frontotemporal dementia is caused by mutant valosin-containing protein. *Nature genetics*, 36(4), pp.377–381.

Weberruss, M.H. et al., 2013. Blm10 facilitates nuclear import of proteasome core particles. *The EMBO journal*, 32(20), pp.2697–2707.

Wenzel, D.M. et al., 2011. UBCH7 reactivity profile reveals parkin and HHARI to be RING/HECT hybrids. *Nature*, 474(7349), pp.105–108.

Wenzel, T. & Baumeister, W., 1995. Conformational constraints in protein degradation by the 20S proteasome. *Nature Structural Biology*, 2(3), pp.199–204.

West, M.L. & Corden, J.L., 1995. Construction and analysis of yeast RNA polymerase II CTD deletion and substitution mutations. *Genetics*, 140(4), pp.1223–1233.

Wilkinson, K.D., Urban, M.K. & Haas, A.L., 1980. Ubiquitin is the ATP-dependent proteolysis factor I of rabbit reticulocytes. *The Journal of biological chemistry*, 255(16), pp.7529–7532.

Wilson, M.D. et al., 2012. MultiDsk: A Ubiquitin-Specific Affinity Resin. *PloS one*, 7(10), p.e46398.

Wilson, M.D., Harreman, M. & Svejstrup, J.Q., 2013. Ubiquitylation and degradation of elongating RNA polymerase II: the last resort. *Biochimica et biophysica acta*, 1829(1), pp.151–157.

Wilson, M.D., Harreman, M., Taschner, M., et al., 2013. Proteasome-mediated processing of Def1, a critical step in the cellular response to transcription stress. *Cell*, 154(5), pp.983–995.

Wohlschlegel, J.A. et al., 2004. Global analysis of protein sumoylation in Saccharomyces cerevisiae. *The Journal of biological chemistry*, 279(44), pp.45662–45668.

Woudstra, E.C. et al., 2002. A Rad26-Def1 complex coordinates repair and RNA pol II proteolysis in response to DNA damage. *Nature*, 415(6874), pp.929–933.

Xie, Y. & Varshavsky, A., 2001. RPN4 is a ligand, substrate, and transcriptional regulator of the 26S proteasome: a negative feedback circuit. *Proceedings of the National Academy of Sciences of the United States of America*, 98(6), pp.3056–3061.

Xu, Z. et al., 2009. Bidirectional promoters generate pervasive transcription in yeast. *Nature*, 457(7232), pp.1033–1037.

Yamamoto, S. et al., 2004. Expression of valosin-containing protein in colorectal carcinomas as a predictor for disease recurrence and prognosis. *Clinical cancer research : an official journal of the American Association for Cancer Research*, 10(2), pp.651–657.

Ye, Yihong, Meyer, H.H. & Rapoport, T.A., 2003. Function of the p97-Ufd1-Npl4 complex in retrotranslocation from the ER to the cytosol: dual recognition of nonubiquitinated polypeptide segments and polyubiquitin chains. *The Journal of cell biology*, 162(1), pp.71–84.

Ye, Yu et al., 2012. Ubiquitin chain conformation regulates recognition and activity of interacting proteins. *Nature*, 492(7428), pp.266–270.

Yeung, H.O. et al., 2008. Insights into adaptor binding to the AAA protein p97. *Biochemical Society transactions*, 36(Pt 1), pp.62–67.

Yu, S.-L. et al., 2003. The stalling of transcription at abasic sites is highly mutagenic. *Molecular and cellular biology*, 23(1), pp.382–388.

Yuan, W.-C. et al., 2014. K33-Linked Polyubiquitination of Coronin 7 by Cul3-KLHL20 Ubiquitin E3 Ligase Regulates Protein Trafficking. *Molecular cell*, 54(4), pp.586–600.

Zhang, H & Lawrence, C.W., 2005. The error-free component of the RAD6/RAD18 DNA damage tolerance pathway of budding yeast employs sister-strand recombination. *Proceedings of the National Academy of Sciences of the United States of America*, 102(44), pp.15954–15959.

Zhang, M, Pickart, C.M. & Coffino, P., 2003. Determinants of proteasome recognition of ornithine decarboxylase, a ubiquitin-independent substrate | The EMBO Journal. *The EMBO journal*.

Zhang, S, Guha, S. & Volkert, F.C., 1995. The Saccharomyces SHP1 gene, which encodes a regulator of phosphoprotein phosphatase 1 with differential effects on glycogen metabolism, meiotic differentiation, and mitotic cell cycle progression. *Molecular and cellular biology*, 15(4), pp.2037–2050.

Zhang, S, Skalsky, Y. & Garfinkel, D.J., 1999. MGA2 or SPT23 is required for transcription of the delta9 fatty acid desaturase gene, OLE1, and nuclear membrane integrity in Saccharomyces cerevisiae. *Genetics*, 151(2), pp.473–483.

Zhang, Xiaoyi et al., 2015. Altered cofactor regulation with disease-associated p97/VCP mutations. *Proceedings of the National Academy of Sciences of the United States of America*, 112(14), pp.E1705–14.

Zhang, Yi, 2003. Transcriptional regulation by histone ubiquitination and deubiquitination. *Genes & development*, 17(22), pp.2733–2740.

Zhang, Yuan et al., 2015. The contribution of GIGYF2 to Parkinson's disease: a meta-analysis. *Neurological sciences : official journal of the Italian Neurological Society and of the Italian Society of Clinical Neurophysiology*, 36(11), pp.2073–2079.

Zhou, J., Schweikhard, V. & Block, S.M., 2013. Single-molecule studies of RNAPII elongation. *Biochimica et biophysica acta*, 1829(1), pp.29–38.

Zhou, W. & Doetsch, P.W., 1993. Effects of abasic sites and DNA single-strand breaks on prokaryotic RNA polymerases. *Proceedings of the National Academy of Sciences of the United States of America*, 90(14), pp.6601–6605.

Zhou, W., Reines, D. & Doetsch, P.W., 1995. T7 RNA polymerase bypass of large gaps on the template strand reveals a critical role of the nontemplate strand in elongation. *Cell*, 82(4), pp.577–585.